

**ESIPT Based Imidazole Probes for Fluoride ion Detection:
Design, Syntheses and Photophysical Properties of *N,O*- and *N,C*-
Chelate Organoboron Compounds**

By

DHANUNJAYARAO KUNCHALA

CHEM11201104011

**National Institute of Science Education and Research,
Bhubaneswar, Odisha**

*A thesis submitted to the
Board of Studies in Chemical Sciences
In partial fulfillment of requirements
for the Degree of*

DOCTOR OF PHILOSOPHY

Of

HOMI BHABHA NATIONAL INSTITUTE



November, 2017

Homi Bhabha National Institute

Recommendations of the Viva Voce Committee

As members of the Viva Voce Committee, we certify that we have read the dissertation prepared by **Dhanunjayarao Kunchala** entitled "ESIPT Based Imidazole Probes for Fluoride ion Detection: Design, Syntheses and Photophysical Properties of *N,O*- and *N,C*-Chelate Organoboron Compounds" and recommend that it may be accepted as fulfilling the thesis requirement for the award of Degree of Doctor of Philosophy.

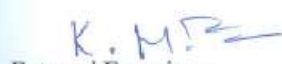
Chairman: Prof. A. Srinivasan



Date: 8.03.2018


Guide: Dr. V. Krishnan

Date: 8/3/18


External Examiner:
Prof. K. Muralidharan

Date: 8/3/18

Member 1- Dr. C. Gunanathan



Date: 8/3/18

Member 2- Dr. U. Lourderaj



Date: 8/2/18

Member 3- Dr. Praful Singru



Date: 8.3.2018

Final approval and acceptance of this thesis is contingent upon the candidate's submission of the final copies of the thesis to HBNI.

I hereby certify that I have read this thesis prepared under my direction and recommend that it may be accepted as fulfilling the thesis requirement.

Date: 8/3/18


(Dr. V. Krishnan)

Place: Bhubaneswar

Guide

STATEMENT BY AUTHOR

This dissertation has been submitted in partial fulfillment of requirements for an advanced degree at Homi Bhabha National Institute (HBNI) and is deposited in the Library to be made available to borrowers under rules of the HBNI.

Brief quotations from this dissertation are allowable without special permission, provided that accurate acknowledgement of source is made. Requests for permission for extended quotation from or reproduction of this manuscript in whole or in part may be granted by the Competent Authority of HBNI when in his or her judgment the proposed use of the material is in the interests of scholarship. In all other instances, however, permission must be obtained from the author.

Dhanunjayarao Kunchala

DECLARATION

I, hereby declare that the investigation presented in the thesis has been carried out by me. The work is original and has not been submitted earlier as a whole or in part for a degree / diploma at this or any other Institution / University.

Dhanunjayarao Kunchala

LIST OF PUBLICATIONS

Published

1. ***Dhanunjavarao, K.**; Mukundam, V.; Ramesh, M.; Venkatasubbaiah, K. Synthesis and Optical Properties of Salicylaldimine-Based Diboron Complexes. *Eur. J. Inorg. Chem.* **2014**, 539.
2. ***Dhanunjavarao, K.**; Mukundam, V.; Venkatasubbaiah, K. A Highly Selective Ratiometric Detection of F⁻ based on Excited-State Intramolecular Proton-Transfer (Imidazole) Materials. *J. Mater. Chem. C.* **2014**, 2, 8599.
3. ***Dhanunjavarao, K.**; Mukundam, V.; Venkatasubbaiah, K. Ratiometric sensing of fluoride anion through selective cleavage of Si-O bond. *Sensors and Actuators B.* **2016**, 232, 175.
4. ***Dhanunjavarao, K.**; Mukundam, V.; Venkatasubbaiah, K. Tetracoordinate Imidazole-Based Boron Complexes for the Selective Detection of Picric Acid. *Inorg. Chem.* **2016**, 55, 11153
5. Mukundam, V.; **Dhanunjavarao, K.**; Chuang, C.-N.; Kang, D.-Y.; Leung, M.-k.; Hsieh, K.-H.; Venkatasubbaiah, K. Design, Synthesis, Photophysical and Electrochemical Properties of 2-(4,5-diphenyl-1-p-aryl-1H-imidazol-2-yl)phenol-based Boron Complexes. *Dalton Trans.* **2015**, 44, 10228.
6. Mukundam, V.; Kumar, A.; **Dhanunjavarao, K.**; Ravi, A.; Peruncheralathan, S.; Venkatasubbaiah, K. Tetraaryl Pyrazole Polymers: Versatile Synthesis, Aggregation Induced Emission Enhancement and Detection of Explosives. *Polym. Chem.* **2015**, 6, 7764.
7. Mukundam, V.; **Dhanunjavarao, K.**; Mamidala, R.; Venkatasubbaiah, K. Synthesis, Characterization and Aggregation Induced Enhanced Emission Properties of Tetraaryl Pyrazole Decorated Cyclophosphazenes. *J. Mater. Chem. C.* **2016**, 4, 3523.
8. Mamidala, R.; Mukundam, V.; **Dhanunjavarao, K.**; Venkatasubbaiah, K. Synthesis of a Cyclometalated 1,3,5-Triphenylpyrazole Palladium Dimer and its Activity Towards Cross Coupling Reactions. *Dalton Trans.* **2015**, 44, 5805.
9. Mamidala, R.; Mukundam, V.; **Dhanunjavarao, K.**; Venkatasubbaiah, K. Cyclometalated palladium pre-catalyst for N-alkylation of amines using

alcohols and regioselective alkylation of sulfanilamide using aryl alcohols.
Tetrahedron. **2017**,73,2225.

10. Mukundam, V.; **Dhanunjayarao, K.**; Samal, S.; Venkatasubbaiah, K. Variation of *para* Substituent on 2-Phenol of Tetraaryl-Substituted Imidazole-Boron Difluoride Complexes: Synthesis, Characterization, and Photophysical Properties. *Asian J. Org. Chem.* **2017**, 6, 1054.

* Pertaining to thesis

Manuscript under preparation

1. * **Dhanunjayarao, K.**; Mukundam, V.; Venkatasubbaiah, K. *N,C*- Chelate mono & dinuclear boron compounds based on phenanthrene imidazole: Synthesis, characterization and photophysical properties.
2. **Dhanunjayarao, K.**; Mukundam, V.; Venkatasubbaiah, K. Synthesis and photophysical properties of Phenanthridine based *N,C*- Chelate boron compounds.

CONFERENCES

- “Synthesis and Characterization of New Fluorescent Salicylaldiimine Based Diboron Complexes”- **Dhanunjayarao, K.**; Mukundam, V.; Ramesh, M.; Venkatasubbaiah, K. in Indo-French Symposium on Functional Metal-Organics: Applications in Materials and catalysis, held on (24-26)th February 2014, NISER Bhubaneswar, India. (**Poster presentation**)

- “Imidazole based probes for the selective detection of fluoride ion” **Dhanunjayarao, K.**; Mukundam, V.; Venkatasubbaiah, K. in 19th CRSI National Symposium in Chemistry held on (14-16)th July 2016, University of North Bengal, Darjeeling, India. (**Poster presentation**)

Dhanunjayarao Kunchala



Dedicated to
Sir V. Krishnan

ACKNOWLEDGEMENTS

*I would like to express my sincere gratitude to my supervisor **Dr. V. Krishnan** for his patient guidance, insightful advice and invaluable encouragements throughout my time as his student.*

*I would like to thank my thesis monitoring committee members **Prof. A. Srinivasan, Dr. C. Gunanathan, Dr. Upakarasamy Lourderaj, Dr. Praful Singru**, for their useful suggestions and **Dr. S. Peruncheralathan**, for his support on several occasions.*

*I am thankful to **Prof. S. Panda**, Director, **Prof. V. Chandrasekhar** and **Prof. T. k. Chandrashekar** previous Directors NISER for providing the laboratory facilities, I am very much thankful to all the **faculty members** of school chemical sciences, NISER for their cooperation and support to adjust me in this environment. I am also thankful to all the **staff members** and **research fellows** of Chemistry, NISER for their necessary help and kind co-operation.*

*It gives me immense pleasure to thank **all the members of the Krishnan group**, past and present, for sharing their experience and knowledge and for their friendship during the past six years. I also thank the seniors, friends and juniors who made my life at NISER really enjoyable and memorable, and special thanks to my seniors **G S Reddy, Pardu** for their encouragement.*

*I am deeply grateful to my beloved, brother **Damodar** and sisters **Bhargavi, Sujatha** for their unconditional love, sacrifices, and blessings which has motivated me to achieve this goal.*

*Finally, I would like to acknowledge **CSIR** for fellowship and **NISER** for research facilities.*

Dhanunjayarao Kunchala

CONTENTS

	Page No.
Synopsis	xi
List of Tables	1
List of Schemes	2
List of Figures	3
List of Abbreviations	10
Chapter 1	13
Chapter 2	63
Chapter 3	97
Chapter 4	153
Summary	207

SYNOPSIS

This will sets the stage for part of the work carried out in this thesis. This thesis has been organized into four chapters.

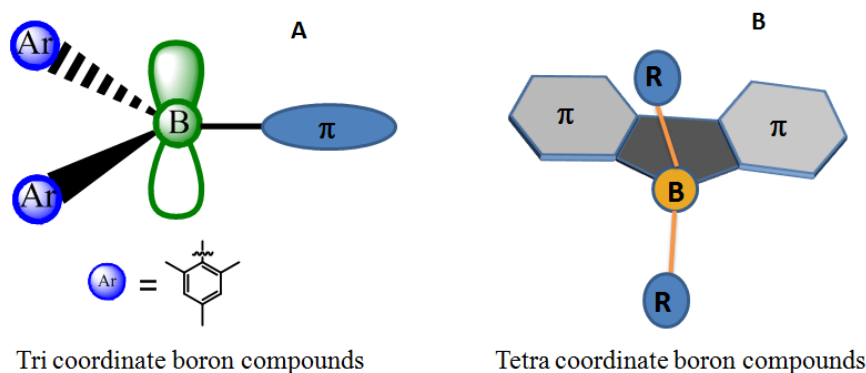
Chapter 1: General introduction

First part of this chapter contains brief introduction on fluoride ion sensing. Fluoride, the smallest inorganic anion, naturally occurs in rocks, soils, ground water, and also presents in animal (mainly in teeth and bone) and plants. Small amounts of fluoride ion is used for the preventions of dental caries¹ and also used in the treatment of osteoporosis. However high consumption of fluoride ion causes dental and skeletal fluorosis and also been accused for many fatal diseases. Hence, it is obvious the regulation and selective detection of fluoride ion become growing interest in research community. Among several detection techniques developed, electrochemical and NMR analysis have disadvantages such as low sensitivity and associates with big instrument setup. Colorimetric (UV) and fluorescence sensors have been paid attention because of their high sensitivity and ease of monitoring in intracellular system.²

Over the year's large member of optical sensor systems were developed for the detection of fluoride ion, based on hydrogen bonding,³ interaction between fluoride ion and Lewis acidic boron.⁴ However many of these methods suffers from low selectivity. Recently, a reaction based chemodosimeters particularly fluoride ion triggered silicon-oxygen bond cleavage based sensors⁵ gained attention because of their high selectivity and sensitivity.⁶

Second part of this chapter comprise brief introduction of fluorescent organoboron compounds. Fluorescent boron compounds⁷ mainly classified into two types as tri-coordinate⁸ and tetra-coordinate⁹ boron compounds. The overlap of empty *p* orbital

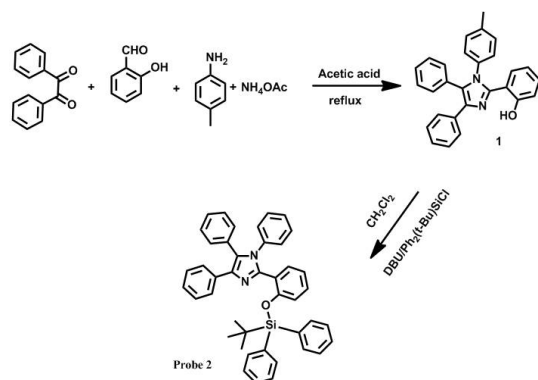
with π -conjugated system in tri-coordinate boron makes it an excellent π -acceptor in conjugated organic molecules.¹⁰ The interaction between Lewis acidic boron and small nucleophiles leads, interesting application in sensing for the selective detection of fluoride and cyanide.¹¹ However the chemistry of tri-coordinate boron is limited because of their instability, and need of sterically demanding bulky groups such as mesityl, triply groups in order to get kinetic stability, which involves tedious synthetic procedures. Meanwhile tetra-coordinate boron compounds paid much attention because of their high stability towards air and moisture.



Tetra-coordinate boron compounds further classified into four types, namely *N,N*-, *N,O*-, *N,C*-, and *O,O*- chelate organoboron compounds based on the chelating atom. Boron-dipyrromethenes (BODIPY's) are well known studied four coordinate organoboron compound with *N,N*- chelation, because of their excellent properties such as high molar extension coefficients, environment independent fluorescence leads potential applications in fluorescent imaging, chemical sensors and near-infrared emitting materials¹². However, BODIPY suffers from small stokes shift and weak emission in solid state which limits their application solid state. In order to overcome these drawbacks recently many boron fluorophores with different chelating ligands have been synthesized¹³ and successfully used as organic field transistors, biological imaging materials, photo chromic materials,¹⁴ and in OLED'S as a emissive layer, as well as electron transporting material.¹⁵

Chapter 2: Synthesis and study of imidazole based probes for the selective detection of fluoride ion via ESIPT mechanism.

By using commercially available simple starting materials, we synthesized probe **2** (2-*tert*-butyldiphenylsiloxy) phenyl-4,5-diphenyl-*p*-tolyl-1H-imidazole) in two steps as shown scheme 2.1. The probe **2** was characterized by ^1H NMR, ^{13}C NMR,



Scheme 2.1 Synthetic route for probe **2**

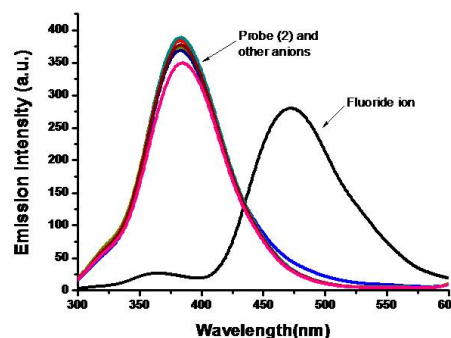


Figure 2.1 Emission spectra of probe **2** and with 15 eq. of Cl^- , Br^- , I^- , CN^- , OAc^- , NO_2^- , NO_3^- , HSO_4^- and F^- in CH_2Cl_2

^{29}Si NMR, HRMS, and single crystal X-ray analysis. Probe **2** exhibited one absorption maxima at 278 nm and an emission band at 386 nm in CH_2Cl_2 . We studied the sensing ability of probe **2** in CH_2Cl_2 , and evaluated its response to fluoride ion by absorption as well as emission spectroscopy. In the absorbance spectra a new band appeared at 318 nm after the addition of F^- ion. In the emission spectra we have seen ratiometric response to the fluoride ion, emission intensity at 386 nm gradually decreased and simultaneously a new band appeared at 473 nm with a clear isoemission point at 436 nm. Probe **2** displayed excellent selectivity and sensitivity towards fluoride ion over other anions (figure 2.1) through the selective cleavage of Si-O bond. However this probe failed to detect fluoride ion in more polar solvents using sodium salts in water. In order to improve the solubility of the sensor in more polar solvents, we introduced hydrophilic moieties. We made the design (probe **4**) much simpler by removing tolyl group on the 1-position of the imidazole **1**; at same

time it introduced NH functionality which helped to solubilize the molecule in more polar solvents (scheme 2.2). Probe 4 displayed good selectivity and sensitivity towards inorganic fluoride and acetate anions in DMSO/water mixed system. The absorption, emission and NMR spectroscopy reveals that the signal transfer occurs *via* Si-O bond cleavage that results in the formation of ESIPT activated imidazole (compound 3).

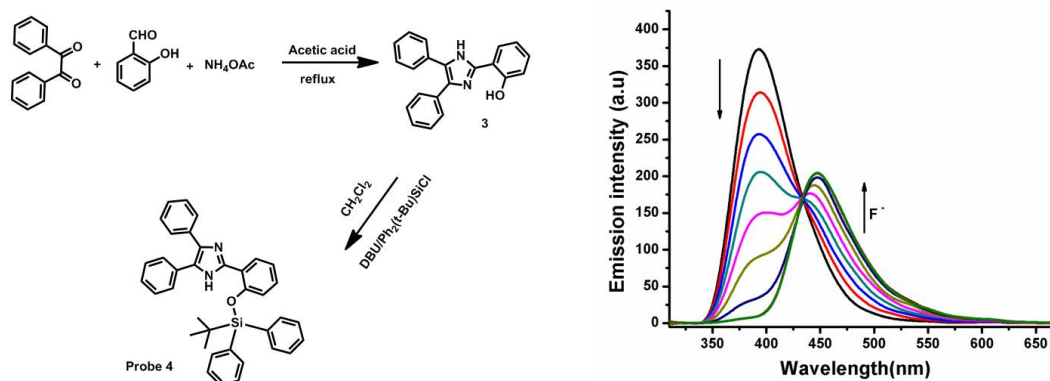
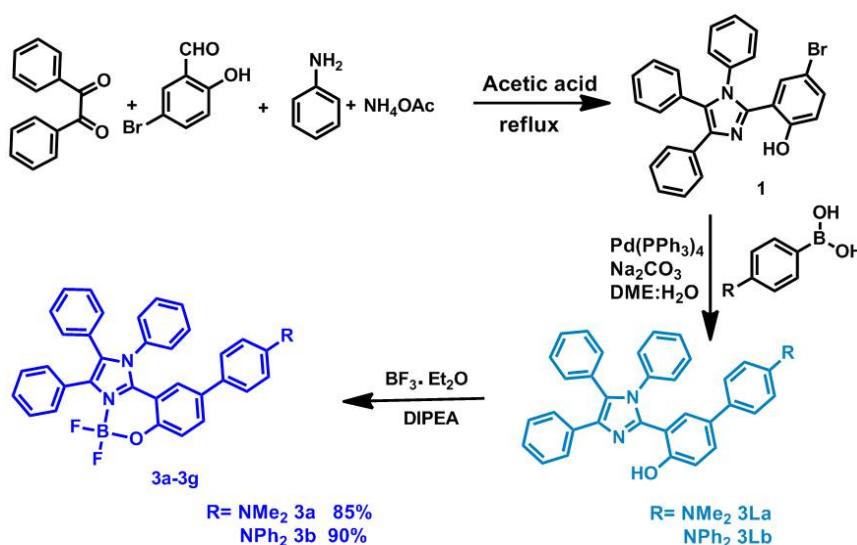


Figure 2.2 Emission spectra of probe 4 (17.6 μM) in DMSO with the addition of NaF in Water (0, to 1.35 equi. excited at 302 nm)

Scheme 2.2 Synthetic route for probe 4

Chapter 3: *N,O*- Chelate organoboron compounds: Synthesis, photophysical properties and their application in explosive detection.



Scheme 3.1 Synthesis of compounds 3a and 3b

This chapter divided into two parts. First part of this chapter describes the synthesis of

N,O-chelate imidazole boron compounds **3a** & **3b** (scheme 3.1) and characterization of the same by ^1H , ^{13}C , ^{11}B , ^{19}F NMR and HRMS analysis. We studied their photo physical properties in different solvents. Compounds **3a** & **3b** were investigated as new sensors for the selective detection of picric acid (PA).

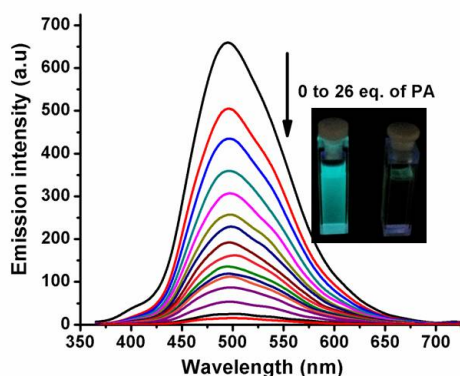


Figure 3.1 Emission changes of **3a** ($43\mu\text{M}$) with addition of PA when excited at 358 nm

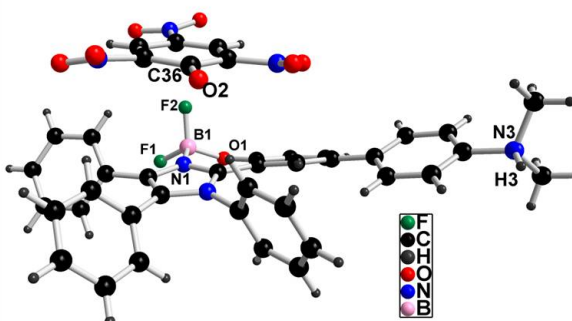
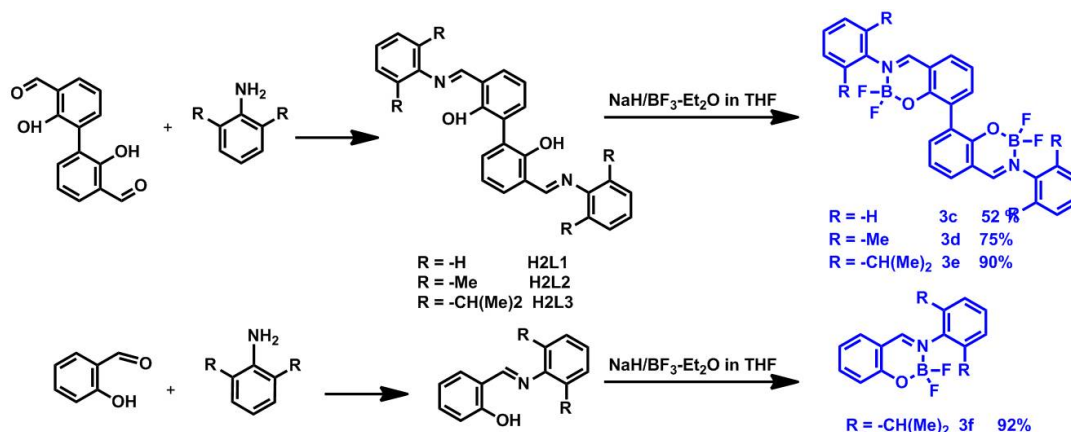


Figure 3.2 Molecular structure of the probe **3a.PA**

Fluorescence quenching by PA (figure 3.1) was analyzed by stern volmer equation and by fluorescence lifetime studies; suggesting that quenching follows a static quenching mechanism through a ground state complex formation between Probe and PA. We grew single crystals of probe **3a** and PA (figure 3.2). X-ray analysis reveal that proton transfer between PA and the imidazole based boron complexes is the origin for the selectivity. Also we made test strips of compound **3a** by whatman filter paper and used for solid state detection of PA.

Second part of this chapter contains *N,O*-chelate disalicyladiimine based diboron complexes **3c-3e**. As shown in scheme 3.2 Schiff base ligands were synthesized by acid catalyzed condensation reaction between aldehyde and amine. In the second step all Schiff base ligands were deprotonated by sodium hydride and complexated by using $\text{BF}_3\cdot\text{Et}_2\text{O}$ to form the desired products **3c-3e** in good yield.



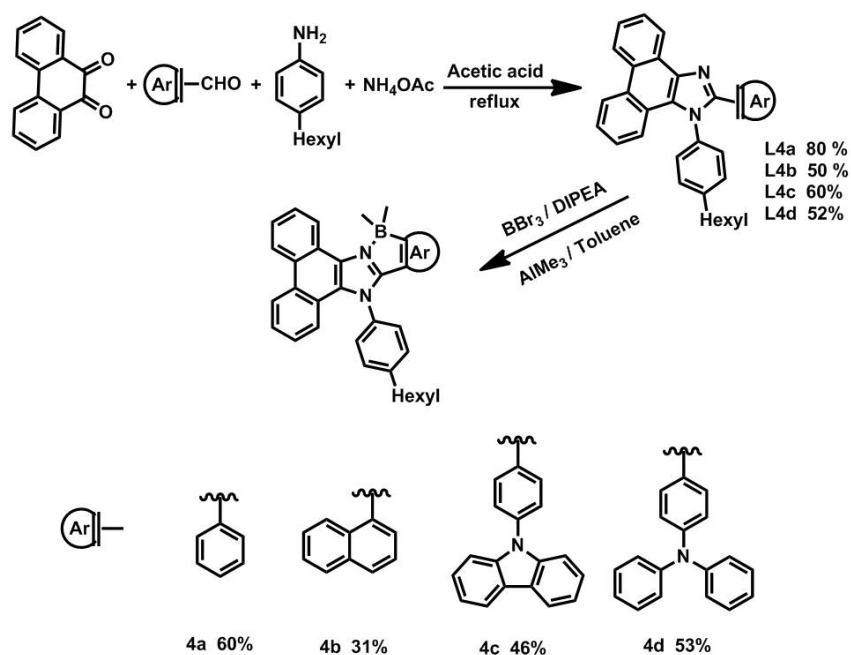
Scheme 3.2 Synthesis of compounds **3c-3f**

All Schiff bases and boron complexes **3c-3e** were well characterized by multinuclear NMR, HRMS and by single crystal X-ray analysis (ligands, **3c & 3e**). We studied the photophysical properties of boron complexes **3c-3e** in THF. Photophysical properties of diboron complex **3e** were compared with its monoboron complex **3f**. The electron accepting abilities of diboron compounds were performed by cyclic voltametry in DMF. These properties suggest that salicylaldimine-boron compounds could have potential applications for the manufacture of optoelectronic devices.

Chapter 4: Synthesis and photophysical properties of *N,C*-chelate organoboron compounds.

In the process of finding new fluorophores with high quantum yields in solutions as well as in solid state, we made *N,C*-chelate organoborons by simple electrophilic borylation method¹⁶.

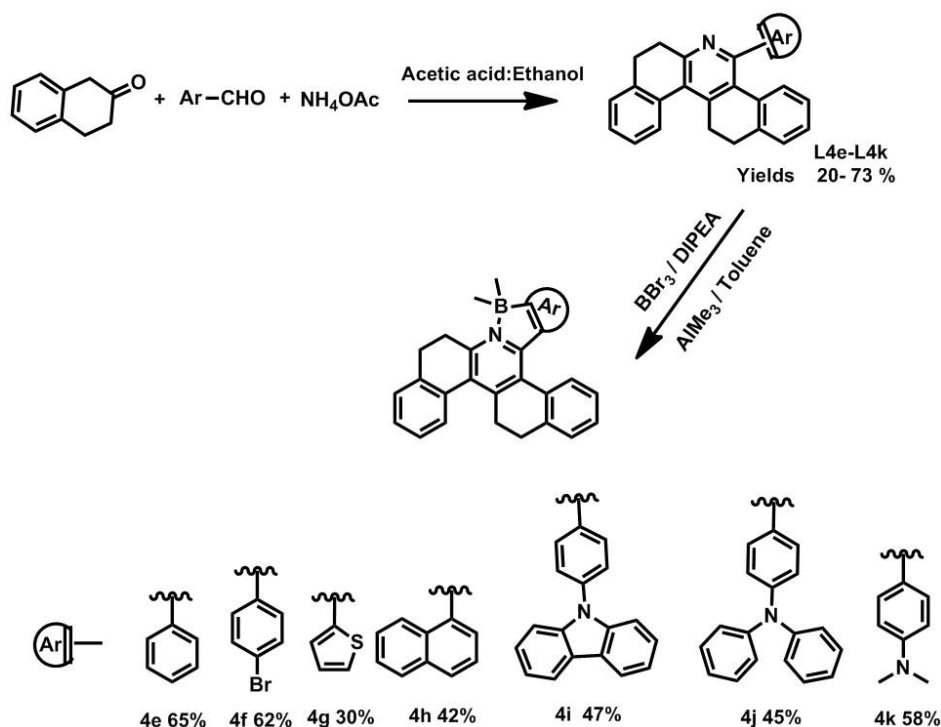
First part of this chapter describes synthesis of phenanthrene imidazole based *N,C*-chelate boron compounds (**4a-4d**) (scheme 4.1), and characterization of these compounds by multinuclear NMR, ESI mass analysis, and also by single crystal X-ray analysis (**4a&4c**). TGA analysis of these boron compounds revealed their high



Scheme 4.1 Synthesis of compounds **4a-4d**

thermal stabilities upto 450 °C. Photophysical properties of these compounds **4a-4d**, studied in different solvents. All the boron compounds were showing good emission properties in solution as well as in solid state.

Second part of this chapter describes the synthesis of tetrahydro phenanthridine based *N,C*-chelate boron compounds (**4e-4l**). All the new boron compounds (**4e-4l**) were characterized by ¹H, ¹¹B NMR, ESI mass, and also by single crystal analysis for **4e**, **4f**, **4h** & **4k**. Thermal properties of these boron compounds were studied by TGA & DSC. Photophysical properties were investigated in both polar and non polar solvents. Both absorption (364 to 420 nm) and emission maxima (402-494 nm) of boron compounds were affected by changing the substitution. All these boron compounds showed moderate to good quantum yields in solution as well in solid state.



Scheme 4.2 Synthesis of compounds 4a-4d

References:

1. Newbrun, E., What we know and do not know about fluoride. *Journal of Public Health Dentistry* **2010**, *70* (3), 227-233.
- 2.(a) Li, L.; Ji, Y.; Tang, X., Quaternary Ammonium Promoted Ultra Selective and Sensitive Fluorescence Detection of Fluoride Ion in Water and Living Cells. *Anal. Chem. (Washington, DC, U. S.)* **2014**, *86* (20), 10006-10009; (b) Zhou, Y.; Zhang, J. F.; Yoon, J., Fluorescence and Colorimetric Chemosensors for Fluoride-Ion Detection. *Chem. Rev. (Washington, DC, U. S.)* **2014**, *114* (10), 5511-5571.
- 3.(a) Guha, S.; Saha, S., Fluoride Ion Sensing by an Anion- π Interaction. *J. Am. Chem. Soc.* **2010**, *132* (50), 17674-17677; (b) Thiagarajan, V.; Ramamurthy, P.; Thirumalai, D.; Ramakrishnan, V. T., A Novel Colorimetric and Fluorescent Chemosensor for Anions Involving PET and ICT Pathways. *Org. Lett.* **2005**, *7* (4), 657-660; (c) Kim, H. J.; Kim, S. K.; Lee, J. Y.; Kim, J. S., Fluoride-Sensing Calix-

luminophores Based on Regioselective Binding. *J. Org. Chem* **2006**, *71* (17), 6611-6614.

4.(a) Jaekle, F., Lewis acidic organoboron polymers. *Coord. Chem. Rev.* **2006**, *250* (9-10), 1107-1121; (b) Yamaguchi, S.; Akiyama, S.; Tamao, K., Colorimetric fluoride ion sensing by boron-containing pi-electron systems. *J. Am. Chem. Soc.* **2001**, *123* (46), 11372-5.

5.Hu, R.; Feng, J.; Hu, D.; Wang, S.; Li, S.; Li, Y.; Yang, G., A Rapid Aqueous Fluoride Ion Sensor with Dual Output Modes. *Angew. Chem., Int. Ed.* **2010**, *49* (29), 4915-4918, S4915/1-S4915/3.

6.Kim, T.-H.; Swager, T. M., A fluorescent self-amplifying wavelength-responsive sensory polymer for fluoride ions. *Angew. Chem., Int. Ed.* **2003**, *42* (39), 4803-4806.

7.Jakle, F., Advances in the Synthesis of Organoborane Polymers for Optical, Electronic, and Sensory Applications. *Chem. Rev. (Washington, DC, U. S.)* **2010**, *110* (7), 3985-4022.

8.Entwistle, C. D.; Marder, T. B., Applications of Three-Coordinate Organoboron Compounds and Polymers in Optoelectronics. *Chem. Mater.* **2004**, *16* (23), 4574-4585.

9.Rao, Y.-L.; Wang, S., Four-Coordinate Organoboron Compounds with a π -Conjugated Chelate Ligand for Optoelectronic Applications. *Inorg. Chem.* **2011**, *50* (24), 12263-12274.

10.Ji, L.; Griesbeck, S.; Marder, T. B., Recent developments in and perspectives on three-coordinate boron materials: a bright future. *Chem. Sci.* **2017**.

11.(a) Hudson, Z. M.; Wang, S., Impact of Donor–Acceptor Geometry and Metal Chelation on Photophysical Properties and Applications of Triarylboranes. *Acc. Chem. Res.* **2009**, *42* (10), 1584-1596; (b) Wade, C. R.; Broomsgrove, A. E. J.;

Aldridge, S.; Gabbaï, F. P., Fluoride Ion Complexation and Sensing Using Organoboron Compounds. *Chem. Rev.* **2010**, *110* (7), 3958-3984.

12.Lipunova, G. N.; Nosova, E. V.; Charushin, V. N.; Chupakhin, O. N., Boron(III) Complexes with N,N'- and N,O-Heterocyclic Ligands: Synthesis and Spectroscopic Properties. *Comments Inorg. Chem.* **2016**, *36* (5), 245-303.

13.Frath, D.; Massue, J.; Ulrich, G.; Ziessel, R., Luminescent materials: locking pi-conjugated and heterocyclic ligands with boron(III). *Angew. Chem. Int. Ed. Engl.* **2014**, *53* (9), 2290-310.

14.Rao, Y.-L.; Amarne, H.; Wang, S., Photochromic four-coordinate N,C-chelate boron compounds. *Coord. Chem. Rev.* **2012**, *256* (5–8), 759-770.

15.Li, D.; Zhang, H.; Wang, Y., Four-coordinate organoboron compounds for organic light-emitting diodes (OLEDs). *Chem. Soc. Rev.* **2013**, *42* (21), 8416-8433.

16.Ishida, N.; Moriya, T.; Goya, T.; Murakami, M., Synthesis of Pyridine–Borane Complexes via Electrophilic Aromatic Borylation. *J. Org. Chem.* **2010**, *75* (24), 8709-8712.

List of tables

1	Table 2.1	Selective bond angle and bond lengths of compounds 1a and 1	68
2	Table 2.2	Crystal data and structure refinement parameters for compounds 1a and 1	68
3	Table 2.3	Comparison of geometric parameters from DFT calculations and X-ray analysis of 1a and 1	74
4	Table 2.5	Crystal data and structure refinement parameters for compounds 2	79
5	Table 2.4	Selective bond lengths of compounds 2	80
6	Table 3A.1	Photophysical data of compounds 4 and 5	107
7	Table 3A.2	Crystal data and structure refinement of adduct 4·PA	114
8	Table 3B.1	Crystal data and structure refinement parameters for compounds 1-3	131
9	Table 3B.2	Crystal data and structure refinement parameters of compounds 5 and 7	136
10	Table 3B.3	Photophysical data of compounds 5-7	137
11	Table 3B.4	Calculated electronic transitions for 5-8 from TD-DFT (B3LYP) calculations	139
12	Table 3B.5	Calculated orbital energies (eV) for compound 5-7 from DFT (B3LYP) calculations	140
13	Table 3B.6	Computed orbitals for compounds 5-7	141
14	Table 3B.7	Frontier orbital energies [eV] derived from UV/Vis onset absorption and electrochemical data	143
15	Table 4A.1	Boron deviation from plane, bond angle and bond lengths of compounds B1 and B3	160
16	Table 4A.2	Crystal data and structure refinement parameters for compounds B1 and B3	161
17	Table 4A.3	Photophysical data of compounds B1-B4	166
18	Table 4B.1	Boron deviation from plane, bond angle and bond length angles of compounds 1, 2, 4, 7 and 8	186
19	Table 4B.2	Crystal data and structure refinement parameters for	186

	compounds 1, 2 and 4	
20	Table 4B.3 Crystal data and structure refinement parameters for compounds 7 and 8	187
21	Table 4B.4 Photophysical data of compounds 1-8	192

List of schemes

1	Scheme 2.1	Synthetic route to probe 1	65
2	Scheme 2.2	Sensing mechanism of the probe 1	72
3	Scheme 2.3	Synthetic route to probe 2	75
4	Scheme 3A.1	Synthetic route to N,O chelate imidazole boron compounds 4 and 5	102
5	Scheme 3B.1	Synthetic route to bis-salicylaldimine Schiff bases 1–3	129
6	Scheme 3B.2	Synthetic route to Schiff bases boron compounds 5–8	132
7	Scheme 4A.1	Synthetic route to compounds L1-L4	156
8	Scheme 4A.2	Synthetic route to <i>N,C</i> - chelate boron compounds B1	158
9	Scheme 4B.1	Synthetic route to compounds 1a-1g	180
10	Scheme 4B.2	Synthetic route to <i>N,C</i> - chelate boron compound 1 and chemdraw representations of compounds 2-7	182
11	Scheme 4B.3	Synthetic route to compound 8	183

List of figures

1	Figure 1.1	Sensors based on hydrogen bonding interactions (1-8)	17
2	Figure 1.2	Sensor based on hydrogen bonding interactions (9).	17
3	Figure 1.3	Sensors based on interaction between Lewis acidic boron and fluoride (10-14).	19
4	Figure 1.4	Sensor 15 based on O-Si bond cleavage reaction	19
5	Figure 1.5	Sensors based on O-Si bond cleavage reaction (17-25)	22
6	Figure 1.6	Schematic representation of (left) tri-coordinate boron; (right) tetra-coordinate boron compounds	23
7	Figure 1.7	<i>N,N</i> -chelate tetra-coordinate boron complexes (26-31).	25
8	Figure 1.8	<i>N,N</i> -chelate tetra-coordinate boron complexes (32-41)	26
9	Figure 1.9	<i>N,N</i> -chelate tetra-coordinate boron complexes (42-51)	26
10	Figure 1.10	<i>N,N</i> -chelate tetra-coordinate boron complexes (52-67).	27
11	Figure 1.11	<i>N,N</i> -chelate tetra-coordinate boron complexes (68-75)	28
12	Figure 1.12	<i>N,O</i> -chelate tetra-coordinate boron complexes (76-101).	29
13	Figure 1.13	<i>N,O</i> -chelate tetra-coordinate boron complexes (102-115).	31
14	Figure 1.14	<i>N,O</i> -chelate tetra-coordinate boron complexes (116-141).	33
15	Figure 1.15	<i>N,O</i> -chelate tetra-coordinate boron complexes (142-158)	34
16	Figure 1.16	<i>N,O</i> -chelate tetra-coordinate boron complexes (159-192).	36
17	Figure 1.17	<i>N,O</i> -chelate tetra-coordinate boron complexes (193-204)	37
18	Figure 1.18	<i>N,O</i> -chelate tetra-coordinate boron complexes (205-217)	37
19	Figure 1.19	<i>N,O</i> -chelate tetra-coordinate boron complexes (218-240).	38
20	Figure 1.20	<i>N,O</i> -chelate tetra-coordinate boron complexes (241-253).	39
21	Figure 1.21	<i>N,C</i> -chelate tetra-coordinate boron complexes (254-259).	41
22	Figure 1.22	<i>N,C</i> -chelate tetra-coordinate boron complexes (260-269).	42
23	Figure 1.23	<i>N,C</i> -chelate tetra-coordinate boron complexes (270-271)	44
24	Figure 1.24	<i>N,C</i> -chelate tetra-coordinate boron complexes (272-279)	44
25	Figure 1.25	<i>N,C</i> -chelate tetra-coordinate boron complexes (280-282)	45
26	Figure 1.26	<i>N,C</i> -chelate tetra-coordinate boron complexes (283-287)	45

27	Figure 1.27	<i>N,C</i> - chelate tetra-coordinate boron complexes (288-309)	46
28	Figure 1.28	<i>N,C</i> - chelate tetra-coordinate boron complexes (310-316)	47
29	Figure 1.29	<i>N,C</i> - chelate tetra-coordinate boron complexes (317-322).	48
30	Figure 1.30	<i>N,C</i> - chelate tetra-coordinate boron complexes (323-326)	49
31	Figure 1.31	<i>N,C</i> - chelate tetra-coordinate boron complexes (327-333).	50
32	Figure 1.32	<i>N,C</i> - chelate tetra-coordinate boron complexes (334-347)	50
33	Figure 1.33	<i>N,C</i> - chelate tetra-coordinate boron complexes (348-355)	51
34	Figure 1.34	<i>N,C</i> - chelate tetra-coordinate boron complexes (356-357)	51
35	Figure 2.1	¹ H NMR spectrum of compound 1a	65
36	Figure 2.2	²⁹ Si NMR spectrum of compound 1	66
37	Figure 2.3	¹ H NMR spectrum of compound 1	67
38	Figure 2.4	HRMS spectrum of compound 1	67
39	Figure 2.5	Molecular structure of compounds 1a (left) and 1 (right). Hydrogen atoms are omitted for clarity	68
40	Figure 2.6	Absorption spectra of Probe 1 (24 μM) with different concentrations of F ⁻ (0, 0.39, 0.78, 1.17, 1.56, 1.95, 2.34, 2.73, 3.12, 3.51, 3.90, 4.29, 4.68, 5.07, 5.46, 5.85, 6.24, 6.63, 9.36, 17.16 equiv.) in THF	70
41	Figure 2.7	Fluorescence spectra of probe 1 (24 μM) with different concentrations of F ⁻ (0, 0.39, 0.78, 1.17, 1.56, 1.95, 2.34, 2.73, 3.12, 3.51, 3.9, 4.29, 4.68, 5.07, 5.46, 5.85, 6.24, 6.63, 9.36, 17.16 equiv) in THF when excited at 278 nm.	71
42	Figure 2.8	Emission changes of probe 1 (24 μM) between 386 and 473 nm with 15 equiv. of Cl ⁻ , Br ⁻ , CN ⁻ , OAc ⁻ , NO ₂ ⁻ ,	72

		NO_3^- , HSO_4^- , F^- .	
43	Figure 2.9	^1H NMR titration spectra of 1 (16 mM) with 0.25, 0.50, 0.75 and 1.00 equivalents of F^- ions in CDCl_3 (bottom to top 0, 0.25...).	73
44	Figure 2.10	HOMO and LUMO diagrams of 1a and 1 (contour value 0.02).	73
45	Figure 2.11	^1H NMR spectrum of compound 2	76
46	Figure 2.12	^{13}C NMR spectrum of compound 2	77
47	Figure 2.13	HRMS spectrum of compound 2	77
48	Figure 2.14	^{29}Si NMR spectrum of compound 2	78
49	Figure 2.15	Molecular structure of compounds 2 . Hydrogen atoms are omitted for clarity	79
50	Figure 2.16	Absorption (left) and emission (right) spectra of probe 2 (17.6 μM) with the addition of TBAF (0, 0.15, 0.3, 0.45, 0.6, 0.75, 0.9, 1.05, 1.20, 1.35 equiv.) in DMSO	80
51	Figure 2.17	Absorption spectra of compound 2 (17.6 μM) in DMSO with the addition of NaF (0, 0.15, 0.3, 0.45, 0.6, 0.75, 0.9, 1.05, 1.20, 1.35 equivi. excited at 302 nm)	81
52	Figure 2.18	Emission spectra of compound 2 (17.6 μM) in DMSO with the addition of NaF (0, 0.15, 0.3, 0.45, 0.6, 0.75, 0.9, 1.05, 1.20, 1.35 equivi. excited at 302 nm)	81
53	Figure 2.19	Fluorescence changes of probe 2 upon addition of NaF^- under hand held UV lamp of 365 nm.	82
54	Figure 2.20	Emission spectra of probe 2 (17.6 μM) in DMSO/ H_2O with time interval 0, 20, 40, 60, 80, 100, 120, 140 minutes (excited at 301 nm).	82
55	Figure 2.21	Fluorescence emission changes of compound 2 (17.6 μM) between 448 and 392nm in DMSO with the addition of one equivalent of different anions (F^- , Cl^- , Br^- , I^- , CO_3^{2-} , SO_4^{2-} , NO_2^- , OAc^- , HSO_3^- , HCO_3^-) of sodium salts in water.	83
56	Figure 2.22	Absorption (left) and emission (right) spectra 2 (17.6mM) with addition of TBOAc^- (0, 0.2, 0.4, 0.6,	83

		0.8, 1.6, 3.2, 4.8, 5.6, 6.4, 8.4 equiv.) in DMSO	
57	Figure 2.23	¹ H NMR spectral changes of the probe 2 (21.8 mM) with addition of 0, 0.2, 0.4, 0.6, 0.8, and 1 equivalent of F ⁻ respectively from bottom to top	85
58	Figure 3A.1	Examples of nitro explosives	99
59	Figure 3A.2	BODIPY based sensors for PA detection	101
60	Figure 3A.3	HRMS of compound 4	102
61	Figure 3A.4	HRMS of compound 5	103
62	Figure 3A.5	¹ H NMR Spectrum of compound 2 and 4	104
63	Figure 3A.6	¹ H NMR Spectrum of compound 5	104
64	Figure 3A.7	¹¹ B NMR (left) and ¹⁹ F NMR Spectrum of compound 4 and 5	105
65	Figure 3A.8	Normalized absorption and emission spectra of probe 4 (43 μM)	106
66	Figure 3A.9	Normalized absorption and emission spectra of probe 5 (43 μM)	106
67	Figure 3A.10	Photographs of probes 4 (left) and 5 (right) under UV lamp	107
68	Figure 3A.11	Emission changes of probes 4 (left) and 5 (right) (43 μM) with the addition of different concentrations of PA (0, 1, 2, 3, 4, 5, 6, 7, 8, 9,10, 11, 12, 14, 16, 18, 20, and 26 equiv of PA) in THF when excited at 358 nm (4) and 327 nm (5) in THF	108
69	Figure 3A.12	Stern-Volmer plots of probe 4 (left) and 5 (right) (43 μM) with addition of different concentration of PA in THF	109
70	Figure 3A.13	Fluorescence lifetime decay of probes 4 (left) and 5 (right) after the addition of 0, 2, and 4 equiv of PA in THF, where the emission is at 496 and 457 nm respectively for probes 4 and 5	109
71	Figure 3A.14	Emission quenching efficiencies of probes (43 μM) after the addition of 8 equiv of different nitroaromatics and other analytes in THF	110

72	Figure 3A.15	Emission changes of probe 4 with TFA (left) and 5 with diff. time interval (right) in THF	111
73	Figure 3A.16	¹ H NMR titration of probe 4 upon the addition of 0, 1, 2, 3, 4, 5, 6, 7, and 8 equiv of PA in DMSO-d ₆	111
74	Figure 3A.17	Molecular structure of the probe 4 ·PA adduct	113
75	Figure 3A.18	Packing of probe 4 ·PA with hydrogen bonding	114
76	Figure 3A.19	Photographs of paper test strips of probe 4 under UV light with the addition of different concentrations of PA: (i) blank; (ii) 10 ⁻² M; (iii) 10 ⁻³ M; (iv) 10 ⁻⁴ M; (v) 10 ⁻⁵ M; (vi) 10 ⁻⁶ M	115
77	Figure 3A.20	¹⁹ F NMR spectra of probe 4 with 0, 1, 4 and 8 equivalents of picric acid in CDCl ₃	115
78	Figure 3A.21	¹¹ B NMR spectra of probe 4 with 0, 1, 4 and 8 equivalents of picric acid in CDCl ₃	116
79	Figure 3B.1	Schematic representation of the skeleton of (i) boron dipyrromethene, (ii) boron quinolate, and (iii) Schiff base boron compounds	127
80	Figure 3B.2	¹ H NMR spectrum of compound 3 .	130
81	Figure 3B.3	Molecular structure of compounds 1-3 . Hydrogen atoms are omitted for clarity.	130
82	Figure 3B.4	¹ H NMR spectrum of compound 7	132
83	Figure 3B.5	¹¹ B (left) and ¹⁹ F NMR (right) spectrum of compounds 5-7	133
84	Figure 3B.6	Molecular structure of compounds 5 . Hydrogen atoms are omitted for clarity	134
85	Figure 3B.7	Molecular structure of compounds 7 . Hydrogen atoms are omitted for clarity	134
86	Figure 3B.8	Normalized absorption (left) and fluorescence emission (right) spectra of 5-7 in THF (43 μM). Excited at the longer wavelength absorption maxima	137
87	Figure 3B.9	Absorption (left) and normalized fluorescence emission	137

		(right) spectra of 7 and 8 in THF. Excited at the longer wavelength absorption maxim	
88	Figure 3B.10	Photograph of compounds 5-7 in THF under hand held UV lamp of 365 nm.	138
89	Figure 3B.11	Computed orbitals for 1-3 .	138
90	Figure 3B.12	Cyclic voltammograms of 5-7 with 0.1 m Bu ₄ N(PF ₆) in DMF as the supporting electrolyte (scan rate 100 mV/s). Referenced relative to Fc/Fc ⁺ couple	142
91	Figure 4A.1	¹ H NMR spectrum of compound L1	156
92	Figure 4A.2	HRMS of compound L3	157
93	Figure 4A.3	¹ H NMR spectrum of compound B1	158
94	Figure 4A.4	¹³ C NMR spectrum of compound B1	159
95	Figure 4A.5	ESI-MS spectrum of compound B1	159
96	Figure 4A.6	Molecular structure of compounds B1 (top) and B3 (bottom). Hydrogen atoms are omitted for clarity	160
97	Figure 4A.7	TGA curves of B1-B4 at a heating rate of 10 °C/min	162
98	Figure 4A.8	DSC curves of B1-B4 at a heating rate of 10 °C/min	163
99	Figure 4A.9	Absorption spectra of boron compounds B1-B4 (22 μM) in CH ₂ Cl ₂	164
100	Figure 4A.10	Normalized emission spectra of boron compounds B1-B4 (22 μM) in CH ₂ Cl ₂ excited at longer wavelength absorption	164
101	Figure 4A.11	Photograph of compounds B1-B4 in CH ₂ Cl ₂ under hand held UV lamp of 365 nm	165
102	Figure 4A.12	Normalized emission spectra of compound B4 with increasing solvent polarity (22 μM) (left) and a comparison of emission spectra of boron compounds B1-B4 in solid state (right)	165
103	Figure 4B.1	¹ H NMR spectrum of compound 1a	181
104	Figure 4B.2	HRMS of compound 1f	181
105	Figure 4B.3	¹ H NMR spectrum of compound 2 (bottom) and 8 (top)	183
106	Figure 4B.4	¹ H NMR spectrum of compound 2 (bottom) and 8 (top)	184

107	Figure 4B.5	ESI-MS spectrum of compound 5	184
108	Figure 4B.6	Molecular structure of compounds 1, 2, 4, 7 and 8 . Hydrogen atoms are omitted. Thermal ellipsoids are drawn at 30% probability level	185
109	Figure 4B.7	TGA curves of 1-6 and 8 at a heating rate of 10 °C/min	189
110	Figure 4B.8	DSC curves of 1-6 and 8 at a heating rate of 10 °C/min	189
111	Figure 4B.9	Absorption spectra of boron compounds 1-8 (24 μM) in CH ₂ Cl ₂	190
112	Figure 4B.10	Normalized emission spectra of boron compounds 1-8 (24 μM) in CH ₂ Cl ₂ excited at longer wavelength absorption maxima	190
113	Figure 4B.11	Normalized emission spectra of compounds 1 (left) and 6 (right) with increasing solvent polarity (24 μM)	191
114	Figure 4B.12	Photograph of compounds 1-8 in THF under hand held UV lamp of 365 nm	191
115	Figure 4B.13	A comparison of normalized emission spectra of boron compounds 1-8 in solid state	194

List of Abbreviations

^1H NMR	Proton nuclear magnetic resonance
^{13}C NMR	Carbon-13 nuclear magnetic resonance
^{11}B NMR	Boron-11 nuclear magnetic resonance
^{19}F NMR	Fluorine-19 nuclear magnetic resonance
^{29}Si NMR	Silicon-29 nuclear magnetic resonance
NIR	Near-infrared region
UV-Vis	Ultraviolet–Visible
CV	Cyclic voltammetry
SCE	Saturated calomel electrode
ESI	Electrospray ionization
DFT	Density functional theory
TGA	Thermogravimetric analysis
DSC	Differential scanning calorimetry
HRMS	High-resolution mass spectrometry
GPC	Gel permeation chromatography
XRD	X-ray diffraction
ETL	Electron transport layer
HTL	Hole transport layer
OLEDs	Organic light emitting diodes
HOMO	Highest occupied molecular orbital
LUMO	Lowest unoccupied molecular orbital
eV	Electronvolt
EL	Electroluminescence
ACQ	Aggregation caused quenching
AIE	Aggregation induced emission
AIEE	Aggregation induced emission enhancement
ESIPT	Excited state intramolecular proton transfer
BODIPY	Boron dipyrromethene
ppm	Parts per million
CH_2Cl_2	Dichloromethane
CHCl_3	Chloroform

DCE	1,2-Dichloroethane
CH ₃ CN	Acetonitrile
EtOH	Ethanol
THF	Tetrahydrofuran
DMSO	Dimethyl sulfoxide
DMF	Dimethylformamide
CDCl ₃	Deuterated chloroform
NH ₄ OAc	Ammonium acetate
AcOH	Acetic acid
Na ₂ CO ₃	Sodium carbonate
K ₂ CO ₃	Potassium carbonate
Cs ₂ CO ₃	Cesium carbonate
NAF	Sodium fluoride
Na ₂ SO ₄	Sodium sulfate
CaH ₂	Calcium hydride
BBr ₃	Boron tribromide
Bu ₄ NPF ₆	Tetrabutylammonium hexafluorophosphate
AlMe ₃	Trimethylaluminium
<i>n</i> -BuLi	<i>n</i> -Butyllithium
(Bpin) ₂	bis(pinacolato)diboron
<i>i</i> -Pr ₂ NEt	N,N-Diisopropylethylamine
NaH	Sodium hydride
Pd(PPh ₃) ₄	Tetrakis(triphenylphosphine)palladium(0)
Pd(dppf)Cl ₂	[1,1'-Bis(diphenylphosphino)ferrocene]dichloropalladium(II)
PA	Picric acid
Mes	Mesityl
TBDPS	<i>t</i> -Butyldiphenylsilyl
TBDMS	<i>tert</i> -Butyldimethylsilyl
TIPS	Triisopropylsilyl
PET	Photoinduced electron transfer
FRET	Fluorescence resonance energy transfer
ICT	Intramolecular charge transfer

CHAPTER 1

INTRODUCTION

1.1 Fluorescent probes for fluoride ion sensing	
1.1.1 Importance of fluoride ion	15
1.1.2 Detection methods for fluoride ion	15
1.1.2.1 Sensors based on hydrogen bonding interactions	16
1.1.2.2 Sensors based on interaction between Lewis acidic boron and fluoride	18
1.1.2.3 O-Si bond cleavage reactions for fluoride ion detection	18
1.2 Fluorescent boron compounds	21
1.2.1 Tri-coordinate boron compounds	21
1.2.2 Tetra-coordinate boron compounds	22
1.2.2.1 <i>N,N</i>-chelate boron compounds	24
1.2.2.2 <i>N,O</i>-chelate boron compounds	28
1.2.2.3 <i>N,C</i>-Chelate boron compounds	40
1.3 References	52

1 Fluorescent probes for fluoride ion sensing

1.1.1 Importance of fluoride ion

In recent years, different methods to recognize and sense biologically and environmentally important anions have become an emerging field in the area of chemical sensors.¹⁻⁴ Among the different anions, fluoride ion attracted interest in the research community. Fluoride ion play important role in human health,⁵ often small amounts of fluoride ion added to tooth paste for the prevention of dental caries.⁶ This anion is also administered in the treatment of osteoporosis.^{7,8} However, high doses of fluoride ion can cause acute toxicity in humans and animals. There are many reports for dental and skeletal fluorosis because of the consumption of drinking water with high fluoride ion content across the world. According to the national health portal of India report 2014 over 11.7 million peoples in India from various states are at risk due to high dose of fluoride. Fluoride is easily absorbed by the body but dissipated slowly, because of this it is blamed for acute liver and kidney diseases.⁹ Therefore it is not surprising that the selective detection of fluoride ion is growing among research community.¹⁰

1.1.2 Detection methods for fluoride ion

Many sensors based on ^{19}F NMR¹¹ and (or) electrochemical methods¹² have been developed. Neither NMR nor electrochemical methods can be used for intracellular fluoride ion monitoring. In this circumstance colorimetric and fluorometric probes gained much attention due to their high sensitivities and the capabilities of fluoride ion monitoring in biological process.

Over the years a large number of optical sensor systems have been developed. Most of these methods employed hydrogen bonding interaction and interaction between fluoride and Lewis acidic boron. Apart from these methods reaction based fluorescent

chemodosimeters have also been developed. In this part of the thesis, recent studies on the development of fluorescent sensors and the chemistry leading to optical responses will be presented.

1.1.2.1 Sensors based on hydrogen bonding interactions

During the past decade many fluorescent probes utilizing hydrogen bonding interactions has been developed. Duke *et. al* developed naphthalimide thiourea (**1-4**)^{13,14} a fluorophore-spacer–receptor principle for fluoride ion detection. The emission intensities of **1** and **2** were quenched due to enhanced photoinduced electron transfer (PET) process from receptor to fluorophore upon addition of fluoride ion in DMSO. In case of sensors **3** and **4** the emission intensities at 528 and 533 nm got quenched upon addition of acetate, phosphate and fluoride *via* PET process. However an effective quenching was seen in the case of **3** by the addition of fluoride ion (*ca.* 90%) with no changes in absorption spectra. These results suggest that bi-directional single-electron transfer (SET) process is responsible for the selective sensing by these naphthalimide based probes. The probes **5**, **6**, **7**^{15,16} also operates *via* similar SET quenching mechanism for the selective detection of fluoride ion. Thiocalix[4]arene anchored with two naphthylthiourea groups, **8**¹⁷ acts as a fluorescent sensor. The addition of fluoride ion to **8** triggers the intramolecular π - π interactions between two naphthyl groups, which leads to the formation excimer emission enhancement. It showed 1:1 complex formation between the probe **8** and F⁻. Based on fluorescence resonance energy transfer (FRET) mechanism several probes have been developed for the selective detection of F⁻. Kim and co-workers reported calix[4]arene based sensor **9**¹⁸ having amide receptor.

1.1.2.2 Sensors based on interaction between Lewis acidic boron and fluoride

Triarylboranes readily reacts with small nucleophiles such as fluorides and cyanides

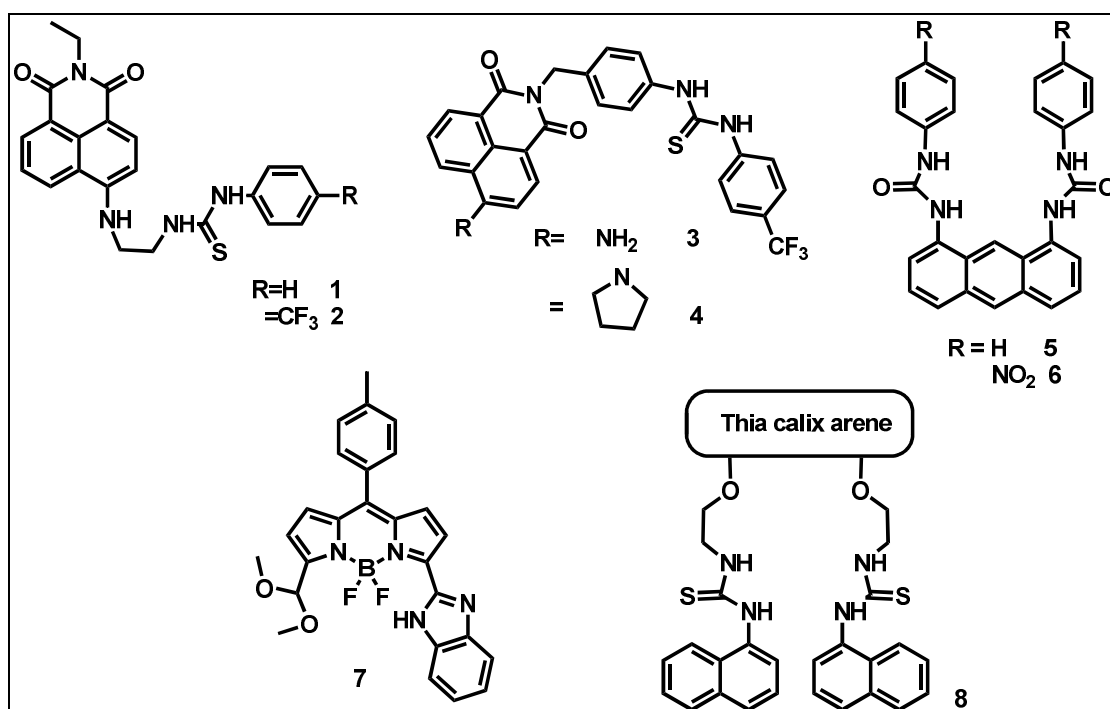


Figure 1.1: Sensors based on hydrogen bonding interactions (1-8).

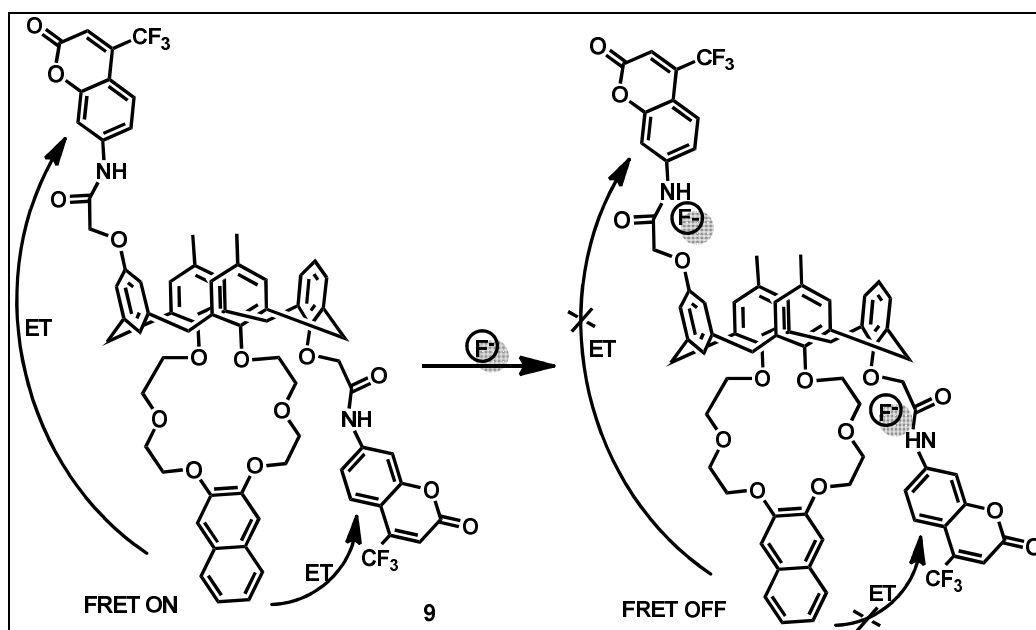


Figure 1.2: Sensor based on hydrogen bonding interactions (9).

to give fluoroborates. This reaction occurs *via* donation of electron pair of fluoride anion to the vacant *p* orbital of the boron centre.¹⁹ By keeping appropriate aryl

substitution and steric bulk around the boron centre, the selectivity of triarylboranes for fluoride ion got achieved. Yamaguchi and coworkers has reported the boron containing π -system, tri(9-anthryl)borane (**10**) as colorimetric sensor for the detection of fluoride ion. Addition of F^- ion to **10** triggers colour changes from orange to colourless and, in the absorption spectra, the characteristic band of **10** at 470 nm disappeared and new band around 360-400 nm appeared.²⁰ From the same group dibenzoborole with (*N,N*-diphenylamino)phenyl group at 3,7-position (**11**) has been investigated as fluorescent probe for fluoride ion. Upon complexation of **11** with F^- , the emission maxima got blue-shifted about 100 nm with 20 fold increment in quantum yield was observed *via* on/off control of the $p\pi-\pi^*$ conjugation of LUMO level.²¹ Wang and coworkers invented two fluorescent probes **12**, **13** based on charge transfer mechanism.²² Sensor **13**, where the donor N(Ph)(1-naphthyl) and the acceptor B(mesityl)₂ groups in a nonplanar arrangement, showed turn on response selectively for fluoride ion. More recently Thilagar group introduced two dissimilar acceptors (triarylborane and BODIPY) on a single donor (**14**) that operates *via* similar intramolecular charge transfer (ICT) mechanism for the selective fluoride ion detection.²³

1.1.2.3 O-Si bond cleavage reactions for fluoride ion detection

In recent year's reaction based chemodosimeters are gaining attention because of their high selectivity. Silyl protection is a well known organic chemistry reaction used for the protection of alcohols and has become key factor for the development of chemodosimeters for the selective fluoride ion detection. In 2003, Swager developed a semiconducting polymer **15** for F^- ion detection. Fluoride ion induced lactonization triggers highly fluorescent coumarin derivatives in the side chain (**16**) which produces small band gap trapping site. The recombination of excitons in the backbone results new emission signal. This method directly interconnects the fluoride ion with polymer

developed a tris (N-salicylideneamine) based fluorophore **17** which showed emission enhancement at 460 nm²⁵ after addition of fluoride ion. The chemodosimeter **18** developed by Kim *et al.*, triggers Si-O bond cleavage results in phenolate anion after the addition of fluoride ion, which further undergoes cleavage to form *p*-quinomethane and resorufin. Here, resorufin acts as a fluorophore for the emission changes.²⁶ Two years later the same group reported coumarin based probe **19** for the detection of fluoride in HEPES buffer where TBDPS used as a silyl group. Probe **19** was also studied for fluorescence cell bioimaging for the detection of NaF in A549 human lung carcinoma cells under physiological conditions.²⁷ In 2010 Hu *et al.* developed probe **20** with dual wavelength emissive ability. Addition of fluoride ion triggers Si-O bond cleavage to form an ESIPT activated benzothiazole moiety which leads emission colour changes from blue-violet to bright yellow ratiometrically.²⁸ Si-O bond cleavage strategy was also studied on BODIPY system (**21**, **22**), and were fabricated for the fluoride ion detection by Akkaya group. Addition of fluoride ion to **21** generates phenolic group on the meso position of BODIPY which leads emission quenching *via* PET quenching mechanism. Whereas in probe **22**, the addition of fluoride ion, which triggers a strong ICT process in leads emission quenching at 560 nm.²⁹ In 2011, ICT based probe **23** was developed, which showed colorimetric and ratiometric emission response for fluoride ion.³⁰ A near infrared fluorescent probe **24** was developed by Cao *et al.* in 2012. Addition of 400 equiv. of fluoride to **24**, results 1000 fold emission enhancement at 718 nm in DMSO/water system.³¹ A sugar modified sensor **25** was developed for fluoride ion detection in 100% water medium. This probe showed turn on emission response with detection limit as low as 1.5 mg/L with significant naked eye colour changes.³² Recently silica supported hybrid material was studied for fluoride ion detection. Addition of fluoride ion detaches the

fluorophore from non emissive solid support and makes free fluorophore in solution which gives its original emission *via* turn on response.³³

1.2 Fluorescent boron compounds

The continuous development of highly conjugated luminescent organic molecules have drawn great attention from chemists, physicists, and biochemists, due to their wide spread applications in organic light emitting diodes (OLED's), organic solid state lasers, sensors, bioimaging, solar energy concentrators and nano emitters. Recently, it has been demonstrated that incorporation of boron into π -conjugated system offers considerable promise for the development of new functional materials with outstanding photophysical and electronic properties. In general, fluorescent boron compounds are divided into two types namely i) tri-coordinate boron compounds and ii) tetra-coordinate boron compounds.

1.2.1 Tri-coordinate boron compounds

The boron atom in the tri-coordinate boron compounds possesses sp^2 hybridization with vacant p_z orbital. The presence of empty p -orbital on boron makes tri-coordinate boron compounds excellent π - acceptors, which can lead significant delocalization with adjacent π -conjugated system. Because of the vacant coordination site on boron, these compounds are unstable, often attacked by nucleophiles such as water. This leads either bond cleavage or formation of tetra coordinate boron species which are not effective in conjugation with adjacent π -system. A common strategy for the stabilization of three coordinate boron compounds is applied by providing steric bulk around the boron center; generally mesityl (2,4,6-trimethylphenyl), fluoromesityl (2,4,6-tris(trifluoromethyl)phenyl), triptyl (2,4,6-triisopropylphenyl) groups are often used to provide steric bulk around boron. These bulky groups are not only preventing

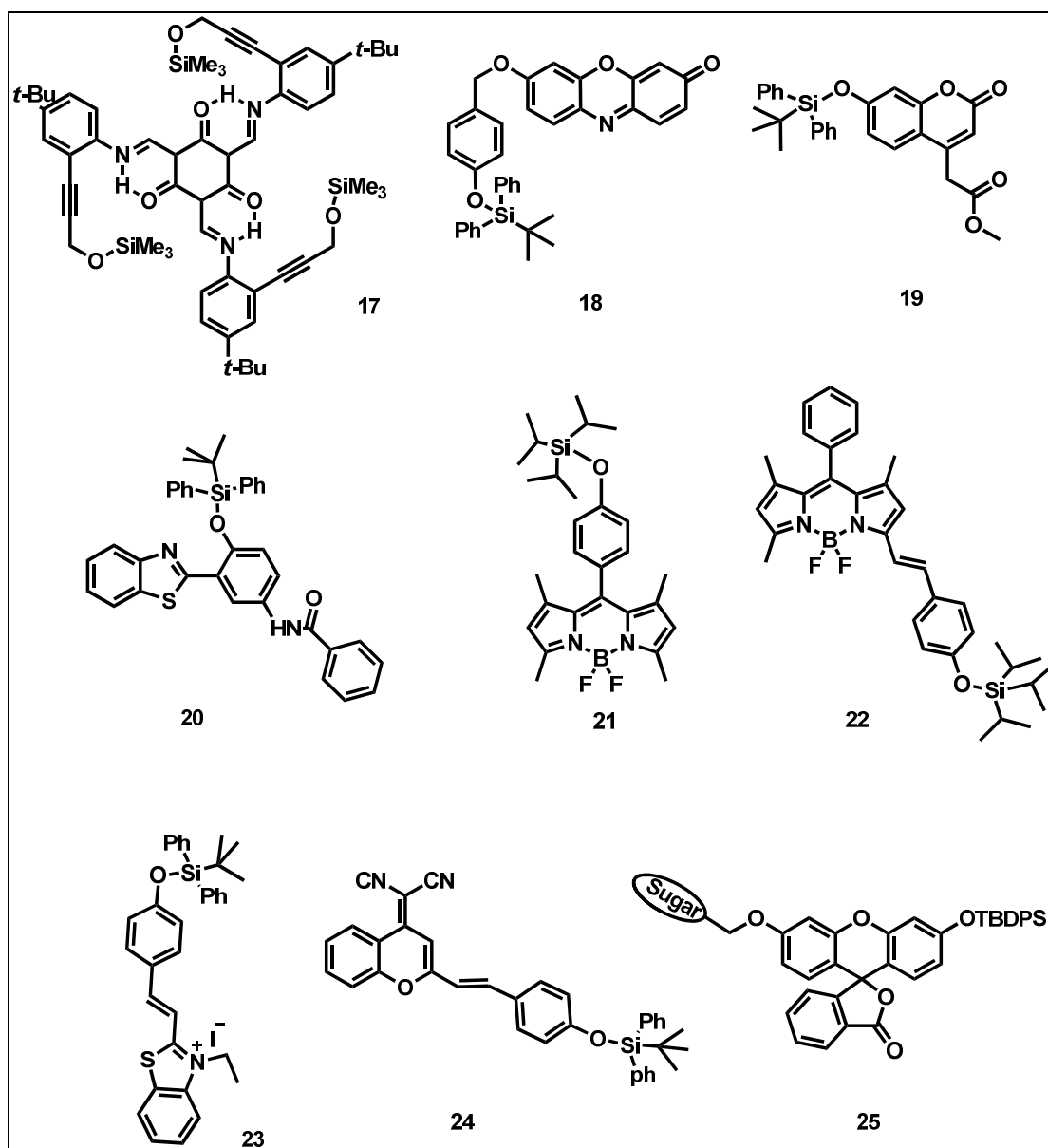


Figure 1.5: Sensors based on O-Si bond cleavage reaction (17-25).

nucleophilic attack on boron but also restrict intermolecular stacking which results in intense solid state emission. Small nucleophiles such as fluoride and cyanide can easily bind to the Lewis acidic boron which makes tri-aryl boron compounds as promising materials for fluoride and cyanide ion sensors. Apart from sensing, triaryl

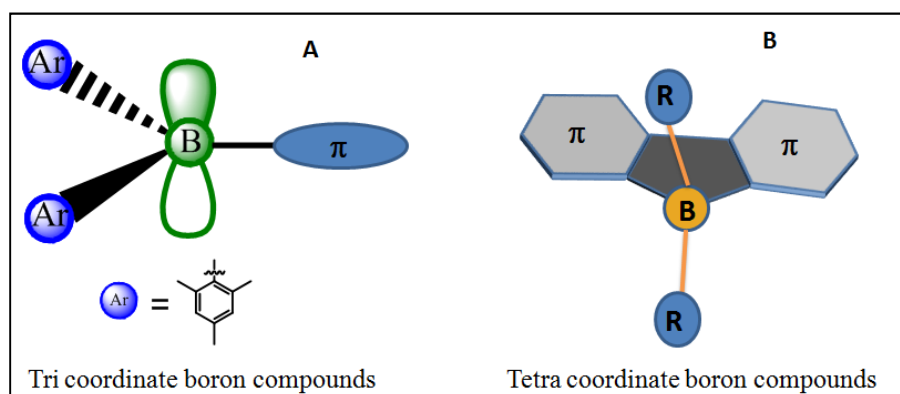


Figure 1.6: Schematic representation of (left) tri-coordinate boron; (right) tetra-coordinate boron compounds.

boranes have been used as emissive as well as charge transport materials in OLED's, non linear optics materials and fluorescent indicators in bioimaging.³⁴

1.2.2 Tetra-coordinate boron compounds

The first organic light emitting diode (OLED) was reported by Tang in 1987 with a double layered structure where organic diamine compound as a (hole transporting layer) HTL and tris(8-hydroxyquinolato)aluminium (Alq_3) as an (electron transporting layer) ETL and as an emitter.³⁵ Although its performance was good but it has drawbacks such as poor long term stability, and tendency to undergo irreversible degradation. In the search of efficient emitters, researchers have been driven into the development of tetra-coordinate boron based materials for their potential use in optoelectronics including OLEDs,³⁶ organic field effect transistors, photoresponsive materials, sensory and biological imaging materials.^{37,38} The main advantage of boron compounds is the formation of stronger covalent B-O, B-N and B-C bonds compared to aluminium Al-O, Al-N and Al-C bonds. The boron saturation in tetra-coordinate boranes, confers increased chemical stability, rigidity, often accompanied by higher

luminescence intensities. In most of these compounds, the ligand is generally mono anionic (*O* or *N* donors) in order to get charge neutral boron compounds. The key role of Lewis acidic boron atom is to stabilize the anionic chelating ligand by forming strong covalent bonds with dissipating the negative charge on the ligand and also planarizes the ligand thus enhancing the π -system conjugation. In tetra-coordinate boron compounds, lowest unoccupied molecular orbital (LUMO) is generally located on π -conjugated ligand while highest occupied molecular orbital (HOMO) is localized on either ligand or the R group (figure 1.6). π - π^* transitions of the ligand or the charge transfer transitions from R group to the chelate are usually responsible for the luminescent properties of this class of compounds.³⁹ Based on chelating donor atoms, tetra-coordinate boron compounds are mainly classified into four different types, namely (i) *N,O*- chelate boron compounds, (ii) *N,N*- chelate boron compounds, (iii) *N,C*- chelate boron compounds, and (iv) other chelate boron compounds like *C,C*-, *C,O*-, *O,O*-.

1.2.2.1 *N,N*- chelate boron compounds

In this type of compounds, boron is chelated with an *N,N*- ligand, in which one of the nitrogen donate its lone pair of electrons in an intramolecular fashion. The 4,4-difluoro-4-bora-3a,4a-diaza-s-indacen (or) boron dipyrromethene (BODIPY) dyes are well known *N,N*- chelate five membered boron compounds. These BODIPYs have excellent spectroscopic properties such as narrow absorption and emission bands, high molar extinction coefficients, high fluorescence quantum yields, strong chemical and photochemical stability in solution and solid state.⁴⁰ Owing to these excellent characteristics, BODIPY dyes have been studied to a greater extent in artificial light harvesters, laser dyes, fluorescent sensors, sensitizers for solar cells, molecular photonic wires and as well as in photodynamic therapy.⁴¹ However BODIPY dyes are

weak emissive in the solid state, which limits their optoelectronic applications. Wang group reported a series of *N,N*-chelate boron compounds (**26-31**) based on pyridylindole, substituted pyridylindole, pyridyl-7-azaindole, pyridylbenzimidazole, thiazolylindole, 8-quinolylindole, and 8-quinolyl-7-azaindole ligands, where boron atom is having two phenyl groups. All these compounds were studied for their photophysical properties and also used as emissive layer in OLEDs.⁴²⁻⁴⁴ Gardinier and co-workers reported a series of diphenylboron complexes based on (2-pyrazolyl)-4-R-anilines or BORAZANS (boron azoanilines) (**32-38**).⁴⁵ The BORAZANS with electron-withdrawing substituents showed high chemical stability and blue fluorescent emission, while the electron-donating groups showed green emission which were susceptible towards hydrolysis. Piers group synthesized difluoroboron compounds based on anilido-pyridine moiety (**39-41**), that exhibited, high photostability, large Stokes shifts with good quantum yields both in solution and solid state.⁴⁶ In a series of papers, Gomes and co-workers reported several

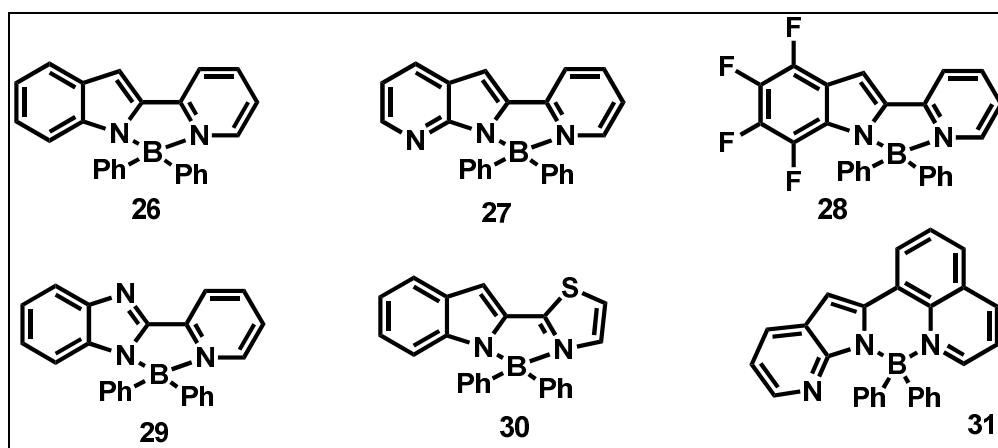


Figure 1.7: *N,N*-chelate tetra-coordinate boron complexes (**26-31**).

mono- and di-nuclear organoboron compounds based on 2-(*N*-aryl)formiminopyrrolyl ligands.⁴⁷⁻⁴⁹ All these compounds were fabricated *via* solution processed method in OLEDs as emissive layer.⁵⁰ Jingsong You and co-workers

reported an unsymmetric boron dyes *via* palladium catalyzed regioselective N-heteroarylation of amidines with various 2-halo-N-heteroarenes, followed by boron complexation with $\text{BF}_3 \cdot \text{Et}_2\text{O}$. The emission colour of these dyes were finely tuned from blue (**42**: 451 nm) to deep red (**51**: 649 nm). These compounds exhibited tunable mechanofluorochromism.⁵¹

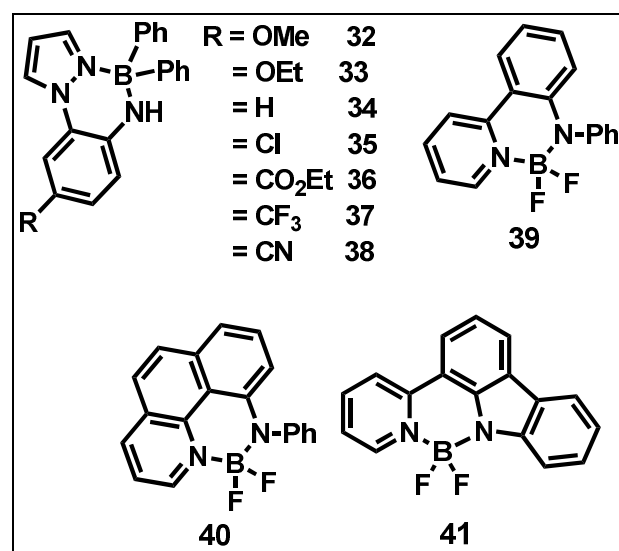


Figure 1.8: *N,N*-chelate tetra-coordinate boron complexes (**32-41**).

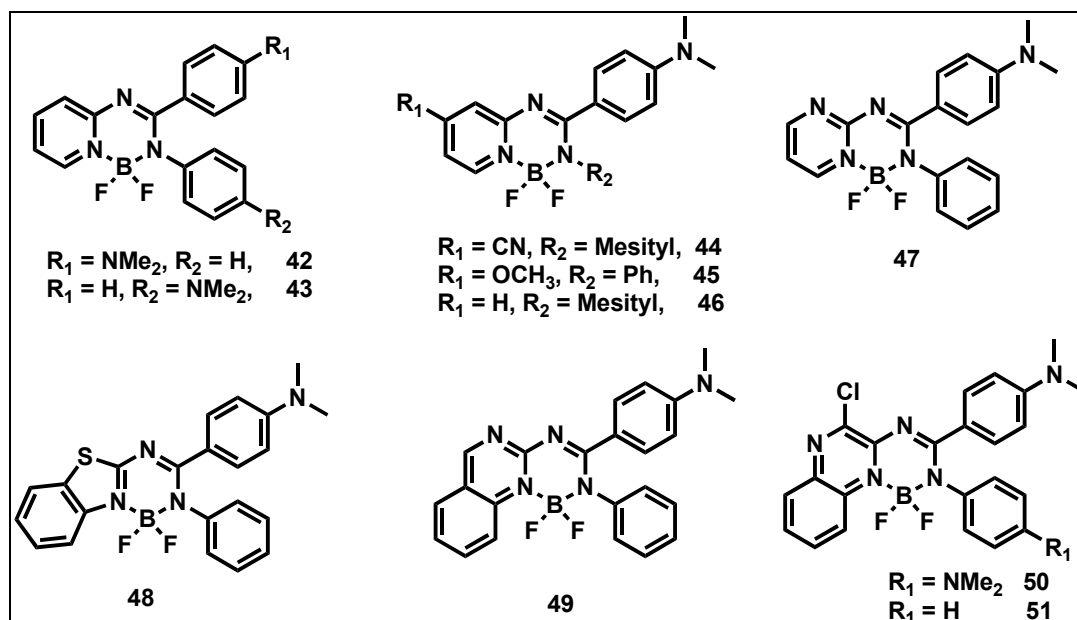


Figure 1.9: *N,N*-chelate tetra-coordinate boron complexes (**42-51**).

Gilroy and Otten groups have synthesized several boron complexes based on formazanate ligands (52-58) and studied for their spectroscopic and electrochemical properties⁵². Later they synthesized complexes 62-64 and studied the effect of extended conjugation on formazanate boron compounds⁵³. The potential application of formazanate complexes as efficient electrochemiluminophores⁵⁴ as AIEE fluorophores⁵⁵, and as bioimaging fluorophores⁵⁶ were also studied⁵⁷.

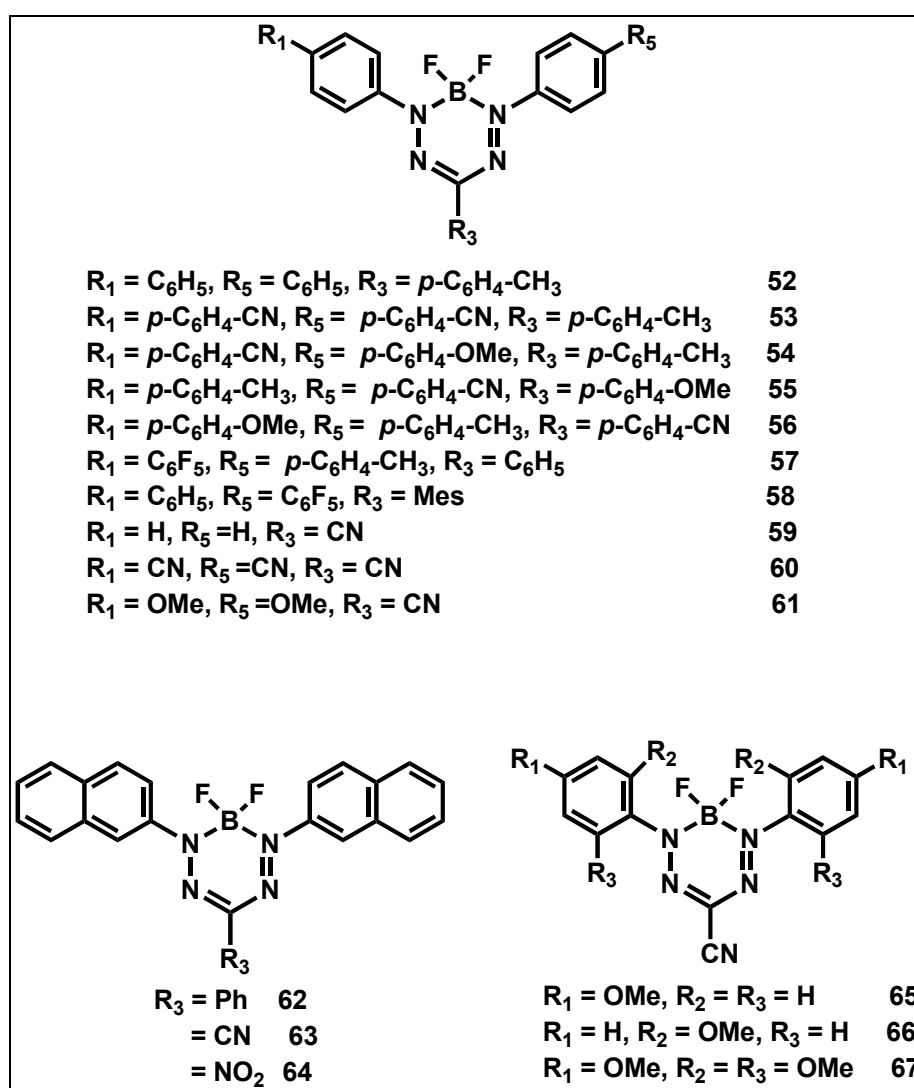


Figure 1.10: *N,N*-chelate tetra-coordinate boron complexes (52-67).

Liu and co-workers developed a series of emission colour tunable fluorophores based on pyridyl enamido boron compounds (68-71). These compounds showed large

Stokes shift emission as well as aggregation induced emission (AIE) property.⁵⁸

Recently, Feng and co-workers reported fluorophores **72-75** based on 5,11,17-triazatrinaphthylene derivative and ligands, where multiple boron atoms were grafted.⁵⁹

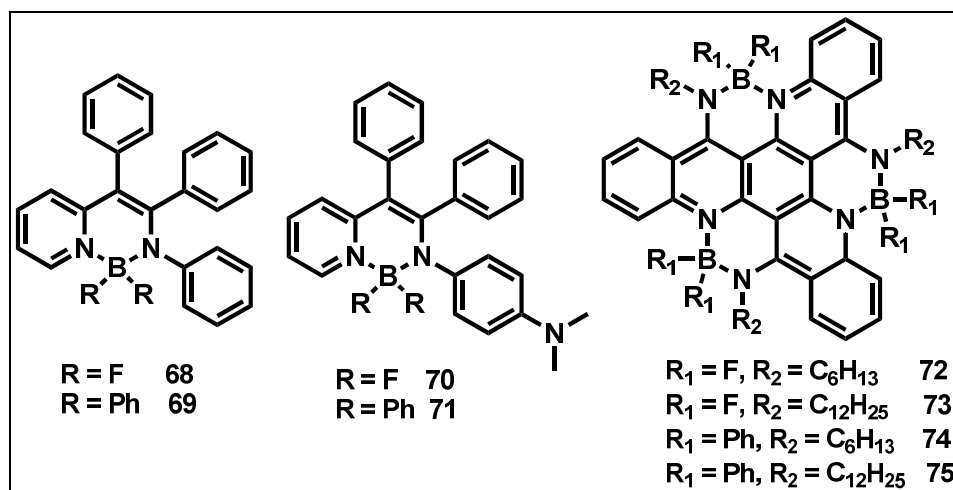
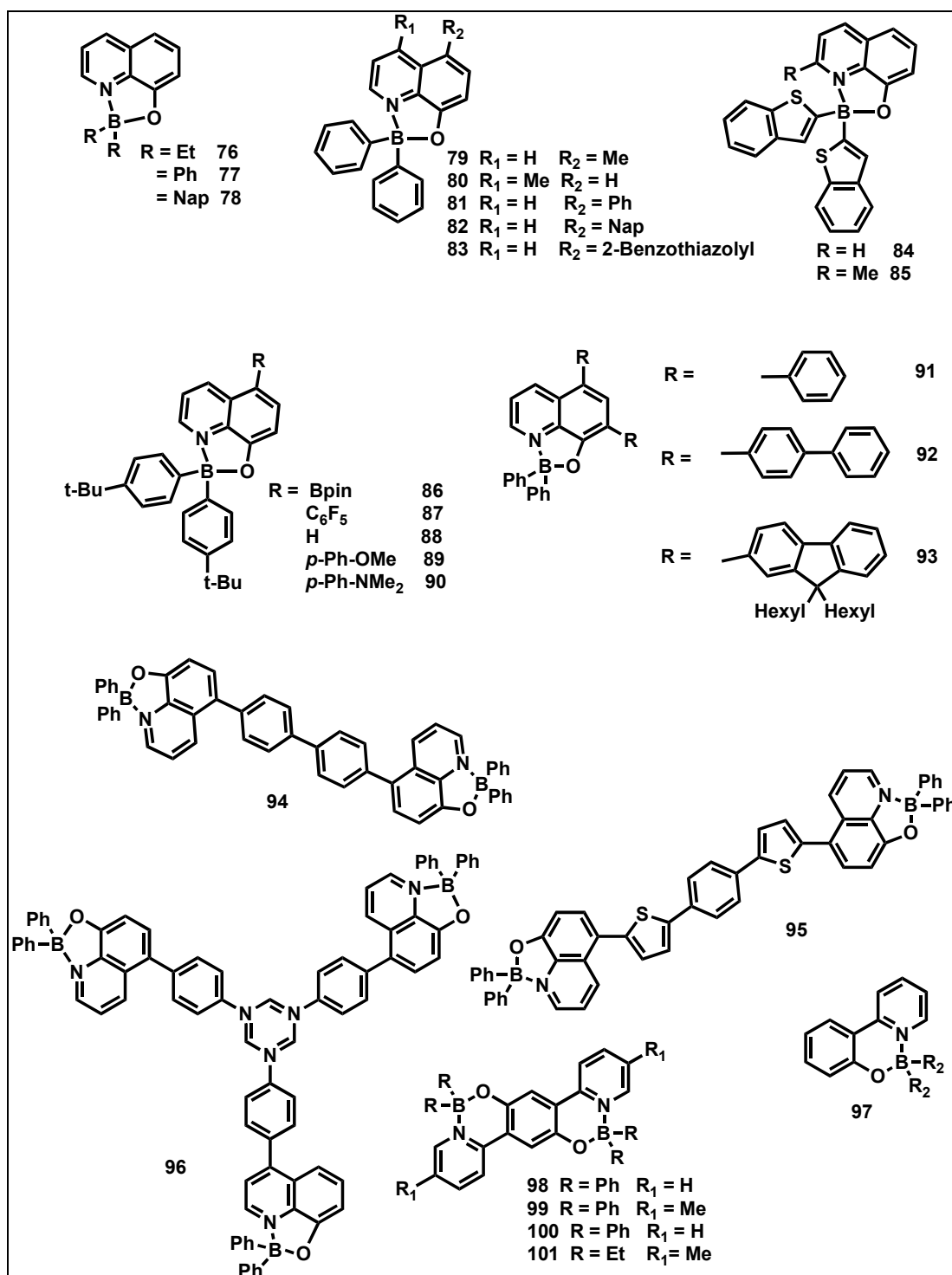


Figure 1.11: *N,N*-chelate tetra-coordinate boron complexes (**68-75**).

1.2.2.2 *N,O*-chelate boron compounds

In 1999, Wang and co-workers studied a series of 8-hydroxyquinolate (q) boron compounds (**76-83**) with general formula (BR₂q) where R = Ethyl, phenyl, naphthyl. These compounds displayed a greenish blue emission (495-500 nm) which are mainly originated from π (Ph-O) $-\pi^*$ (py) transitions.⁶⁰ OLEDs were fabricated using these boron compounds as an emitter/ETL. In 2000 Anderson group studied the effect of methyl group at various positions of BPh₂(Me-q) (**79-80**). The methyl group at the 4-position (**80**) induced a large blue shift of emission (483 nm) while at the 5-position exhibited red shift emission (529 nm).⁶¹ Later, Wang group substituted phenyl, naphthyl and benzothiazole groups at the 5-position of BPh₂q (**81-83**), which were shown red shifted emission with λ_{em} 530, 534, 565 nm respectively. At the time they

Figure 1.12: *N,O*-chelate tetra-coordinate boron complexes (76-101).

also introduced 2-benzothienyl moieties on the boron (**84**, **85**) which showed low lying LUMO levels (~ -3.0 eV). Compounds **84** and **85** were investigated in OLEDs as both emitter and ETL and shown high turn on voltage at 10 V with a maximum brightness of 1050 cd m^{-2} .^{62,63} Compounds **91-93**, were synthesized in 2006 by Slugovc and co-workers. These compounds were shown significant red shift in emission with good quantum yields (22-30 %). Electroluminescent devices were fabricated using compounds **91-93**, showed much lower turn on voltages with higher brightness. Notably, in these complexes no exciplex emission was seen may be because of rise of HOMO level compared to 5-position substituted boron compounds.⁶⁴ Wang and co-workers reported 8-hydroxyquinolate ligand based linear and star shaped multi nuclear boron compounds (**94-96**). The mutual effect of boron centers on π -conjugation, molecular packing and intermolecular interactions were studied.⁶⁵ Yue Wang and coworkers reported a ladder type π -conjugated dinuclear boron compounds (**98-101**). These compounds showed emission maxima ranging from 584-604 nm both in solution and solid state, which were about 100 nm red shifted compared to its mono boron compound **97**. EL devices based on compounds **98** and **99**, showed the maximum brightness exceeding 8000 cd/m^2 with no exciplex emission.⁶⁶

Schiff base boron compounds are another important class of compounds, the first report came from Jiang group in 2006 using *N,N*-*o*-phenylenebis (salicylideneimine) and *N,N*-*p*-phenylenebis (salicylideneimine) as ligands (**102**, **103**). Using compounds **102** and **103** as emitting materials EL devices were fabricated by vacuum deposition and showed blue green emission at 500 nm.⁶⁷ Ziessel, Ulrich, and co-workers reported a series of boron complexes **104-112**, by complexation of anils (aniline-imines) with boron (III) precursors like $\text{BF}_3 \cdot \text{Et}_2\text{O}$ or BPh_3 . They observed an interesting

phenomena “energy transfer through bond” in case of **112** and **111** where the boranil dye was linearly attached to bodipy and subphthalocyanine dyes respectively.⁶⁸ Later they successfully functionalized the boranil dye by taking boranil bearing nitro group which has been reduced to its anilino form and then successfully converted to amide, imine, urea, and thiourea derivatives. The isothiocyanate derivative **113** was utilized as an interesting candidate for bioconjugation to proteins; isolated labeled-BSA protein **113** showed strong emission ($\Phi_f = 47\%$) in biological media.⁶⁹ Recently two more boranil dyes **114** and **115** were reported by Muthusubramanian group, which were studied for the selective detection of hydrogen peroxide in living cells.⁷⁰

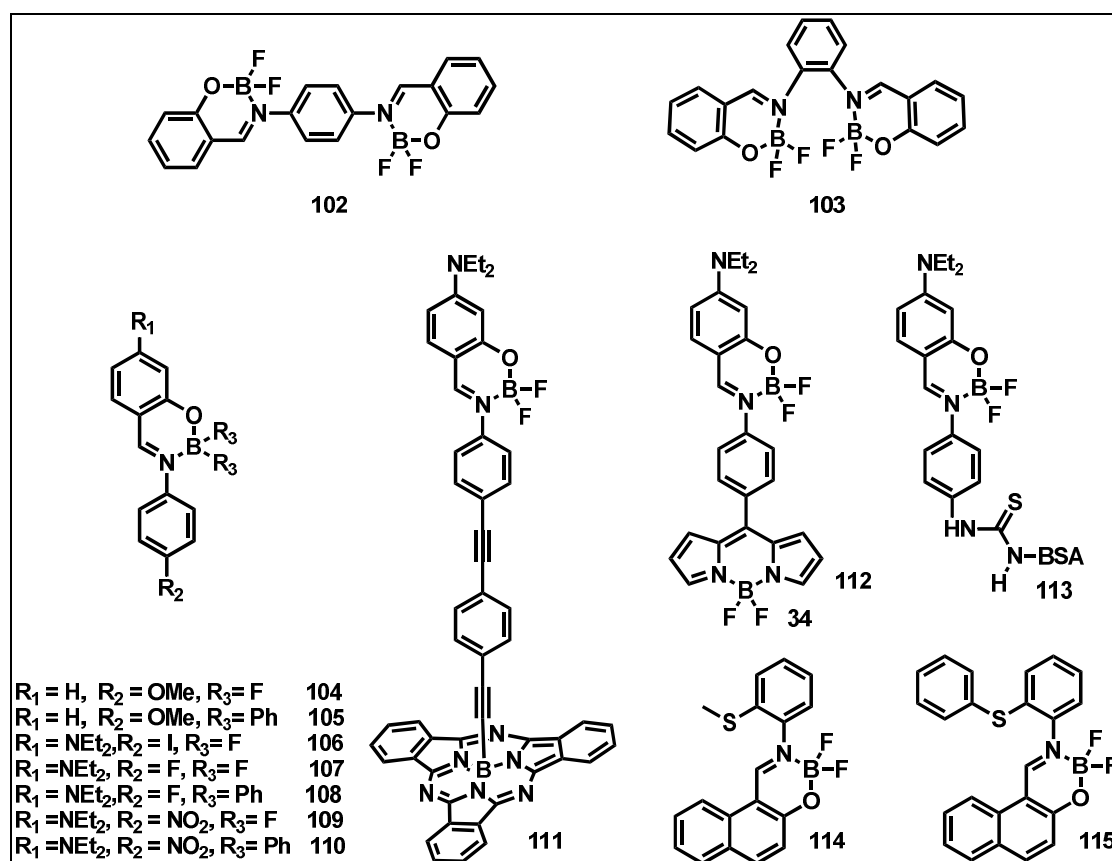


Figure 1.13: *N,O*-chelate tetra-coordinate boron complexes (**102-115**).

β -Iminoenolate based boron compounds are another important class of compounds. Kubota and co-workers reported pyrazine based β -ketoiminate boron compounds **116-121**. All these boron compounds exhibited emission in both solution ($\lambda_{\text{em}} 472\text{-}604 \text{ nm}$)

as well as in solid state (λ_{em} 496-624 nm) with large Stokes shifts.⁷¹ Later they reported thiazole- boron compounds **122-125** and studied their photophysical properties. The BF_2 complex **122** is non fluorescent in hexane, however in the solid state it is highly fluorescent because of restriction of C-Ph intramolecular rotation in the solid state. The BPh_2 complex **123** exhibited higher emission efficiencies over **122**, both in solution and solid state.⁷² They also reported pyrimidine-based mono (**126-135**) and di nuclear (**136-141**) β -iminoenolate boron compounds⁷³⁻⁷⁵ and studied their emission properties in solution and solid state. The diboron compounds **137-141** with D- π -A systems, showed red shifted emission (λ_{em} 583-639 nm) with Φ_f values ranges from 0.57-0.06 in solution and their solid state emission fallen in the NIR region. Ran Lu group synthesized β -iminoenolate boron compounds with different substituents such as triphenylamine (**142**), carbazole (**143**), tertbutyl carbazole (**144**) phenothiazine (**145, 146**), and phenothiazine S,S-dioxide (**147, 148**), and studied their mechanofluorochromism.^{76,77} In grounded form all these compounds exhibited red shifted emission compared to their crystalline or as synthesized state. Sun and co-workers reported quinoxaline- β -ketoiminate boron difluoride complexes **149-153**. These compounds were studied as fluorescent molecular switches by acid/base fuming process.⁷⁸ Structurally similar boron compounds **154-158** developed by Ran Lu group, showed AIEE phenomenon and also they explored their utility as low molecular weight nontraditional π -gelators.⁷⁹ Wang group reported new propeller shaped pyridine, benzothiazole (**159-160**) based ketoiminate boron compounds.⁸⁰ All these complexes exhibited large Stokes shift both in solution as well as in solid state and also showed AIEE phenomenon. Compounds **161-164** studied as solid-state luminescent sensors for acidic vapours.⁸¹ Later, the same group reported similar type

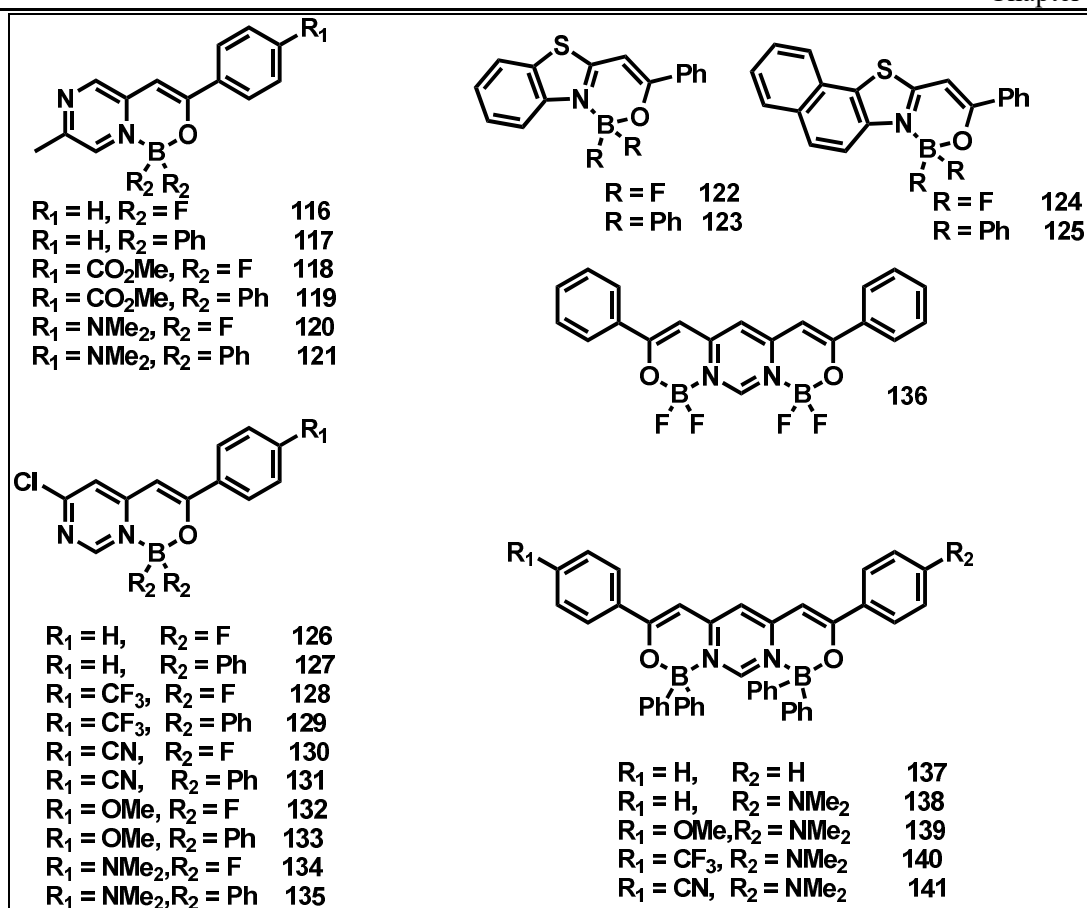


Figure 1.14: *N,O*-chelate tetra-coordinate boron complexes (116-141).

of boron compounds with pyrimidine moiety (165-168) and studied their AIEE and mechanochromic luminescence properties.⁸² Zhao and co-workers reported D- π -A type triphenylamine-functionalized thiazole based β -ketoiminate boron complexes 169-172. All these compounds exhibited strong intramolecular charge transition emission and strong cyano-dependent aggregation induced emission and mechanofluorochromic properties.^{83,84} Li and co-workers reported D- π -A type thiazole based β -ketoiminate boron complexes (173, 174) connected with tetraphenylethene, which exhibits twisted intramolecular transition emission, strong AIE phenomenon and significant mechanofluorochromic properties.⁸⁵ Miałowski and co-workers synthesized 2-benzoylmethylenequinoline (175-183), 1-benzoylmethyleneisoquinoline (184-192) based boron complexes and studied the

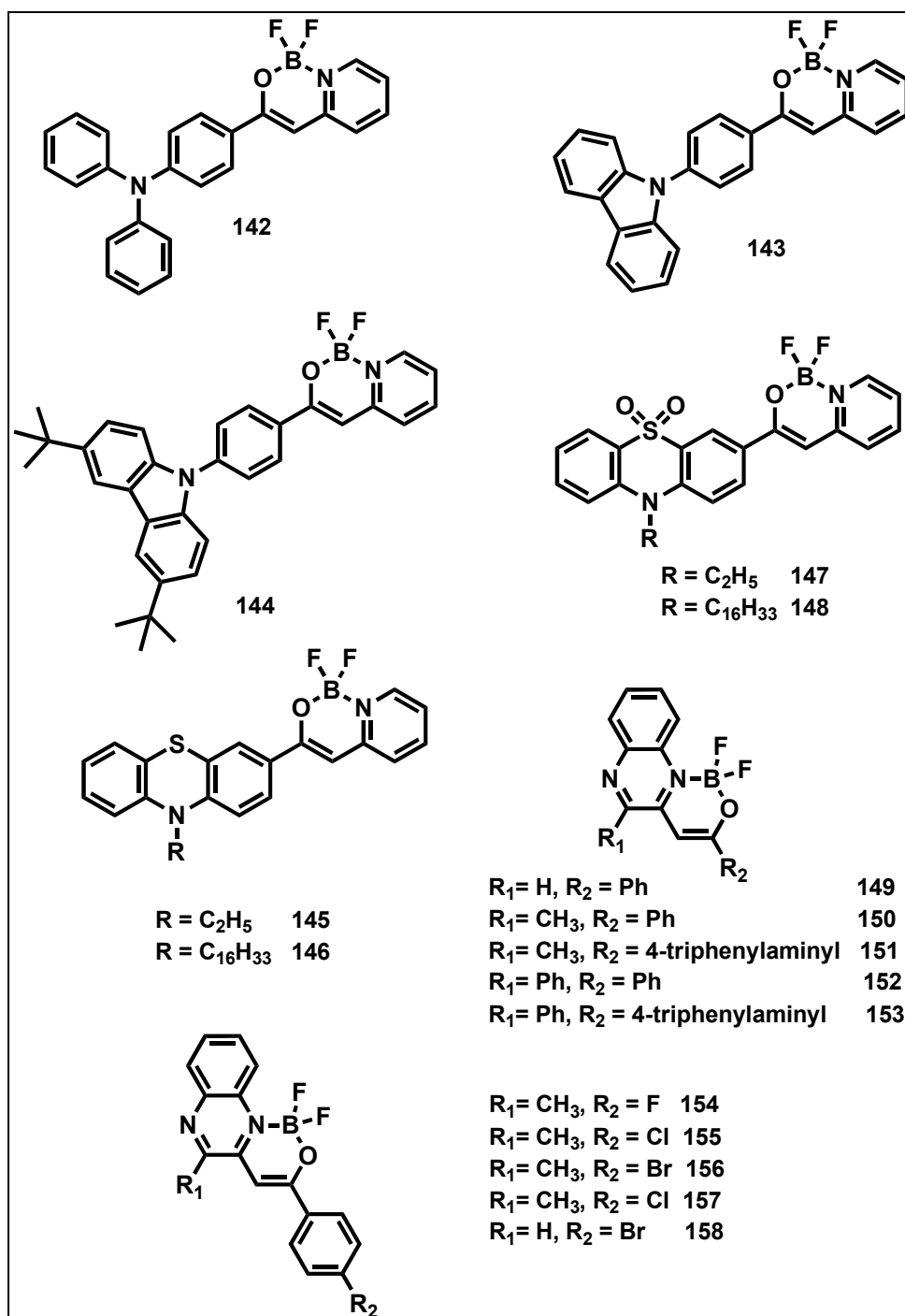


Figure 1.15: *N,O*-chelate tetra-coordinate boron complexes (142-158).

substitution effect to tune the photophysical properties.⁸⁶ Yoshiki Chujo and coworkers reported a new class of AIEE boron ketoiminates (193-195) which showed higher emission quantum yields ($\Phi_f \leq 0.3-0.76$) in the solid state compared to the

solution state ($\Phi_f \leq 0.01$). They were able to control the optical properties of these compounds by using sterically hindered substituent on the nitrogen atom.⁸⁷ Liu and coworkers reported a new class of D- π -A type triphenylamine boron compound **196** which showed high solvent dependent emission.⁸⁸ A significant AIEE character was seen for this compound in the aggregated form (70 % of THF/Water) with a factor of 100 compared to its emission in THF. Yam and co-workers reported a series of dithienylethene-containing boron (III) ketoiminates (**197-204**) for photochromic applications. They observed that the photochromic behavior of these compounds were dependent on the imine R-group (R1) of the boron (III) ketoiminate core. The photocyclization has not been observed in case of **197** and **201** because of considerable non radiative relaxation process, in contrast restriction of such rotation by bulky N-mesityl substituent, photocyclization effect got recovered without direct changes on core dithienylethene moiety.⁸⁹ Kwak and Kim synthesized 2-(2'-hydroxyphenyl)benzoxazole (**205**) and 2-(2'-hydroxyphenyl)benzothiazole (**206**) based difluoroboron complexes and explored them as a candidate for blue luminescent materials. These dyes exhibited high fluorescence quantum yields and good photostability.⁹⁰ Zhang and co-workers reported two boron compounds (**212-213**) with rigid frame work by introducing phenyl groups on boron which resulted good thermal stability and high solid state emissions. Compound **212** exhibited red emission at 632 nm ($\Phi_f = 30$) while compound **213** showed deep red emission at 670 nm ($\Phi_f = 41$). Electroluminescent devices were fabricated employing compound **212** or **213** as non doped emitters for bright red and near infrared emission.⁹¹ In 2012 the same group reported benzoxazole (**207**) and benzthiazole (**208-211**) boron complexes by introducing various amine substituents. The emission colour of these compounds

covered a broad range from deep blue to saturated red in both solution and solid state with high quantum yields.

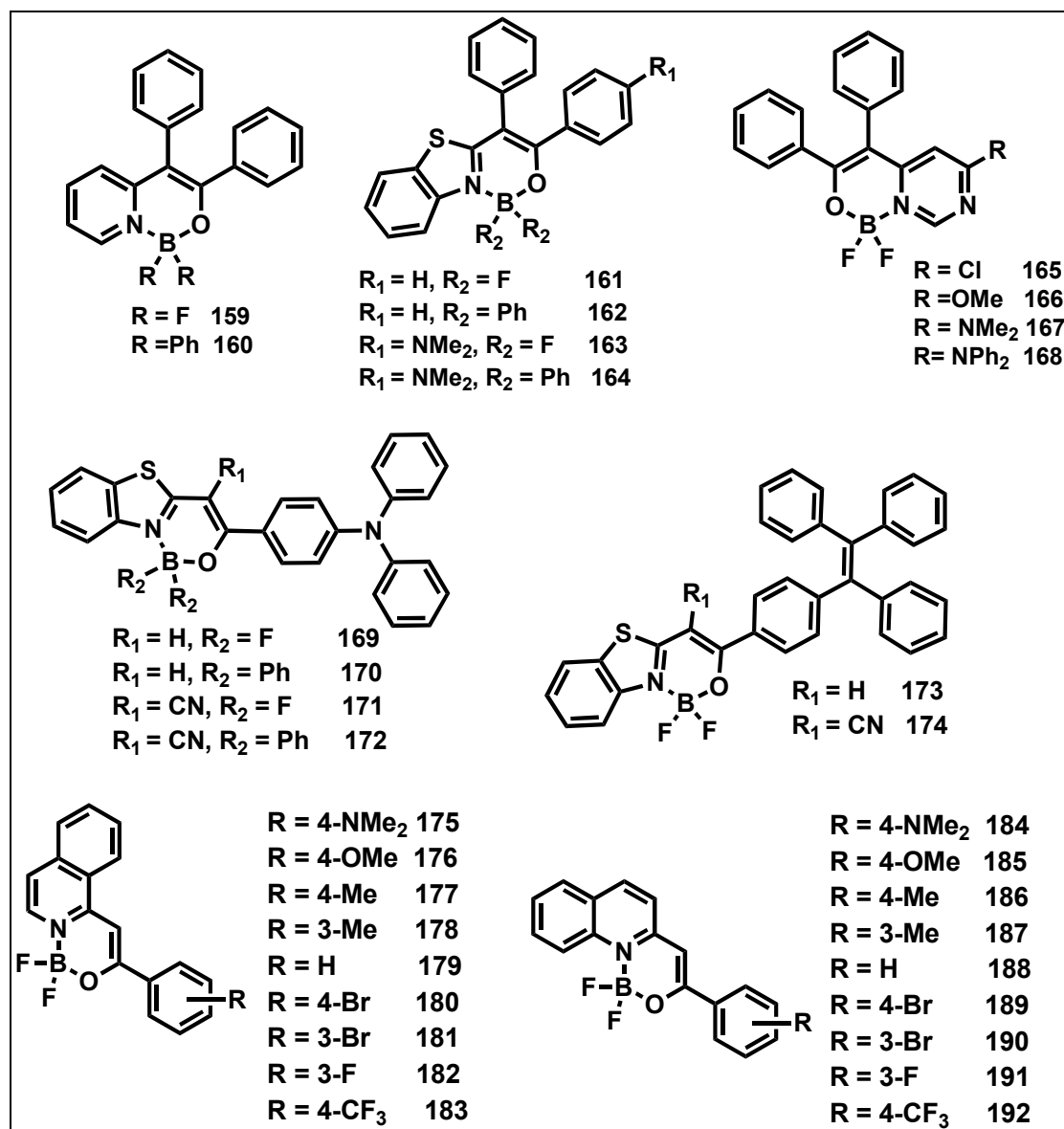


Figure 1.16: *N,O*-chelate tetra-coordinate boron complexes (159-192).

The OLED devices using these boron compounds retained their full colour tunable emission.⁸³ Device based on **206** exhibited greenish blue emission with the highest efficiency of 7.8 cd A^{-1} while **207** showed yellow emission with the highest brightness of 31220 cd m^{-2} . Later they designed diboron bridged ladder type compounds **214-217**

and studied their thermal, photophysical, electrochemical properties. These compounds revealed good thermal stability, high fluorescence quantum yields and

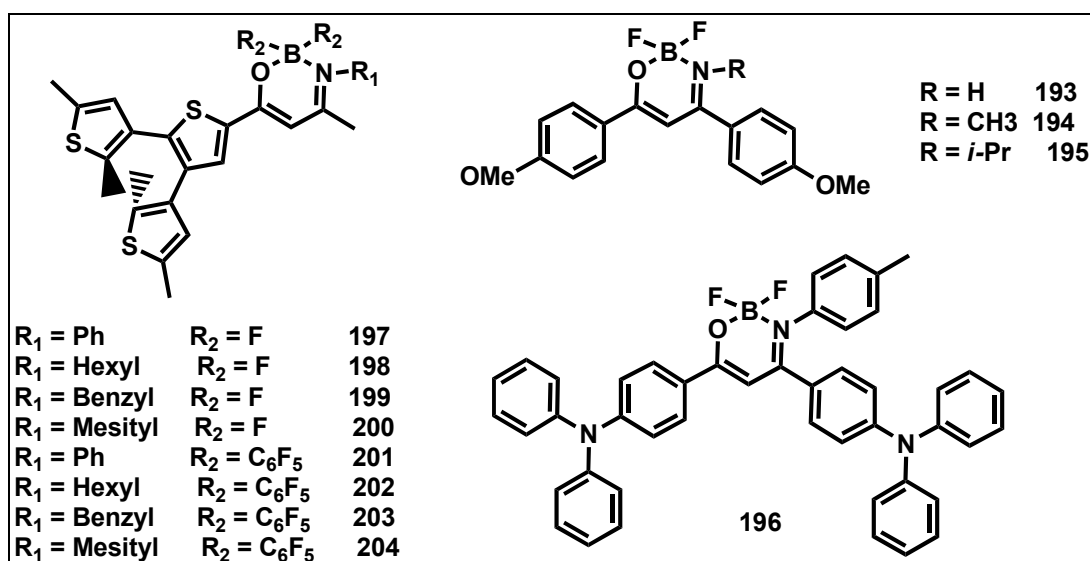


Figure 1.17: *N,O*-chelate tetra-coordinate boron complexes (193-204).

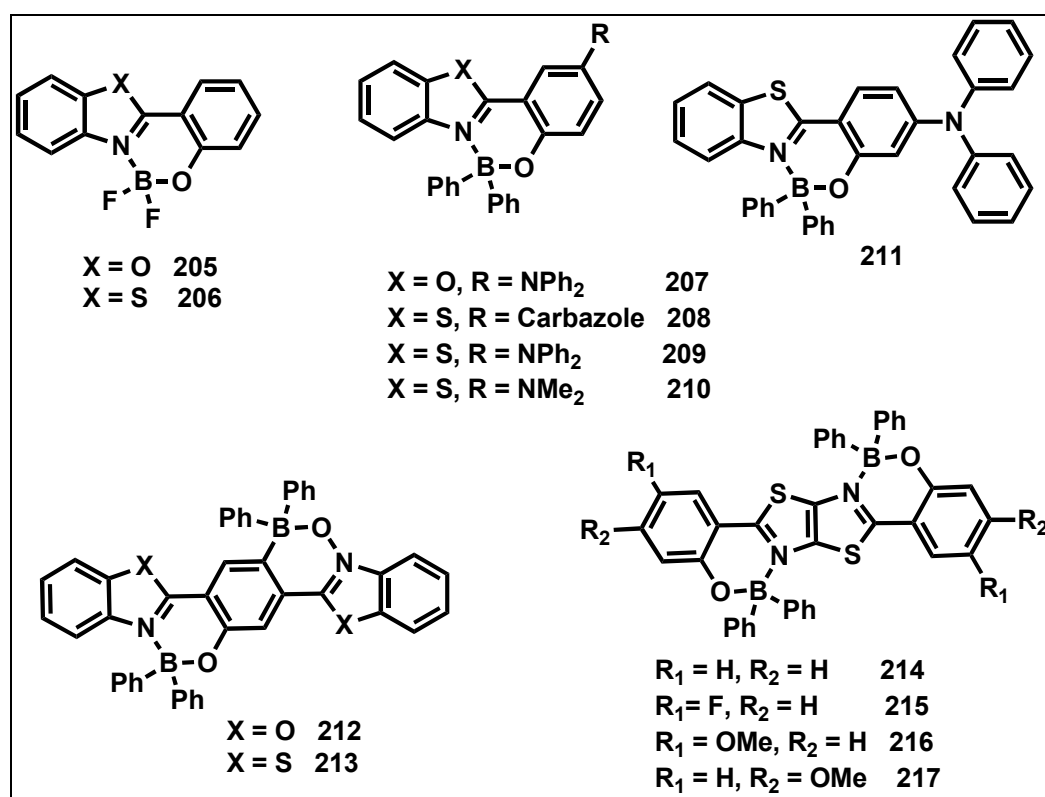


Figure 1.18: *N,O*-chelate tetra-coordinate boron complexes (205-217).

strong electron affinity. OLEDs were also fabricated employing these compounds as electron transporting as well as non doped emitters.⁹²

A Coumarin based 8-benzothiazole boron dye **218** was studied by Lijuan and coworkers which showed absorption at 322 nm and emission at 340, 514 nm ($\Phi_f = 0.76$).⁹³ Ziessel and co-workers reported a series of boron compounds **219-227** based on electron donor/acceptor substituted 2-(2'-hydroxy phenyl)benzoxazole ligands (HBO) with an emission wavelength ranging from 385-425 in CH_2Cl_2 .⁹⁴ Later they synthesized ethynyl extended boron compounds **228-238**, with substituent variation at 3-, 4- and 5- position of the phenolate side of the HBO core.⁹⁵⁻⁹⁷ Crystal packing

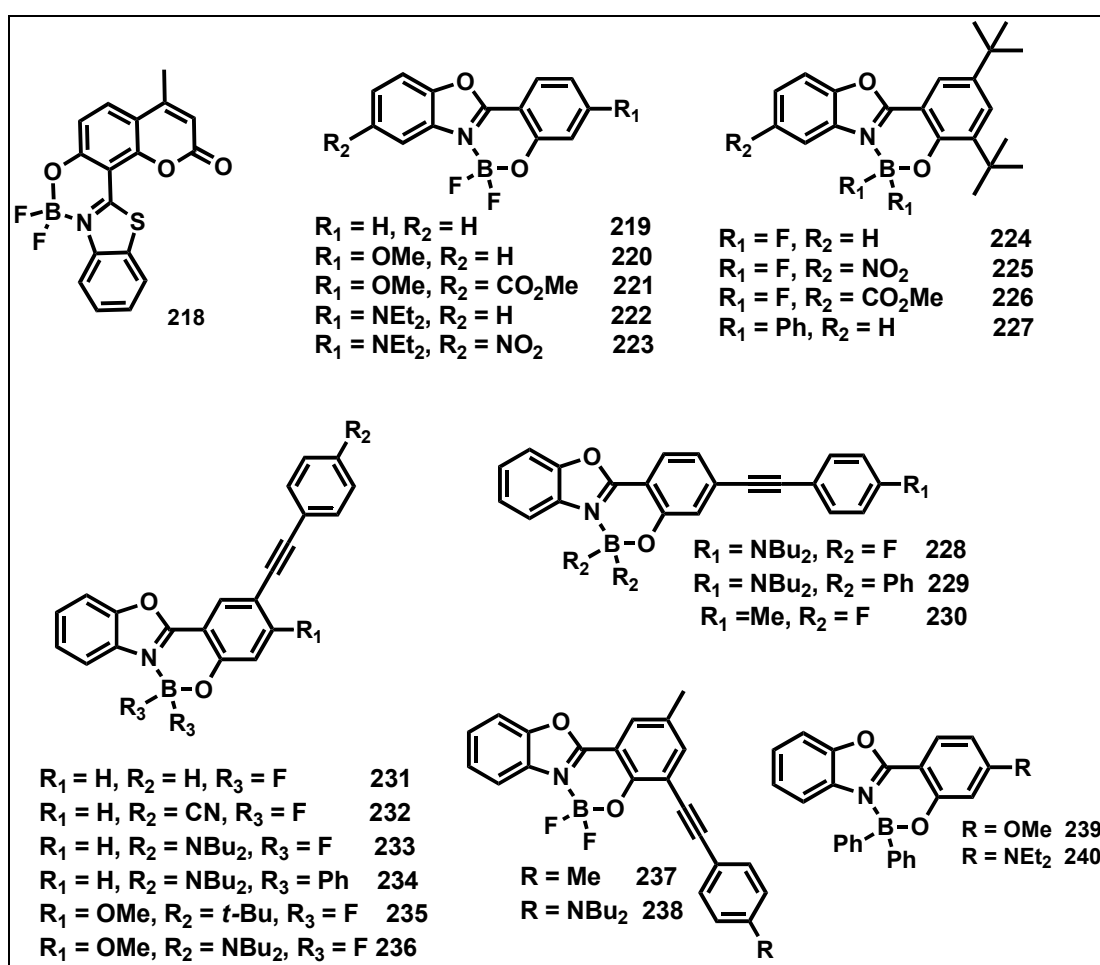


Figure 1.19: *N,O*-chelate tetra-coordinate boron complexes (**218-240**).

analysis of these compounds revealed, intense red shifted emission of BPh₂ complexes compared to BF₂ complex. They concluded that the ethynyl extension in these compounds provided extended conjugation and there by red shifted emission in both

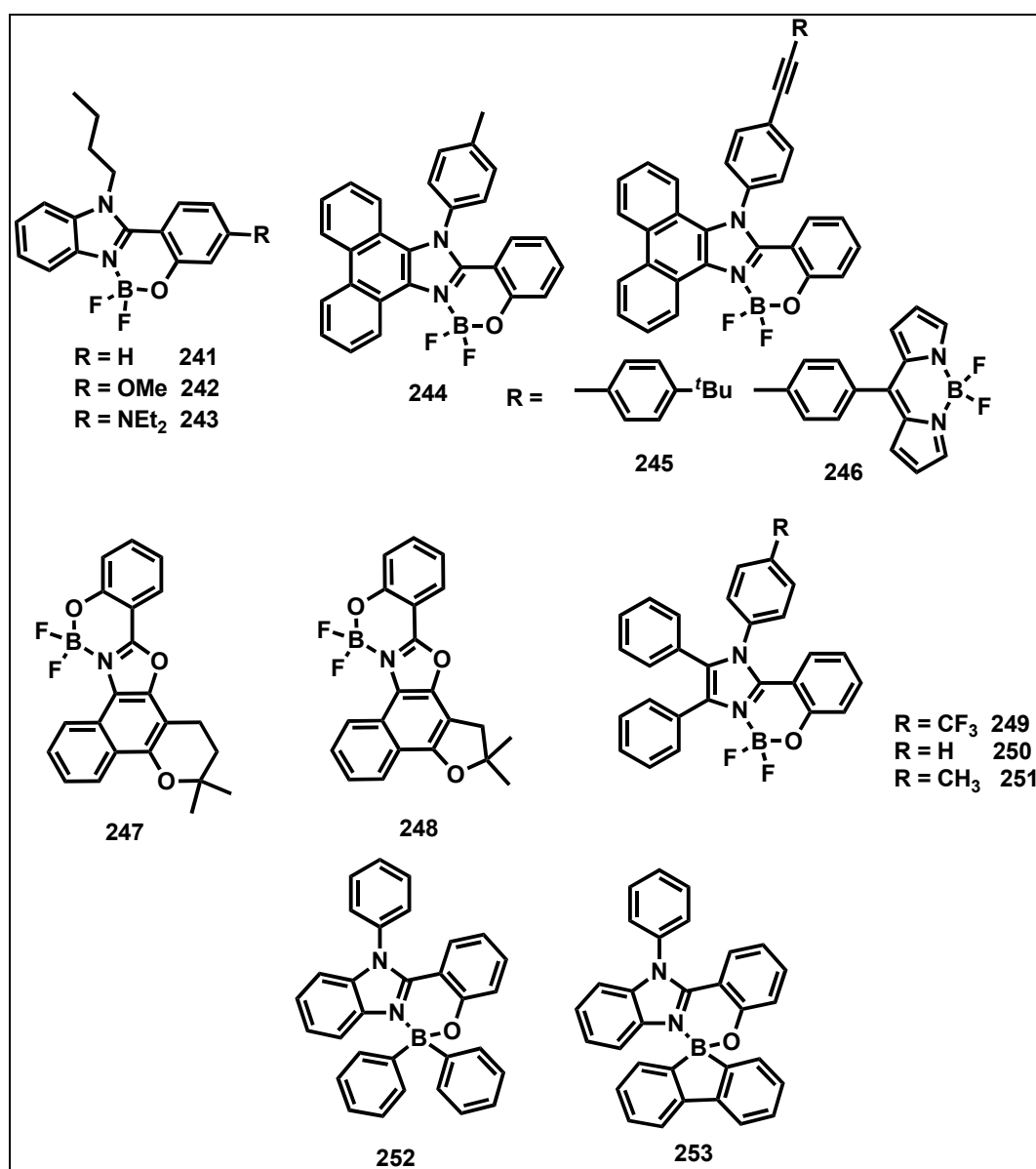


Figure 1.20: *N,O*-chelate tetra-coordinate boron complexes (241-253).

solution and solid state. They also synthesized a series of difluoroboron complexes **241-246**, based on N-alkylated 2-(2'-hydroxyphenyl)benzimidazole (HBI) or 2-(2'-hydroxyphenyl)-9,10-phenanthroimidazole (HPI) ESIPT ligands and studied their optical properties in both solution and solid state. These compounds showed efficient emission from blue to green colour with quantum yields up to 91% in CH₂Cl₂ and 27% in solid state.⁹⁸ Silva group synthesized fluorescent naphthoxazole boron complexes **247** and **248**, and used them as efficient bioprobes for endocytic pathway tracking in live cancer cells and showed far better selectivity compared to commercially available acridine orange.⁹⁹ Recently Mukundam *et.al* synthesized tetraphenylimidazole boron compounds (**249-251**) in two simple steps from commercially available starting materials and studied their optical properties. Electroluminescent devices were fabricated using compounds (**249-251**) as electron transporting layer. A maximum brightness of 6450 cd m⁻² was achieved with good efficiency (10.6 cd A⁻¹) for compound **249**.¹⁰⁰ Hongyu Zhang and coworkers reported benzimidazole based spiroborate complexes **252** and **253**. Both the compounds showed intense blue emission in both solution ($\Phi_f \sim 0.70$) and solid state ($\Phi_f \sim 0.50$). These compounds also exhibited high hole and electron transport ability and high decomposition temperatures (362 °C for **252** & 383 °C for **253**). By employing these compounds as emitting materials, OLEDs were fabricated, which showed deep-blue light emission with CIE coordinates of (X = 0.15, Y = 0.09) and (X = 0.16, Y = 0.08) respectively.¹⁰¹

1.2.2.3 N,C – Chelate boron compounds

Shigehiro Yamaguchi and co-workers reported the N,C- chelate boron compound **254** based on thienylthiazole ligand. The regioselective functionalization of **254**, followed by coupling reactions, achieved three isomers of ladder type boron compounds **255-**

257. The boron chelation makes thienylthiazole skeleton more planar with increased conjugation which leads them low lying LUMO levels.¹⁰² Later the same group reported thiazolyl capped π -conjugated compounds (**258**, **259**) by employing coordination/cyclization protocol with $B(C_6F_5)_3$. These two products showed yellow emission at 476, 548 with red shifted emission maxima by 63, 72 nm compared to those of un cyclized compounds. The electrochemical studies of these compounds revealed their two step reduction waves at $E_{pc} = -1.81$ V and -1.96 V for **258** and -1.70 V and -1.89 V for **259**, with increased reversibility for the first reduction waves. Theoretical calculations of these compounds showed reduced band gap energy (2.96 eV for **258**) with lowered LUMO level by

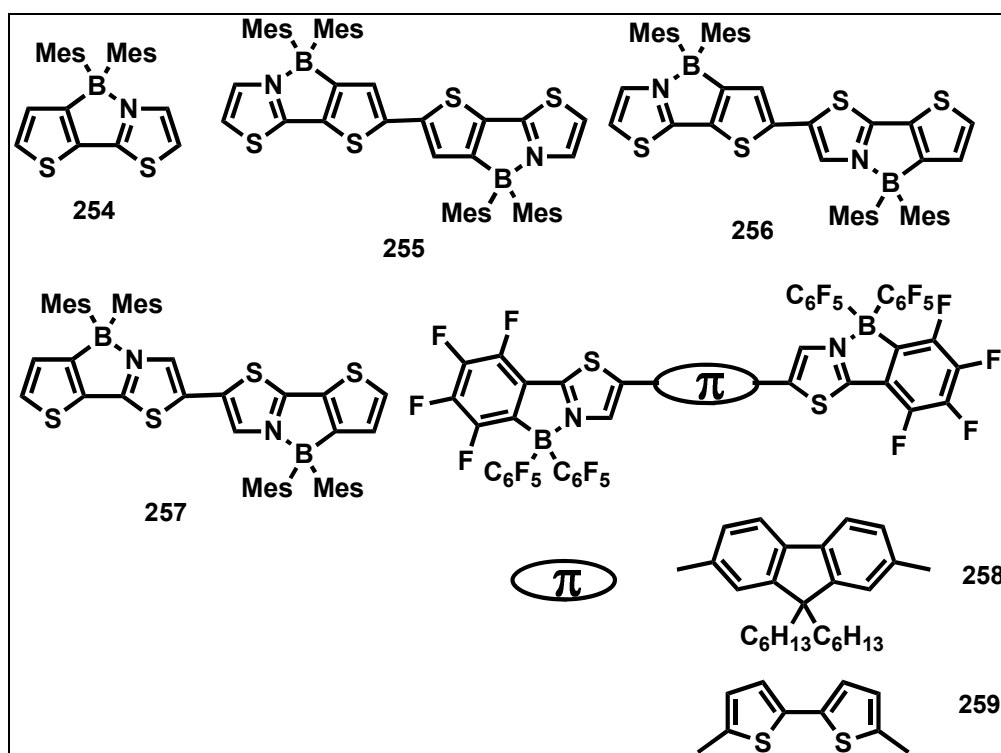


Figure 1.21: *N,C*-chelate tetra-coordinate boron complexes (**254-259**).

0.13 eV compared to its precursor.¹⁰³ By using simple synthetic strategies, Zhang group synthesized a series of ladder type π -conjugated boron compounds **260-263** with electron donating/withdrawing groups on thiazole backbone. All these

complexes exhibited high decomposition temperatures with 5% weight loss (T_{d5} : 343-400 °C) and melting points (275-380 °C), suggested their high thermal stabilities. Absorption and emission maxima of these compounds ranging from 404-450 nm and 439-515 nm respectively with good quantum yields in CH_2Cl_2 . Cyclic voltammetry of these compounds showed first reversible reduction waves in the ranges from -1.73 to -1.92 V; the values are less positive compared to the starting material ($E_{1/2} = -2.33$). They concluded that these compounds could be potential candidates as efficient emitters in optoelectronics.¹⁰⁴ Uwe Pischel and co-workers reported six new fluorescent boron compounds **264-269** based

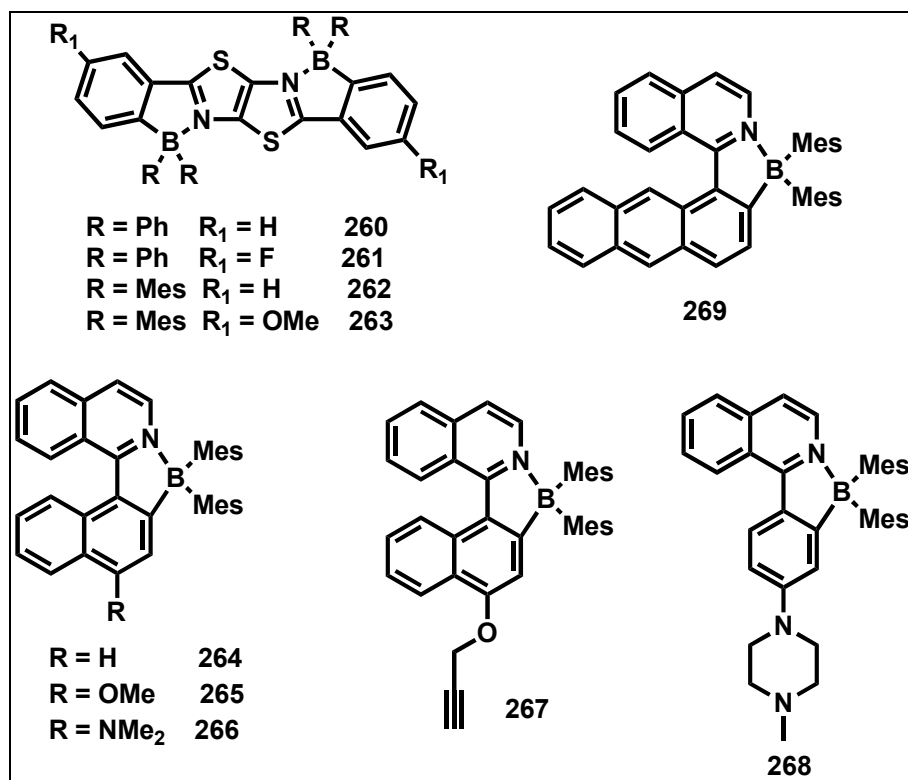


Figure 1.22: *N,C*-chelate tetra-coordinate boron complexes (**260-269**).

on aryl isoquinoline moiety with various electron donating groups. Toluene solutions of these complexes emits in the ranges from 487 to 547 nm with maximum quantum yields upto 0.62. All these boron complexes exhibited intense excited state

intramolecular charge transfer behavior with high solvent dependent emission from toluene to DMSO with large Stokes shifts. All these boron compounds showed high photostability in contrast to photochromic B(ppy)Mes₂ *N,C*-chelates which will be discussed in the next paragraph. More over these compounds showed significant two photon absorption cross sections (up to 61 GM) which allows the use of excitation wavelengths in the NIR region (> 800 nm). Dye **266** was studied in confocal microscopy for imaging of N13 mouse microglial cell line.¹⁰⁵ Suning Wang group synthesized dimesitylboron compound **270** based on 2- phenylpyridine and studied for their photochromic applications.¹⁰⁶

When irradiated by hand held UV lamp of 365 nm, toluene solution of compound **270** turns dark navy blue, with a rapid loss of fluorescence. In the absorption spectrum, a new band appeared at 599 nm, the same changes were also established by ¹H NMR spectra. NMR analysis, confirmed the formation of isomerized product **271**, where a C-C bond is formed between the phenyl and one of the mesityls. Moreover, the reversibility of **271** to **270** was observed when heated under nitrogen. However this compound was not stable with oxygen under light, and readily converted to **271A**. Later they synthesized compounds **272-275** in order to check the substituent effect on the photoisomerization phenomena.¹⁰⁷ These compounds showed photoisomerization similar to **270**. The absorption spectra of the dark isomer was red shifted with electron withdrawing group and blue shifted with an electron donating group such as SiMe₃ in the same manner as **270** (light colored isomer). The photoisomerization process can be thermally reversible for compounds **274** and **275**, but in case of dark isomer **273**, a gradual decomposition occurred at ambient temperature. Compounds **276-279** showed much lower photoisomerization quantum efficiency than that of **270**. Compound **279** did not undergo photoisomerization at all because of significant pi-conjugation. They

also synthesized compounds **280-282**, where the olefin conjugates with ppy-BMes₂ unit. No colour change was observed in compound **280**, when irradiated at 365 nm, instead trans-cis isomerization occurred at the olefin centre without altering the boron core. In case of compounds **281** and **282**, only one olefin bond underwent trans-cis isomerization. Later they synthesized N,C- chelate BMes₂ compounds with other ligand systems (**283-287**) such as benzofuryl, benzothieryl, and N-phenyl indolyl, and studied their photochromic behavior.¹⁰⁸

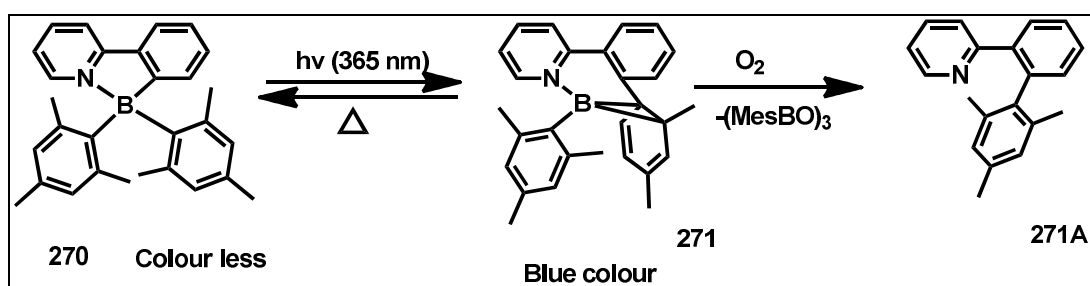


Figure 1.23: N,C- chelate tetra-coordinate boron complexes (**270-271**).

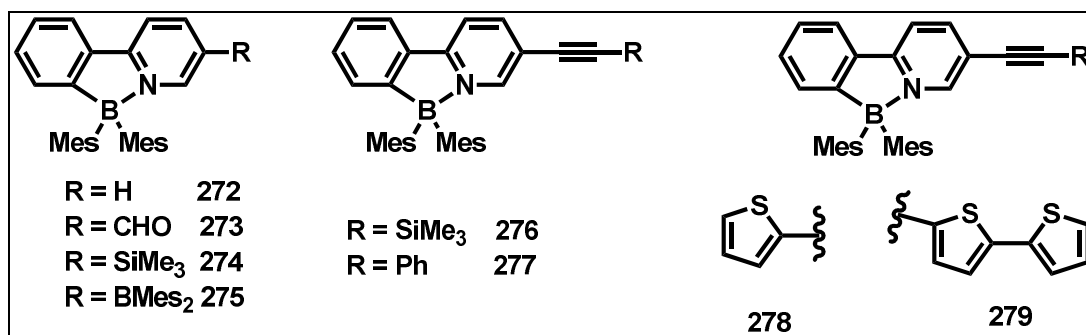


Figure 1.24: N,C- chelate tetra-coordinate boron complexes (**272-279**).

Kawashima and co-workers reported azobenzene based pentafluorophenyl boron compounds (**288-295**) with various substituents at the 4- and 4'- positions of phenyl.¹⁰⁹ These compounds showed yellow, green, orange, red fluorescence with emission ranging from 503 nm (**293**) to 634 nm (**294**); the quantum yields observed up to 0.9 (**290**) in hexane. The substituent effect and fluorescence properties were

well correlated by TD-DFT studies. The electron donating group at the 4'- position was mainly responsible for an intense emission of these compounds. In order to study the effect of pentafluorophenyl groups on boron, they also synthesized compound **300** which was non emissive. Moreover, these 2-borylazobenzenes were studied as fluorescent vital stain for the visualization of living tissues by microinjection into *Xenopus* embryos.

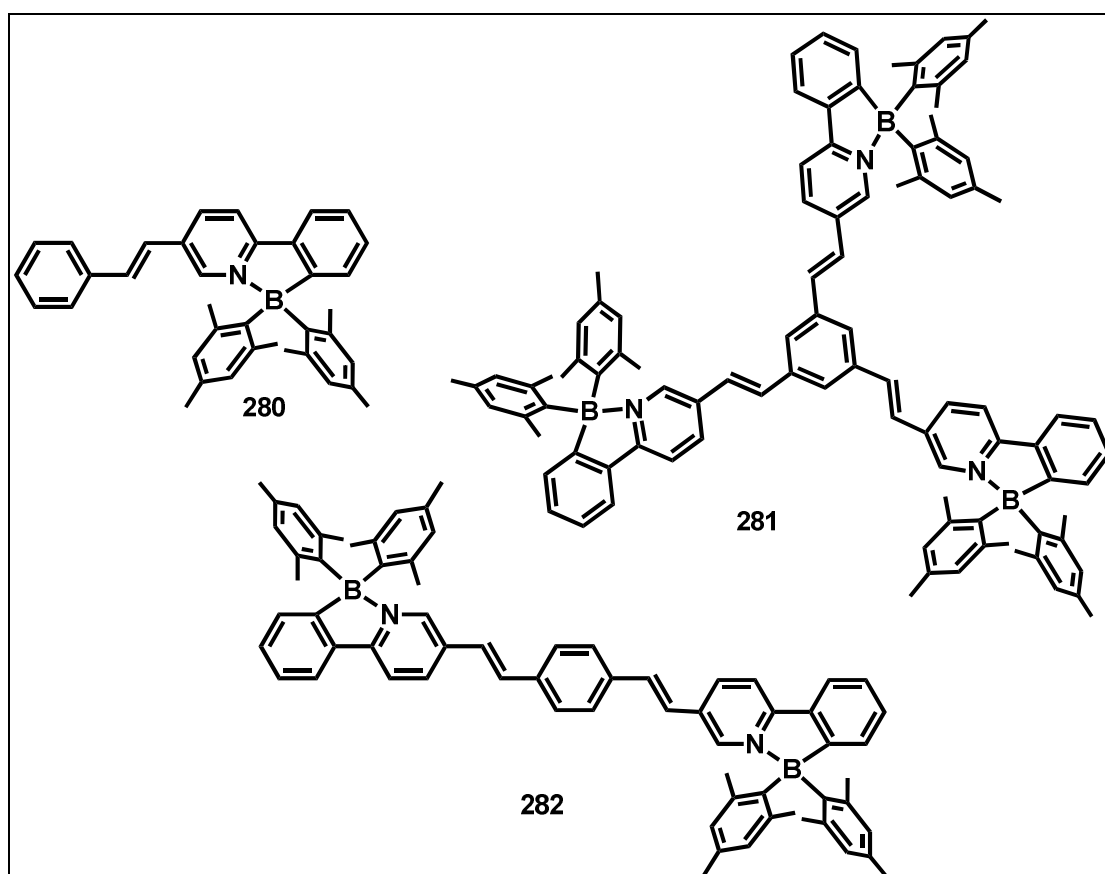


Figure 1.25: *N,C*-chelate tetra-coordinate boron complexes (280-282).

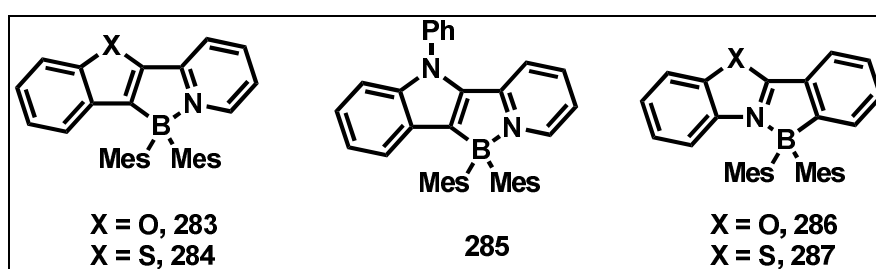


Figure 1.26: *N,C*-chelate tetra-coordinate boron complexes (283-287).

Later, they synthesized 2,2'-diborylazobenzenes (**296-299**) with double intramolecular N-B coordination. These four compounds showed orange and red colour emission with quantum yields ranging from 0.20 to 0.73, which were highly red shifted in both

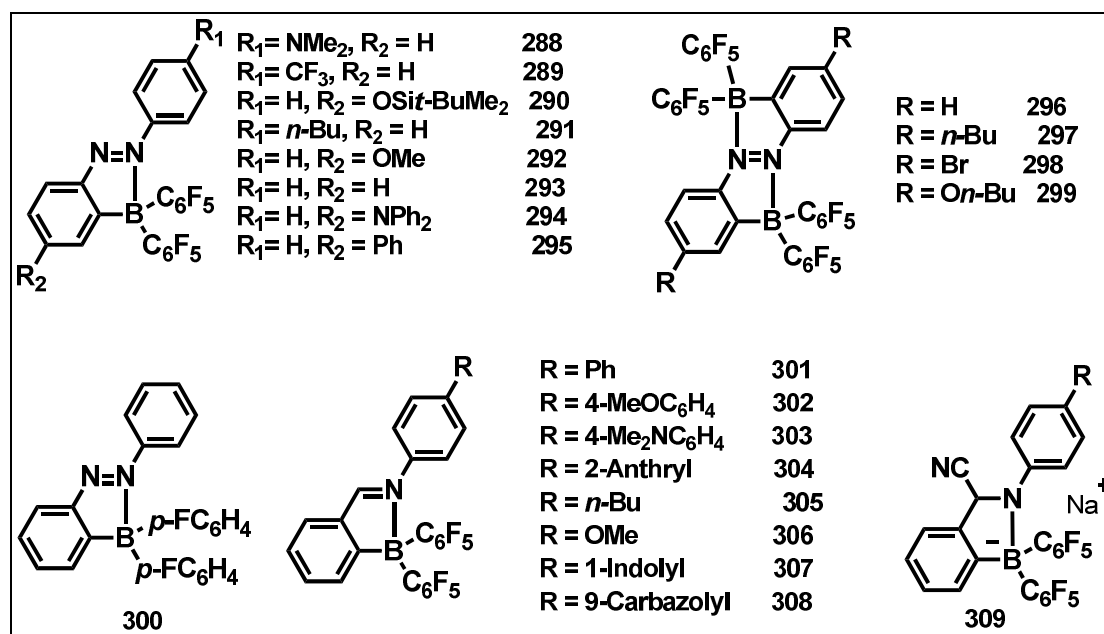


Figure 1.27: *N,C*-chelate tetra-coordinate boron complexes (**288-309**).

absorption and emission maxima compared to their monomeric boron compounds. Cyclic voltammetry of these compounds showed one electron reduction. Compound **297** (λ_{abs} THF: 547 and 582 nm) chemically reduced using decamethylcobaltocene to its non fluorescent azobenzene radical anion (λ_{abs} THF: 613 nm) and was confirmed by EPR spectroscopy. The air oxidation of radical anion recovered the original absorption and emission properties of compound **297**.¹¹⁰ The same group reported imine based boron compounds **301-308** with different substituents at the para position of the N-phenyl. All these compounds showed blue to green emission in hexane. In particular, the borylated *N*-(4-dimethylaminophenyl)imine (**303**) showed intense green emission (Φ_f 0.73) which is 7000 times higher compared to *N*-benzylideneaniline. Boron compounds with *N*-(1-indolyl)- (**307**) and *N*-(9-

carbazolyl)- (**308**) substituents showed dual emissions, as a result of moderately perpendicular structure of the imine moieties.¹¹¹ The formation of adduct **309** by the addition of cyanide to arylimine boron compounds makes them as potential candidates for cyanide ion sensing.¹¹²

Wuerthwein and co-workers reported N-aryl-2-borylbenzaldimines (**310-312**) and their extended π -conjugated compounds where two 2-borylbenzaldimine (**313-316**) units connects *via* spacer. They observed that, the dinuclear boron compounds with extended conjugation exhibited, large Stokes shifts and high electrochemical stability than the mononuclear compounds. Moreover these compounds showed better photochemical stability over Wang's 2-phenylpyridine based dimesityl boron compounds.¹¹³

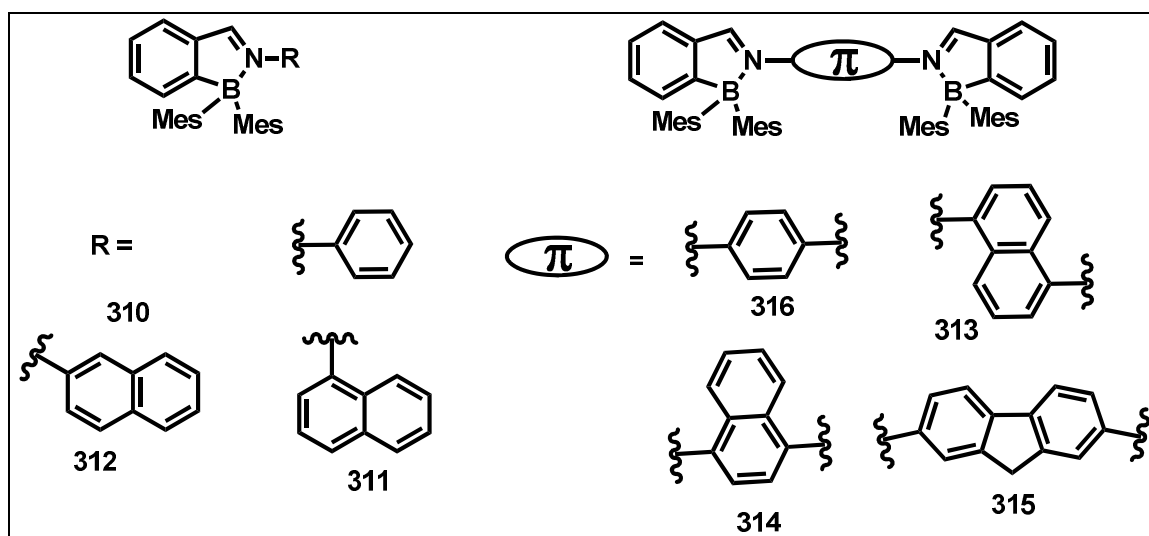


Figure 1.28: *N,C*- chelate tetra-coordinate boron complexes (**310-316**).

Murakami group reported the electrophilic aromatic borylation strategy to prepare the *N,C*- chelate boron compounds.¹¹⁴ Later, the electrophilic aromatic borylation strategy has been utilized by Yam and co-workers to synthesize a series of diarylethene-containing *N,C*- chelate thienylpyridine-bis(alkynyl)borane compounds

(317-322). These compounds showed absorption at *ca.* 380-450 nm and solvent dependent emission at *ca.* 460-580 nm. Cyclic voltammetry showed two irreversible oxidation waves at *ca.* +1.3 V and *ca.* +1.6 V and one reduction wave at *ca.* -1.55 or -1.98 V vs SCE. The photochromic behaviour of these compounds were also studied.¹¹⁵

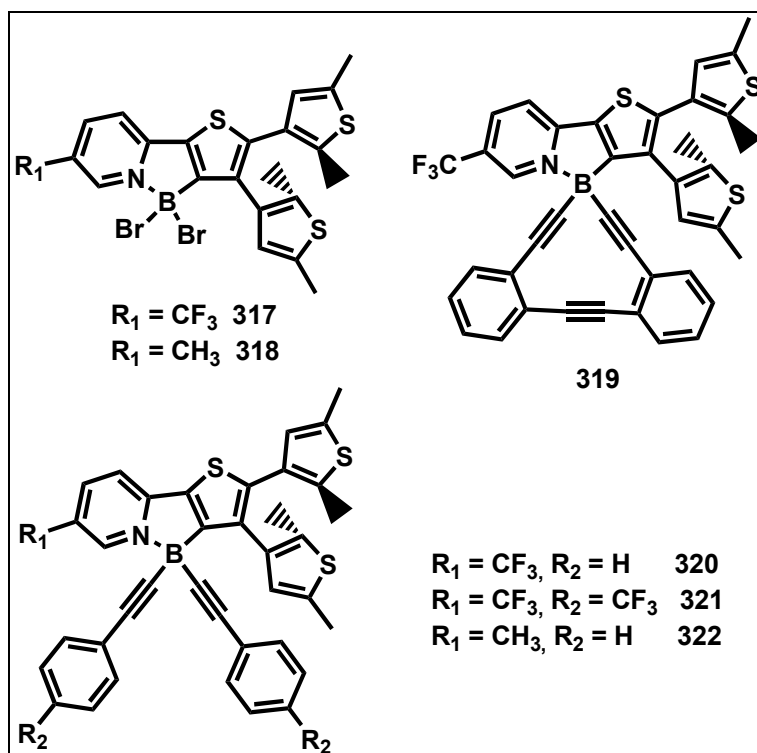


Figure 1.29: *N,C*-chelate tetra-coordinate boron complexes (317-322).

Qiu and co-workers synthesized tetraphenylethene containing *N,C*-chelate boron compounds **323** and **324**. These compounds exhibit aggregation induced emission due to the presence of tetraphenylethene moiety and also shown good thermal stability with quantum yield near to unity.¹¹⁶ Later the same group synthesised boron compounds **325** and **326** which exhibit aggregation induced emission, high thermal stability with excellent solid state fluorescence quantum yields up to unity. These

compounds were utilized as emitters in OLED and shown superior electroluminescent efficiencies over their corresponding ligands.¹¹⁷

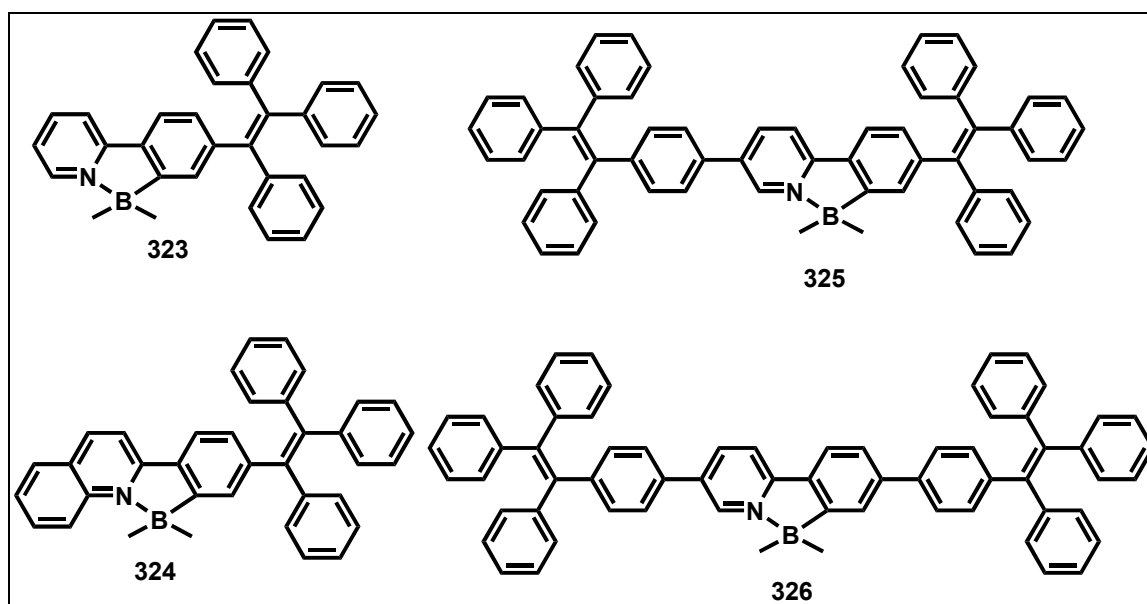


Figure 1.30: *N,C*-chelate tetra-coordinate boron complexes (**323-326**).

Baranov and co-workers reported conformationally locked green fluorescent protein (GFP) chromophores **327-333**. These compounds showed high fluorescence quantum yields and pH dependence of spectra in physiological range. Compound **329** was studied for fluorescent labelling in cellular lipid organelles, including inner and outer membranes and lipid drops.¹¹⁸

Patil and co-workers synthesized a series of boron compounds (**334-347**) based on 2-aryl quinoline ligands. The tuning of emission colour in both solution and solid state was achieved from blue to red by simply varying the substituents on either quinolines or the boron centre. Feasibility of these molecules for bio-imaging was studied by confocal imaging in the MCF-7 cancer cell line.¹¹⁹ Wah Yam and co-workers reported a series of spiro-fused ladder type boron compounds **348-355**. The emission colour of these compounds were finely tuned from blue to red by varying substituents on the pyridine ring and extending the π -conjugation of the spiro framework. Solution

processed OLED devices were fabricated using some of these compounds as blue, green and red dopant

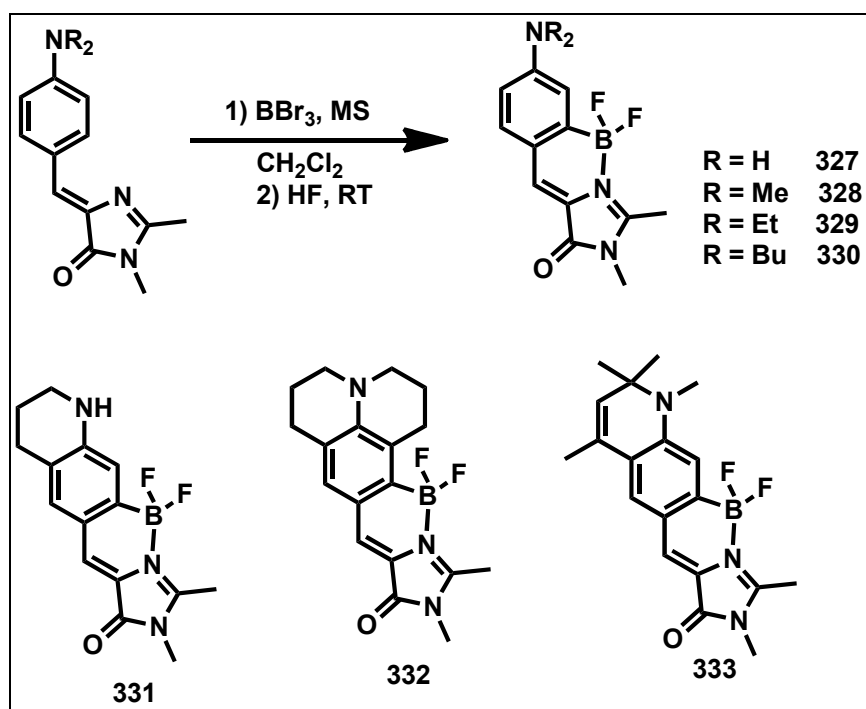


Figure 1.31: *N,C*-chelate tetra-coordinate boron complexes (327-333).

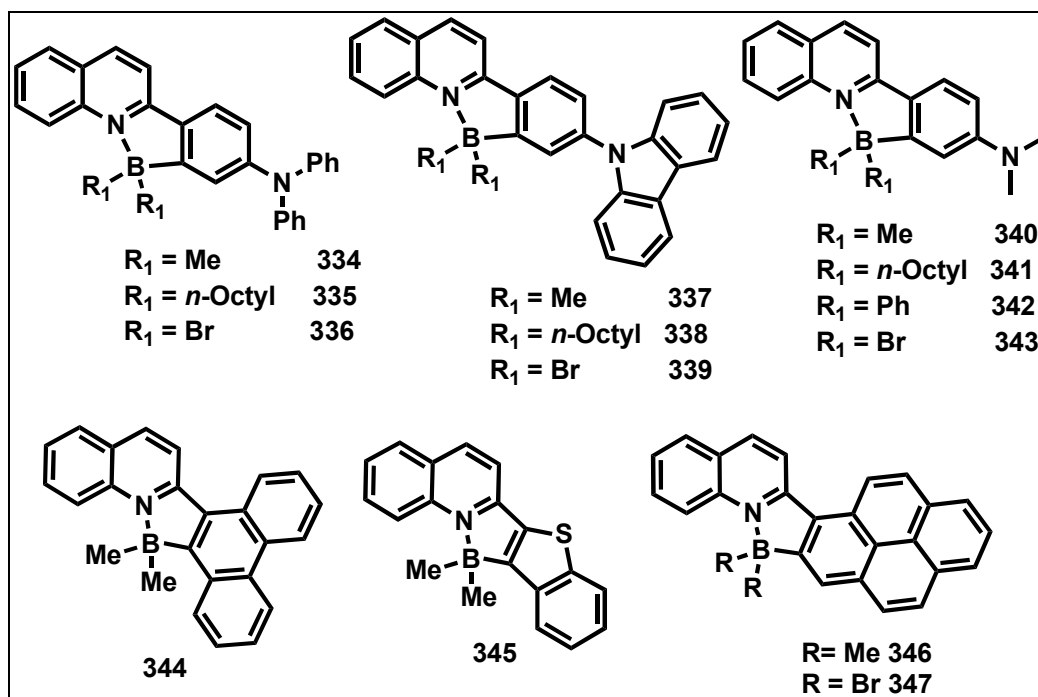


Figure 1.32: *N,C*-chelate tetra-coordinate boron complexes (334-347).

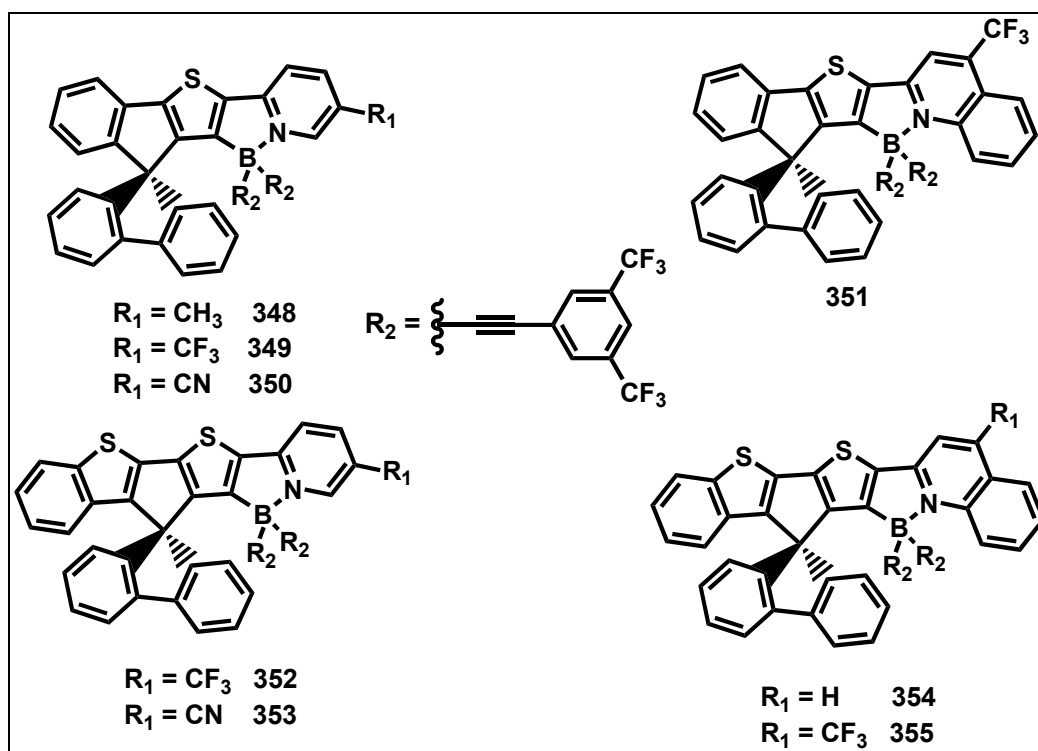


Figure 1.33: *N,C*-chelate tetra-coordinate boron complexes (348-355).

material in the emissive layer.¹²⁰ Jäkle and co-workers reported conjugated ladder type organoboron compounds **356** and **357**, by the reaction of 2,7-dibromo-9,9-dihexylfluorene with 6-methylpyridin-2-yl(pivaloyloxy)zinc *via* Negishi coupling, followed by aromatic electrophilic borylation method. These boron compounds showed strong blue emission with high quantum yields and underwent multistep reversible reduction and oxidation processes.¹²¹

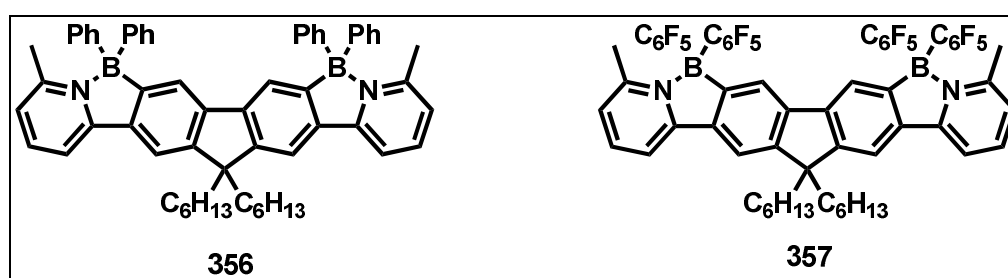


Figure 1.34: *N,C*-chelate tetra-coordinate boron complexes (356-357).

1.3 References

- (1) Beer, P. D.; Gale, P. A. *Angew. Chem., Int. Ed.* **2001**, *40*, 486.
- (2) Gunnlaugsson, T.; Glynn, M.; Tocci, G. M.; Kruger, P. E.; Pfeffer, F. M. *Coord. Chem. Rev.* **2006**, *250*, 3094.
- (3) Kubik, S. *Chem. Soc. Rev.* **2010**, *39*, 3648.
- (4) Martinez-Manez, R.; Sancenon, F. *Chem. Rev. (Washington, DC, U. S.)* **2003**, *103*, 4419.
- (5) Kirk, K. L. *Biochemistry of the Halogens and Inorganic Halides* **1991**, 58.
- (6) Newbrun, E. J. *Public Health Dent.* **2010**, *70*, 227.
- (7) Briancon, D. *Rev. Rhum.* **1997**, *64*, 78.
- (8) Kleerekoper, M. *Endocrinol. Metab. Clin. North Am.* **1998**, *27*, 441.
- (9) Michigami, Y.; Kuroda, Y.; Ueda, K.; Yamamoto, Y. *Anal. Chim. Acta* **1993**, *274*, 299.
- (10) Zhou, Y.; Zhang, J. F.; Yoon, J. *Chem. Rev. (Washington, DC, U. S.)* **2014**, *114*, 5511.
- (11) Konieczka, P.; Zygmunt, B.; Namieśnik, J. *J. Bull. Environ. Contam. Toxicol.* **2000**, *64*, 794.
- (12) Cosentino, P.; Grossman, B.; Shieh, C.; Doi, S.; Xi, H.; Erbland, P. J. *Geotech. Eng.* **1995**, *121*, 610.
- (13) Duke, R. M.; Gunnlaugsson, T. *Tetra. lett* **2007**, *48*, 8043.
- (14) Veale, E. B.; Gunnlaugsson, T. *J. Org. Chem.* **2008**, *73*, 8073.
- (15) Kwon, J. Y.; Jang, Y. J.; Kim, S. K.; Lee, K.-H.; Kim, J. S.; Yoon, J. *J. Org. Chem* **2004**, *69*, 5155.
- (16) Madhu, S.; Ravikanth, M. *Inorg. Chem.* **2014**, *53*, 1646.

-
- (17) Kumar, M.; Kumar, R.; Bhalla, V. *Tetrahedron* **2009**, *65*, 4340.
- (18) Lee, M. H.; Quang, D. T.; Jung, H. S.; Yoon, J.; Lee, C.-H.; Kim, J. S. *J. Org. Chem* **2007**, *72*, 4242.
- (19) Wade, C. R.; Broomsgrove, A. E. J.; Aldridge, S.; Gabbai, F. P. *Chem. Rev.* **2010**, *110*, 3958.
- (20) Yamaguchi, S.; Akiyama, S.; Tamao, K. *J. Am. Chem. Soc.* **2001**, *123*, 11372.
- (21) Yamaguchi, S.; Shirasaka, T.; Akiyama, S.; Tamao, K. *J. Am. Chem. Soc.* **2002**, *124*, 8816.
- (22) Liu, X. Y.; Bai, D. R.; Wang, S. *Angew. Chem. Int. Ed.* **2006**, *45*, 5475.
- (23) P, C. A. S.; Thilagar, P. *Inorg. Chem.* **2014**, *53*, 2776.
- (24) Kim, T.-H.; Swager, T. M. *Angew. Chem., Int. Ed.* **2003**, *42*, 4803.
- (25) Jiang, X.; Vieweger, M. C.; Bollinger, J. C.; Dragnea, B.; Lee, D. *Org. Lett.* **2007**, *9*, 3579.
- (26) Kim, S. Y.; Hong, J. I. *Org. Lett.* **2007**, *9*, 3109.
- (27) Kim, S. Y.; Park, J.; Koh, M.; Park, S. B.; Hong, J. I. *Chem. Commun.* **2009**, 4735.
- (28) Hu, R.; Feng, J.; Hu, D.; Wang, S.; Li, S.; Li, Y.; Yang, G. *Angew. Chem. Int. Ed.* **2010**, *49*, 4915.
- (29) Bozdemir, O. A.; Sozmen, F.; Buyukcakir, O.; Guliyev, R.; Cakmak, Y.; Akkaya, E. U. *Org. Lett.* **2010**, *12*, 1400.
- (30) Zhu, B.; Yuan, F.; Li, R.; Li, Y.; Wei, Q.; Ma, Z.; Du, B.; Zhang, X. *Chem. Commun.* **2011**, *47*, 7098.
- (31) Cao, J.; Zhao, C.; Zhu, W. *Tetra. lett* **2012**, *53*, 2107.
- (32) Wei, G.; Yin, J.; Ma, X.; Yu, S.; Wei, D.; Du, Y. *Anal. Chim. Acta* **2011**, *703*, 219.
-

-
- (33) Jha, G.; N, A.; Rahaman, A.; Sarkar, M. *Phys. Chem. Chem. Phys.* **2015**, *17*, 3525.
- (34) Ji, L.; Griesbeck, S.; Marder, T. B. *Chem. Sci.* **2017**.
- (35) Tang, C. W.; Vanslyke, S. A. *Appl. Phys. Lett.* **1987**, *51*, 913.
- (36) Li, D.; Zhang, H.; Wang, Y. *Chem. Soc. Rev.* **2013**, *42*, 8416.
- (37) Frath, D.; Massue, J.; Ulrich, G.; Ziessel, R. *Angew. Chem. Int. Ed.* **2014**, *53*, 2290.
- (38) Jäkle, F. *Chem. Rev.* **2010**, *110*, 3985.
- (39) Rao, Y.-L.; Wang, S. *Inorg. Chem.* **2011**, *50*, 12263.
- (40) Boens, N.; Leen, V.; Dehaen, W. *Chem. Soc. Rev.* **2012**, *41*, 1130.
- (41) Loudet, A.; Burgess, K. *Chem. Rev.* **2007**, *107*, 4891.
- (42) Liu, Q.; Mudadu, M. S.; Schmider, H.; Thummel, R.; Tao, Y.; Wang, S. *Organometallics* **2002**, *21*, 4743.
- (43) Chen, H. Y.; Chi, Y.; Liu, C. S.; Yu, J. K.; Cheng, Y. M.; Chen, K. S.; Chou, P. T.; Peng, S. M.; Lee, G. H.; Carty, A. J.; Yeh, S. J.; Chen, C. T. *Adv. Funct. Mater.* **2005**, *15*, 567.
- (44) Liu, Q. D.; Mudadu, M. S.; Thummel, R.; Tao, Y.; Wang, S. *Adv. Funct. Mater.* **2005**, *15*, 143.
- (45) Liddle, B. J.; Silva, R. M.; Morin, T. J.; Macedo, F. P.; Shukla, R.; Lindeman, S. V.; Gardinier, J. R. *J. Org. Chem.* **2007**, *72*, 5637.
- (46) Araneda, J. F.; Piers, W. E.; Heyne, B.; Parvez, M.; McDonald, R. *Angew. Chem. Int. Ed.* **2011**, *50*, 12214.
- (47) Calhorda, M. J.; Suresh, D.; Gomes, P. T.; Di Paolo, R. E.; Macanita, A. L. *Dalton Trans.* **2012**, *41*, 13210.
-

-
- (48) Suresh, D.; Gomes, C. S. B.; Gomes, P. T.; Di Paolo, R. E.; Macanita, A. L.; Calhorda, M. J.; Charas, A.; Morgado, J.; Teresa Duarte, M. *Dalton Trans.* **2012**, *41*, 8502.
- (49) Suresh, D.; Gomes, C. S. B.; Lopes, P. S.; Figueira, C. A.; Ferreira, B.; Gomes, P. T.; Di Paolo, R. E.; Macanita, A. L.; Duarte, M. T.; Charas, A.; Morgado, J.; Vila-Vicosa, D.; Calhorda, M. J. *Chem. Eur. J.* **2015**, *21*, 9133.
- (50) Suresh, D.; Lopes, P. S.; Ferreira, B.; Figueira, C. A.; Gomes, C. S. B.; Gomes, P. T.; Di Paolo, R. E.; Macanita, A. L.; Duarte, M. T.; Charas, A.; Morgado, J.; Calhorda, M. J. *Chem. Eur. J.* **2014**, *20*, 4126.
- (51) Zhao, D.; Li, G.; Wu, D.; Qin, X.; Neuhaus, P.; Cheng, Y.; Yang, S.; Lu, Z.; Pu, X.; Long, C.; You, J. *Angew. Chem. Int. Ed.* **2013**, *52*, 13676.
- (52) Barbon, S. M.; Reinkeluers, P. A.; Price, J. T.; Staroverov, V. N.; Gilroy, J. B. *Chem. Eur. J.* **2014**, *20*, 11340.
- (53) Barbon, S. M.; Staroverov, V. N.; Gilroy, J. B. *J. Org. Chem.* **2015**, *80*, 5226.
- (54) Hesari, M.; Barbon, S. M.; Staroverov, V. N.; Ding, Z.; Gilroy, J. B. *Chem. Commun.* **2015**, *51*, 3766.
- (55) Maar, R. R.; Gilroy, J. B. *J. Mater. Chem. C.* **2016**, *4*, 6478.
- (56) Maar, R. R.; Barbon, S. M.; Sharma, N.; Groom, H.; Luyt, L. G.; Gilroy, J. B. *Chem. Eur. J.* **2015**, *21*, 15589.
- (57) Barbon, S. M.; Gilroy, J. B. *Polym. Chem.* **2016**, *7*, 3589.
- (58) Wang, X.; Wu, Y.; Liu, Q.; Li, Z.; Yan, H.; Ji, C.; Duan, J.; Liu, Z. *Chem. Commun.* **2015**, *51*, 784.
- (59) Qiu, F.; Zhang, F.; Tang, R.; Fu, Y.; Wang, X.; Han, S.; Zhuang, X.; Feng, X. *Org. Lett.* **2016**, *18*, 1398.
-

-
- (60) Wu, Q.; Esteghamatian, M.; Hu, N.-X.; Popovic, Z.; Enright, G.; Tao, Y.; D'Iorio, M.; Wang, S. *Chem. Mater.* **1999**, *12*, 79.
- (61) Anderson, S.; Weaver, M. S.; Hudson, A. J. *Synth. Met.* **2000**, *111*, 459.
- (62) Cui, Y.; Liu, Q. D.; Bai, D. R.; Jia, W. L.; Tao, Y.; Wang, S. *Inorg. Chem.* **2005**, *44*, 601.
- (63) Qin, Y.; Kiburu, I.; Shah, S.; Jäkle, F. *Org. Lett.* **2006**, *8*, 5227.
- (64) Kappaun, S.; Rentenberger, S.; Pogantsch, A.; Zojer, E.; Mereiter, K.; Trimmel, G.; Saf, R.; Möller, K. C.; Stelzer, F.; Slugovc, C. *Chem. Mater.* **2006**, *18*, 3539.
- (65) Cui, Y.; Wang, S. *J. Org. Chem.* **2006**, *71*, 6485.
- (66) Zhang, Z.; Bi, H.; Zhang, Y.; Yao, D.; Gao, H.; Fan, Y.; Zhang, H.; Wang, Y.; Wang, Y.; Chen, Z.; Ma, D. *Inorg. Chem.* **2009**, *48*, 7230.
- (67) Hou, Q.; Zhao, L.; Zhang, H.; Wang, Y.; Jiang, S. *J. Lumin.* **2007**, *126*, 447.
- (68) Frath, D.; Azizi, S.; Ulrich, G.; Retailleau, P.; Ziessel, R. *Org. Lett.* **2011**, *13*, 3414.
- (69) Frath, D.; Azizi, S.; Ulrich, G.; Ziessel, R. *Org. Lett.* **2012**, *14*, 4774.
- (70) Shanmugapriya, J.; Rajaguru, K.; Sivaraman, G.; Muthusubramanian, S.; Bhuvanesh, N. *RSC Adv.* **2016**, *6*, 85838.
- (71) Kubota, Y.; Hara, H.; Tanaka, S.; Funabiki, K.; Matsui, M. *Org. Lett.* **2011**, *13*, 6544.
- (72) Kubota, Y.; Tanaka, S.; Funabiki, K.; Matsui, M. *Org. Lett.* **2012**, *14*, 4682.
- (73) Kubota, Y.; Ozaki, Y.; Funabiki, K.; Matsui, M. *J. Org. Chem.* **2013**, *78*, 7058.
- (74) Kubota, Y.; Kasatani, K.; Takai, H.; Funabiki, K.; Matsui, M. *Dalton Trans.* **2015**, *44*, 3326.
-

-
- (75) Kubota, Y.; Kasatani, K.; Niwa, T.; Sato, H.; Funabiki, K.; Matsui, M. *Chem. Eur. J.* **2016**, *22*, 1816.
- (76) Zhang, Z.; Xue, P.; Gong, P.; Zhang, G.; Peng, J.; Lu, R. *J. Mater. Chem. C.* **2014**, *2*, 9543.
- (77) Zhang, Z.; Wu, Z.; Sun, J.; Yao, B.; Zhang, G.; Xue, P.; Lu, R. *J. Mater. Chem. C.* **2015**, *3*, 4921.
- (78) Liao, C.-W.; Rao M, R.; Sun, S.-S. *Chem. Commun.* **2015**, *51*, 2656.
- (79) Wu, Z.; Sun, J.; Zhang, Z.; Yang, H.; Xue, P.; Lu, R. *Chem. Eur. J.* **2017**, *23*, 1901.
- (80) Wu, Y.; Li, Z.; Liu, Q.; Wang, X.; Yan, H.; Gong, S.; Liu, Z.; He, W. *Org. Biomol. Chem.* **2015**, *13*, 5775.
- (81) Gong, S.; Liu, Q.; Wang, X.; Xia, B.; Liu, Z.; He, W. *Dalton Trans.* **2015**, *44*, 14063.
- (82) Qi, F.; Lin, J.; Wang, X.; Cui, P.; Yan, H.; Gong, S.; Ma, C.; Liu, Z.; Huang, W. *Dalton Trans.* **2016**, *45*, 7278.
- (83) Li, D.; Zhang, H.; Wang, C.; Huang, S.; Guo, J.; Wang, Y. *J. Mater. Chem.* **2012**, *22*, 4319.
- (84) Zhou, L.; Xu, D.; Gao, H.; Han, A.; Yang, Y.; Zhang, C.; Liu, X.; Zhao, F. *RSC Adv.* **2016**, *6*, 69560.
- (85) Gao, H.; Xu, D.; Liu, X.; Han, A.; Zhou, L.; Zhang, C.; Yang, Y.; Li, W. *RSC Adv.* **2017**, *7*, 1348.
- (86) Ośmiałowski, B.; Zakrzewska, A.; Jędrzejewska, B.; Grabarz, A.; Zalesny, R.; Bartkowiak, W.; Kolehmainen, E. *J. Org. Chem.* **2015**, *80*, 2072.
- (87) Yoshii, R.; Nagai, A.; Tanaka, K.; Chujo, Y. *Chem. Eur. J.* **2013**, *19*, 4506.
-

-
- (88) Zhou, L.; Xu, D.; Gao, H.; Han, A.; Liu, X.; Zhang, C.; Li, Z.; Yang, Y. *Dyes Pigm.* **2017**, *137*, 200.
- (89) Wong, C.-L.; Poon, C.-T.; Yam, V. W.-W. *Chem. Eur. J.* **2016**, *22*, 12931.
- (90) Kwak, M.-J.; Kim, Y.-M. *Bull. Korean Chem. Soc.* **2009**, *30*, 2865.
- (91) Li, D.; Wang, K.; Huang, S.; Qu, S.; Liu, X.; Zhu, Q.; Zhang, H.; Wang, Y. *J. Mater. Chem.* **2011**, *21*, 15298.
- (92) Li, D.; Yuan, Y.; Bi, H.; Yao, D.; Zhao, X.; Tian, W.; Wang, Y.; Zhang, H. *Inorg. Chem.* **2011**, *50*, 4825.
- (93) Xie, L.; Chen, Y.; Wu, W.; Guo, H.; Zhao, J.; Yu, X. *Dyes Pigm.* **2012**, *92*, 1361.
- (94) Massue, J.; Frath, D.; Ulrich, G.; Retailleau, P.; Ziessel, R. *Org. Lett.* **2012**, *14*, 230.
- (95) Massue, J.; Frath, D.; Retailleau, P.; Ulrich, G.; Ziessel, R. *Chem. Eur. J.* **2013**, *19*, 5375.
- (96) Massue, J.; Retailleau, P.; Ulrich, G.; Ziessel, R. *New J. Chem.* **2013**, *37*, 1224.
- (97) Massue, J.; Ulrich, G.; Ziessel, R. *Eur. J. Org. Chem.* **2013**, *2013*, 5701.
- (98) Benelhadj, K.; Massue, J.; Retailleau, P.; Ulrich, G.; Ziessel, R. *Org. Lett.* **2013**, *15*, 2918.
- (99) Dias, G. G.; Rodrigues, B. L.; Resende, J. M.; Calado, H. D. R.; de Simone, C. A.; Silva, V. H. C.; Neto, B. A. D.; Goulart, M. O. F.; Ferreira, F. R.; Meira, A. S.; Pessoa, C.; Correa, J. R.; da Silva Junior, E. N. *Chem. Commun.* **2015**, *51*, 9141.
- (100) Mukundam, V.; Dhanunjayarao, K.; Chuang, C. N.; Kang, D. Y.; Leung, M. K.; Hsieh, K. H.; Venkatasubbaiah, K. *Dalton Trans.* **2015**, *44*, 10228.
-

-
- (101) Zhang, Z.; Zhang, H.; Jiao, C.; Ye, K.; Zhang, H.; Zhang, J.; Wang, Y. *Inorg. Chem.* **2015**, *54*, 2652.
- (102) Wakamiya, A.; Taniguchi, T.; Yamaguchi, S. *Angew. Chem. Int. Ed.* **2006**, *45*, 3170.
- (103) Job, A.; Wakamiya, A.; Kehr, G.; Erker, G.; Yamaguchi, S. *Org. Lett.* **2010**, *12*, 5470.
- (104) Li, D.; Zhang, Z.; Zhao, S.; Wang, Y.; Zhang, H. *Dalton Trans.* **2011**, *40*, 1279.
- (105) Pais, V. F.; Alcaide, M. M.; Lopez-Rodriguez, R.; Collado, D.; Najera, F.; Perez-Inestrosa, E.; Alvarez, E.; Lassaletta, J. M.; Fernandez, R.; Ros, A.; Pischel, U. *Chem. Eur. J.* **2015**, *21*, 15369.
- (106) Rao, Y.-L.; Amarne, H.; Zhao, S.-B.; McCormick, T. M.; Martić, S.; Sun, Y.; Wang, R.-Y.; Wang, S. *J. Am. Chem. Soc.* **2008**, *130*, 12898.
- (107) Amarne, H.; Baik, C.; Murphy, S. K.; Wang, S. *Chem. Eur. J.* **2010**, *16*, 4750.
- (108) Rao, Y.-L.; Amarne, H.; Wang, S. *Coord. Chem. Rev.* **2012**, *256*, 759.
- (109) Yoshino, J.; Kano, N.; Kawashima, T. *Chem. Commun.* **2007**, 559.
- (110) Kano, N.; Furuta, A.; Kambe, T.; Yoshino, J.; Shibata, Y.; Kawashima, T.; Mizorogi, N.; Nagase, S. *Eur. J. Inorg. Chem.* **2012**, *2012*, 1584.
- (111) Yoshino, J.; Kano, N.; Kawashima, T. *J. Org. Chem.* **2009**, *74*, 7496.
- (112) Yoshino, J.; Kano, N.; Kawashima, T. *Dalton Trans.* **2013**, *42*, 15826.
- (113) Neue, B.; Froehlich, R.; Wibbeling, B.; Fukazawa, A.; Wakamiya, A.; Yamaguchi, S.; Wuerthwein, E.-U. *J. Org. Chem.* **2012**, *77*, 2176.
- (114) Ishida, N.; Moriya, T.; Goya, T.; Murakami, M. *J. Org. Chem.* **2010**, *75*, 8709.
- (115) Wong, H.-L.; Wong, W.-T.; Yam, V. W.-W. *Org. Lett.* **2012**, *14*, 1862.
-

-
- (116) Zhao, Z.; Chang, Z.; He, B.; Chen, B.; Deng, C.; Lu, P.; Qiu, H.; Tang, B. Z. *Chem. Eur. J.* **2013**, *19*, 11512.
- (117) He, B.; Chang, Z.; Jiang, Y.; Chen, B.; Lu, P.; Kwok, H. S.; Qin, A.; Zhao, Z.; Qiu, H. *Dyes Pigm.* **2014**, *101*, 247.
- (118) Baranov, M. S.; Solntsev, K. M.; Baleeva, N. S.; Mishin, A. S.; Lukyanov, S. A.; Lukyanov, K. A.; Yampolsky, I. V. *Chem. Eur. J.* **2014**, *20*, 13234.
- (119) Shaikh, A. C.; Ranade, D. S.; Thorat, S.; Maity, A.; Kulkarni, P. P.; Gonnade, R. G.; Munshi, P.; Patil, N. T. *Chem. Commun.* **2015**, *51*, 16115.
- (120) Wong, B. Y.-W.; Wong, H.-L.; Wong, Y.-C.; Chan, M.-Y.; Yam, V. W.-W. *Chem. Eur. J.* **2016**, *22*, 15095.
- (121) Yusuf, M.; Liu, K.; Guo, F.; Lalancette, R. A.; Jakle, F. *Dalton Trans.* **2016**, *45*, 4580.

CHAPTER 2

Synthesis and study of imidazole based probes for the selective detection of fluoride ion *via* ESIPT mechanism

2.1 Introduction	63
2.2 Results and discussion	64
2.2.1 Synthesis and characterization of probe 1	64
2.2.2 Probe 1 for fluoride ion sensing	69
2.2.3 Synthesis and characterization of probe 2	75
2.2.4 Probe 2 for fluoride ion sensing	78
2.3 Conclusions	84
2.4 Experimental section	85
2.4.1 General information	85
2.4.2 Synthetic procedure and spectral characterization	87
2.5 References	90

2.1 Introduction

In recent years, the field of anion recognition has grown exponentially due to the significant role of anions in environmental, biological and industrial systems.¹⁻³ Fluoride is a small inorganic anion often added to toothpaste owing to its beneficial role in dental health.⁴ This anion is also administered in the treatment of osteoporosis. However, high dosage of fluoride can result in skeletal and dental fluorosis in humans.⁵ Hence, the regulation and detection of fluoride attracted considerable attention. Over the past decade, a number of fluoride ion sensors based on different signalling mechanisms, such as intramolecular charge transfer,^{6,7} photo-induced electron transfer,⁸⁻¹³ fluorescence resonance energy transfer,¹⁴⁻¹⁷ twisted intramolecular charge transfer,^{18,19} excited state proton transfer,²⁰⁻²⁹ metal-ligand charge transfer,³⁰⁻³² and excimer/exciplex³³⁻³⁵ formation have been used. However, most of the reported probes suffer from low sensitivity (or) slow response, turn-off fluorescence response and complicated synthetic procedures. Therefore, it is important (a) to develop easier and convenient synthetic methodology and (b) highly selective and rapid detection methods. High selectivity and sensitivity was achieved mostly through hydrogen bonding or Lewis acid coordination.³⁶⁻³⁸ The performance of fluoride sensors was improved by taking advantage of chemical affinity between silicon and fluoride.^{14,39-45} Early examples include Swager's⁴⁶ fluoride-induced lactonization, Yang's³⁹ dual emissive N-(3-benzo[d]thiazol-2-yl)-4-*tert*-butyldiphenylsilyloxy)phenyl)-benzamide and Hong's *tert*-butyldiphenyl-7-hydroxycoumarin-4-acetic acid methyl ester.⁴⁰ These and related reaction based sensors served as a good candidate for fluoride detection, but most of them suffer from complicated synthetic procedures.

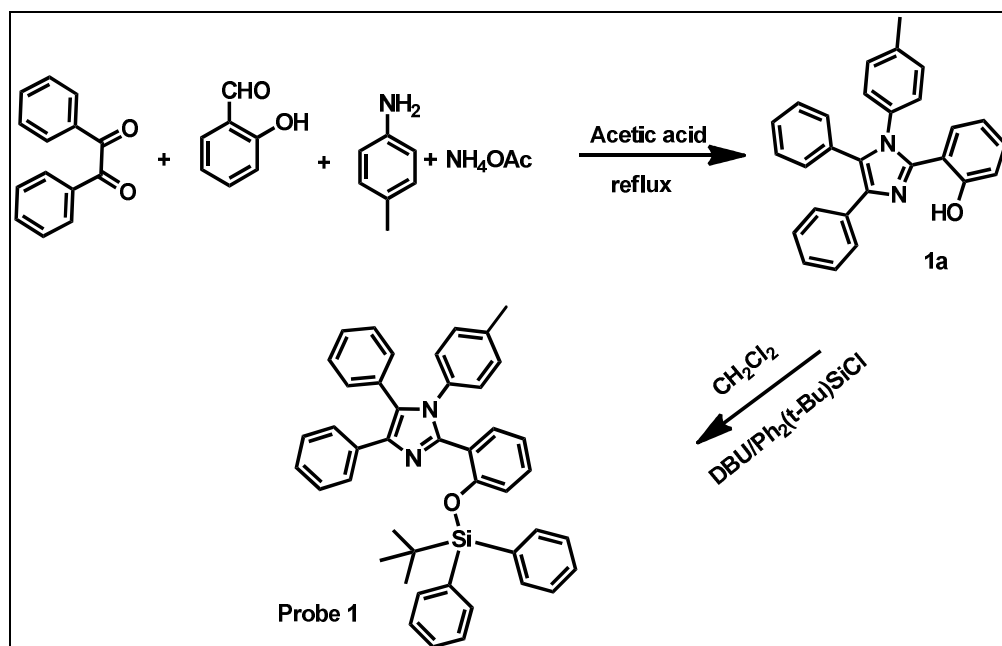
Imidazoles are versatile molecules and extensively studied for their application in

biological systems,⁴⁷⁻⁴⁹ as sensors for anions^{50,51} and in the fabrication of light-emitting devices.⁵²⁻⁵⁵ In particular, 2-hydroxyl-substituted tetraphenyl imidazoles have been extensively studied for their peculiar photophysical process owing to the excited-state intramolecular proton transfer (ESIPT) reaction as well as potential applications in chemosensors, solar energy concentrators, laser dyes and electroluminescent materials.⁵⁶⁻⁶⁰ Taking the advantage of ESIPT chromophores several anion selective probes have been developed.⁶¹⁻⁶⁴ In our endeavour to develop a simple synthetic methodology from simple starting materials, In this chapter, the synthesis of **2-(2-*tert*-butyldiphenylsiloxy)phenyl-4,5-diphenyl-1-*p*-tolyl-1H-imidazole**, 2-(2-((*tert*-butyldiphenylsilyl) oxy)phenyl)-4,5-diphenyl-1H-imidazole and its sensing ability towards fluoride anion are discussed.^{65,66}

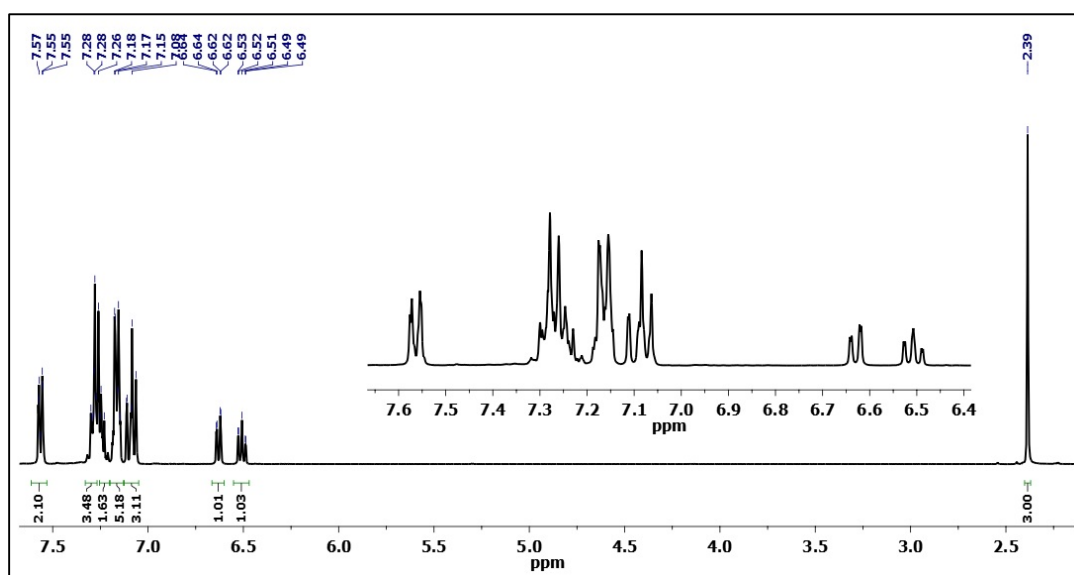
2.2 Results and discussion

2.2.1 Synthesis and Characterization of probe 1

First, we synthesized probe **1** as shown in scheme 2.1. The ESIPT imidazole compound **1a** was synthesized by a four component reaction involving cheap reagents, salicylaldehyde, toluidine, benzil, ammonium acetate in glacial acetic acid under reflux condition by a literature reported procedure⁶⁷. In a second step the targeted probe **1** was obtained by the reaction of compound **1a** with *tert*-butyl(chloro) diphenylsilane in presence of a base 1,8-diazabicyclo[5.4.0]undec-7-ene (DBU) in 82 % yield. The compound **1a** was characterized by ¹H, ¹³C, HRMS and by single crystal analysis. ¹H NMR spectrum of compound **1a** was recorded in CDCl₃. As shown in figure 2.1. Toly group resonates at δ 2.3 ppm and all aromatic protons appeared between δ 6.5-7.6 ppm. Single crystals of ESIPT imidazole compound **1a** shown in figure 2.5. Probe **1** was also characterized by multinuclear NMR analysis. When compared with compound **1a**, in the ¹H NMR spectra (figure 2.3) of probe **1**, the tolyl



Scheme 2.1: Synthetic route to probe 1.

Figure 2.1: ^1H NMR spectrum of compound 1a.

group resonated slightly upfield and a new peak appeared at δ 2.3 ppm, which represents the tert-butyl group.

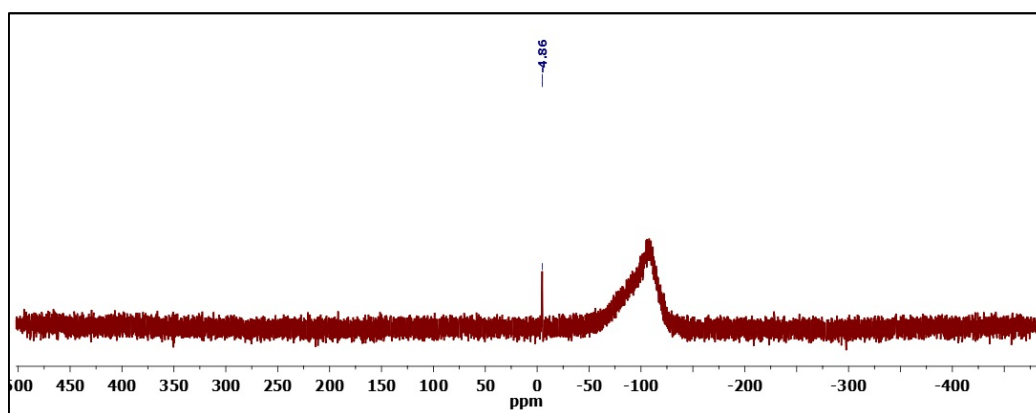


Figure 2.2: ^{29}Si NMR spectrum of compound **1**.

The silylation of probe **1** was also confirmed by ^{29}Si NMR spectra (figure 2.2) where probe **1** exhibited one peak at δ -4 ppm which is the characteristic peak for tetra coordinate silicon atom. HRMS of probe **1** is shown in figure 2.4. Single crystal was obtained by slow evaporation of compound **1** in dichloromethane and confirmed by XRD analysis (figure 2.5) and we also compared with its starting material compound **1a** (table 2.1). The starting material crystallizes in the triclinic space group $P\bar{1}$, whereas the probe **1** crystallizes in monoclinic space group $P2_1/n$. Compound **1a** shows an H-bonded, nearly planar conformation consisting of a central imidazole and two phenyl rings at the 1-and 2-positions. The ring twist between the imidazole and the phenyl ring at the 1-position (8.30°) is smaller than the ring twist between the imidazole and the phenyl ring at the 2-position (23.16°). The phenyl rings at the 1 & 5- positions of compound **1a** were severely twisted (84.8° & 83.7°). Upon silylation of the imidazole, a remarkable ring twist was observed for the phenyl ring at the 1-position of the probe **1** (88.9°). Probe **1** showed good solubility in organic solvents

like dichloromethane and THF. The probe **1** exhibited one absorption band at 273 nm and an emission band at 386 nm.

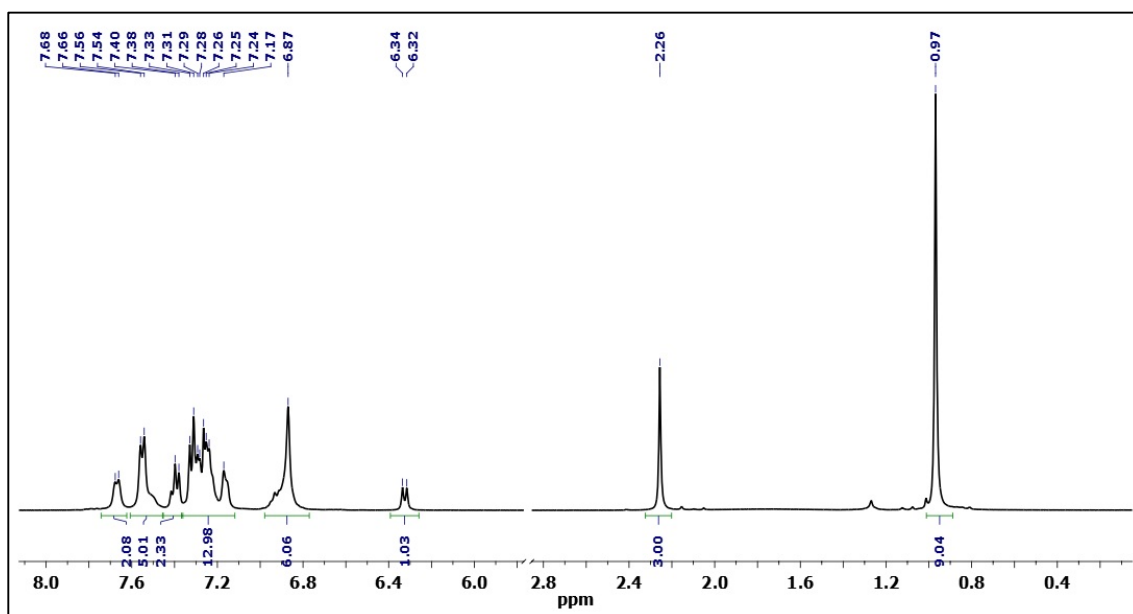


Figure 2.3: ^1H NMR spectrum of compound **1**.

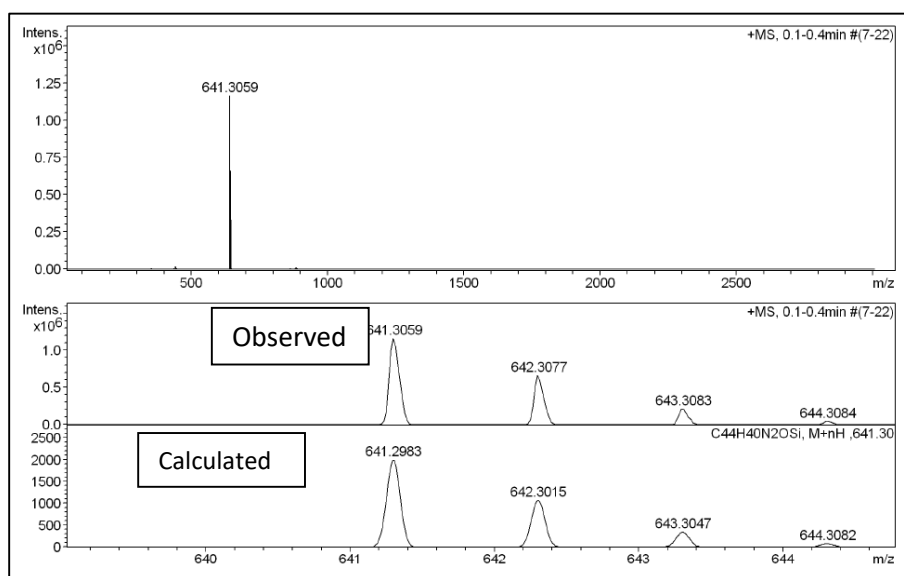


Figure 2.4: HRMS spectrum of compound **1**.

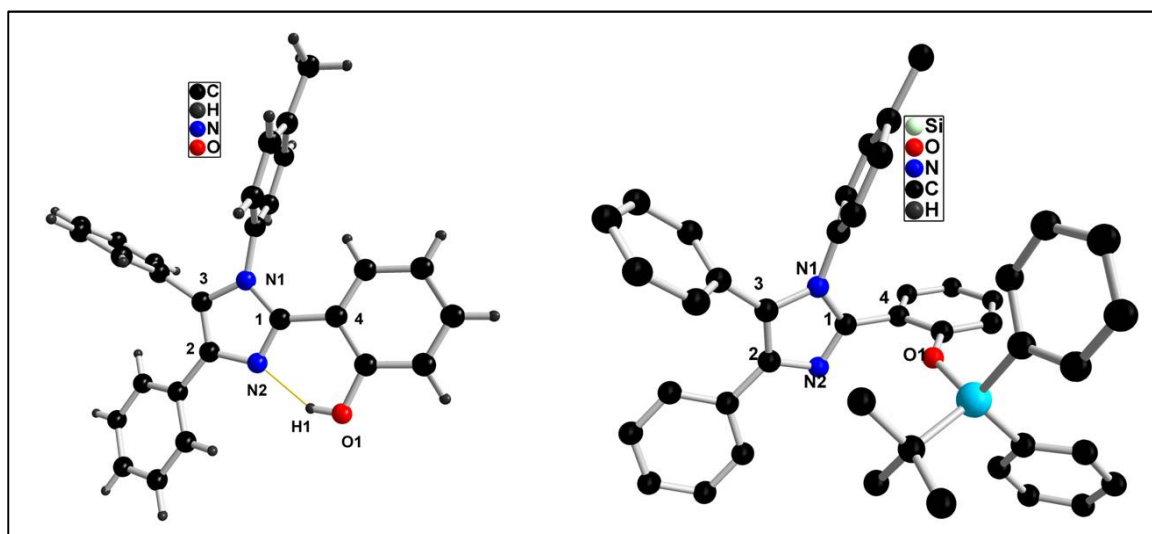


Figure 2.5: Molecular structure of compounds **1a** (left) and **1** (right). Hydrogen atoms are omitted for clarity.

Table 2.1: Selective bond angle and bond lengths of compounds **1a** and **1**.

Bond length (Å)	Compound 1a	Probe 1	Ring twist of phenyls around imidazole	Compound 1a	Probe 1
N1–C1	1.375(2)	1.370(2)	C-1	8.30 °	88.9 °
N1–C3	1.395(2)	1.391(2)	C-2	23.16 °	21.72 °
N2–C1	1.326(2)	1.311(2)	C-3	84.8 °	67.57 °
N2–C2	1.379(2)	1.383(2)	N-1	83.77 °	68.16 °
C2–C3	1.374(2)	1.376(3)			
C1–C4	1.468(2)	1.475(3)			
N2–H1	1.824	1.6461(14)			

Table 2.2: Crystal data and structure refinement parameters for compounds **1a** and **1**.

	1a	1
empirical formula	C ₂₈ H ₂₂ N ₂ O	C ₄₄ H ₄₀ N ₂ O Si
MW	402.48	640.87
T, K	296(2)	296(2)
wavelength, Å	0.71073 Å	0.71073 Å
crystal system	Triclinic	Monoclinic
space group	P-1	P2(1)/n
a/Å	10.0790(3)	14.8683(6)

b/Å	10.2068(3)	10.4772(4)
c/Å	10.6405(3)	23.5294(10)
$\alpha/^\circ$	89.314(2)	90
$\beta/^\circ$	76.447(2)	91.515(3)
$\gamma/^\circ$	86.532(2)	90
V/Å ³	1062.20(5)	3664.1(3)
Z	2	4
ρ_{calc} , g cm ⁻³	1.258	1.162
μ (MoK α), mm ⁻¹	0.077	0.100
F (000)	424	1360
θ range, deg	1.97 – 30.07	2.13 – 28.33
limiting indices	-13 \leq h \leq 14 -12 \leq k \leq 14 -14 \leq l \leq 14	-19 \leq h \leq 19 -13 \leq k \leq 13 -31 \leq l \leq 31
reflns collected	18495	55590
independent reflns	6183 [R(int) = 0.0477]	9104 [R(int) = 0.0814]
absorption correction	Semi-empirical from equivalents	Semi-empirical from equivalents
refinement method	Full-matrix least square on F ²	Full-matrix least square on F ²
data / restraints / parameters	6183 / 0 / 283	9104 / 0 / 438
Goodness-of-fit on F ²	0.971	0.995
final R indices [I > 2 σ (I)] ^[a]	R ₁ = 0.0608 wR ₂ = 0.1502	R ₁ = 0.0525 wR ₂ = 0.1243
R indices (all data) ^[a]	R ₁ = 0.1240 wR ₂ = 0.1882	R ₁ = 0.1277 wR ₂ = 0.1545
peak _{max} /hole _{min} (e Å ⁻³)	0.271 and -0.234	0.189 and -0.196
[a] R ₁ = $\Sigma F_o - F_c /\Sigma F_o $; wR ₂ = $\{\Sigma[w(F_o^2 - F_c^2)^2]/\Sigma[w(F_o^2)^2]\}^{1/2}$		

2.2.2 Probe 1 for fluoride ion sensing

In order to test the sensing ability of probe **1** in organic solvents, we added different quantities of tetra butyl ammonium fluoride and the response was estimated by absorption as well as emission spectroscopy. Upon gradual addition of fluoride ion to compound **1** in THF solution, results in the gradual formation of new absorption band at 318 nm (figure 2.6). As shown in figure 2.7 probe **1** displayed a ratiometric fluorescent behaviour to the fluoride ion. Probe **1** displayed maximum emission at

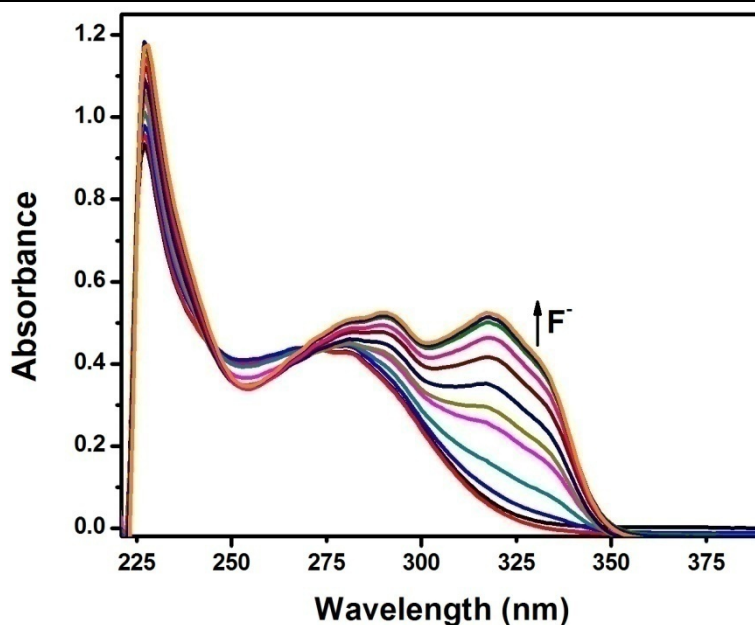


Figure 2.6: Absorption spectra of Probe **1** (24 μM) with different concentrations of F^- (0, 0.39, 0.78, 1.17, 1.56, 1.95, 2.34, 2.73, 3.12, 3.51, 3.90, 4.29, 4.68, 5.07, 5.46, 5.85, 6.24, 6.63, 9.36, 17.16 equiv.) in THF.

386 nm when excited at 278 nm. An emission titration was carried out by addition of small amounts of fluoride ion, the band intensity at 386 nm was steadily decreased with gradual appearance of a new band at 473 nm with an isoemission point at 436 nm, which clearly indicates the formation of new species. When fluoride ion was added we observed color changes of probe **1** from colorless to sky blue under hand held UV lamp. To further confirm the fluoride ion promoted selective Si-O bond cleavage, we tested the emission response of probe **1** with various other tetra butyl ammonium anions such as Cl^- , Br^- , NO_3^- , NO_2^- , AcO^- , HSO_4^- , and CN^- . As shown in figure 2.8, only F^- induced an immediate red shift in the emission maximum from 386 nm to 473 nm and all the other anions did not cause any emission intensity change at 473 nm. This result indicates that our probe **1** is very good sensor for recognizing fluoride ion over other anions through “off-on” mechanism.

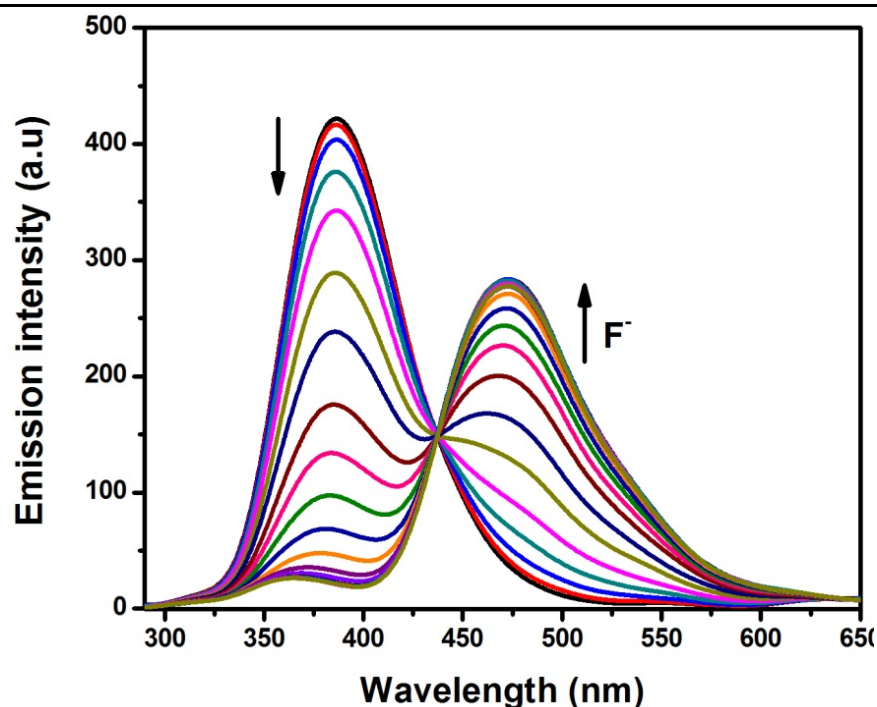


Figure 2.7: Fluorescence spectra of probe **1** (24 μM) with different concentrations of F^- (0, 0.39, 0.78, 1.17, 1.56, 1.95, 2.34, 2.73, 3.12, 3.51, 3.9, 4.29, 4.68, 5.07, 5.46, 5.85, 6.24, 6.63, 9.36, 17.16 equiv.) in THF when excited at 278 nm.

The excellent selectivity is attributed to the selective cleavage of the Si-O bond by fluoride ion (Scheme 2.2). It is known that ESIPT chromophores will show large Stokes' shifted emissions compared to non-ESIPT chromophores. As expected, probe **1** showed normal Stokes shifted emission, upon addition of fluoride ion selective cleavage of Si-O bond results in the formation of a desilylated product which is an ESIPT chromophore (compound **1a**). Mass spectrometry analysis confirmed the formation of the deprotected product. For further studies of the fluoride ion sensing ability of probe **1**, we carried out ^1H NMR titrations in CDCl_3 . Upon addition of TBAF the peaks at 2.26 ppm and 6.33 ppm were significantly downfielded. As shown in figure 2.9, the ^1H NMR spectra of the probe at the end of the titration was resemblance to ESIPT imidazole compound **1a**, which suggests that the desilylation reaction take places smoothly by the addition of fluoride anion. To gain insight of

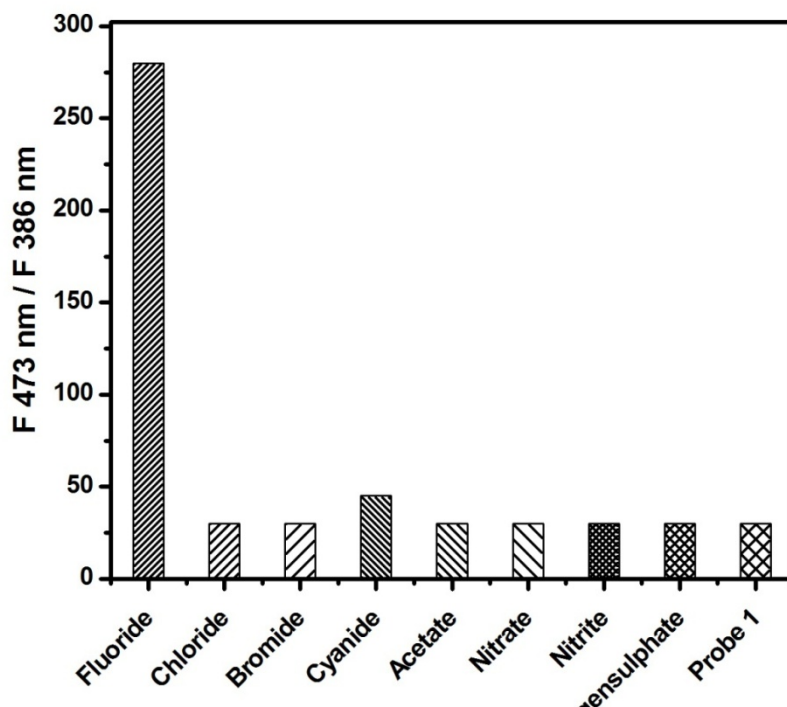
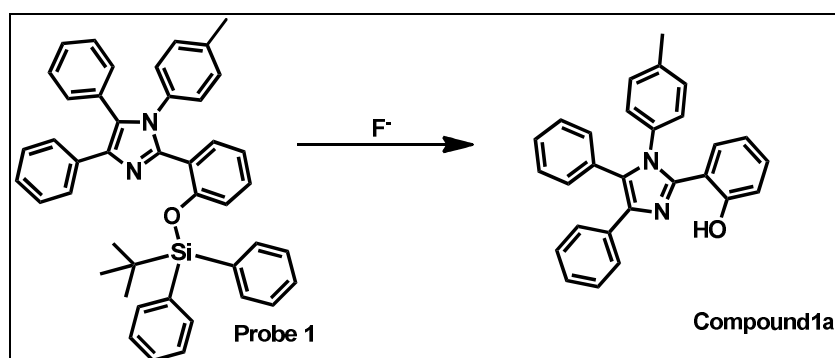


Figure 2.8: Emission changes of probe **1** (24 μM) between 386 and 473 nm with 15 equiv. of Cl^- , Br^- , CN^- , OAc^- , NO_2^- , NO_3^- , HSO_4^- , F^- .

optical properties of probe **1** and deprotected ESIPT imidazole, we performed DFT studies with the B3LYP exchange functional (6-31G (d) basis set) using Gaussian 03 programmes. Both product and compound **1a** were optimized and their structural parameters were compared with single crystal X-ray diffraction data. The calculation proves that the structural data parameters of probe **1** and compound **1a** are same as



Scheme 2.2: Sensing mechanism of the probe **1**

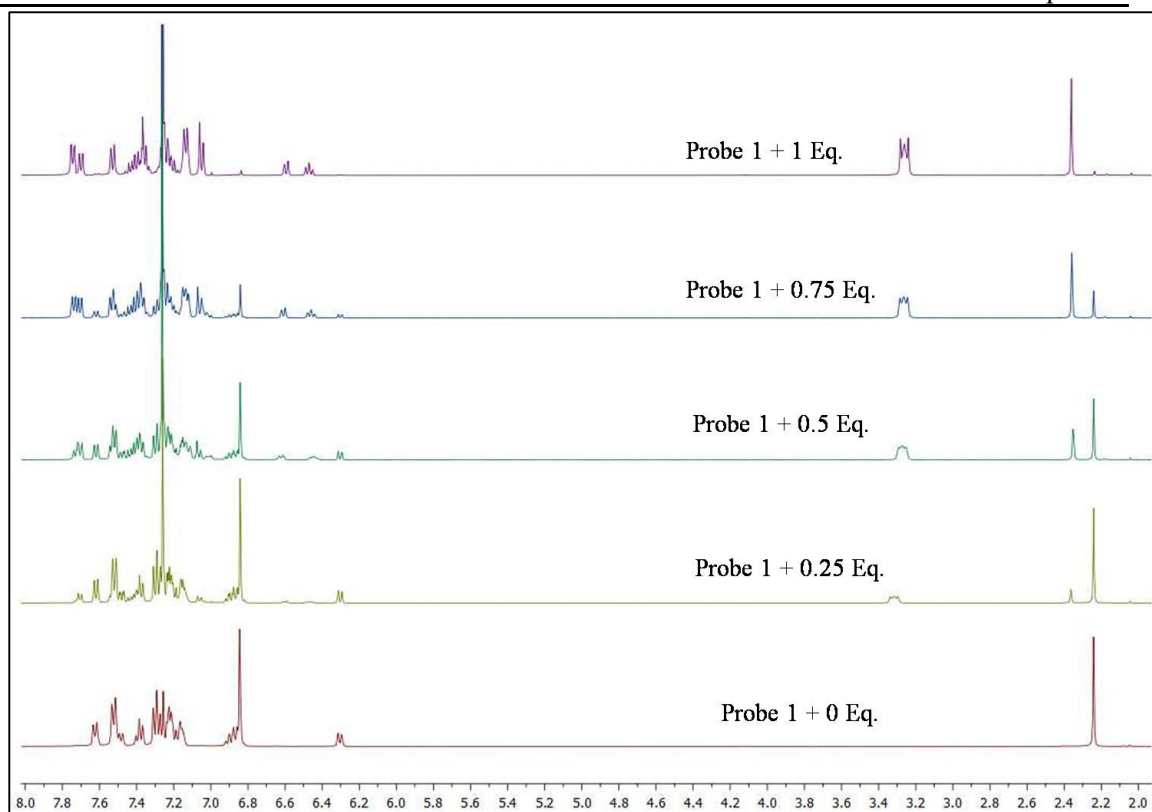


Figure 2.9: ^1H NMR titration spectra of **1** (16 mM) with 0.25, 0.50, 0.75 and 1.00 equivalents of F^- ions in CDCl_3 (bottom to top 0, 0.25...).

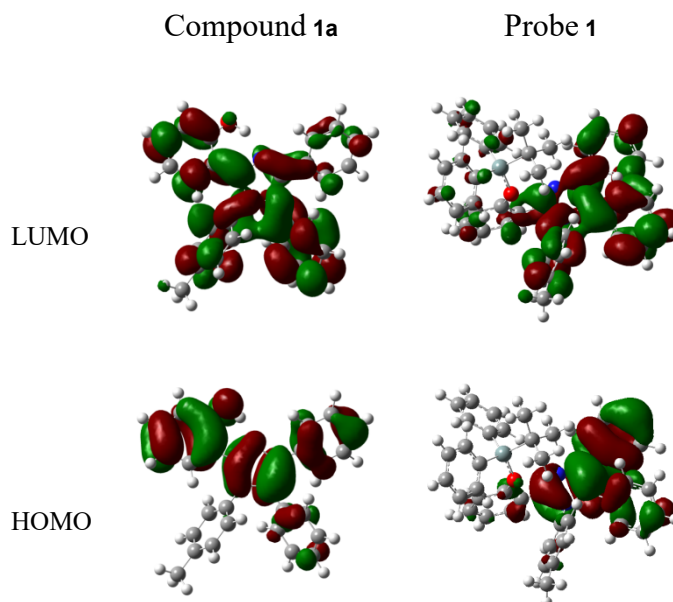
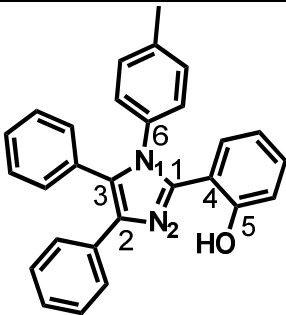
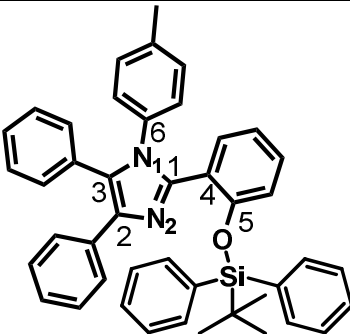


Figure 2.10: HOMO and LUMO diagrams of **1a** and **1** (contour value 0.02).

obtained by X-ray diffraction (table 2.3). We also performed time-dependent density functional theory (TD-DFT) calculations for probe **1** and compound **1a**. The calculations showed that, for both Probe **1** and compound **1a** the lowest energy transitions correspond to HOMO to the LUMO (oscillator strength $f= 0.23$ for **1** and $f= 0.19$ for **1a**). The DFT calculations reveals that the HOMO levels of probe **1**

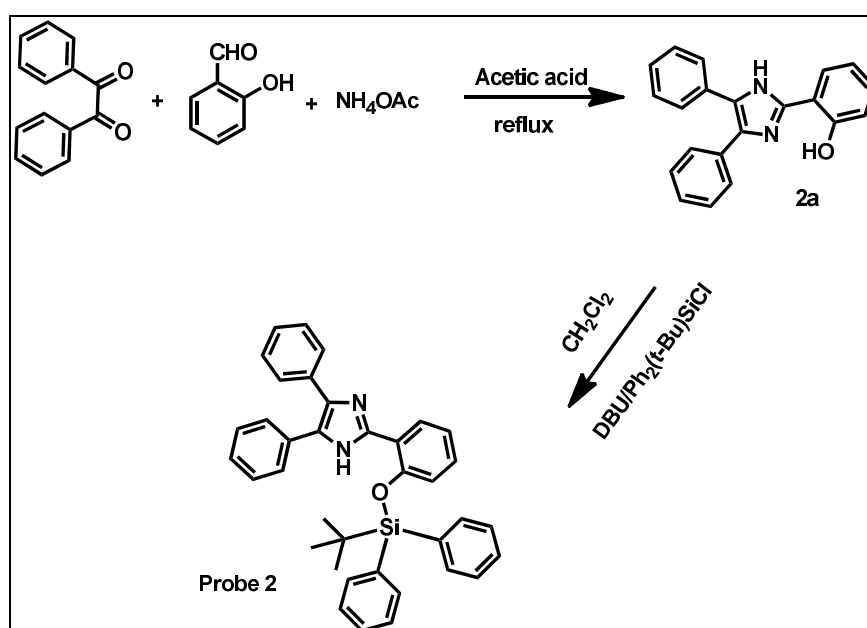
Table 2.3: Comparison of geometric parameters from DFT calculations and X-ray analysis of **1a** and **1**

Compound		DFT (Å)	X-ray(Å)
	N1-C1	1.3827	1.375(2)
	N1-C3	1.4036	1.395(2)
	N2-C1	1.3283	1.326(2)
	N2-C2	1.375	1.379(2)
	C2-C3	1.3847	1.374(2)
	O-C5	1.3462	1.356(2)
	C1-C4	1.4682	1.468(2)
	N1-C6	1.4345	1.445(2)
	N1-C1	1.3818	1.370(2)
	N1-C3	1.4001	1.391(2)
	N2-C1	1.3154	1.311(2)
	N2-C2	1.3814	1.383(2)
	C2-C3	1.3889	1.376(3)
	O-C5	1.3693	1.362(2)
	C1-C4	1.4817	1.475(3)
	N1-C6	1.4311	1.441(2)
	O-Si	1.6999	1.6461(14)

mainly contributed from imidazole ring and phenyl rings at the 4 & 5-position while the LUMO levels mainly situated on imidazole ring and phenyl rings at 1, 4 & 5-position. But in case of ES IPT imidazole (deprotected compound) the HOMO and LUMO levels contributed from extended conjugation between the imidazole and the phenyl ring at the 2-position (figure 2.10). DFT further reveals that the HOMO-LUMO gap of compound **1a** is reduced by 0.327 eV in comparison to that of the probe **1** and the LUMO level is lowered by 0.27 eV.

2.2.3 Synthesis and Characterization of probe 2

Although, the simple design of probe **1** for the detection of fluoride ion *via* ES IPT off-on mechanism was successfully employed in organic solvents, but failed to detect the fluoride ion in more polar solvents using sodium salts was unsuccessful. In order to improve the solubility of the sensor in more polar solvents, we introduced hydrophilic moieties. We made probe design much simpler by removing tolyl group on the 1-position of the imidazole (introduced NH functionality), which helped us to improve the solubility of the sensor in more polar solvents.



Scheme 2.3: Synthetic route to probe 2.

As shown in scheme 2.3, probe **2** was readily synthesized in good yields by the reaction of 2-(4,5-diphenyl-1H-imidazol-2-yl)phenol and *tert*-butyl(chloro)diphenylsilane in presence of a base diazabicyclo[5.4.0]undec-7-ene (DBU). The starting material 2-(4,5-diphenyl-1H-imidazol-2-yl)phenol (compound **2a**) was prepared by a multicomponent reaction using commercially available chemicals; salicylaldehyde, ammonium acetate and benzil following literature reported procedure. Probe **2** was fully characterized by ^1H , ^{13}C , ^{29}Si NMR and by HRMS analysis. The ^1H NMR spectrum of probe **2** (figure 2.11) showing a peak at δ 0.98 ppm corresponds to isopropyl group and another significant peak at δ 13.5 ppm represents the NH functionality. The characteristic peak at δ -2.89 ppm in ^{29}Si NMR corresponds to tetra coordinate silicon in probe **2** (figure 2.14).

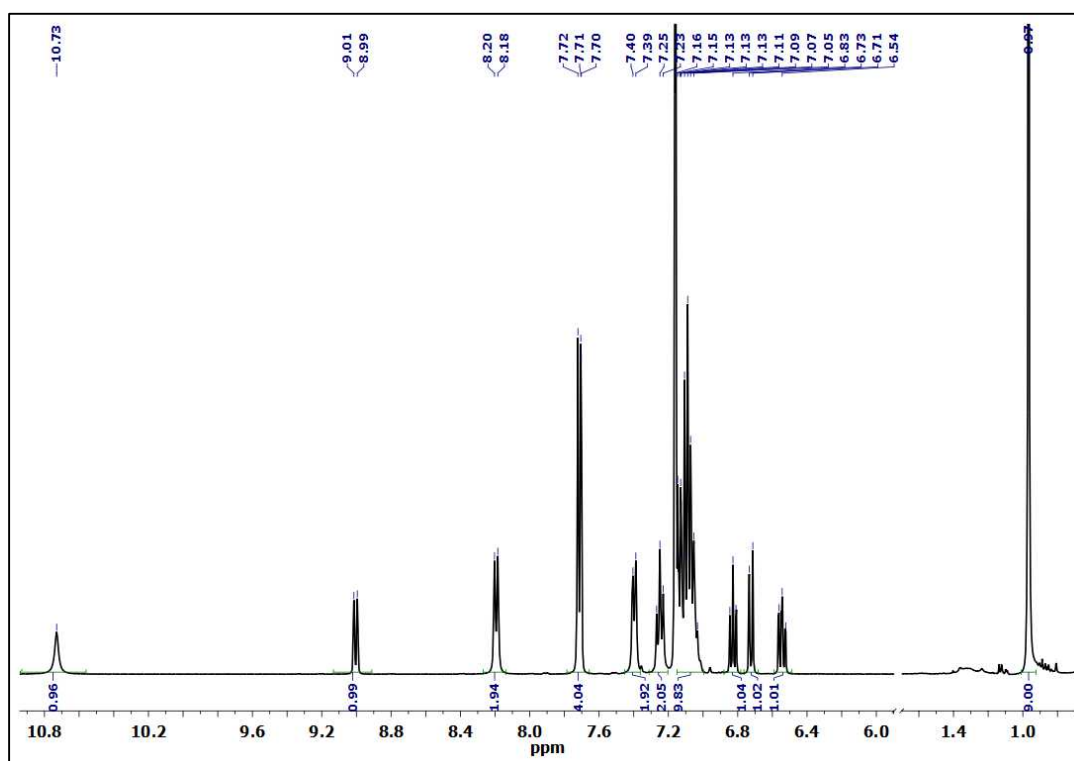


Figure 2.11: ^1H NMR spectrum of compound **2**.

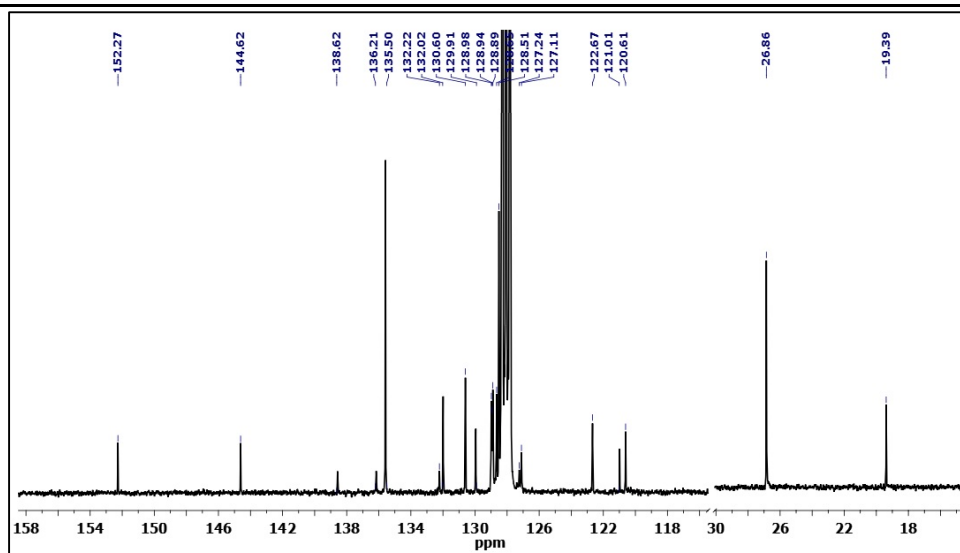


Figure 2.12: ^{13}C NMR spectrum of compound 2.

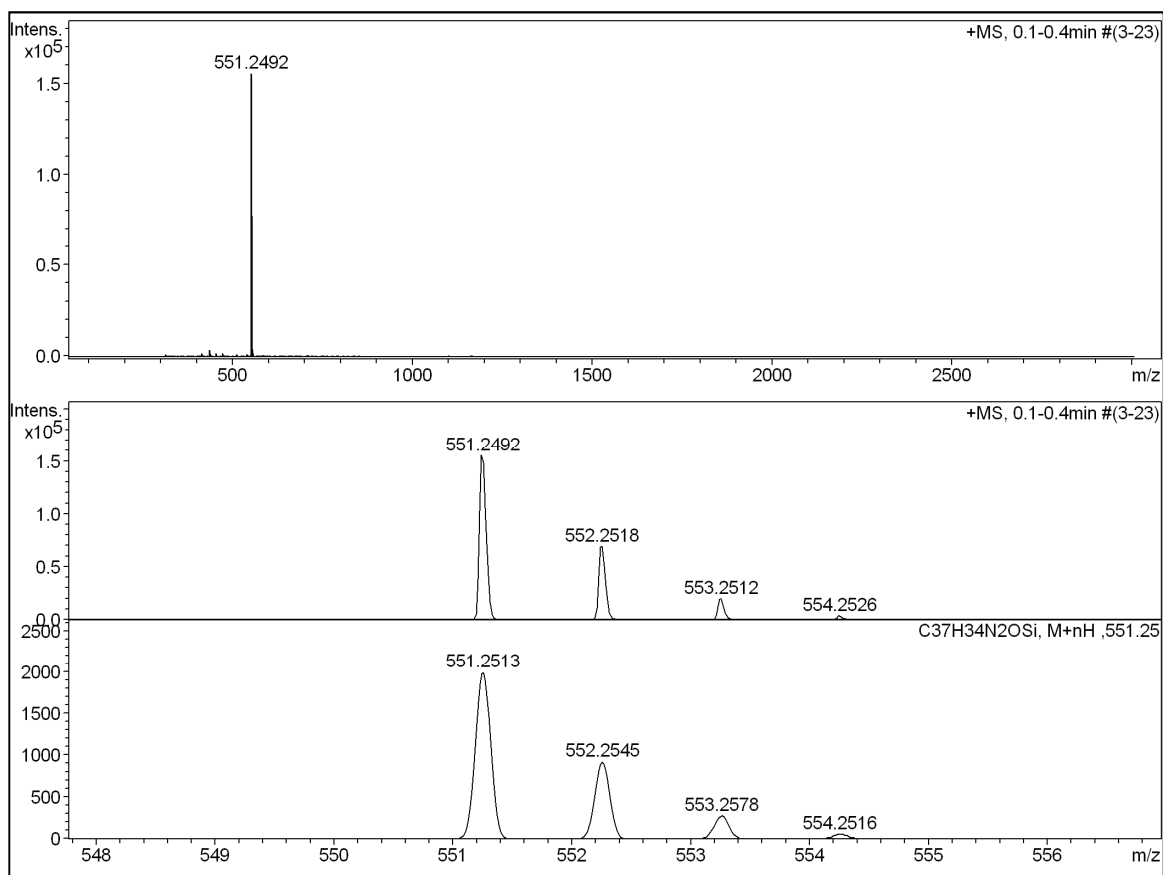


Figure 2.13: HRMS spectrum of compound 2.

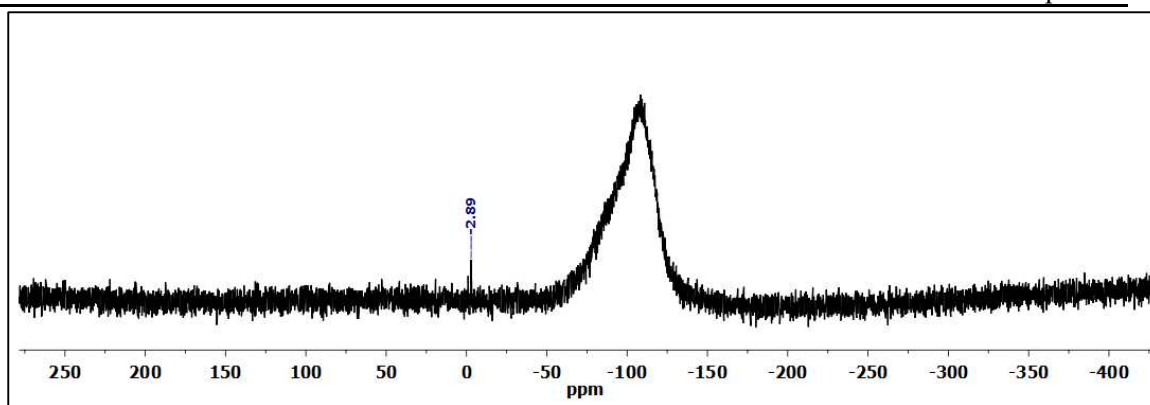


Figure 2.14: ^{29}Si NMR spectrum of compound **2**.

ESI-HRMS analysis of probe **2** shows parent ion peak at m/z 551.2513 ($[\text{M} + \text{H}]^+$) confirms the compound formation (figure 2.13). Single crystals of the probe **2** were grown from CH_2Cl_2 -hexane solvent and analyzed using single crystal X-ray diffraction study. Molecular structure of the probe **2** is shown in figure 2.15. The X-ray crystal data and structure refinement are provided in the table 2.4. Compound **2** crystallizes in monoclinic space group C2/c and the X-ray analysis of the probe reveals that the dihedral angle between the planes passing through central imidazole and the phenyl groups at 9- and 8- position are 30.01° and 42.59° respectively. The ring distortion between the imidazole and phenyl ring at the 7-position of the probe **2** (21.95°) is more pronounced when compared to its starting material (3.47°). The probe **2** showing good solubility in dichloromethane, THF and also in more polar solvents like DMSO. Probe **2** displayed absorption and emission band centres at 320 and 392 nm respectively in DMSO.

2.2.4 Probe **2** for fluoride ion sensing

We tested the sensing abilities of Probe **2** by absorption and also by emission spectroscopy. Initial studies were carried out in polar aprotic solvent DMSO. The probe **2** exhibited one absorption band at 302 nm. Addition of tetra-*n*-

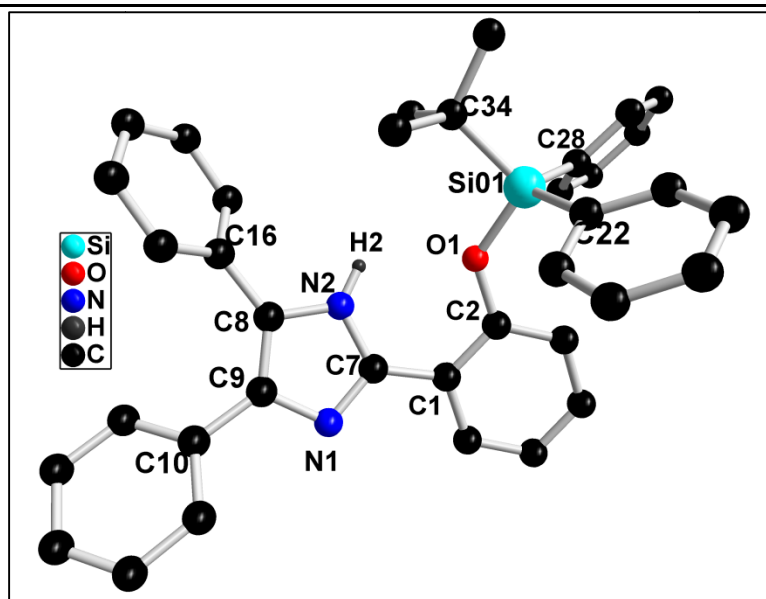


Figure 2.15: Molecular structure of compounds **2**. Hydrogen atoms are omitted for clarity.

Table 2.5: Crystal data and structure refinement parameters for compounds **2**.

	2
Empirical formula	C ₃₇ H ₃₄ N ₂ OSi
Formula weight	550.75
Temperature/K	296.15
Crystal system	monoclinic
Space group	C2/c
a/Å	35.2300(10)
b/Å	10.3909(3)
c/Å	19.4085(5)
$\alpha/^\circ$	90
$\beta/^\circ$	119.129(3)
$\gamma/^\circ$	90
V/Å ³	6206.3(3)
Z	8
$\rho_{\text{calc}}/\text{cm}^3$	1.179
μ/mm^{-1}	0.107
F(000)	2336.0
Radiation	MoK α ($\lambda = 0.71073$)
2 θ range for data collection/ $^\circ$	4.138 to 58.33
Index ranges	-48 \leq h \leq 47, -14 \leq k \leq 13, -26 \leq l \leq 26

Reflections collected	46921
Independent reflections	8361 [$R_{\text{int}} = 0.0499$, $R_{\text{sigma}} = 0.0365$]
Data/restraints/parameters	8361/0/373
Goodness-of-fit on F^2	1.056
Final R indexes [$I > 2\sigma(I)$]	$R_1 = 0.0515$, $wR_2 = 0.1319$
Final R indexes [all data]	$R_1 = 0.0868$, $wR_2 = 0.1513$
Largest diff. peak/hole / $e \text{ \AA}^{-3}$	0.32/-0.22

Table 2.4: Selective bond lengths of compounds **2**.

Atom	Length/ \AA
Si-O	1.6753(12)
Si-C28	1.8621(17)
Si-C22	1.8667(19)
O1-C2	1.3758(18)
N1-C7	1.3198(19)
N1-C9	1.3816(19)
N2-C8	1.378(2)
N2-C7	1.3556(18)
C7-C1	1.462(2)

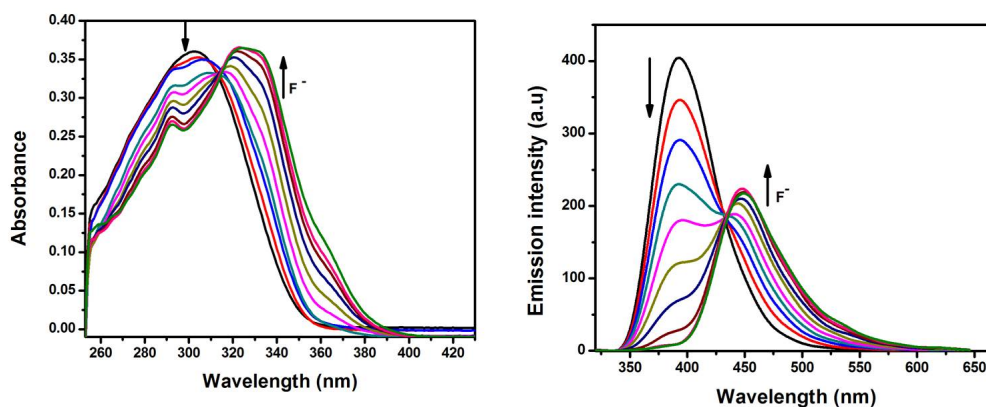


Figure 2.16: Absorption (left) and emission (right) spectra of probe **2** ($17.6 \mu\text{M}$) with the addition of TBAF (0, 0.15, 0.3, 0.45, 0.6, 0.75, 0.9, 1.05, 1.20, 1.35 equiv.) in DMSO.

butylammonium fluoride in DMSO results a gradual appearance of new absorption band at 327 nm (figure. 2.16). When excited at 302 nm, the probe **2** displayed a strong fluorescence at 392 nm. As shown in fig. 2.16, ratiometric fluorescence titration was carried out by introduction of fluoride ion, the band at 392 nm was steadily decreased

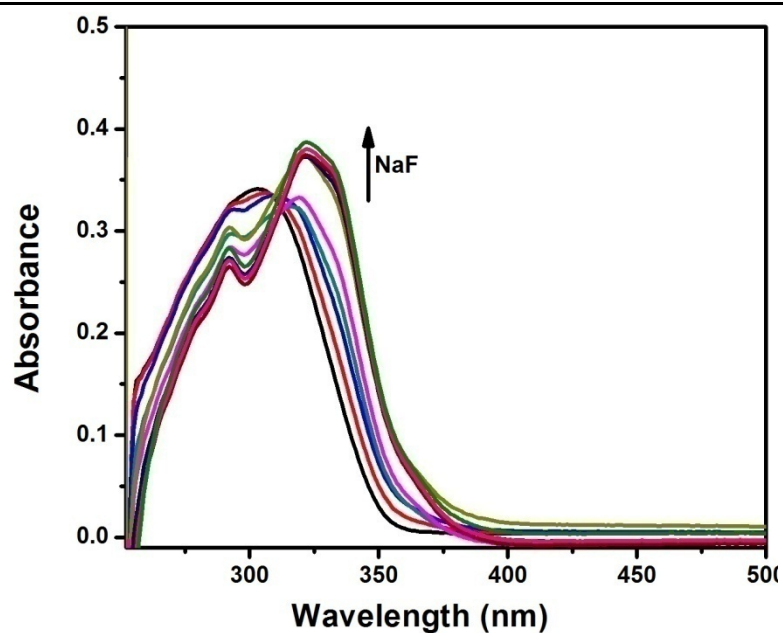


Figure 2.17: Absorption spectra of compound **2** (17.6 μM) in DMSO with the addition of NaF (0, 0.15, 0.3, 0.45, 0.6, 0.75, 0.9, 1.05, 1.20, 1.35 equiv. excited at 302 nm).

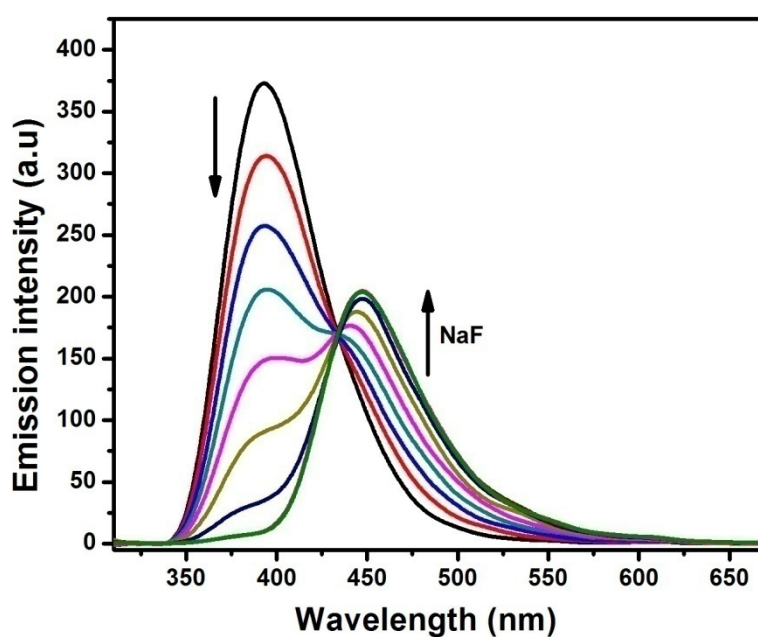


Figure 2.18: Emission spectra of compound **2** (17.6 μM) in DMSO with the addition of NaF (0, 0.15, 0.3, 0.45, 0.6, 0.75, 0.9, 1.05, 1.20, 1.35 equiv. excited at 302 nm).

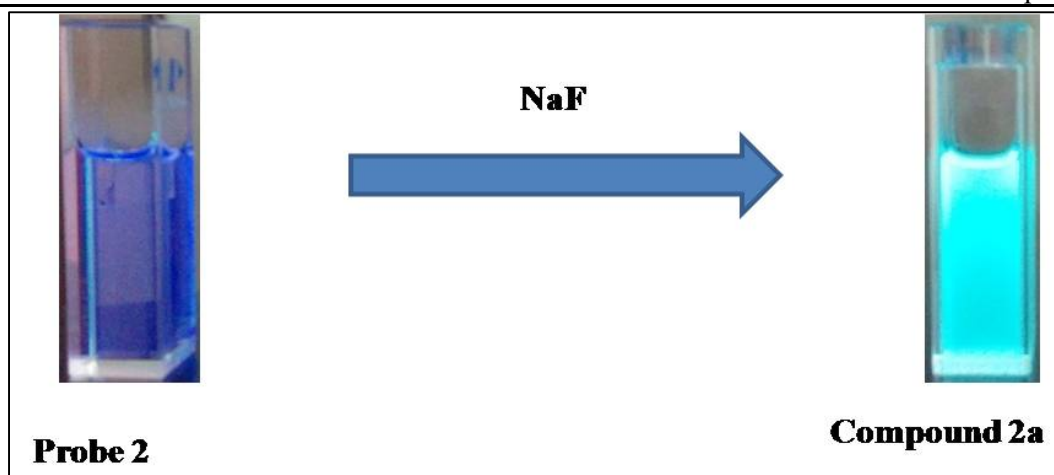


Figure 2.19: Fluorescence changes of probe **2** upon addition of NaF^- under hand held UV lamp of 365 nm.

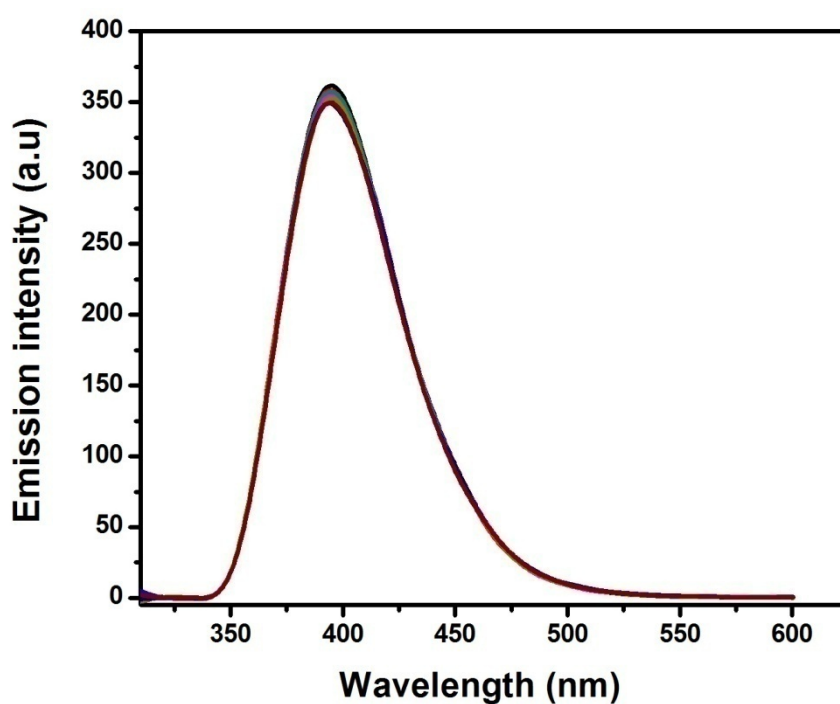


Figure 2.20: Emission spectra of probe **2** ($17.6 \mu\text{M}$) in DMSO/ H_2O with time interval 0, 20, 40, 60, 80, 100, 120, 140 minutes (excited at 301 nm).

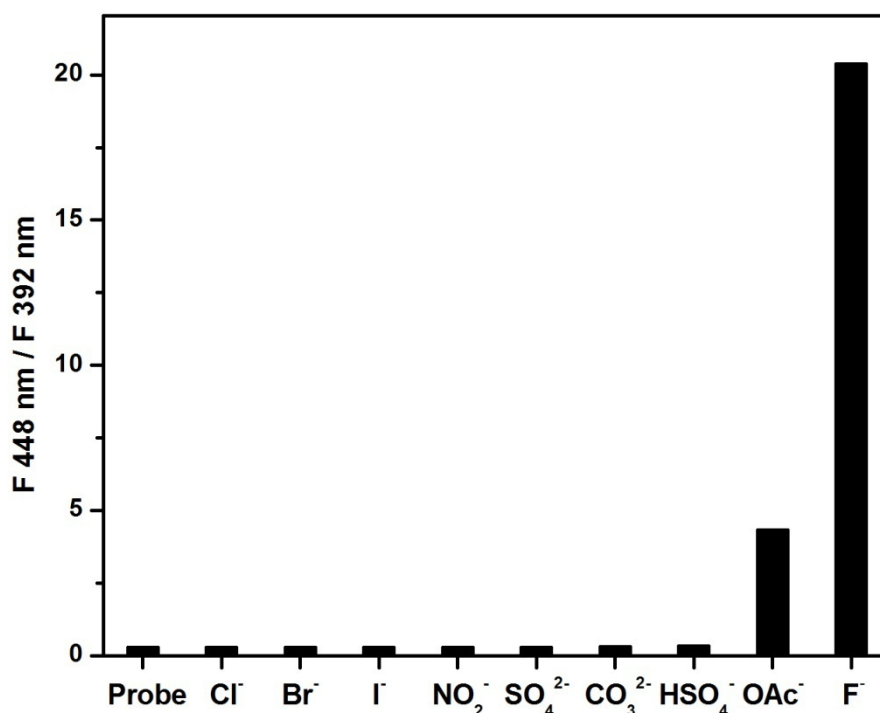


Figure 2.21: Fluorescence emission changes of compound **2** (17.6 μ M) between 448 and 392nm in DMSO with the addition of one equivalent of different anions (F⁻, Cl⁻, Br⁻, I⁻, CO₃²⁻, SO₄²⁻, NO₂⁻, OAc⁻, HSO₃⁻, HCO₃⁻) of sodium salts in water.

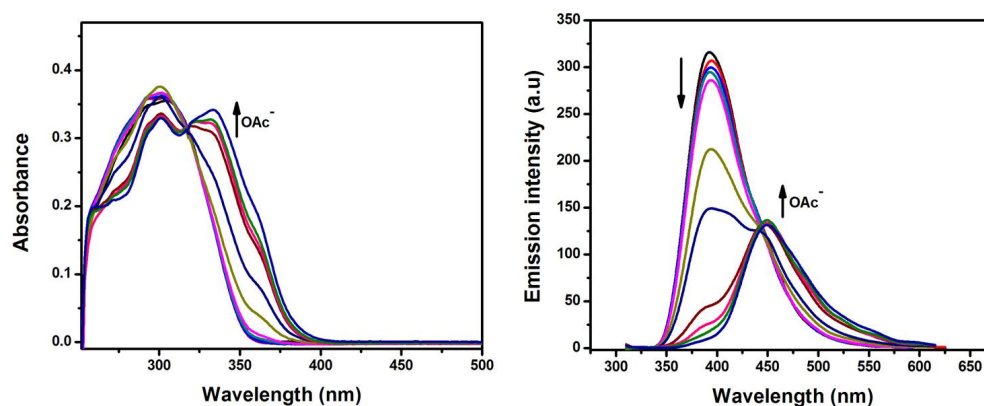


Figure 2.22: Absorption (left) and emission (right) spectra **2** (17.6mM) with addition of TBOAc⁻ (0, 0.2, 0.4, 0.6, 0.8, 1.6, 3.2, 4.8, 5.6, 6.4, 8.4 equiv.) in DMSO.

with simultaneous appearance of a new band at 448 nm. A clear isoemission point at 433 nm was established, which indicates the creation of new species. After addition of 1 equivalent of fluoride ion the band at 392 nm was fully saturated and the resultant emission band was superimposable with its imidazole emission (starting material),

which clearly indicates the triggering of ESIPT emission with large Stoke shift (56 nm). The probe was insoluble in water and DMSO mixture. In order to judge the sensing ability of fluoride anion in aqueous medium, small portions of sodium fluoride in water was added to the probe in DMSO solution, the resultant UV-visible and emission spectra were recorded which were reminiscent to those observed in DMSO using tetra-*n*-butylammonium fluoride (figure 2.17 and figure 2.18). Figure 2.19 represents the naked eye colour changes of the probe **2** under UV lamp. In order to check the stability, the solution of probe **2** (43 μM) was evaluated by its emission spectra with varying time (figure 2.20). Probe **2** results in no changes of emission intensity even after 3 hours, proves its stability under experimental conditions. As expected our new probe achieved excellent selective emission response, through ESIPT off-on mechanism towards sodium fluoride anion, unlike other anions Cl^- , Br^- , I^- , CO_3^{2-} , SO_4^{2-} , NO_2^- , OAc^- , HSO_3^- , HCO_3^- which showed no emission changes (figure 2.21). However, when we added more than one equivalent of OAc^- anion, a gradual appearance of new bands at 327 nm and 448 nm in the absorption and fluorescence spectra respectively were observed (figure 2.22). ^1H NMR experiment was performed to investigate the species formed at the end of addition of fluoride. As shown in figure 2.23, upon sequential addition of fluoride ion, a gradual disappearance of peaks corresponding to the probe was observed.

2.3 Conclusions

In conclusion, we have rationally designed and synthesized novel ESIPT-based ratiometric fluorescent sensors from simple synthetic starting materials. The probes which are non-ESIPT chromophores gave normal Stokes' shifted emission however, upon addition of the fluoride ion, probes got converted to ESIPT active chromophores produces large Stokes' shifted emission. The probes exhibit high fluoride ion

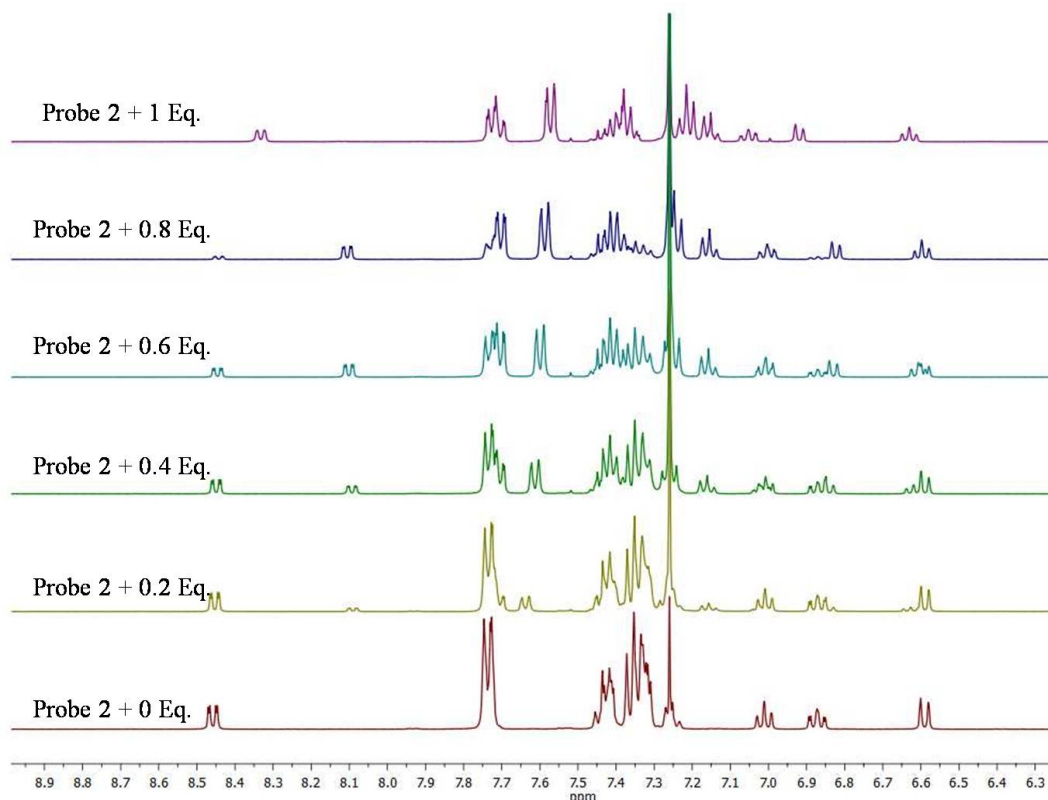


Figure 2.23: ^1H NMR spectral changes of the probe **2** (21.8 mM) with addition of 0, 0.2, 0.4, 0.6, 0.8, and 1 equivalent of F^- respectively from bottom to top.

selectivity over various other anions in organic solvents, which is due to the strong affinity of the fluoride ion toward silicon. Importantly in case of probe **2** we could also be able to detect inorganic fluoride and acetate anion in DMSO-water system. The optical response of the probe **1** was rationalized using density functional theory and time-dependent density function theory calculation. We expect that the unique ES IPT character of the imidazole will be useful to construct a wide variety of ratiometric sensors based on the ES IPT signalling mechanism.

2.4 Experimental section

2.4.1 General information

Benzil, salicylaldehyde, *p*-toluidine and ammonium acetate were received from Sigma-Aldrich. *tert*-butyl(chloro)diphenylsilane and 1,8-diazabicyclo[5.4.0]undec-7-

ene (DBU) were purchased from Alfa-Aesar. Acetic acid and dichloromethane (DCM), dimethyl sulfoxide (DMSO), tetrahydrofuran (THF) were obtained from Spectrochem India. All tetra butyl ammonium, sodium and potassium salts of anions were used and obtained from Sigma-Aldrich. Dichloromethane and DMSO were dried using calcium hydride and distilled and stored in over 4Å molecular sieve prior to use. Tetrahydrofuran (THF) was initially distilled over KOH, followed by distillation over sodium metal (using benzophenone). Deionized water was from Millipore. ^1H NMR (400 MHz), ^{13}C NMR (100 MHz), ^{29}Si NMR (79.49 MHz), spectra were recorded on a Bruker ARX 400 spectrometer operating at 400 MHz. All ^1H and ^{13}C NMR spectra were referenced internally to residual solvent signals namely chloroform (δ 7.26 ^1H ; δ 77.16 ^{13}C in ppm), benzene (δ 7.16 ^1H ; δ 128.06 ^{13}C in ppm), DMSO (δ 2.5 ^1H ; δ 39.52 ^{13}C in ppm). ^{29}Si NMR spectra were referenced externally to TMS in CDCl_3 (δ = 0). All NMR spectra were recorded at ambient temperature. Chemical shifts are reported in ppm (δ); multiplicities are indicated by s (singlet), d (doublet), t (triplet), q (quartet), m (multiplet) dd (doublet of doublet) and br (broad). Coupling constants, J, are reported in Hertz. Melting points (mp) were determined on a Fischer John's melting point apparatus and are uncorrected. Elemental analyses were carried out by using a Thermo quest CE instrument model EA/110 CHNS-O elemental analyzer. ESI mass spectra were recorded on Bruker, microTOF-QII mass spectrometer. Infrared (IR) spectrum of compounds was recorded on Perkin Elmer FT-IR spectrometer in solid state using KBR pellet, spectrum RXI. UV-Visible spectra were recorded on Perkin-Elmer Lambda 750 UV/Visible spectrometer. The fluorescence spectra were recorded with a Perkin-Elmer LS-55 Fluorescence spectrometer and corrected for the instrumental response. The raw data collected were analyzed using Origin Pro 8 software. Distilled solvents were used for all photophysical studies.

Single crystal X-ray diffraction data were collected on Bruker APEX-II CCD diffractometer at 296 K using Mo-K α radiation ($\lambda = 0.71073 \text{ \AA}$). The structures were solved by direct methods using shelXT program and refined with least squares minimization with shelXL⁶⁸ using Olex2⁶⁹. All non-hydrogen atoms were refined with anisotropic displacement coefficients. The H- atoms were assigned at calculated positions and were refined as riding atoms. Crystal data for compounds **1a**, **1**, **2** has been deposited in Cambridge Crystallographic Data Centre with CCDC-1019160, CCDC-1019161 and CCDC- 1429413 respectively. DFT calculations were performed with the Gaussian03 program.⁷⁰ Excitation data were determined using TD-DFT (B3LYP) calculations.

2.4.2 Synthetic procedure and spectral characterization

Synthesis of 2-(4,5-diphenyl-1-*p*-tolyl-1H-imidazol-2-yl)phenol (**1a**)

Benzil (3.00 g, 14.27 mmol) and salicylaldehyde (1.52 mL, 14.27 mmol) were taken in acetic acid, to this mixture toluidine (1.68 g, 15.69 mmol) and ammonium acetate (1.64 g, 21.40 mmol) were added subsequently and refluxed for 24 h. Later the reaction mixture was cooled to room temperature and then water was added, the obtained precipitate was collected by filtration. The white solid was recrystallized from ethyl acetate to get the pure product. Yield: 3.70 g, 65 %. ¹H NMR (400 MHz, CDCl₃): $\delta = 2.39$ (s, 3H, ArCH₃), 6.48-6.53 (m, 1H, ArH), 6.63 (dd, J=8.0 & 1.6 Hz, 1H, ArH), 7.05-7.12 (m, 3H, ArH), 7.13-7.19 (m, 5H, ArH), 7.20-7.25 (m, 2H, ArH), 7.27-7.32 (m, 4H, ArH), 7.54-7.59 (m, 2H, ArH). ¹³C NMR (100 MHz, CDCl₃): $\delta = 21.39$ (Ar-CH₃), 113.08, 117.89, 118.11, 126.40, 127.10, 127.22, 128.39, 128.42, 128.59, 129.85, 130.18, 130.33, 130.66, 131.46, 132.87, 134.38, 134.86, 139.40, 144.99, 158.48 (ArC). IR (KBr): ν (cm⁻¹) = 3056(m), 3030(w), 2849(w), 2644(w),

1902(m), 1601(m), 1587(s), 1499(s), 1483(s), 1414(s), 1383(s), 1293(s), 1256(m), 1165(m), 1105(s), 1044(s), 971(s), 821(s), 722(m), 694(m), 537(m). HRMS (ESI): calcd. for $C_{28}H_{22}N_2O$ ($[M + H]^+$) : 403.1805, found : 403.1859. Elemental analysis calcd (%) for $C_{28}H_{22}N_2O$: C 83.56, H 5.51, N 6.96; found: C 83.61, H 5.65, N 6.81.

Synthesis of Probe, 2-(2-*tert*-butyldiphenyl siloxy)phenyl-4,5-diphenyl-1-*p*-tolyl-1H-imidazol (1)

To a solution of imidazole (0.6 g, 1.49 mmol) in dichloromethane, 1,8-diazabicyclo[5.4.0]undec-7-ene (DBU) (0.44 mL, 2.98 mmol) was added at -20 °C and stirred for 20 min. at this temperature, then *tert*-butyl(chloro)diphenylsilane (0.77 mL, 2.98 mmol) was added and the solution was allowed to warm up to room temperature and stirred at the same temperature for 12 h. After water workup, the organic layer was separated and dried over sodium sulphate and concentrated using rotary evaporator. The product was separated by silica gel column chromatography using ethyl acetate and hexanes mixture as the eluent. Yield: 0.79 g, 82.5 %. m.p. 203-205 °C. 1H NMR (400 MHz, $CDCl_3$): δ = 0.96 (s, 9H, Si- CH_3), 2.26 (s, 3H, Ar- CH_3), 6.33 (d, $J=8.0$ Hz, 1H, ArH), 6.77-7.00 (m, 6H, ArH), 7.15 (d, $J=7.0$ Hz, 2H, ArH), 7.19-7.25 (m, 2H, ArH), 7.26-7.35 (m, 7H, ArH), 7.40 (t, $J=7.0$ Hz, 2H, ArH), 7.44-7.61 (m, 5H, ArH), 7.62-7.80 (m, 2H, ArH), ^{13}C NMR (100 MHz, $CDCl_3$): δ = 19.63 (Si- CH_3), 21.22 (Ar- CH_3), 26.64 (C- CH_3), 119.24, 120.69, 123.28, 126.44, 127.74, 127.78, 127.83, 128.17, 128.47, 129.08, 129.75, 129.96, 130.13, 131.08, 131.26, 132.39, 132.70, 134.10, 135.07, 135.57, 137.33, 137.86, 145.79, 154.36 (ArC). ^{29}Si NMR (79.49 MHz, $CDCl_3$): δ = -4.86. IR (KBr): ν (cm^{-1}) = 3070(m), 2931(m), 2893(m), 2857(s), 1604(m), 1575(m), 1502(s), 1471(m), 1443(m), 1428(m), 1395(s), 1367(s), 1284(s), 1256(s), 1107(s), 961(s), 928(s), 824(s), 757(s) 748(m), 614(s), 500(s). HR-MS (ESI): calcd. for $C_{44}H_{40}N_2OSi$ ($[M + H]^+$) : 641.2983, found :

641.3059. Elemental analysis calcd (%) for $C_{44}H_{40}N_2OSi$: C 82.46, H 6.29, N 4.37; found: C 82.23, H 6.41, N 4.28. 1H NMR (400 MHz, C_6D_6): δ = 1.1 (s, 9H, CH_3), 1.75 (s, 3H, Ar CH_3) 6.55 (d, $J=8.0$ Hz, 3H, ArH), 6.58-6.65 (m, 2H, ArH), 6.92-7.03 (m, 5H, ArH), 7.08 (t, $J=8.0$ Hz, 1H, ArH), 7.17(m, 6H, ArH) 7.23 (t, $J=8.0$ Hz, 2H, ArH), 7.34 (d, $J=8.0$ Hz, 2H, ArH), 7.45-7.47 (m, 1H, ArH), 7.76-7.78 (m, 4H, ArH), 8.18 (d, $J=8.0$ Hz, 2H, ArH) . ^{13}C NMR (100 MHz, C_6D_6): δ = 20.16 (Si- CH_3), 21.11 (Ar- CH_3), 27.09 (Ar- CH_3), 120.03, 121.27, 124.83, 127.10, 128.30, 128.46, 128.53, 128.91, 129.10, 129.67, 130.52, 131.84, 132.60, 133.01, 133.58, 135.22, 136.28, 136.48, 137.69, 139.06, 146.26, 155.34 (ArC). ^{29}Si NMR (79.49 MHz, C_6D_6): δ = -4.80.

Synthesis of 2-(2-hydroxyphenyl)-4, 5-diphenyl-1H-imidazole (2a)

Benzil (1.50 g, 7.13 mmol), salicylaldehyde (0.76 mL, 7.13 mmol) and ammonium acetate (1.64 g, 21.40 mmol) were taken in acetic acid, and refluxed for 12 h. Later the reaction mixture was cooled to room temperature and then water was added, the obtained precipitate was collected by filtration. The white solid was recrystallized from ethyl acetate to get the pure product. Yield: 1.89 g, 85 %. 1H NMR (400 MHz, C_6D_6): δ 13.29 (bS, 1H), 8.36 (S, 1H), 7.74 (S, 2H), 7.30 (d, $J = 8$ Hz, 1H), 7.13 – 6.99 (m, 8H), 6.69 (d, $J = 4$ Hz, 2H). HR-MS (ESI): calcd. for $C_{21}H_{17}N_2O$ ($[M + H]^+$): 313.1335, found: 313.1347.

Synthesis of 2-(2-((tert-butyldiphenylsilyl)oxy)phenyl)-4,5-diphenyl-1H-imidazole (2)

Under nitrogen atmosphere in a two neck round bottom flask, imidazole (0.38 g, 1.24 mmol) was taken in dichloromethane, to this solution DBU (0.37 mL, 2.48 mmol) was added at -10 °C and stirred for 20 min., at this temperature, *tert*-butyl(chloro)diphenylsilane (0.64 mL, 2.48 mmol) was added and warmed up to room

temperature and stirred for overnight. Water was added, the organic layer was extracted and dried over sodium sulphate and concentrated using rotary evaporator. The product was separated by silica gel (100-200 mesh) column chromatography using ethyl acetate in hexane as eluent. Yield: 0.41 g (60 %). m.p. 97-100 °C. ^1H NMR (400 MHz, C_6D_6): δ = 0.97 (s, 9H, CH_3), 6.54 (t, J = 8 Hz, 1H, ArH), 6.72 (d, J = 8 Hz, 1H, ArH), 6.83 (t, J = 8 Hz, 1H, ArH), 7.03-7.15 (m, 10H, ArH), 7.25 (t, J = 8 Hz, 2H, ArH), 7.40 (d, J = 4 Hz, 2H, ArH), 7.71 (d, 4H, ArH), 8.19 (d, J = 8 Hz, 2H, ArH), 9.00 (d, J = 8 Hz, 1H, ArH) 10.73 (s, 1H, ArNH) ppm. ^{13}C NMR (100 MHz, C_6D_6): δ = 19.39 ($-\text{CH}_3$), 26.85 (C- CH_3), 120.61, 120.98, 122.67, 127.11, 127.24, 128.51, 128.65, 128.89, 128.94, 128.98, 129.95, 130.60, 131.99, 132.22, 135.58, 136.16, 138.57, 144.62, 152.27 ppm. ^{29}Si NMR (79.49 MHz, C_6D_6): δ = -2.89 ppm. IR (KBr): $\nu(\text{cm}^{-1})$ = 3069(m), 2952(s), 2928(m), 2859(s), 1952(b), 1885(b), 1602(s), 1583(m), 1527(m), 1467(s), 1232(s), 1114(s), 1095(m), 892(s), 820(s), 698(s). HR-MS (ESI): calcd. for $\text{C}_{37}\text{H}_{34}\text{N}_2\text{OSi}$ ($[\text{M} + \text{H}]^+$): 551.2513, found: 551.2492.

2.5 References

- (1) Martinez-Manez, R.; Sancenon, F. *Chem. Rev. (Washington, DC, U. S.)* **2003**, *103*, 4419.
- (2) Kubik, S. *Chem. Soc. Rev.* **2010**, *39*, 3648.
- (3) Gunnlaugsson, T.; Glynn, M.; Tocci, G. M.; Kruger, P. E.; Pfeffer, F. M. *Coord. Chem. Rev.* **2006**, *250*, 3094.
- (4) Newbrun, E. *J. Public Health Dent.*, **2010**, *70*, 227.
- (5) Horowitz, H. S. *J. Public Health Dent.*, **2003**, *63*, 3.
- (6) Kumari, N.; Jha, S.; Bhattacharya, S. *J. Org. Chem.*, **2011**, *76*, 8215.
- (7) Madhuprasad; Shetty, A. N.; Trivedi, D. R. *RSC Adv.* **2012**, *2*, 10499.

-
- (8) Thiagarajan, V.; Ramamurthy, P.; Thirumalai, D.; Ramakrishnan, V. T. *Org. Lett.* **2005**, *7*, 657.
- (9) Veale, E. B.; Gunnlaugsson, T. *J. Org. Chem.* **2008**, *73*, 8073.
- (10) Zhang, H.; Hu, J.; Qu, D.-H. *Org. Lett.* **2012**, *14*, 2334.
- (11) Bozdemir, O. A.; Sozmen, F.; Buyukcakir, O.; Guliyev, R.; Cakmak, Y.; Akkaya, E. U. *Org. Lett.* **2010**, *12*, 1400.
- (12) Vadavi, R. S.; Kim, H.; Lee, K. M.; Kim, T.; Lee, J.; Lee, Y. S.; Lee, M. H. *Organometallics* **2012**, *31*, 31.
- (13) Misra, A.; Shahid, M.; Dwivedi, P.; Srivastava, P.; Ali, R.; Razi, S. S. *ARKIVOC (Gainesville, FL, U. S.)* **2013**, 133.
- (14) Kim, T.-H.; Swager, T. M. *Angew. Chem., Int. Ed.* **2003**, *42*, 4803.
- (15) Xue, M.; Wang, X.; Wang, H.; Chen, D.; Tang, B. *Chem. Commun. (Cambridge, U. K.)* **2011**, *47*, 4986.
- (16) Xu, W.; Liu, S.; Sun, H.; Zhao, X.; Zhao, Q.; Sun, S.; Cheng, S.; Ma, T.; Zhou, L.; Huang, W. *J. Mater. Chem.* **2011**, *21*, 7572.
- (17) Hu, J.; Zhang, G.; Geng, Y.; Liu, S. *Macromolecules (Washington, DC, U. S.)* **2011**, *44*, 8207.
- (18) Tan, W.; Zhang, D.; Zhu, D. *Bioorg. Med. Chem. Lett.* **2007**, *17*, 2629.
- (19) Kolos, R.; Grabowski, Z. R. *J. Mol. Struct.* **1982**, *84*, 251.
- (20) Peng, X.; Wu, Y.; Fan, J.; Tian, M.; Han, K. *J. Org. Chem.* **2005**, *70*, 10524.
- (21) Wu, Y.; Peng, X.; Fan, J.; Gao, S.; Tian, M.; Zhao, J.; Sun, S. *J. Org. Chem.* **2007**, *72*, 62.
- (22) Goswami, S.; Das, A. K.; Manna, A.; Maity, A. K.; Fun, H.-K.; Quah, C. K.; Saha, P. *Tetrahedron Lett.* **2014**, *55*, 2633.
- (23) Chen, J.-S.; Zhou, P.-W.; Zhao, L.; Chu, T.-S. *RSC Adv.* **2014**, *4*, 254.
-

-
- (24) Kanagaraj, K.; Pitchumani, K. *Chem. - Asian J.* **2014**, *9*, 146.
- (25) Liu, K.; Huo, J.; Zhu, B.; Huo, R. *J. Fluoresc.* **2012**, *22*, 1231.
- (26) Wang, F.; Wu, J.; Zhuang, X.; Zhang, W.; Liu, W.; Wang, P.; Wu, S. *Sens. Actuators, B* **2010**, *146*, 260.
- (27) Yang, X.-F.; Qi, H.; Wang, L.; Su, Z.; Wang, G. *Talanta* **2009**, *80*, 92.
- (28) Jung, H. S.; Kim, H. J.; Vicens, J.; Kim, J. S. *Tetrahedron Lett.* **2009**, *50*, 983.
- (29) Chu, Q.; Medvetz, D. A.; Pang, Y. *Chem. Mater.* **2007**, *19*, 6421.
- (30) Elmes, R. B. P.; Gunnlaugsson, T. *Tetrahedron Lett.* **2010**, *51*, 4082.
- (31) Wade, C. R.; Broomsgrove, A. E. J.; Aldridge, S.; Gabbai, F. P. *Chem. Rev. (Washington, DC, U. S.)* **2010**, *110*, 3958.
- (32) Zhao, S.-B.; McCormick, T.; Wang, S. *Inorg. Chem.* **2007**, *46*, 10965.
- (33) Kim, S. K.; Bok, J. H.; Bartsch, R. A.; Lee, J. Y.; Kim, J. S. *Org. Lett.* **2005**, *7*, 4839.
- (34) Gai, L.; Chen, H.; Zou, B.; Lu, H.; Lai, G.; Li, Z.; Shen, Z. *Chem. Commun. (Cambridge, U. K.)* **2012**, *48*, 10721.
- (35) Song, Q.; Bamesberger, A.; Yang, L.; Houtwed, H.; Cao, H. *Analyst (Cambridge, U. K.)* **2014**, *139*, 3588.
- (36) Hudnall, T. W.; Chiu, C.-W.; Gabbai, F. P. *Acc. Chem. Res.* **2009**, *42*, 388.
- (37) Hudson, Z. M.; Wang, S. *Acc. Chem. Res.* **2009**, *42*, 1584.
- (38) Yamaguchi, S.; Akiyama, S.; Tamao, K. *J. Am. Chem. Soc.* **2001**, *123*, 11372.
- (39) Hu, R.; Feng, J.; Hu, D.; Wang, S.; Li, S.; Li, Y.; Yang, G. *Angew. Chem., Int. Ed.* **2010**, *49*, 4915.
- (40) Kim, S. Y.; Park, J.; Koh, M.; Park, S. B.; Hong, J.-I. *Chem. Commun. (Cambridge, U. K.)* **2009**, 4735.
- (41) Cao, J.; Zhao, C.; Feng, P.; Zhang, Y.; Zhu, W. *RSC Adv.* **2012**, *2*, 418.
-

-
- (42) Zhu, B.; Yuan, F.; Li, R.; Li, Y.; Wei, Q.; Ma, Z.; Du, B.; Zhang, X. *Chem. Commun. (Cambridge, U. K.)* **2011**, *47*, 7098.
- (43) Bao, Y.; Liu, B.; Wang, H.; Tian, J.; Bai, R. *Chem. Commun. (Cambridge, U. K.)* **2011**, *47*, 3957.
- (44) Ren, J.; Wu, Z.; Zhou, Y.; Li, Y.; Xu, Z. *Dyes Pigm.* **2011**, *91*, 442.
- (45) Cao, J.; Zhao, C.; Zhu, W. *Tetrahedron Lett.* **2012**, *53*, 2107.
- (46) Kim, T.-H.; Swager, T. M. *Angew. Chem., Int. Ed.* **2003**, *42*, 4803.
- (47) Bellina, F.; Cauteruccio, S.; Monti, S.; Rossi, R. *Bioorg. Med. Chem. Lett.* **2006**, *16*, 5757.
- (48) Vlahakis, J. Z.; Hum, M.; Rahman, M. N.; Jia, Z.; Nakatsu, K.; Szarek, W. A. *Bioorg. Med. Chem.* **2009**, *17*, 2461.
- (49) Bhandari, K.; Srinivas, N.; Marrapu, V. K.; Verma, A.; Srivastava, S.; Gupta, S. *Bioorg. Med. Chem. Lett.* **2010**, *20*, 291.
- (50) Chen, X.; Kang, S.; Kim, M. J.; Kim, J.; Kim, Y. S.; Kim, H.; Chi, B.; Kim, S.-J.; Lee, J. Y.; Yoon, J. *Angew. Chem., Int. Ed.* **2010**, *49*, 1422.
- (51) Coll, C.; Ros-Lis, J. V.; Martinez-Manez, R.; Marcos, M. D.; Sancenon, F.; Soto, J. J. *Mater. Chem.* **2010**, *20*, 1442.
- (52) Ge, Z.; Hayakawa, T.; Ando, S.; Ueda, M.; Akiike, T.; Miyamoto, H.; Kajita, T.; Kakimoto, M.-a. *Chem. Mater.* **2008**, *20*, 2532.
- (53) Lai, M.-Y.; Chen, C.-H.; Huang, W.-S.; Lin, J. T.; Ke, T.-H.; Chen, L.-Y.; Tsai, M.-H.; Wu, C.-C. *Angew. Chem., Int. Ed.* **2008**, *47*, 581.
- (54) Fang, Z.; Wang, S.; Zhao, L.; Xu, Z.; Ren, J.; Wang, X.; Yang, Q. *Mater. Chem. Phys.* **2008**, *107*, 305.
- (55) Chen, C.-H.; Huang, W.-S.; Lai, M.-Y.; Tsao, W.-C.; Lin, J. T.; Wu, Y.-H.; Ke, T.-H.; Chen, L.-Y.; Wu, C.-C. *Adv. Funct. Mater.* **2009**, *19*, 2661.
-

-
- (56) Kim, S.; Chang, D. W.; Park, S. Y.; Kawai, H.; Nagamura, T. *Macromolecules* **2002**, *35*, 2748.
- (57) Park, S.; Kwon, O.-H.; Kim, S.; Park, S.; Choi, M.-G.; Cha, M.; Park, S. Y.; Jang, D.-J. *J. Am. Chem. Soc.* **2005**, *127*, 10070.
- (58) Kwon, J. E.; Park, S. Y. *Adv. Mater. (Weinheim, Ger.)* **2011**, *23*, 3615.
- (59) Lim, S.-J.; Seo, J.; Park, S. Y. *J. Am. Chem. Soc.* **2006**, *128*, 14542.
- (60) Nayak, M. K. *J. Photochem. Photobiol., A* **2012**, *241*, 26.
- (61) Kim, T.-I.; Kang, H. J.; Han, G.; Chung, S. J.; Kim, Y. *Chem. Commun. (Cambridge, U. K.)* **2009**, 5895.
- (62) Jung, H. S.; Kim, H. J.; Vicens, J.; Kim, J. S. *Tetrahedron Lett.* **2009**, *50*, 983.
- (63) Xu, Y.; Pang, Y. *Chem. Commun. (Cambridge, U. K.)* **2010**, *46*, 4070.
- (64) Xu, Z.; Xu, L.; Zhou, J.; Xu, Y.; Zhu, W.; Qian, X. *Chem. Commun. (Cambridge, U. K.)* **2012**, *48*, 10871.
- (65) Dhanunjayarao, K.; Mukundam, V.; Venkatasubbaiah, K. *J. Mater. Chem. C.* **2014**, *2*, 8599.
- (66) Dhanunjayarao, K.; Mukundam, V.; Venkatasubbaiah, K. *Sens. Actuators, B* **2016**, *232*, 175.
- (67) Park, S.; Kwon, O.-H.; Kim, S.; Park, S.; Choi, M.-G.; Cha, M.; Park, S. Y.; Jang, D.-J. *J. Am. Chem. Soc.* **2005**, *127*, 10070.
- (68) Sheldrick, G. M. *Acta Crystallogr. Sect. A: Found. Crystallogr.* **2007**, *64*, 112.
- (69) Dolomanov, O. V.; Bourhis, L. J.; Gildea, R. J.; Howard, J. A. K.; Puschmann, H. *J. Appl. Crystallogr.* **2009**, *42*, 339.
- (70) M. J. Frisch, G. W. T., H. B. Schlegel, G. E. Scuseria, M. A. Robb, J. R. Cheeseman, G. Scalmani, V. Barone, B. Mennucci, G. A. Petersson, H. Nakatsuji, M. Caricato, X. Li, H. P. Hratchian, A. F. Izmaylov, J. Bloino, G. Zheng, J. L.

Sonnenberg, M. Hada, M. Ehara, K. Toyota, R. Fukuda, J. Hasegawa, M. Ishida, T. Nakajima, Y. Honda, O. Kitao, H. Nakai, T. Vreven, J. J. A. Montgomery, J. E. Peralta, F. Ogliaro, M. Bearpark, J. J. Heyd, E. Brothers, K. N. Kudin, V. N. Staroverov, R. Kobayashi, J. Normand, K. Raghavachari, A. Rendell, J. C. Burant, S. S. Iyengar, J. Tomasi, M. Cossi, N. Rega, N. J. Millam, M. Klene, J. E. Knox, J. B. Cross, V. Bakken, C. Adamo, J. Jaramillo, R. Gomperts, R. E. Stratmann, O. Yazyev, A. J. Austin, R. Cammi, C. Pomelli, J. W. Ochterski, R. L. Martin, K. Morokuma, V. G. Zakrzewski, G. A. Voth, P. Salvador, J. J. Dannenberg, S. Dapprich, A. D. Daniels, Ö. Farkas, J. B. Foresman, J. V. Ortiz, J. Cioslowski and D. J. Fox *Gaussian 09 (Rev. C.02)*, Gaussian, Inc., Wallingford CT **2009**.

CHAPTER 3A

Imidazole based *N,O*- chelate boron compounds for the selective detection of picric acid

3A.1 Introduction	99
3A.1.1 Importance of Picric acid	99
3A.1.2 <i>N,O</i> - Chelate tetra coordinate boron compounds	100
3A.2 Results and discussion	101
3A.2.1 Synthesis and characterization	101
3A.2.2 Photophysical properties	107
3A.2.3 <i>N,O</i> - Chelate boron compounds for PA detection	107
3A.3 Conclusions	116
3A.4 Experimental section	117
3A.4.1 General procedures	117
3A.4.2 Synthetic procedure and spectral characterization	118
3A.5 References	121

3A.1 Introduction

3A.1.1 Importance of Picric acid

Polynitrated organic compounds such as trinitrotoluene (TNT), trinitro tri aza cyclohexane (RDX), 2,4,6-trinitrophenol (TNP) are highly explosive and used during

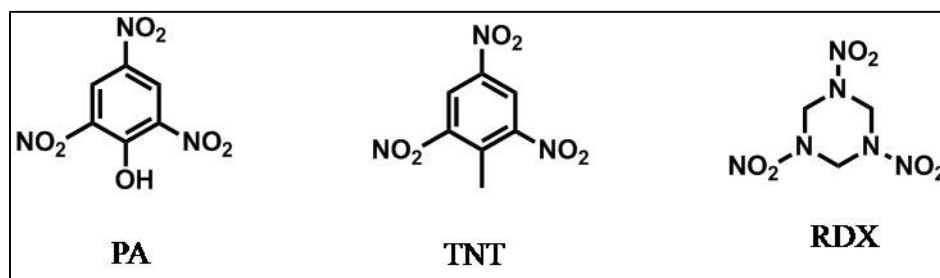


Figure 3A.1: Examples of nitro explosives

world war I and II¹. Among them PA is a widely used explosive because of its superior power compared to TNT.^{2,3} As an explosive, picric acid played an important role; The French used PA as a burst charge for shells under the name of melinite. During the Russo-Japanese war, picric acid was most widely used as a military explosive. Besides its explosive nature, picric acid has been used in optical metallography to reveal prior austenite grain boundaries in ferritic steels and also to etch magnesium alloys, such as AZ31. PA has also been used in clinical chemistry, histology specimens, skin dye, manufacturing rocket fuels, fireworks, matches, dyes, and pharmaceuticals, etc.^{4,5}

PA is water soluble, its extensive use may increase the possibility to be released to the environment, which can finally lead to water and soil pollution. It is an environmentally hazardous chemical and potentially harmful for wildlife and human health.⁶ PA causes skin and eye irritation in contact. Overexposure of PA can produce lung damage, anemia, carcinogenicity, unconsciousness, or death.⁷ Therefore, the detection of PA to avoid terrorist attacks and environmental pollution has been a

matter of concern for scientists. Although several instrumental techniques have been developed⁸⁻¹¹ and used to detect nitroaromatics such as ion mobility spectrometry (IMS), gas chromatography with mass spectrometry (GC-MS), electrochemical methods, surface-enhanced Raman spectroscopy, etc., however, they suffer from high cost, sophisticated protocols, on-field use issues and low selectivity, which limit their practical applications. Recently, fluorescent-based chemodosimeters are gaining attention for the detection of PA owing to their low cost, simplicity, high sensitivity and selectivity.¹² Recently many fluorescent PA sensors have been developed and studied extensively, including small molecular dyes,¹²⁻¹⁵ conjugated polymers,¹⁶⁻¹⁹ fluorescent metal-organic frameworks (MOF),²⁰⁻²² and fluorescent nanomaterials.^{23,24} Although a large number of reports for the detection of polynitroaromatics are available, synthesis of an effective, highly selective, and reliable chemosensor for the detection of PA remains a challenging task because of unavoidable interference from TNT, DNT, and so on.^{3,25}

3A.1.2 *N,O*- Chelate tetra coordinate boron copounds

Tri- and tetracoordinate boron complexes²⁶ have received overwhelming interest because of their applications in various fields like organic-light-emitting diodes, photovoltaics, organic field-effect transistors, and sensor materials. Tunable photophysical properties and better fluorescence quantum yields have made the boron compounds suitable for widespread use in the construction of sensors for different anions such as fluoride, cyanide, and so on.^{27,28} Recently, two approaches have been reported for the detection of PA using boron dipyrromethene (BODIPY) as the fluorophore signaling unit.^{29,30} (figure 3A.2)

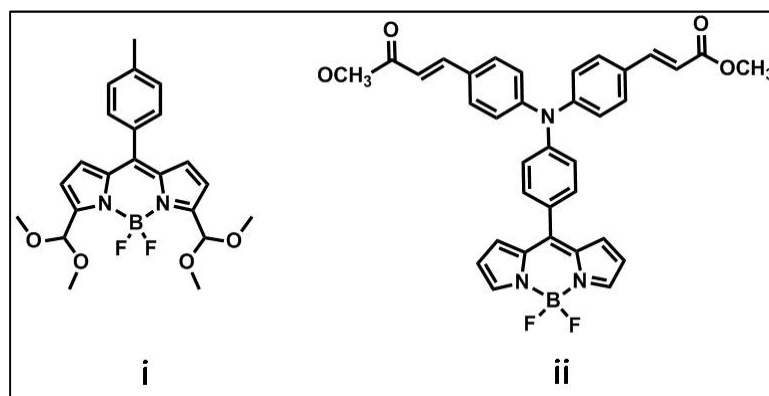


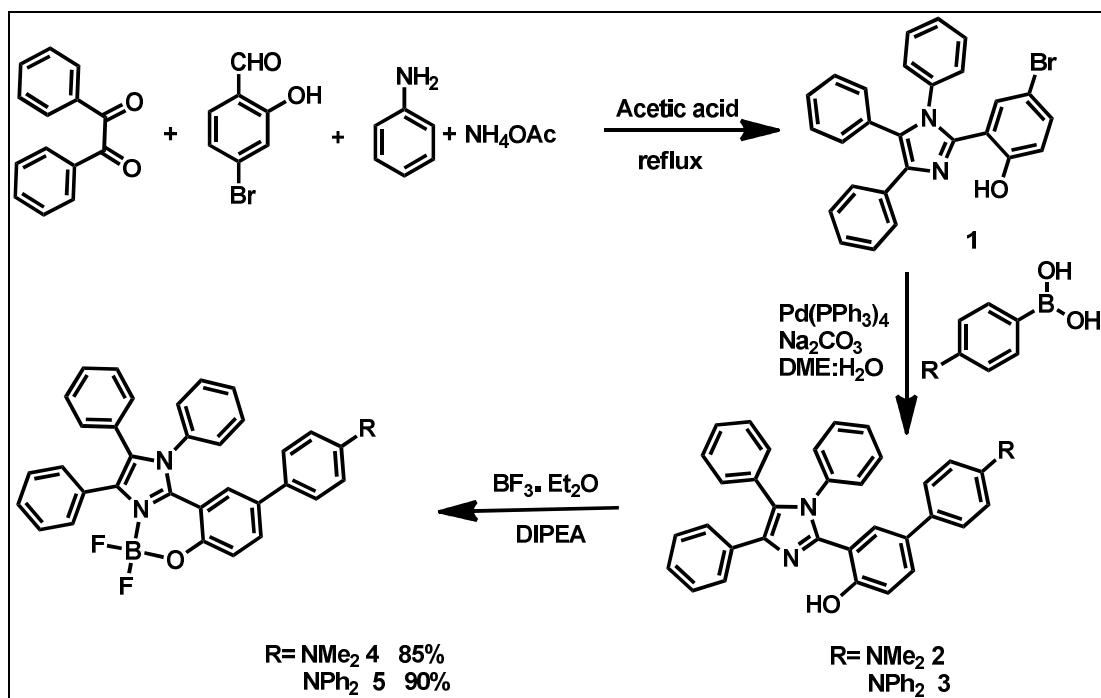
Figure 3A.2: BODIPY based sensors for PA detection

One of the reports demonstrates PA detection without selectivity, while the other report illustrates high sensitivity and selectivity. However, in both instances, structural evidence of the adduct formed between PA and BODIPY is not reported. Considering these factors, we have designed two imidazole-based boron complexes with N,N-dimethylamine and N,N-diphenylamine units at the 4-position of the biphenyl group (scheme 3A.1) for the detection of PA. Although imidazole-based N,O-chelated boron complexes have been studied for their application in electronic materials^{31,32}, they have not yet been explored for the detection of explosives especially PA. Herein, we explored a very efficient and highly selective PA sensor derived from imidazole-based boron complexes.³³

3A.2 Results and Discussions

3A.2.1 Synthesis and characterization of *N,O*-Chelate boron compounds

The *N,O*-chelate imidazole boron complexes **4** and **5** were synthesized in three steps as shown in scheme 3A.1. Firstly bromophenol-substituted imidazole **1** was prepared by four component reaction using bromosalicylaldehyde, aniline, benzil and ammonium acetate under reflux condition in acetic acid according to known reported procedure.^{34,35}



Scheme 3A. 1: Synthetic route to N,O chelate imidazole boron compounds 4 and 5

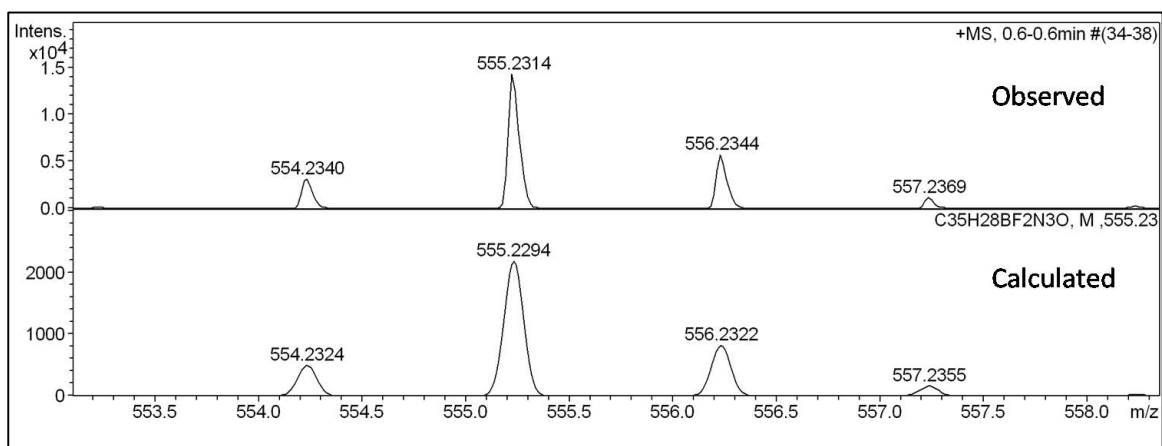


Figure 3A.3: HRMS of compound 4

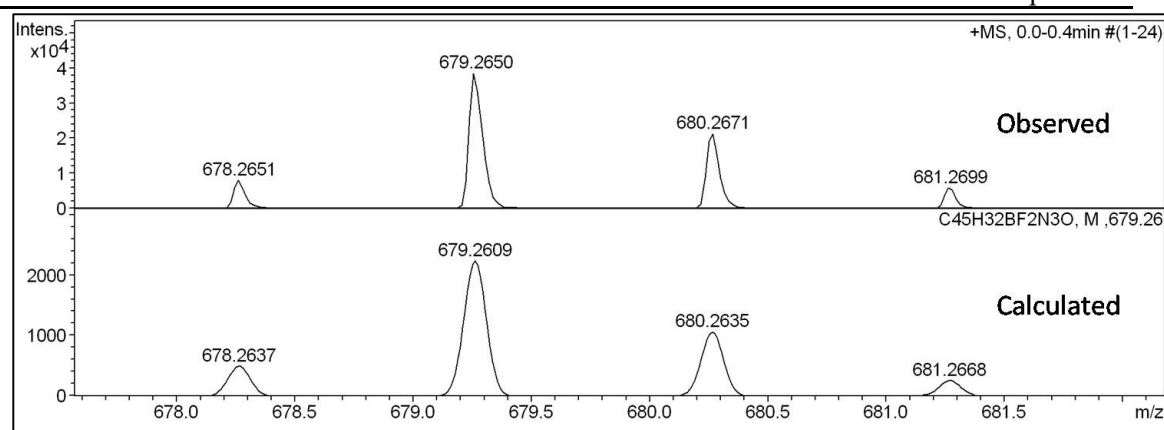


Figure 3A.4: HRMS of compound **5**

In the second step of reaction excited state intramolecular proton transfer imidazole ligands (**2** and **3**) were synthesized *via* Suzuki coupling reaction between bromophenol-substituted imidazole and the corresponding boronic acid in good yield. Finally the target imidazole borate complexes **4** and **5** were synthesized by the complexation of imidazole ligands with BF₃·Et₂O in the presence of base in more than 90 % yield. All compounds were characterized by NMR, HRMS and by CHN analysis (for Compound **4** & **5**). ESI-HRMS analysis of compounds shown parent ion peak at m/z values confirmed the compound formation (figure 3A.3 and 3A.4). In the ¹H NMR spectrum, the broad down fielded singlet of hydroxyl group of ESIPT ligand disappeared in the corresponding boron complex formation. In case of compound **4**, the peak at δ 13.38 ppm got disappeared after complexation with BF₃·Et₂O (figure 3A.5). The two *N,O*-chelate boron complexes (**4** & **5**) were also analyzed by ¹¹B and ¹⁹F NMR (figure 3A.7). The ¹¹B nuclei of both the compounds resonate at around 1 ppm, which indicates the formation of tetracoordinate boron compounds, and the ¹⁹F NMR signal resonate at *ca.* -138 ppm, which is comparable with literature reported compounds of similar type.³⁶⁻³⁸

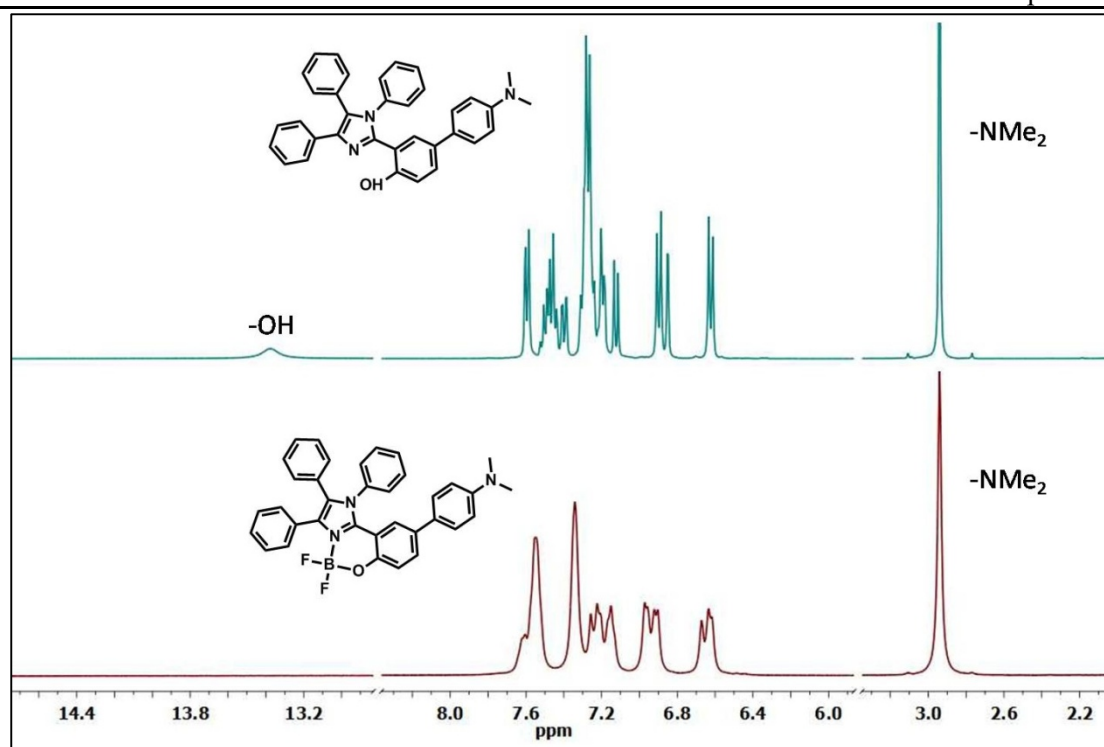


Figure 3A.5: ^1H NMR Spectrum of compound 2 and 4

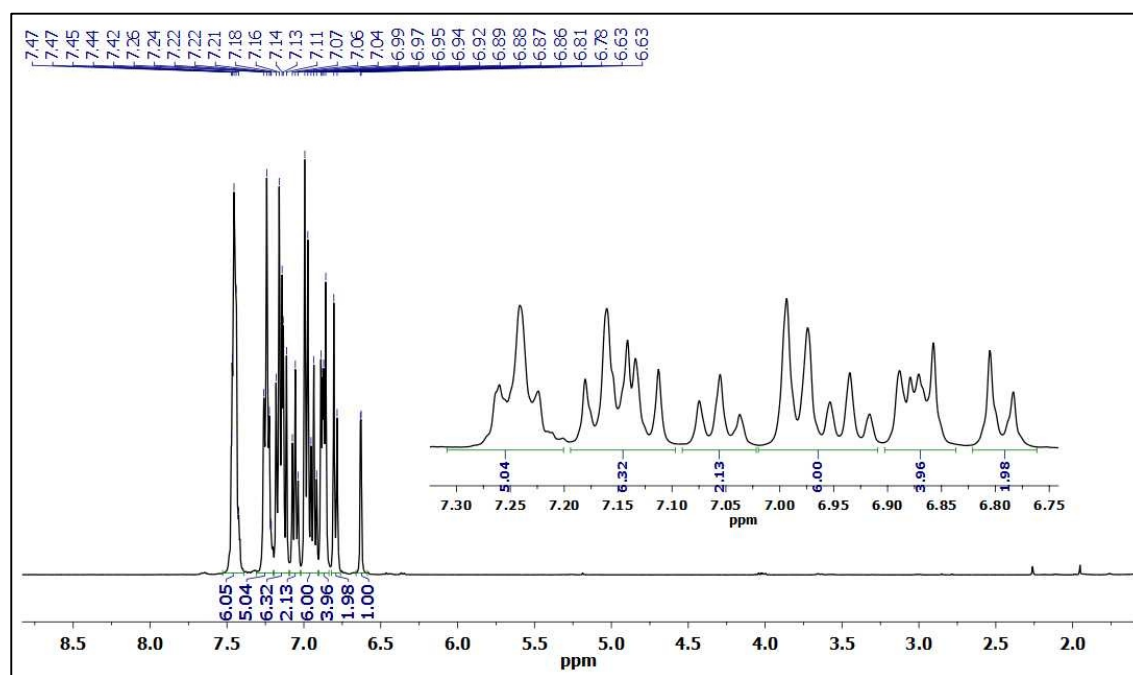


Figure 3A.6: ^1H NMR Spectrum of compound 5

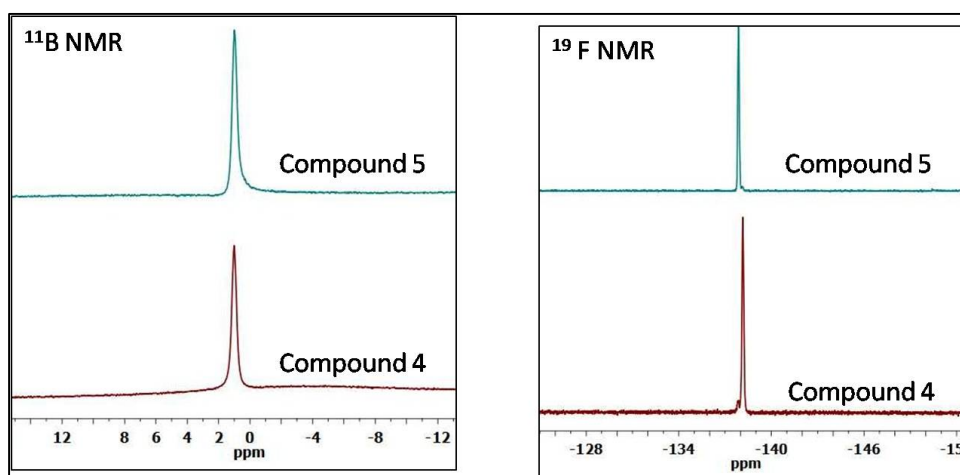


Figure 3A.7: ^{11}B NMR (left) and ^{19}F NMR Spectrum of compound 4 and 5

3A.2.2 Photophysical properties of *N,O*-chelate boron compounds

The boron compounds **4** and **5** showed good solubility in polar protic solvents. Photophysical properties of both the compounds were explored in different solvents and are presented in table 3A.1. The absorption and emission spectra of compounds **4** and **5** recorded in different solvents are shown in figure 3A.8 and 3A.9 respectively. Compound **4** exhibits two major absorption maxima at 306 and 358 nm, and compound **5** also shows two absorption bands at 307 and 327 nm in tetrahydrofuran (THF). The pronounced red shift of compound **4** is due to efficient charge transfer from $-\text{NMe}_2$ to the imidazole moiety. The emission spectrum of compound **4** exhibits one emission band at 496 nm with a quantum yield of 0.21 when excited at 358 nm, while compound **5** emits at 457 nm (excited at 327 nm) with a quantum yield of 0.2. Although there is no significant solvent effect on the absorption bands of compounds **4** and **5**, the emission profile shows a strong positive solvatochromism. The emission maxima λ_{em} shifted from 461 nm (toluene) to 564 nm (acetonitrile) for compound **5**.

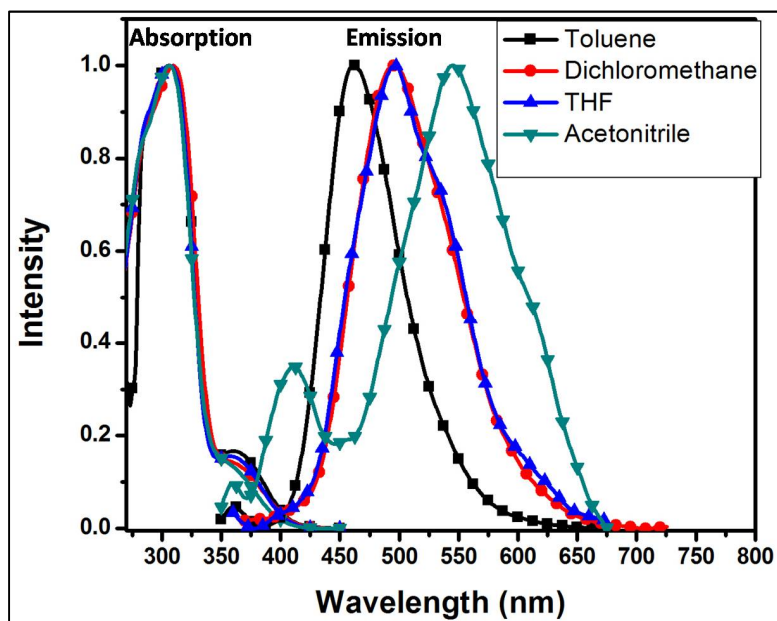


Figure 3A.8: Normalized absorption and emission spectra of probe 4 (43 μM).

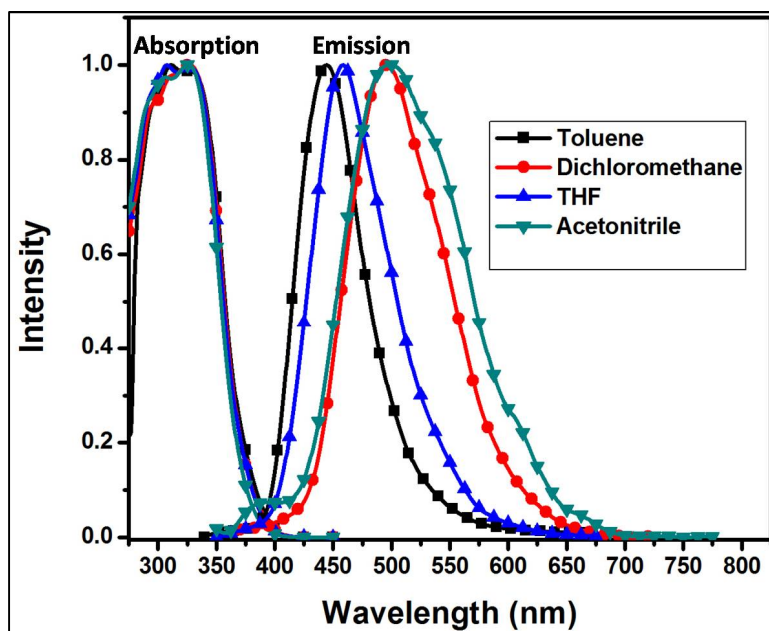


Figure 3A.9: Normalized absorption and emission spectra of probe 5 (43 μM).

Table 3A.1: Photophysical data of compounds **4** and **5**

probe	solvent	$\lambda_{\text{abs}}^{\text{[a]}}$ [nm]	$\epsilon_{\text{max}}^{\text{[c]}}$ ($\text{M}^{-1} \text{cm}^{-1} \times 10^3$)	λ_{em} [nm]	$(\Phi)^{\text{b}}$
5	CH ₃ CN	326	35.4	494	0.23
	THF	327	36.0	457	0.20
	DCM	327	34.1	497	0.17
	Toluene	326	34.5	442	0.27
4	CH ₃ CN	353	5.6	546	0.12
	THF	358	6.7	496	0.21
	DCM	365	6.0	501	0.17

^aAbsorption maximum (concentrations were 4.0×10^{-5} M). ^bExcited at the lowest-energy absorption maximum. ^cQuantum yields were measured according to literature reported methods³⁹ using quinine sulfate as the reference. $\Phi = 0.55$ in 1 M H₂SO₄.

3A.2.3 *N,O*- Chelate boron compounds for PA detection

To explore the potential use of compounds **4** and **5**, we added 30 equivalents of picric acid (PA) in a THF solution. As shown in figure 3A.10, a clear visual color change from yellowish green to colorless was noticed for compound **4**, while in case of compound **5**, the blue color disappeared under a hand held UV lamp.

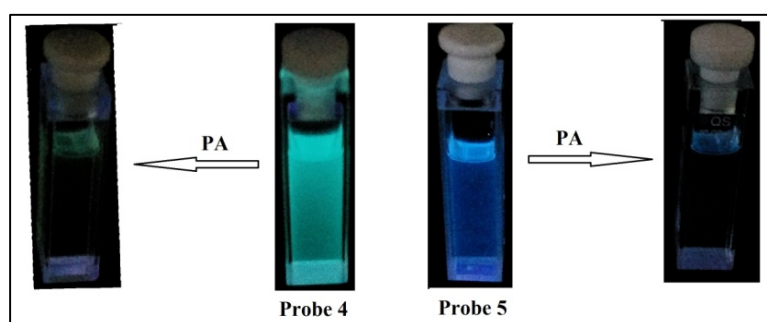


Figure 3A.10: Photographs of probes **4** (left) and **5** (right) under UV lamp

Encouraged by these observations, the sensing ability of these compounds were explored by emission spectroscopy in THF. Figure 3A.11 shows the emission response of compounds with different concentrations of PA. The emission intensity at 496 nm was gradually decreased when small amounts of picric acid was added to the

compound **4**. By the addition of 10 equivalents of PA, almost 90% emission was quenched and complete emission quenching was noticed after addition of 26 equivalents of PA to compound **4**. A similar trend was also seen for compound **5**. The emission intensity of compound **5** at 457 nm was gradually decreased with addition of PA and complete quenching was realized with 20 equivalents of PA.

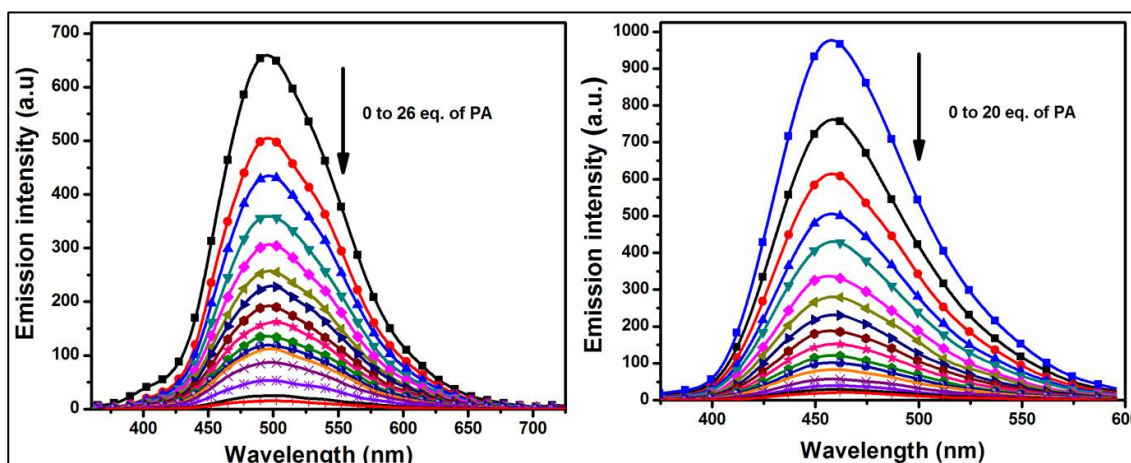


Figure 3A.11: Emission changes of probes **4** (left) and **5** (right) ($43 \mu\text{M}$) with the addition of different concentrations of PA (0, 1, 2, 3, 4, 5, 6, 7, 8, 9, 10, 11, 12, 14, 16, 18, 20, and 26 equiv of PA) in THF when excited at 358 nm (**4**) and 327 nm (**5**) in THF.

Fluorescence quenching by PA was analyzed by stern volmer equation at lower concentrations, and the quenching constant was found to be $0.7 \times 10^4 \text{ M}^{-1}$ for compound **4** and $1 \times 10^4 \text{ M}^{-1}$ for compound **5** (figure 3A.12). The fluorescence lifetimes of probes **4** and **5** were measured in the presence and absence of picric acid (figure 3A.13). The observed lifetime measurements with different concentrations of picric acid were found to be invariant, suggesting that the quenching follows a static quenching mechanism through a ground state complex formed between the probes and PA.

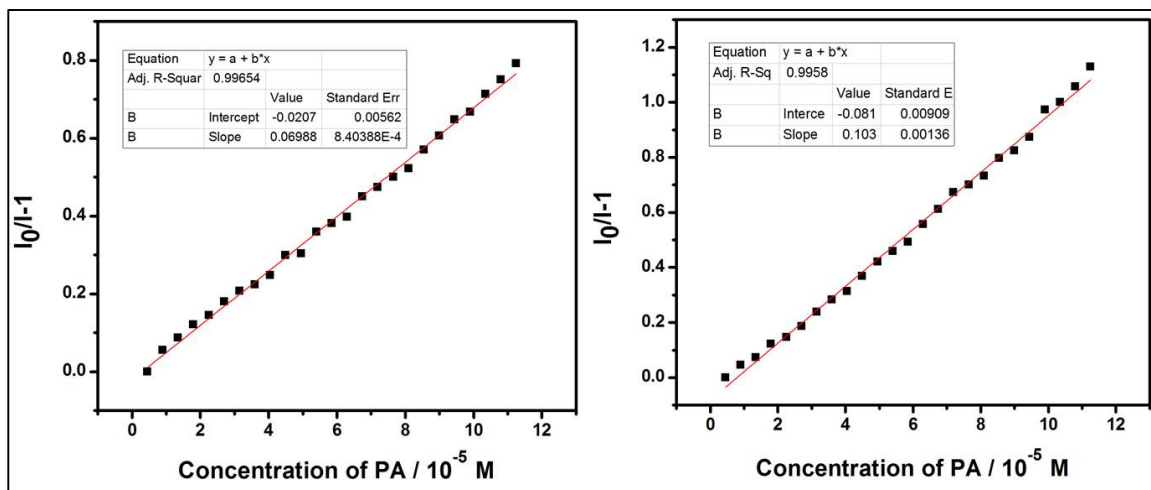


Figure 3A.12: Stern-Volmer plots of probe 4 (left) and 5 (right) (43 μM) with addition of different concentration of PA in THF

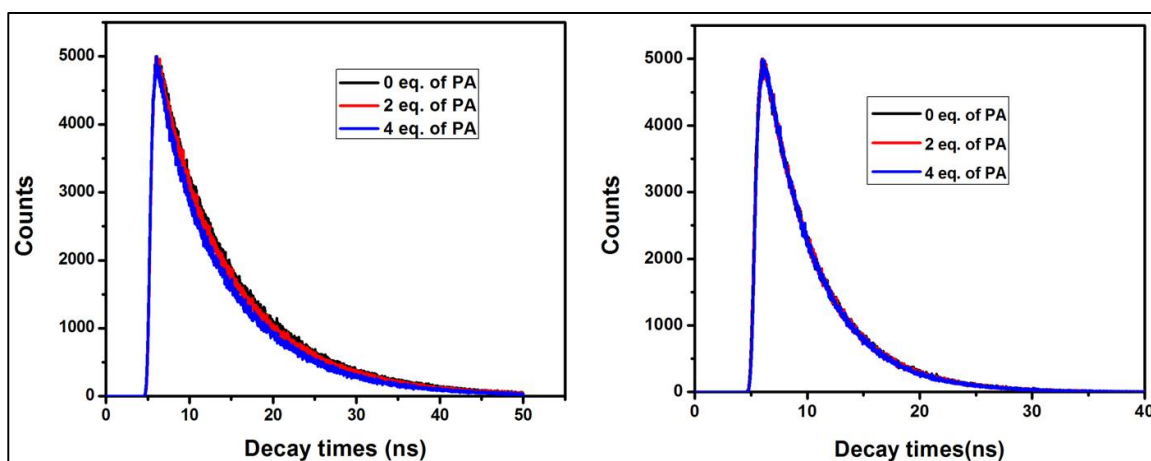


Figure 3A.13: Fluorescence lifetime decay of probes 4 (left) and 5 (right) after the addition of 0, 2, and 4 equiv of PA in THF, where the emission is at 496 and 457 nm respectively for probes 4 and 5.

Furthermore we investigated the emission response of the probes with different nitroaromatics and other interfering analytes like 4-nitrotoluene (4-NT), 2,4-dinitrotoluene (2,4-DNT), 1,3-dinitrobenzene (1,3-DNB), 1,4-dinitrobenzene (1,4-DNB), 2,6-dinitrotoluene (2,6DNT), benzoic acid (BA), phenol, nitromethane (NM), and nitrobenzene (NB) to determine the selectivity. Unlike picric acid, other nitroaromatics and analytes do not show significant emission quenching (figure 3A.14). Among all of these nitroaromatics only PA showed 85% emission quenching

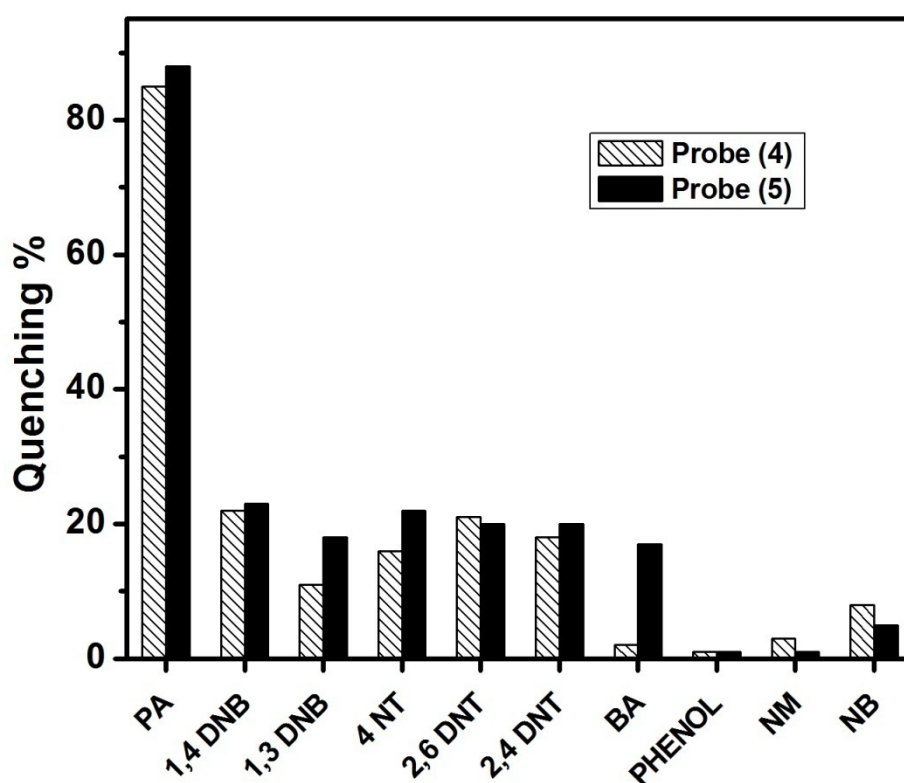


Figure 3A.14: Emission quenching efficiencies of probes (43 μ M) after the addition of 8 equiv of different nitroaromatics and other analytes in THF

when 8 equivalent of the analytes were added. In order to check the stability of boron complex we recorded emission spectrum with different time intervals. As shown in figure 3.15, there is no change in emission intensity of boron complex **5** suggesting its stability under experimental conditions.

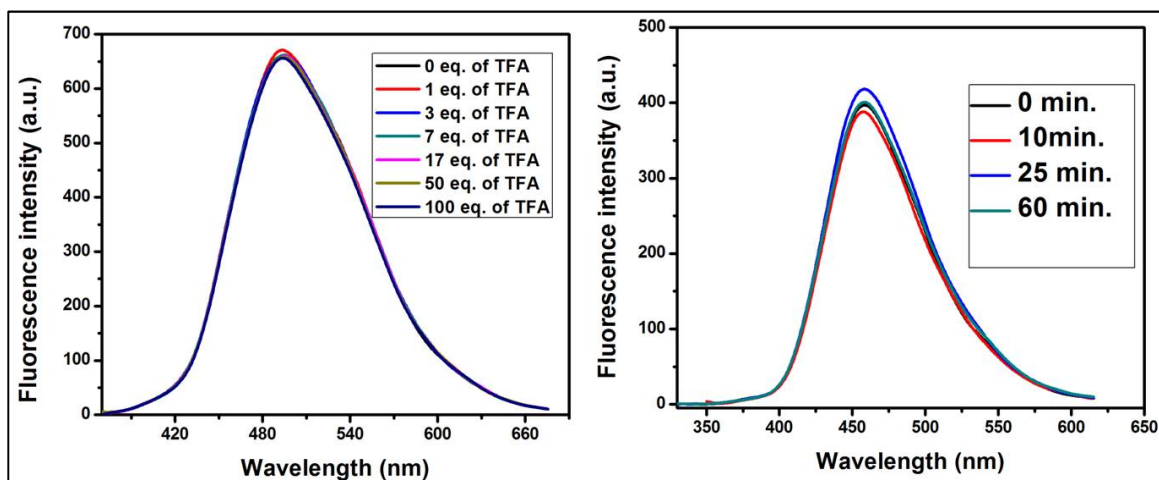


Figure 3A.15: Emission changes of probe **4** with TFA (left) and **5** with diff. time interval (right) in THF.

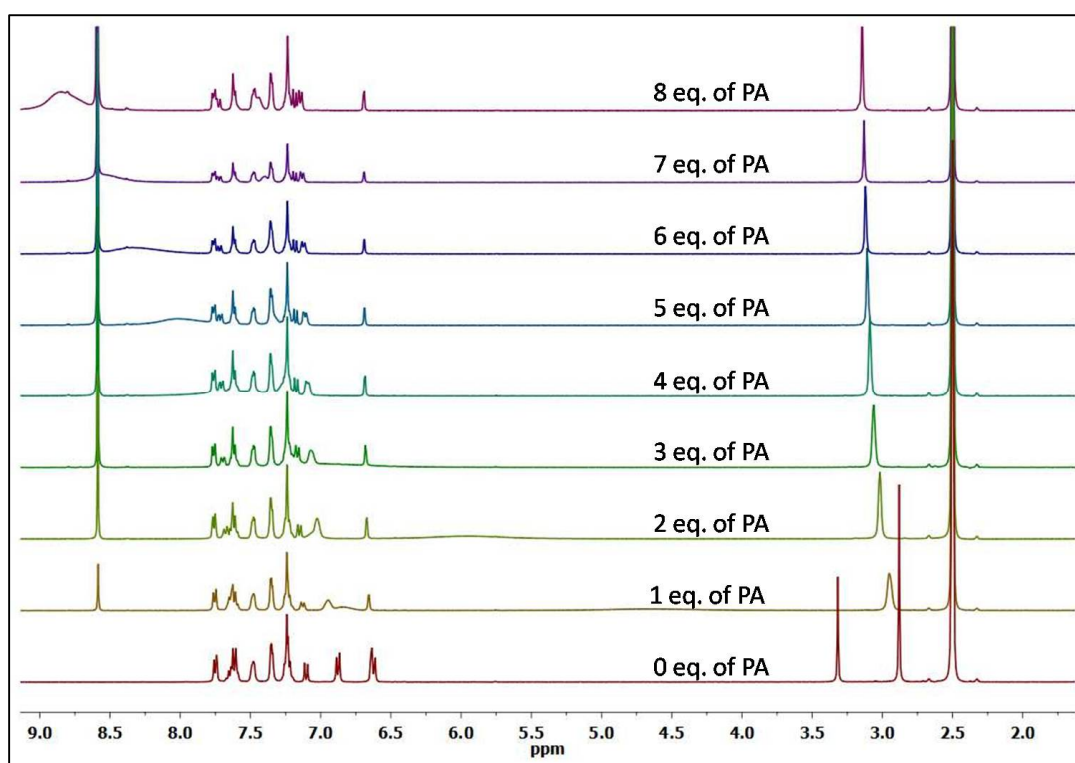


Figure 3A.16: ^1H NMR titration of probe **4** upon the addition of 0, 1, 2, 3, 4, 5, 6, 7, and 8 equiv of PA in DMSO-d_6 .

To gain insights into the mode of interaction between compound **4** and PA in solution, ^1H NMR titrations were performed in DMSO- d_6 (figure 3A.16). By the addition of PA to compound **4**, NMe_2 protons at δ 2.8 ppm shifted to δ 3.1 ppm; in addition all of the aromatic protons were also downfield-shifted, which indicates that there is a strong interaction between compound **4** and PA. Because PA is a strong acid ($\text{p}K_a \approx 0.38$) to nullify the possibility of decomposition of the probe, ^{19}F and ^{11}B NMR studies performed by the addition of PA. Both ^{19}F and ^{11}B NMR titration spectra (figure 3A.20 & 3A.21) revealed that the peak positions are relatively unchanged with respect to the probe, suggesting that the probes remain intact after the addition of PA.

Recently, Hengchang and co-workers³⁰ reported triphenylamine- decorated BODIPY for the detection of PA. The intermolecular photoinduced electron-transfer (PET) process was studied using NMR experiments and proposed that $\text{F}\cdots\text{H}$ hydrogen bonding is responsible for the selectivity. However, structural evidence for the adduct was not reported. In order to investigate the interactions between the probe and PA, we grew single crystals of probe **4** and PA (**4**·PA) by slow evaporation of THF and ethanol. To our delight, single-crystal X-ray diffraction analysis revealed the formation of a 1:1 adduct, in which PA undergoes deprotonation and the $-\text{NMe}_2$ group of probe **4** is protonated to form the picrate anion and $-\text{NMe}_2\text{H}^+$ cation, respectively (figure 3A.17). The hydrogen atom of the $-\text{NMe}_2\text{H}^+$ group and the oxygen atom of the phenolate form a strong $\text{N}-\text{H}\cdots\text{O}$ hydrogen bond ($\text{H}\cdots\text{O} = 1.810$ Å and $\text{N}-\text{H}\cdots\text{O} = 169.96^\circ$). As shown in figure 3A.17, the imidazole ring lies parallel to the picrate plane, suggestive of π - π interactions (4.06 Å). The packing diagram of probe **4**·PA was shown in figure 3A.18. In order to understand the role of proton transfer, the effect on the emission of probe **4** was performed using a stronger acid,

trifluoroacetic acid (TFA) (figure 3A.15). Under the experimental conditions mentioned, the addition of TFA does not quench the fluorescence of probe **4**, which establishes that protonation of the probe does not lead to emission quenching. These results imply that the interactions discussed *vide supra* bring probe **4** and PA into close proximity and facilitate energy transfer and/or charge transfer, thus producing selective quenching toward PA. We believe that a similar fluorescence quenching mechanism operates in probe **5** also. The detection method described above used fluorimeters, which cannot be used for *in situ/on-site* detection. To overcome this, a test-strip method was developed for the detection of picric acid (Figure 3A.19). Test

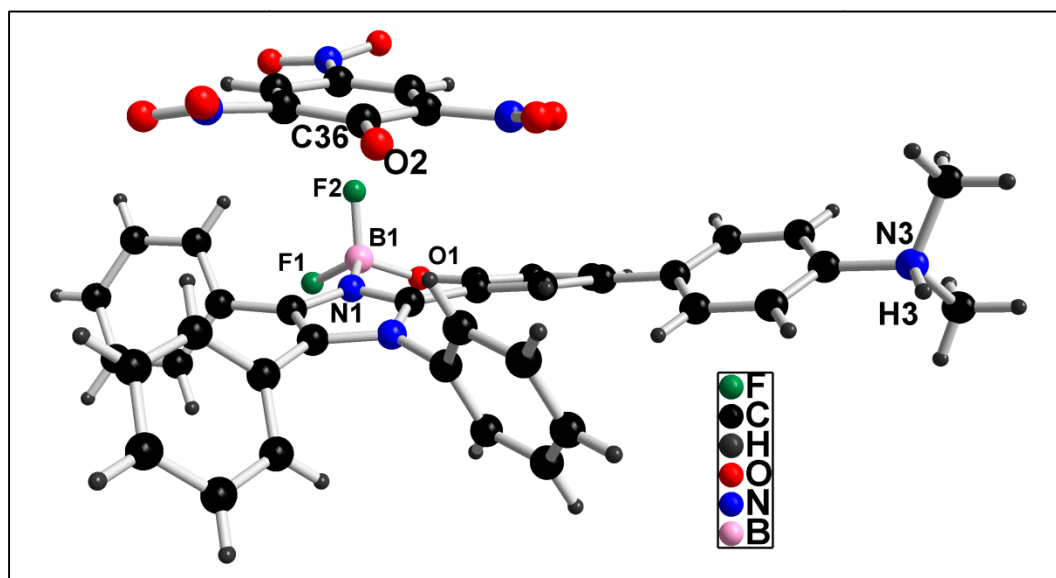


Figure 3A.17: Molecular structure of the probe **4**·PA adduct

strips were made by Whatman filter paper dipped in a solution of probe **4** (10^{-2} M in THF) and dried. A total of 10 μ L of PA was drop-cast onto the test strips at varying concentrations. Upon irradiation with a UV lamp, blue spots appeared in the spotted area. The minimum concentration of PA that could be detected using this technique was found to be ≈ 20 ng.

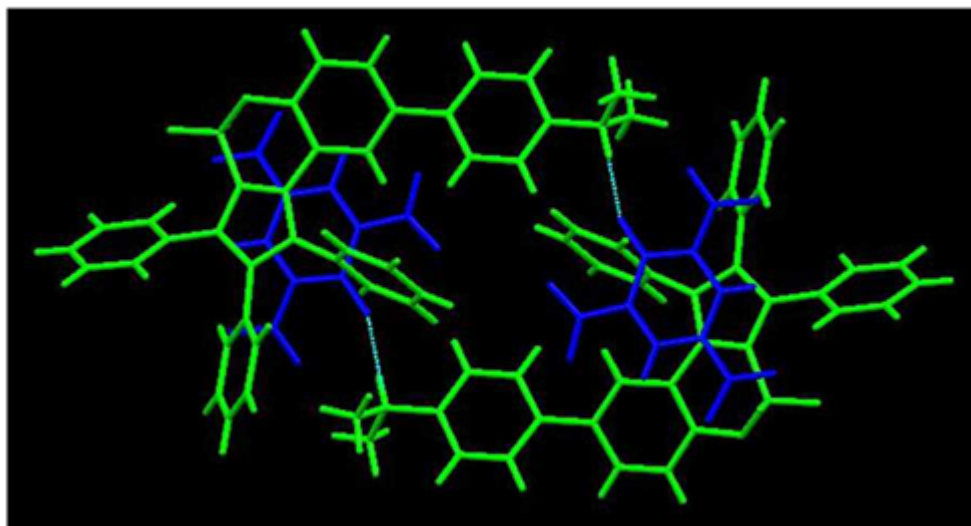


Figure 3A.18: Packing of probe 4·PA with hydrogen bonding.

Table 3A.2: Crystal data and structure refinement of adduct 4·PA

Empirical formula	C ₄₁ H ₃₁ BF ₂ N ₆ O ₈
Formula weight	784.53
Temperature/K	296.15
Crystal system	triclinic
Space group	P-1
a/Å	12.1397(11)
b/Å	12.3267(11)
c/Å	14.5320(14)
α/°	107.347(6)
β/°	93.129(7)
γ/°	113.264(5)
Volume/Å ³	1869.7(3)
Z	2
ρ _{calc} /cm ³	1.393
μ/mm ⁻¹	0.105
F(000)	812.0
Crystal size/mm ³	0.2 × 0.15 × 0.1
Radiation	MoKα (λ = 0.71073)
2θ range for data collection/°	3.724 to 50.998
Index ranges	-14 ≤ h ≤ 14, -14 ≤ k ≤ 14, -17 ≤ l ≤ 17
Reflections collected	20495
Independent reflections	6951 [R _{int} = 0.0336, R _{sigma} = 0.0397]
Data/restraints/parameters	6951/0/519
Goodness-of-fit on F ²	1.024
Final R indexes [I >= 2σ (I)]	R ₁ = 0.0623, wR ₂ = 0.1747
Final R indexes [all data]	R ₁ = 0.1026, wR ₂ = 0.2093
Largest diff. peak/hole / e Å ⁻³	0.43/-0.35

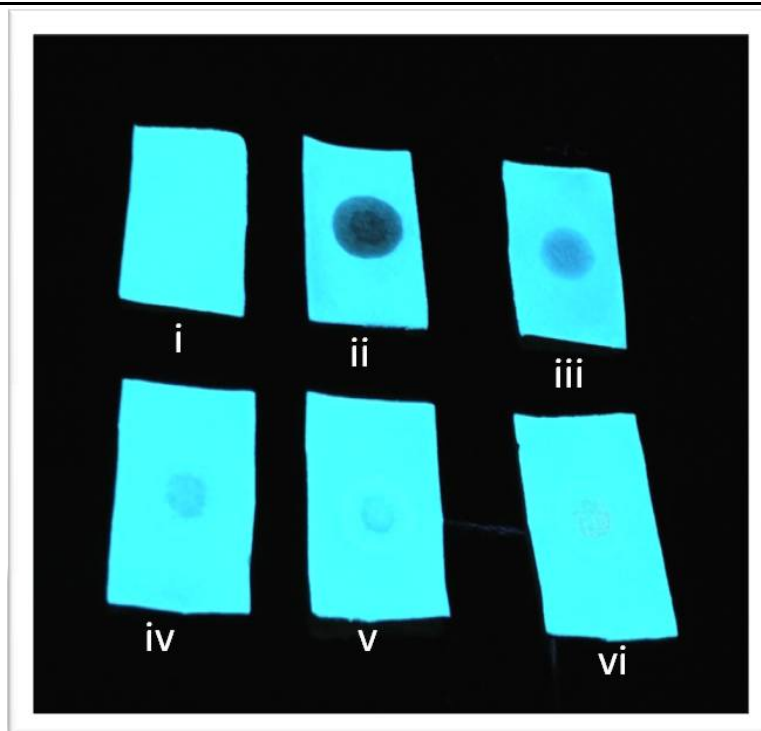


Figure 3A.19: Photographs of paper test strips of probe **4** under UV light with the addition of different concentrations of PA: (i) blank; (ii) 10^{-2} M; (iii) 10^{-3} M; (iv) 10^{-4} M; (v) 10^{-5} M; (vi) 10^{-6} M.

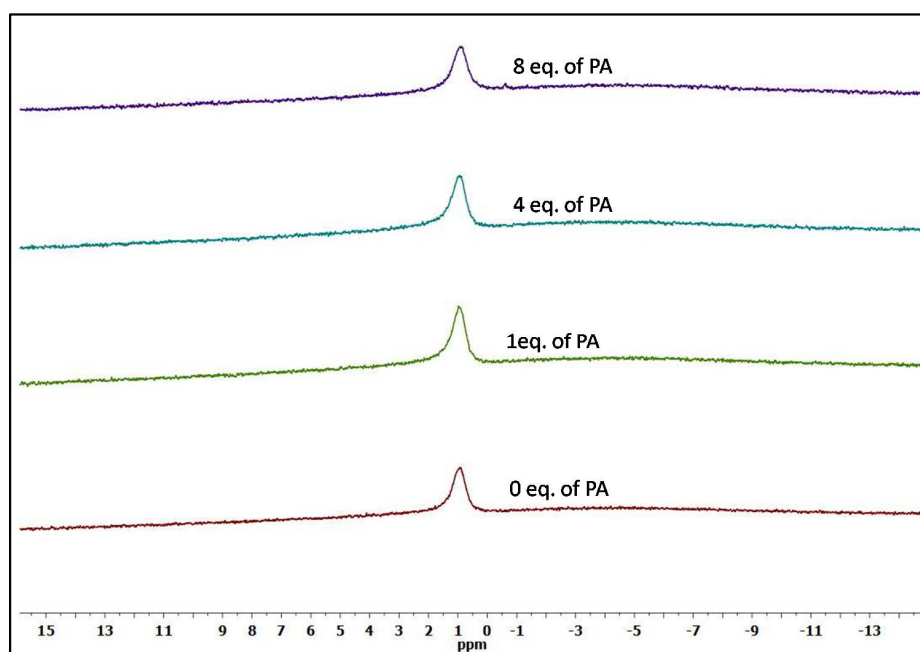


Figure 3A.20: ^{19}F NMR spectra of probe **4** with 0, 1, 4 and 8 equivalents of picric acid in CDCl_3

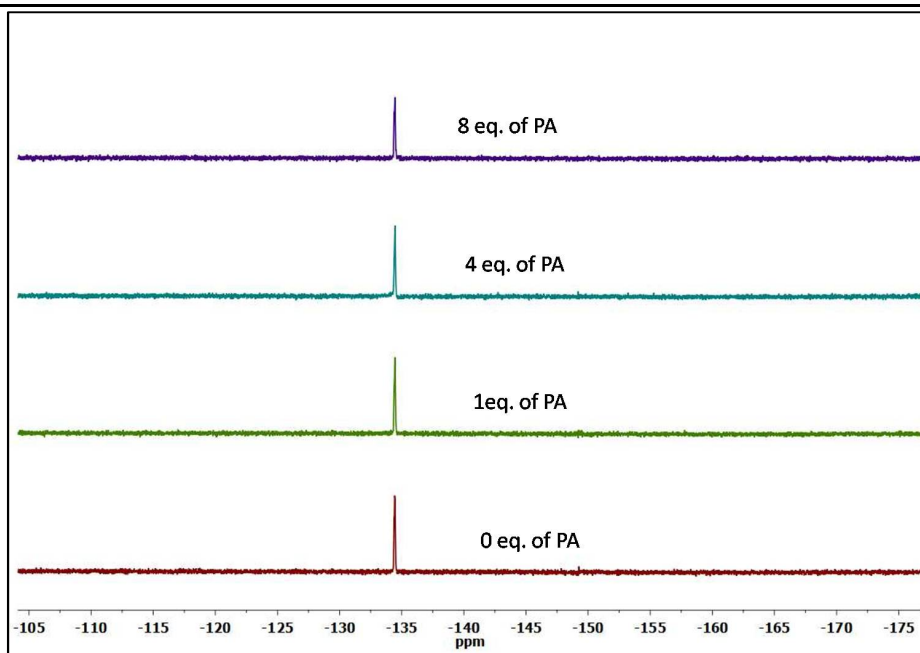


Figure 3A.21: ^{11}B NMR spectra of probe **4** with 0, 1, 4 and 8 equivalents of picric acid in CDCl_3

3A.3 Conclusion

In summary, tertiary amine-decorated imidazole-based *N,O*-chelate boron complexes were designed and synthesized in three simple steps. The boron complexes **4** and **5** were characterized by HRMS, and multi nuclear NMR. The photophysical properties of these complexes were explored in different solvents. Both probes exhibit selective emission quenching toward picric acid over other nitroaromatics and other analytes. Stern Volmer plots and fluorescence lifetime studies on emission quenching of Probes by PA, suggests a static quenching mechanism. ^1H NMR and single-crystal X-ray analysis reveal that proton transfer between PA and the imidazole-based boron complexes is the origin for the selectivity. The results presented in this study hold great potential for the development of new boron-based sensors for the selective detection of PA.

3A.4 Experimental section

3A.4.1 General Procedures

All chemicals were used as received from commercially available sources. 1,2-dichloroethane was distilled over CaH₂, and 1,2-dimethoxyethane was dried using sodium. 4-(dimethylamino)phenylboronic acid⁴⁰ and 4-(diphenylamino)-phenylboronic acid⁴¹ were synthesized by following literature reported methods. NMR spectra were recorded on a Bruker ARX 400 spectrometer at room temperature. ¹H (400 MHz) and ¹³C (100 MHz) NMR chemical shifts in ppm were referenced internally to proton resonances of incomplete deuterated solvent signals. ¹¹B and ¹⁹F NMR spectra were externally referenced to BF₃·Et₂O in CDCl₃ (δ = 0 ppm) and α,α,α-trifluorotoluene in CDCl₃ (δ = -63.73 ppm), respectively. Electrospray ionization (ESI) high-resolution mass spectrometry (HR-MS) spectra were recorded on a Bruker micro-TOF-QII spectrometer. IR spectra were recorded with a PerkinElmer instrument. Time-resolved fluorescence measurements were recorded on an Edinburgh instrument. Absorption measurements were carried out on a PerkinElmer Lambda 750 UV-vis spectrometer. Emission spectra were recorded using a PerkinElmer LS-55 fluorometer. Single crystal X-ray diffraction data were collected on a Bruker APEX-II diffractometer. The data were collected at 296 K using Mo Kα radiation (0.71073 Å). Crystallographic data for **4·PA** and details of X-ray diffraction experiments and crystal structure refinements are given in table 3.2. Using OLEX2⁴², the structure was solved with the SHELXS structure solution program using direct methods and refined with the SHELXL⁴³ refinement package using least-squares minimization. All non-hydrogen atoms were refined with anisotropic

displacement coefficients. The hydrogen atoms were placed at calculated positions and refined as riding atoms.

3A.4.2 Synthetic procedures and spectral characterization

4-Bromo-2-(1,4,5-triphenyl-1H-imidazol-2-yl)phenol (1) To a stirred solution of 5-bromosalicylaldehyde (1.00 g, 4.9 mmol) and aniline (1.13 mL, 12.4 mmol) in acetic acid were added benzil (1.04 g, 4.9 mmol) and ammonium acetate (0.38 g, 4.9 mmol), and the resulting solution was heated to reflux for 12 h. At room temperature, water was added to the reaction mixture, which was extracted with dichloromethane, dried over sodium sulfate, and concentrated using rotavap. The resultant white solid was purified by 100–200 silica gel column chromatography using ethyl acetate in hexane (1:9) as the eluent. Yield: 1.90 g, 82%. Mp: 198 °C. ^1H NMR (400 MHz, CDCl_3): δ 7.58 (d, $J = 4$ Hz, 2H, ArH), 7.48–7.42 (m, 3H, ArH), 7.33–7.27 (m, 6H, ArH), 7.25–7.18 (m, 5H, ArH), 7.00 (d, $J = 8$ Hz, 1H, ArH), 6.64 (d, $J = 4$ Hz, 1H, ArH). ^{13}C NMR (100 MHz, CDCl_3): δ 157.48, 143.53, 136.30, 134.90, 132.98, 132.16, 131.36, 130.90, 129.90, 129.77, 129.20, 129.10, 128.88, 128.71, 128.52, 127.57, 127.20, 119.59, 114.26, 109.83. HR-MS (ESI). Calcd for $\text{C}_{27}\text{H}_{20}\text{Br}_1\text{N}_2\text{O}_1$ ($[\text{M} + \text{H}]^+$): m/z 467.0754. Found: m/z 467.0779.

4'-(Dimethylamino)-3-(1,4,5-triphenyl-1H-imidazol-2-yl)-(1,1'-biphenyl)-4-ol (2) Under a nitrogen atmosphere, a 100 mL two-neck round-bottomed flask with a reflux condenser was charged with bromophenol-substituted imidazole (1.00 g, 2.1 mmol) and $\text{Pd}(\text{PPh}_3)_4$ (0.07 g, 0.06 mmol). To this mixture was added 50 mL of degassed 1,2-dimethoxyethane (DME), and the resulting solution was stirred at room temperature for 30 min. To this stirred solution was added 4-(dimethylamino)phenylboronic acid (0.42 g, 2.6 mmol) and 1.07 M aqueous sodium

carbonate (0.67 g, 6.4 mmol), and the solution was heated to reflux for 20 h. The reaction mixture was cooled to room temperature; water workup was done with dichloromethane. The organic layer was washed with a brine solution, dried over magnesium sulfate, and concentrated by rotavap. The crude product was separated by 100–200 silica gel column chromatography using hexane ethyl acetate (4:1) as the eluent to get a pure product. Yield: 0.80 g, 74%. Mp: 235 °C. ^1H NMR (400 MHz, CDCl_3): δ 13.38 (br s, 1H, ArOH), 7.59 (d, $J = 8$ Hz, 2H, ArH), 7.50–7.44 (m, 3H, ArH), 7.40 (dd, $J = 8$ and 4 Hz, 1H, ArH), 7.31–7.24 (m, 8H, ArH), 7.19 (d, 2H, $J = 8$ Hz, ArH), 7.12 (d, $J = 8$ Hz, 1H, ArH), 6.90 (d, 2H, $J = 8$ Hz, ArH), 6.84 (d, $J = 4$ Hz, 1H, ArH), 6.62 (d, $J = 8$ Hz, 2H, ArH), 2.94 (s, 6H, NMe_2). ^{13}C NMR (100 MHz, CDCl_3): δ 157.15, 149.45, 145.19, 137.65, 135.39, 133.28, 131.50, 130.78, 130.56, 129.99, 129.95, 129.21, 128.98, 128.72, 128.59, 128.56, 128.41, 127.78, 127.12, 127.05, 126.80, 124.00, 117.94, 113.04, 112.72, 40.72 (NMe_2). IR (KBr, cm^{-1}): ν 3056 (m), 3029 (m), 2883 (m), 2799 (m), 1953 (b), 1887 (b), 1609 (s), 1529 (m), 1492 (s), 1443 (s), 1365 (m), 1254 (m), 1168 (m), 1027 (m), 1003 (m), 917 (m), 811 (s), 763 (m), 699 (s), 542 (m). HR-MS (ESI). Calcd for $\text{C}_{35}\text{H}_{30}\text{N}_3\text{O}_1$ ($[\text{M} + \text{H}]^+$): m/z 508.2383. Found: m/z 508.2359. Elem anal. Calcd for $\text{C}_{35}\text{H}_{29}\text{N}_3\text{O}$: C, 82.81; H, 5.76; N, 8.28. Found: C, 82.88; H, 5.80; N, 8.17.

4'-(Diphenylamino)-3-(1,4,5-triphenyl-1H-imidazol-2-yl)-(1,1'-biphenyl)-4-ol

(3) Imidazole 3 was synthesized by the Suzuki coupling conditions used above using bromophenol-substituted imidazole (1.90 g, 4.1 mmol), 4-(diphenylamino)phenylboronic acid (1.40 g, 4.9 mmol), 1.52 M aqueous sodium carbonate (1.27 g, 12.2 mmol), $\text{Pd}(\text{PPh}_3)_4$ (0.14 g, 0.12 mmol), and 70 mL of degassed DME. Yield: 1.74 g, 68%. ^1H NMR (400 MHz, CDCl_3): δ 7.58 (d, $J = 8$ Hz, 2H, ArH), 7.42–7.40 (m, 4H, ArH), 7.30–7.23 (m, 13H, ArH), 7.19–7.14 (m, 3H,

ArH), 7.08 (d, $J = 8$ Hz, 4H, ArH), 7.02 (t, $J = 8$ Hz, 2H, ArH), 6.89 – 6.97 (m, 5H, ArH) ppm. ^{13}C NMR (100 MHz, CDCl_3): δ 157.52, 147.83, 146.48, 144.77, 137.03, 134.51, 131.45, 130.65, 130.35, 129.94, 129.42, 129.34, 128.81, 128.70, 128.53, 127.53, 127.24, 126.85, 124.96, 124.27, 124.18, 122.83, 118.39, 112.76 ppm. IR (KBr, cm^{-1}): ν 3056 (m), 3032 (m), 2755 (m), 2286 (m), 1951 (m), 1888 (m), 1737 (m), 1589 (s), 1485 (s), 1386 (s), 1326 (s), 1269 (s), 1145 (m), 1027 (m), 972 (m), 920 (m), 895 (m), 818 (s), 757 (s), 697 (s), 511 (s). HR-MS (ESI). Calcd for $\text{C}_{45}\text{H}_{34}\text{N}_3\text{O}_1$ ($[\text{M} + \text{H}]^+$): m/z 632.2696. Found: m/z 632.2686. Elem anal. Calcd for $\text{C}_{45}\text{H}_{33}\text{N}_3\text{O}$: C, 85.55; H, 5.26; N, 6.65. Found: C, 85.62; H, 5.18; N, 6.70.

Dimethylimidazole Borane Complex (Probe 4) An oven-dried two-neck round-bottomed flask was charged with imidazole **2** (0.50 g, 1.0 mmol) in 25 mL of 1,2-dichloroethane under an argon atmosphere. To this stirred solution was added $\text{BF}_3 \cdot \text{Et}_2\text{O}$ (0.74 mL, 5.9 mmol), and after 10 min, N,N -diisopropylethylamine (1.03 mL, 5.9 mmol) was added. The reaction mixture was stirred at 40 °C for 1 h and then at room temperature overnight. The crude mixture was passed through a basic alumina column packed in dichloromethane and concentrated in a vacuum to obtain a pure yellow solid compound. Yield: 0.52 g, 95%. Mp: 288 °C (dec). ^1H NMR (400 MHz, CDCl_3): δ 7.62–7.55 (m, 6H, ArH), 7.34–7.15 (m, 9H, ArH), 6.97–6.91 (m, 4H, ArH), 6.67–6.62 (m, 3H, ArH), 2.94 (s, 6H, NCH_3). ^1H NMR (400 MHz, DMSO-d_6): δ 7.75 (d, $J = 8$ Hz, 2H, ArH), 7.67–7.59 (m, 4H, ArH), 7.49–7.47 (m, 2H, ArH), 7.36–7.34 (m, 3H, ArH), 7.26–7.20 (m, 5H, ArH), 7.10 (d, $J = 8$ Hz, 1H, ArH), 6.88 (d, $J = 8$ Hz, 2H, ArH), 6.64–6.61 (m, 3H, ArH), 2.88 (s, 6H, NCH_3). ^{13}C NMR (100 MHz, CDCl_3): δ 155.38, 149.62, 141.71, 135.54, 132.48, 132.40, 132.00, 131.27, 131.15, 130.73, 130.65, 130.60, 129.15, 129.01, 128.56, 128.54, 128.49, 128.25,

128.10, 126.89, 126.79, 122.29, 120.66, 112.79, 109.78, 40.73. ^{11}B NMR (128 MHz, CDCl_3): δ 1.01. ^{19}F NMR (376 MHz, CDCl_3): δ -138.14. IR (KBr, cm^{-1}): ν 3057 (m), 2923 (m), 1897 (m), 1612 (s), 1508 (s), 1440 (m), 1309 (s), 1272 (m), 1171 (m), 1050 (s), 1030 (s), 906 (s), 838 (m), 812 (s), 707 (m), 695 (m). HR-MS (ESI). Calcd for $\text{C}_{35}\text{H}_{28}\text{BF}_2\text{N}_3\text{O}$ ($[\text{M}]^+$): m/z 555.2294. Found: m/z 555.2314. Elem anal. Calcd for $\text{C}_{35}\text{H}_{28}\text{BF}_2\text{N}_3\text{O}$: C, 75.69; H, 5.08; N, 7.57. Found: C, 75.58; H, 5.01; N, 7.49.

Diphenylimidazole Borate Complex (Probe 5) Compound **2** was prepared by adopting a similar protocol as that mentioned for probe **4** (compound **4**). The quantities involved are as follows: imidazole **3** (0.40 g, 0.6 mmol), $\text{BF}_3 \cdot \text{Et}_2\text{O}$ (0.47 mL, 3.8 mmol), *N,N*-diisopropylethylamine (0.66 mL, 3.8 mmol), and 30 mL of 1,2-dichloroethane. A white solid compound was obtained. Yield: 93% (0.40 g). Mp: 283 °C (dec). ^1H NMR (400 MHz, CDCl_3): δ 7.47–7.42 (m, 6H, ArH), 7.26–7.22 (m, 5H, ArH), 7.18–7.11 (m, 6H, ArH), 7.06 (t, $J = 8$ Hz, 2H, ArH), 6.98 (d, $J = 8$ Hz, 4H, ArH), 6.94 (t, $J = 8$ Hz, 2H, ArH), 6.89–6.86 (m, 4H, ArH), 6.81–6.78 (m, 2H, ArH), 6.63 (d, $J = 2$ Hz, 1H, ArH). ^{13}C NMR (100 MHz, CDCl_3): δ 155.91, 147.71, 146.87, 141.45, 135.44, 133.66, 132.52, 132.48, 131.23, 131.16, 130.67, 130.56, 129.39, 129.18, 129.00, 128.56, 128.47, 128.40, 128.23, 126.75, 126.65, 124.46, 123.88, 123.04, 122.61, 120.75, 109.85. ^{11}B NMR (128 MHz, CDCl_3): δ 1.0. ^{19}F NMR (376 MHz, CDCl_3): δ -137.87. IR (KBr, cm^{-1}): ν 3057 (m), 3033 (m), 2359 (m), 1899 (m), 1620 (s), 1588 (s), 1499 (s), 1453 (m), 1311 (m), 1274 (m), 1152 (m), 1038 (m), 911 (s), 822 (s), 696 (s), 621 (m), 509 (m). HRMS (ESI). Calcd for $\text{C}_{45}\text{H}_{32}\text{BF}_2\text{N}_3\text{O}$ ($[\text{M}]^+$): m/z 679.2609. Found: m/z 679.2650. Elem anal. Calcd for $\text{C}_{45}\text{H}_{32}\text{BF}_2\text{N}_3\text{O}$: C, 79.53; H, 4.75; N, 6.18. Found: C, 79.49; H, 4.68; N, 6.10.

3A.5 References

-
- (1) Cooper, P. *Explosive Engineering* **1996**, 33.
 - (2) Caygill, J. S.; Davis, F.; Higson, S. P. J. *Talanta* **2012**, 88, 14.
 - (3) Salinas, Y.; Martínez-Máñez, R.; Marcos, M. D.; Sancenón, F.; Costero, A. M.; Parra, M.; Gil, S. *Chem. Soc. Rev.* **2012**, 41, 1261.
 - (4) Meredith, D. T.; Lee, C. O. *J. Am. Pharm. Assoc.* **1939**, 28.
 - (5) Volwiler, E. H. *Ind. Eng. Chem.* **1926**, 18, 1336.
 - (6) Nipper, M.; Qian, Y.; Carr, R. S.; Miller, K. *Chemosphere* **2004**, 56, 519.
 - (7) Ashbrook, P. C.; Houts, T. A. *Chemical Health and Safety* **2003**, 10, 27.
 - (8) Moore, D. S. *Rev. Sci. Instrum.* **2004**, 75, 2499.
 - (9) Zimmermann, Y.; Broekaert, J. A. C. *Anal. Bioanal. Chem.* **2005**, 383, 998.
 - (10) Steinfeld, J. I.; Wormhoudt, J. In *Annu. Rev. Phys. Chem.* 1998; Vol. 49, p 203.
 - (11) Soltzberg, L. J.; Hagar, A.; Kridaratikorn, S.; Mattson, A.; Newman, R. *J. Am. Soc. Mass. Spectrom.* **2007**, 18, 2001.
 - (12) Dey, N.; Samanta, S. K.; Bhattacharya, S. *ACS Appl. Mater. Interfaces* **2013**, 5, 8394.
 - (13) Peng, Y.; Zhang, A. J.; Dong, M.; Wang, Y. W. *Chem. Commun.* **2011**, 47, 4505.
 - (14) Kartha, K. K.; Babu, S. S.; Srinivasan, S.; Ajayaghosh, A. *J. Am. Chem. Soc.* **2012**, 134, 4834.
 - (15) Roy, B.; Bar, A. K.; Gole, B.; Mukherjee, P. S. *J. Org. Chem.* **2013**, 78, 1306.
 - (16) Sohn, H.; Calhoun, R. M.; Sailor, M. J.; Trogler, W. C. *Angew. Chem. Int. Ed.* **2001**, 40, 2104.
 - (17) Sohn, H.; Sailor, M. J.; Magde, D.; Trogler, W. C. *J. Am. Chem. Soc.* **2003**, 125, 3821.

-
- (18) Liu, J.; Zhong, Y.; Lu, P.; Hong, Y.; Lam, J. W. Y.; Faisal, M.; Yu, Y.; Wong, K. S.; Tang, B. Z. *Polym. Chem.* **2010**, *1*, 426.
- (19) Xu, B.; Wu, X.; Li, H.; Tong, H.; Wang, L. *Macromolecules* **2011**, *44*, 5089.
- (20) Lan, A.; Li, K.; Wu, H.; Olson, D. H.; Emge, T. J.; Ki, W.; Hong, M.; Li, J. *Angew. Chem. Int. Ed.* **2009**, *48*, 2334.
- (21) Gong, Y. N.; Jiang, L.; Lu, T. B. *Chem. Commun.* **2013**, *49*, 11113.
- (22) Nagarkar, S. S.; Joarder, B.; Chaudhari, A. K.; Mukherjee, S.; Ghosh, S. K. *Angew. Chem. Int. Ed.* **2013**, *52*, 2881.
- (23) Dinda, D.; Gupta, A.; Shaw, B. K.; Sadhu, S.; Saha, S. K. *ACS Appl. Mater. Interfaces* **2014**, *6*, 10722.
- (24) Feng, H. T.; Zheng, Y. S. *Chem. Eur. J.* **2014**, *20*, 195.
- (25) Germain, M. E.; Knapp, M. J. *Chem. Soc. Rev.* **2009**, *38*, 2543.
- (26) Entwistle, C. D.; Marder, T. B. *Chem. Mater.* **2004**, *16*, 4574.
- (27) Wade, C. R.; Broomsgrove, A. E. J.; Aldridge, S.; Gabbai, F. P. *Chem. Rev.* **2010**, *110*, 3958.
- (28) Wade, C. R.; Gabbai, F. P. *Inorg. Chem.* **2010**, *49*, 714.
- (29) Madhu, S.; Bandela, A.; Ravikanth, M. *RSC Adv.* **2014**, *4*, 7120.
- (30) Hengchang, M.; Zhongwei, Z.; Yuanyuan, J.; Lajia, Z.; Chunxuan, Q.; Haiying, C.; Zengming, Y.; Zhiwang, Y.; Ziqiang, L. *RSC Adv.* **2015**, *5*, 87157.
- (31) Zhang, Z.; Zhang, Z.; Ye, K.; Zhang, J.; Zhang, H.; Wang, Y. *Dalton Trans.* **2015**, *44*, 14436.
- (32) Mukundam, V.; Dhanunjarao, K.; Chuang, C. N.; Kang, D. Y.; Leung, M. K.; Hsieh, K. H.; Venkatasubbaiah, K. *Dalton Trans.* **2015**, *44*, 10228.
- (33) Dhanunjarao, K.; Mukundam, V.; Venkatasubbaiah, K. *Inorg. Chem.* **2016**, *55*, 11153.

-
- (34) Park, S.; Kwon, O. H.; Kim, S.; Park, S.; Choi, M. G.; Cha, M.; Park, S. Y.; Jang, D. J. *J. Am. Chem. Soc.* **2005**, *127*, 10070.
- (35) Dhanunjayarao, K.; Mukundam, V.; Venkatasubbaiah, K. *J. Mater. Chem. C.* **2014**, *2*, 8599.
- (36) Kubota, Y.; Ozaki, Y.; Funabiki, K.; Matsui, M. *J. Org. Chem.* **2013**, *78*, 7058.
- (37) Kubota, Y.; Tanaka, S.; Funabiki, K.; Matsui, M. *Org. Lett.* **2012**, *14*, 4682.
- (38) Massue, J.; Frath, D.; Ulrich, G.; Retailleau, P.; Ziessel, R. *Org. Lett.* **2012**, *14*, 230.
- (39) Demas, J. N.; Crosby, G. A. *J.chem.Phys.* **1971**, *75*, 991.
- (40) Reiff, A. L.; Garcia-Frutos, E. M.; Gil, J. M.; Anderson, O. P.; Hegedus, L. S. *Inorg. Chem.* **2005**, *44*, 9162.
- (41) Li, Z. H.; Wong, M. S. *Org. Lett.* **2006**, *8*, 1499.
- (42) Dolomanov, O. V.; Bourhis, L. J.; Gildea, R. J.; Howard, J. A. K.; Puschmann, H. *J. Appl. Crystallogr.* **2009**, *42*, 339.
- (43) Sheldrick, G. M. *Acta Crystallogr. Sect. A: Found. Crystallogr.* **2007**, *64*, 112.

CHAPTER 3B**Synthesis and optical properties of
salicylaldimine-based diboron complexes**

3B.1 Introduction	127
3B.2 Results and discussion	128
3B.2.1 Synthesis and characterization of bis-salicylaldimine	128
3B.2.2 Synthesis and characterization of diboron compounds 5-7	129
3B.2.3 Photophysical properties of diboron compounds 5-7	135
3B.2.4 Electrochemical properties of diboron compounds 5-7	141
3B.3 Conclusions	143
3B.4 Experimental section	143
3B.4.1 General information	143
3B.4.2 Synthetic procedure and spectral characterization	144
3B.5 References	149

3B.1 Introduction

In recent years, tri¹⁻³- and tetracoordinate^{4,5} boron compounds have received immense attention owing to their use as new materials in different fields including organic field-effect transistors, sensor materials, organic light-emitting diodes (OLEDs), and photovoltaics. The overlap of the empty *p* orbital of the tricoordinate boron atom with the organic π system leads to interesting optoelectronic properties and also enables the detection of anions such as fluoride and cyanide. Recently, efforts have been devoted to the design and synthesis of tetracoordinate boron compounds with *N,O*-, *N,N*-, and *N,C*-chromophores.⁶⁻¹⁵ Among the tetracoordinate boron compounds, boron dipyrromethene dyes^{16,17} (figure 3B.1, i) have been studied to a greater extent owing to their potential application in artificial light harvesters, fluorescent sensors, laser dyes, sensitizers for solar cells, and molecular photonic wires. Boron quinolate compounds are analogous to aluminium quinolato compounds (Figure 3B.1, ii); the photophysical tuning of R₂BQ compounds (Q = substituted quinolate) was recently studied by Wang and co-workers^{18,19} and Jaekle and coworkers.²⁰⁻²⁴ Schiff base boron compounds (Figure 3B.1, iii) are yet another type of four-coordinate boron complex that has gained interest owing to their

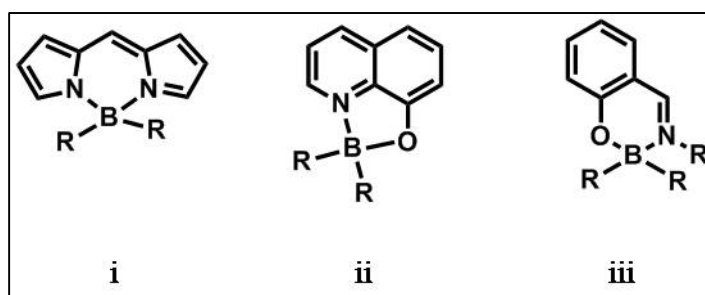


Figure 3B.1: Schematic representation of the skeleton of (i) boron dipyrromethene, (ii) boron quinolate, and (iii) Schiff base boron compounds.

greater stability than tricoordinate boron compounds.^{8,10,13,14} For example, Ziessel, Ulrich, and co-workers reported the synthesis and optical properties of boranil

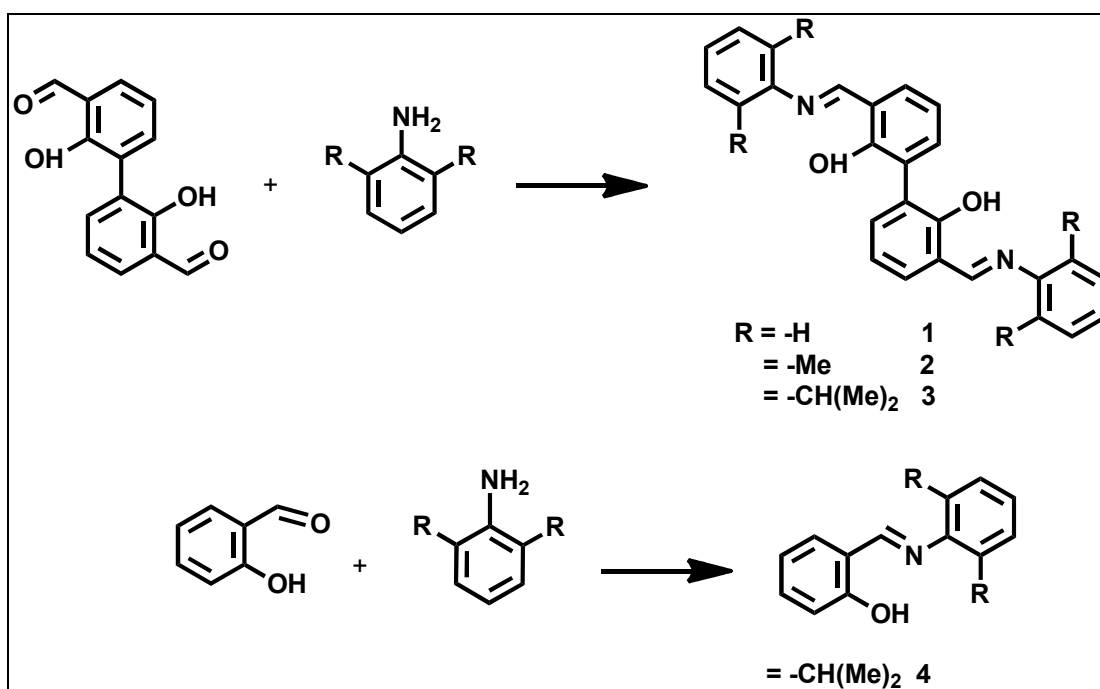
complexes.¹³ Ziessel and Ulrich are also credited for expanding the scope of the boranil complexes in a model labelling experiment with bovine serum albumin.¹⁴ More recently, Lee and co-workers reported a Schiff base route for the synthesis of boron-based stackable pseudo-triphenylenes, which showed interesting increased fluorescence upon aggregation in solution.²⁵

With advances in the design of different boron fluorophores, researchers are continually trying to synthesize conjugated tetracoordinate diboron or multiboron systems to improve fluorescence and electron-transport properties.^{12,26-28} For instance, Yamaguchi and co-workers reported the synthesis of boron-bridged dipyridylvinylenes and dithiazolylvinylenes.²⁶ More recently, Gomes and coworkers revealed the synthesis of an iminopyrrolyl diboron complex and its usefulness in nondoped OLEDs. In view of the important potential applications of boron compounds, in particular, the use of diboron compounds in transistors, OLEDs, and lasers, the search for alternative fluorescent dyes prompted us to synthesize new salicylaldehyde diboron complexes. We expect that a 1,1'-biphenyl backbone will help to increase the conjugation and, thus, result in better luminescent materials. The preparation and structural, photophysical, and electrochemical properties of these compounds have been explored in this chapter.²⁹

3B.2 Results and Discussion

3B.2.1 Synthesis and characterization of bis-salicylaldehyde

The bis-salicylaldehyde Schiff bases **1–3** (scheme 3B.1) were obtained *via* simple condensation reactions between the dialdehyde³⁰ and readily available anilines by using catalytic amount of acid in toluene or dichloromethane at reflux condition. All these starting materials were characterized by ¹H and ¹³C NMR spectrum. In the ¹H NMR spectra of all Schiff bases compounds, we observed a characteristic



Scheme 3B.1: Synthetic route to bis-salicylaldehyde Schiff bases 1–3.

H-bonded downfield phenolic proton at $\delta \approx 13\text{--}14$ ppm (figure 3B.2). All three Schiff bases were also characterized by single-crystal X-ray analysis. The molecular structure of compounds 1–3 were shown in figure 3B.3 and the corresponding crystal data and structure refinement were represented in table 3B.1. Particularly, as shown in figure 3B.3 all three Schiff bases were involved in intramolecular hydrogen bonding by utilizing phenolic hydrogen and the corresponding imine nitrogen atoms to form six membered rings. The observed hydrogen-bonding metric parameters ($H\cdots N$ 1.86–1.89 Å; $N\cdots O$ 2.59–2.62 Å; $O\text{--}H\cdots N$ 147.7–148.6°) showed similar trends to those previously reported for these interacting units.³¹

3B.2.2 Synthesis and characterization of diboron compounds 5-8

The sodium salt of the bis-salicylaldehyde treated with excess $BF_3 \cdot Et_2O$ in Sodium hydride was used for the deprotonation of Schiff bases in tetrahydrofuran.

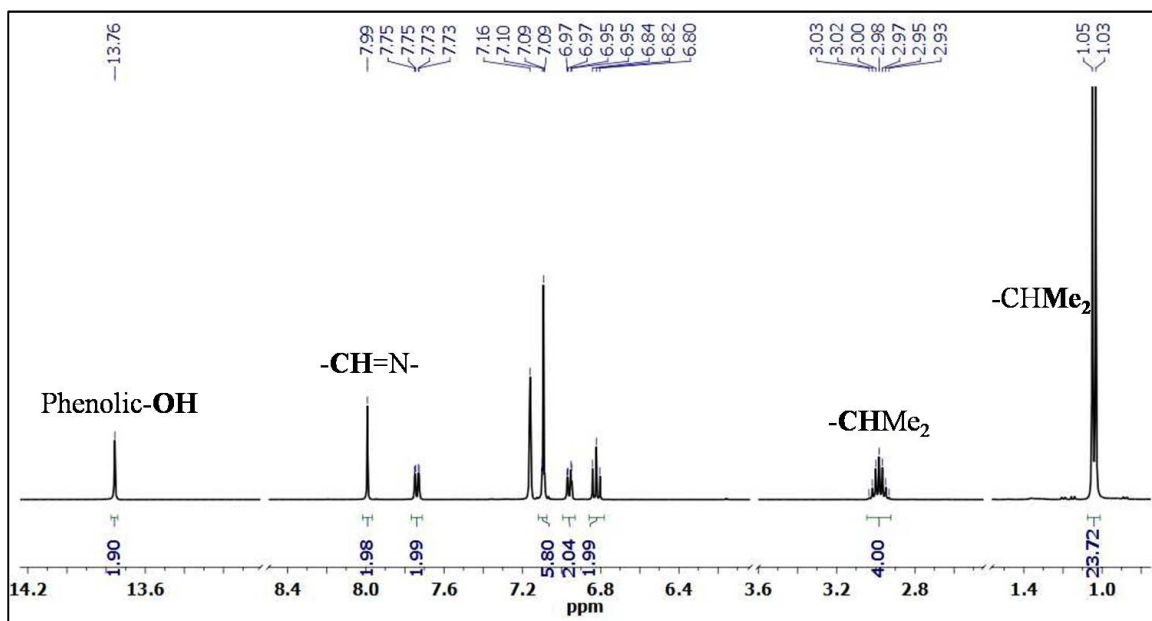


Figure 3B.2: ^1H NMR spectrum of compound 3.

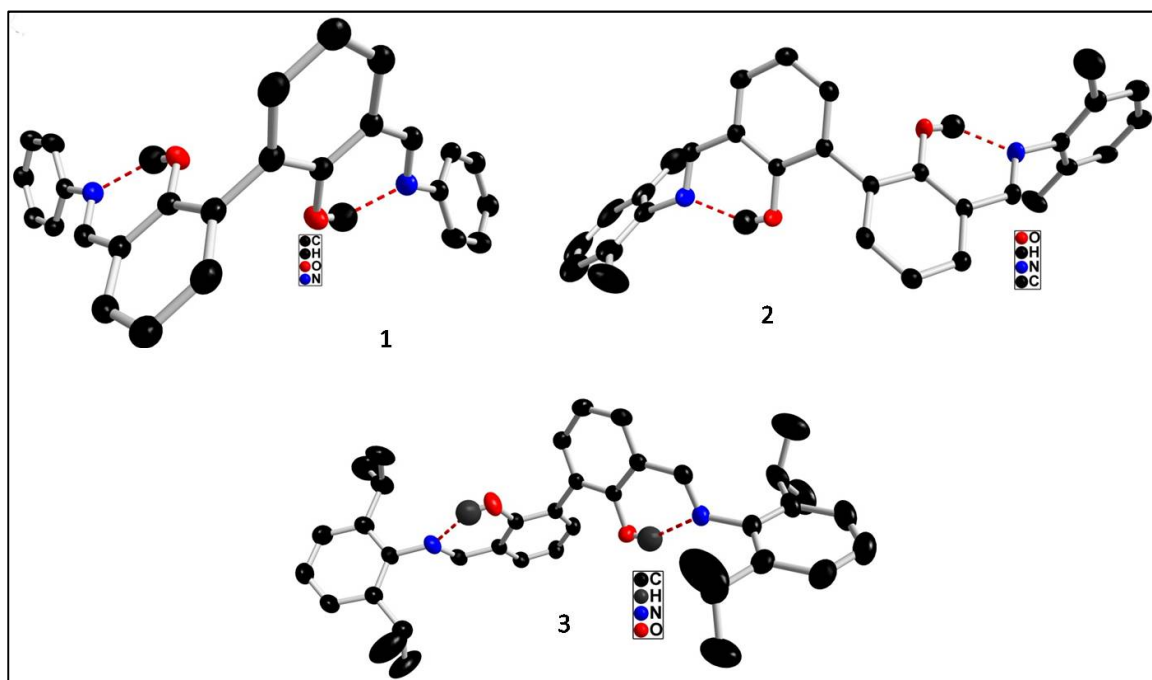
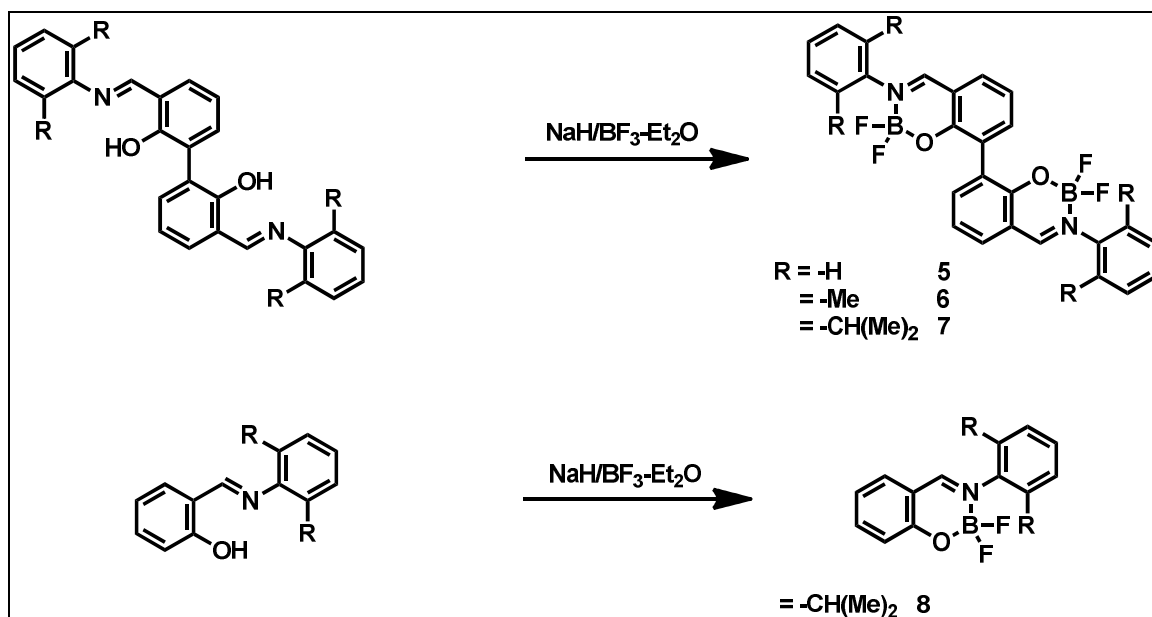


Figure 3B.3: Molecular structure of compounds 1-3. Hydrogen atoms are omitted for clarity.

Table 3B.1: Crystal data and structure refinement parameters for compounds **1-3**.

	1	2	3
Empirical formula	C ₂₆ H ₂₀ N ₂ O ₂	C ₃₀ H ₂₈ N ₂ O ₂	C ₃₈ H ₄₄ N ₂ O ₂
Formula weight	392.44	448.54	560.75
Temperature/K	296 (2)	296(2)	296(2)
Crystal system	Orthorhombic	Monoclinic	Monoclinic
Space group	Pbcn	P2(1)/n	C2/c
a/Å	10.6421(10)	9.3749(2)	37.628(6)
b/Å	9.9084(10)	15.9137(3)	9.1901(14)
c/Å	19.0054(16)	17.3009(4)	20.290(4)
α/°	90	90	90
β/°	90	102.9030(10)	107.919(15)
γ/°	90	90	90
Volume/Å ³	2004.0(3)	2515.94(9)	6676.1(19)
Z	4	4	8
ρ _{calc} /cm ³	1.301	1.184	1.116
μ/mm ⁻¹	0.083	0.074	0.068
F(000)	824.0	952.0	2416.0
Radiation	MoKα (λ = 0.71073)	MoKα (λ = 0.71073)	MoKα (λ = 0.71073)
2 θ range for data collection/°	2.81 – 28.73	2.29 – 30.04	2.07 – 28.34
Index ranges	-14 ≤ h ≤ 14 -13 ≤ k ≤ 13 -25 ≤ l ≤ 25	-13 ≤ h ≤ 13 -14 ≤ k ≤ 22 -24 ≤ l ≤ 24	-49 ≤ h ≤ 50 -12 ≤ k ≤ 12 -27 ≤ l ≤ 15
Reflections collected	28991	42160	53808
Independent reflections	2601 [R(int) = 0.0677]	7364 [R(int) = 0.0384]	8316 [R(int) = 0.0412]
Data/restraints/parameters	2601 / 0 / 138	7364 / 0 / 314	8316 / 0 / 390
Goodness-of-fit on F ²	0.961	1.035	1.035
Final R indexes [I > 2σ(I)]	R _I = 0.0404 wR ₂ = 0.0811	R _I = 0.0490 wR ₂ = 0.1252	R _I = 0.0606 wR ₂ = 0.1734
Final R indexes [all data]	R _I = 0.0799 wR ₂ = 0.0956	R _I = 0.0855 wR ₂ = 0.1448	R _I = 0.1026 wR ₂ = 0.2088
Largest diff. peak/hole / e Å ⁻³	0.146 and -0.141	0.216 and -0.203	0.379 and -0.277



Scheme 3B.2: Synthetic route to Schiff bases boron compounds 5–8.

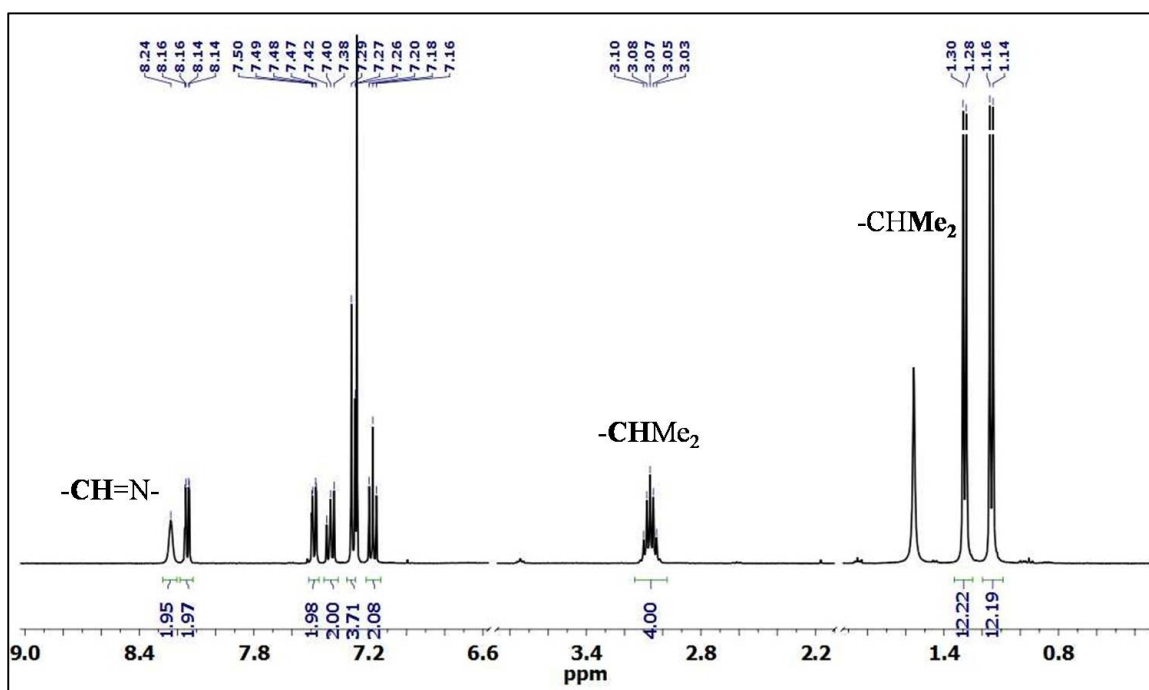


Figure 3B.4: ^1H NMR spectrum of compound 7.

at room temperature for 24 h yields diboron salicylaldehyde complexes. All boron compounds 5–7 were characterized by ^1H , ^{13}C NMR and HRMS. In the ^1H NMR

spectrum the downfield-shifted proton ($\delta \approx 13\text{--}14$ ppm) of starting materials (**1-3**) got disappear in their respective boron compounds (**5-7**) which indicates the product formation. The ^{11}B NMR spectra of the diboron complexes exhibited peak at $\delta \approx 0\text{--}1$ ppm, which indicates the formation of tetracoordinate boron atom. Additionally, these compounds (**5-7**) were also characterized by ^{19}F NMR spectroscopy. The chemical shift values of the fluorine nuclei in the ^{19}F NMR spectra were not strongly affected by the substitution. Fluorine nuclei of compound **6** and **7** resonates at $\delta = -137.2$ and -137.9 ppm respectively and were slightly upfield shifted in comparison to that of **5** ($\delta = -135.4$ ppm). The absence of quartet splitting pattern in ^{19}F NMR spectra reveals

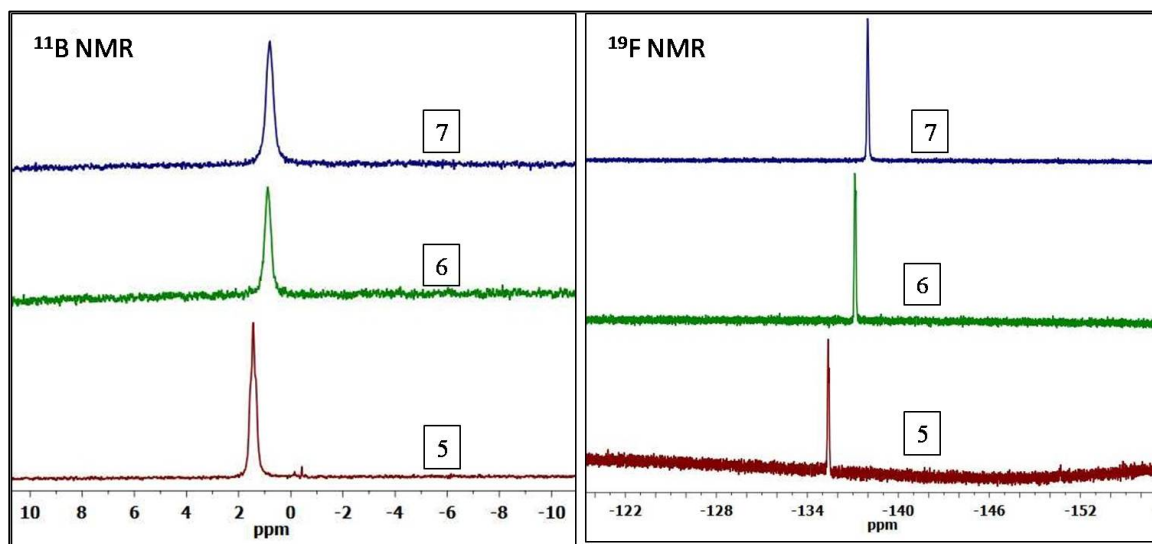


Figure 3B.5: ^{11}B (left) and ^{19}F NMR (right) spectrum of compounds **5-7**.

that there may be fast relaxation of the quadrupolar boron nuclei at room temperature (figure 3B.5). The proposed structures of diboron complexes were further confirmed by $[\text{M} + \text{Na}]^+$ ion peaks in HRMS and also single-crystal X-ray analysis of **5** and **7**. The molecular structures of **5** and **7** are shown in figure 3B.6 and 3B.7 respectively, and crystal data and structure refinement parameters are presented in the table 3B.2. The B–N and B–O bond lengths in **5** and **7** are similar to those of the other reported Schiff base– BF_2 complexes. In both structures, the boron atom deviates from the

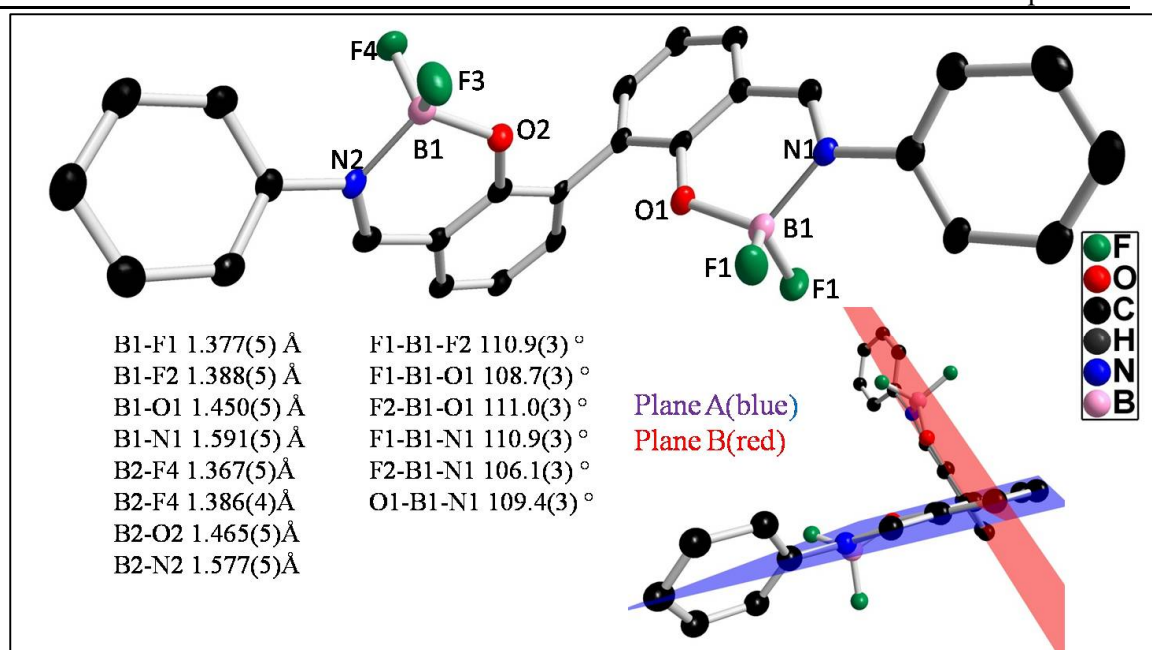


Figure 3B.6: Molecular structure of compounds 5. Hydrogen atoms are omitted for clarity.

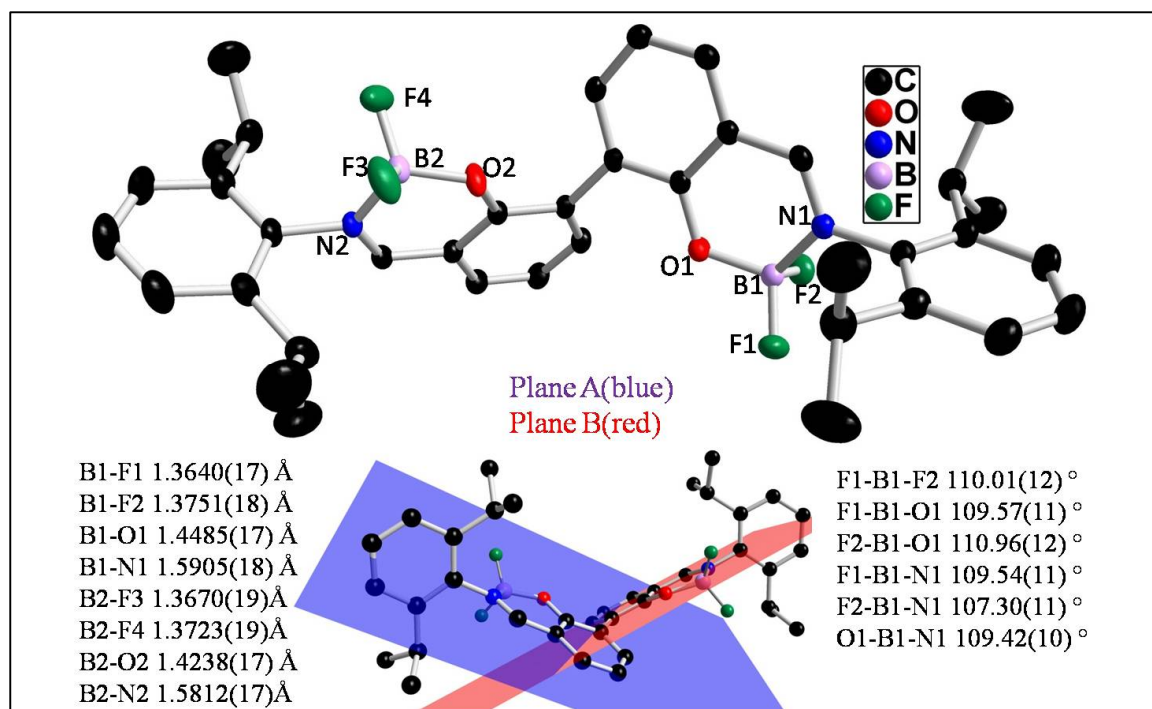


Figure 3B.7: Molecular structure of compounds 7. Hydrogen atoms are omitted for clarity.

nine-atom plane defined by the six biphenyl carbon atoms and the imino carbon, nitrogen, and oxygen atoms (figures 3B.6 and 3B.7); the deviation is more pronounced in **5** (0.39 Å for B1 and 0.37 Å for B2) than in **7** (0.30 Å for B1 and 0.18 Å for B2). The dihedral angles between the two planes (planes A and B,) are 73.45 and 123.21° in **5** and **7**, respectively. Steric hindrance in **7** plays a major role in this drastic difference, as is also seen from the separation distance between the boron atoms; the B–B distance in **5** is 5.74 Å, whereas in **7** it increases to 7.16 Å. Both boron atoms in **5** and **7** have slightly distorted tetrahedral geometries with angles ranging from 106.1(3) to 111.0(3) ° for **5** and 107.30(11) to 110.96(12) ° for **7**. The interplanar angles between planes A or B (six biphenyl carbon atoms and imino carbon, nitrogen, and oxygen atom) and the *N*-phenyl rings in **5** are 44.18 and 48.88°, and in **7** these angles are 77.86 and 85.19°.

3B.2.3 Photophysical properties of di-boron compounds 5-7

All boron complexes **5-7** showed good solubility in polar aprotic solvents. Because of poor solubility in non polar solvents, the photophysical properties of these compounds were studied in tetrahydrofuran. The absorption and fluorescence spectra of diboron compounds **5-7** in tetrahydrofuran are shown in Figure 3B.8. As shown in figure 3B.8 and table 3B.3, all three compounds exhibit absorption at *ca.* 370–380 nm and emission at *ca.* 460–490 nm. Both the absorption and the emission of **5** are redshifted in comparison to those of **6** and **7**. Compounds **5-7** showed moderate quantum yields (12, 28, and 16% respectively); however, a remarkably higher quantum yield was observed for **6** compared to those of **5** and **7**. The photophysical properties of these compounds were unaffected by solvent change; this indicates that the interactions of the fluorophores with solvent molecules in the excited state is less significant. To gain

Table 3B.2: Crystal data and structure refinement parameters of compounds **5** and **7**.

	5	7
Empirical formula	C ₃₀ H ₂₆ B ₂ F ₄ N ₂ O ₃	C ₄₀ H ₄₅ B ₂ F ₄ N ₃ O ₂
Formula weight	560.15	697.41
Temperature/K	150(2)	296(2) K
Crystal system	Triclinic	Monoclinic
Space group	P-1	P2(1)/n
a/Å	9.4177(9)	14.1532(19)
b/Å	9.4194(9)	14.855(2)
c/Å	15.9178(14)	18.101(3)
α/°	92.431(7)	90
β/°	92.202(7)	96.102(7)
γ/°	114.727(6)	90
Volume/Å ³	1279.0(2)	3784.2(9)
Z	2	4
ρ _{calc} /cm ³	1.455	1.224
μ/mm ⁻¹	0.112	0.088
F(000)	580	1472
Radiation	MoKα (λ = 0.71073)	MoKα (λ = 0.71073)
2θ range for data collection/°	2.39 – 26.31	1.99 - 30.16
Index ranges	-11 ≤ h ≤ 11 -11 ≤ k ≤ 11 -19 ≤ l ≤ 19	-19 ≤ h ≤ 14 -20 ≤ k ≤ 20 -25 ≤ l ≤ 25
Reflections collected	15390	63454
Independent reflections	5085 [R(int) = 0.0568]	11054 [R(int) = 0.0328]
Data/restraints/parameters	5085 / 0 / 372	11054 / 0 / 470
Goodness-of-fit on F ²	1.055	1.021
Final R indexes [I ≥ 2σ(I)]	R _I = 0.0571 wR ₂ = 0.1191	R _I = 0.0486 wR ₂ = 0.1238
Final R indexes [all data]	R _I = 0.0901 wR ₂ = 0.1327	R _I = 0.0800 wR ₂ = 0.1436
Largest diff. peak/hole / e Å ⁻³	0.327 and -0.322	0.261 and -0.225

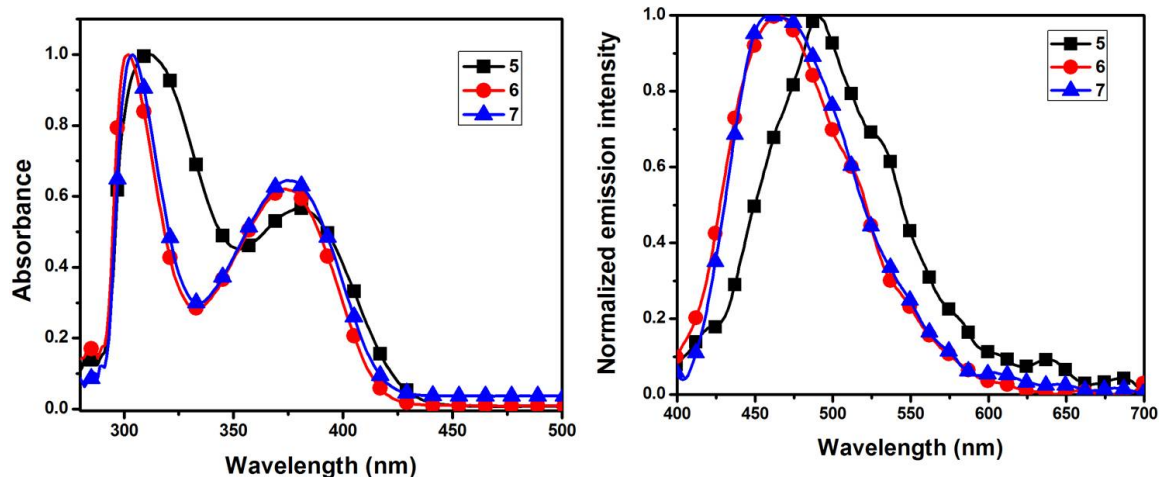


Figure 3B.8: Normalized absorption (left) and fluorescence emission (right) spectra of 5–7 in THF (43 μ M). Excited at the longer wavelength absorption maxima.

Table 3B.3: Photophysical data of compounds 5-7

Compound	$\lambda_{\max}^{[a]}$ (nm)	ϵ (L/mol.cm)	$\lambda_{\text{em}}^{[a,b]}$ (nm) (Φ) ^[c]
5	380	13500	490 (0.12)
6	373	8700	464 (0.28)
7	375	15548	460 (0.16)

^[a] Concentrations were 43 μ M in THF. ^[b] Excited at the absorption maximum. ^[c] Quantum yield measured by using quinine sulfate as a reference $\Phi = 0.54$ in 1 N H₂SO₄.

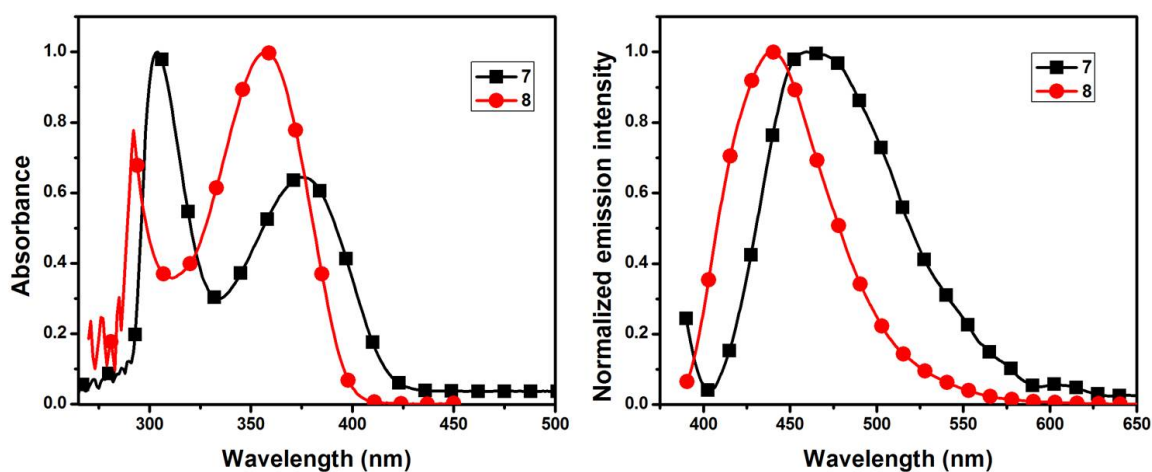


Figure 3B.9: Absorption (left) and normalized fluorescence emission (right) spectra of 7 and 8 in THF. Excited at the longer wavelength absorption maxim.

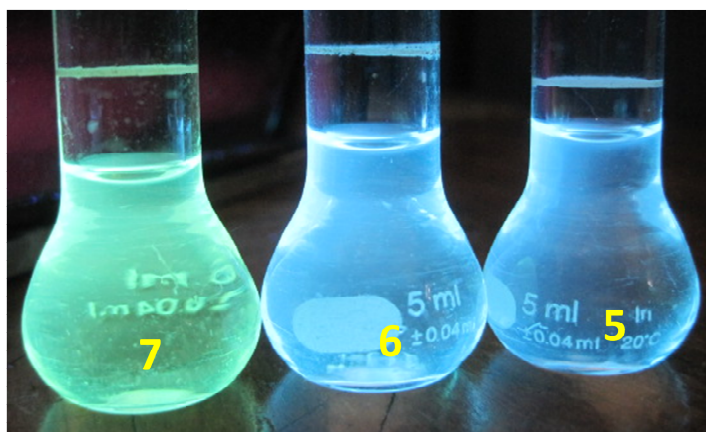


Figure 3B.10: Photograph of compounds 5-7 in THF under hand held UV lamp of 365 nm.

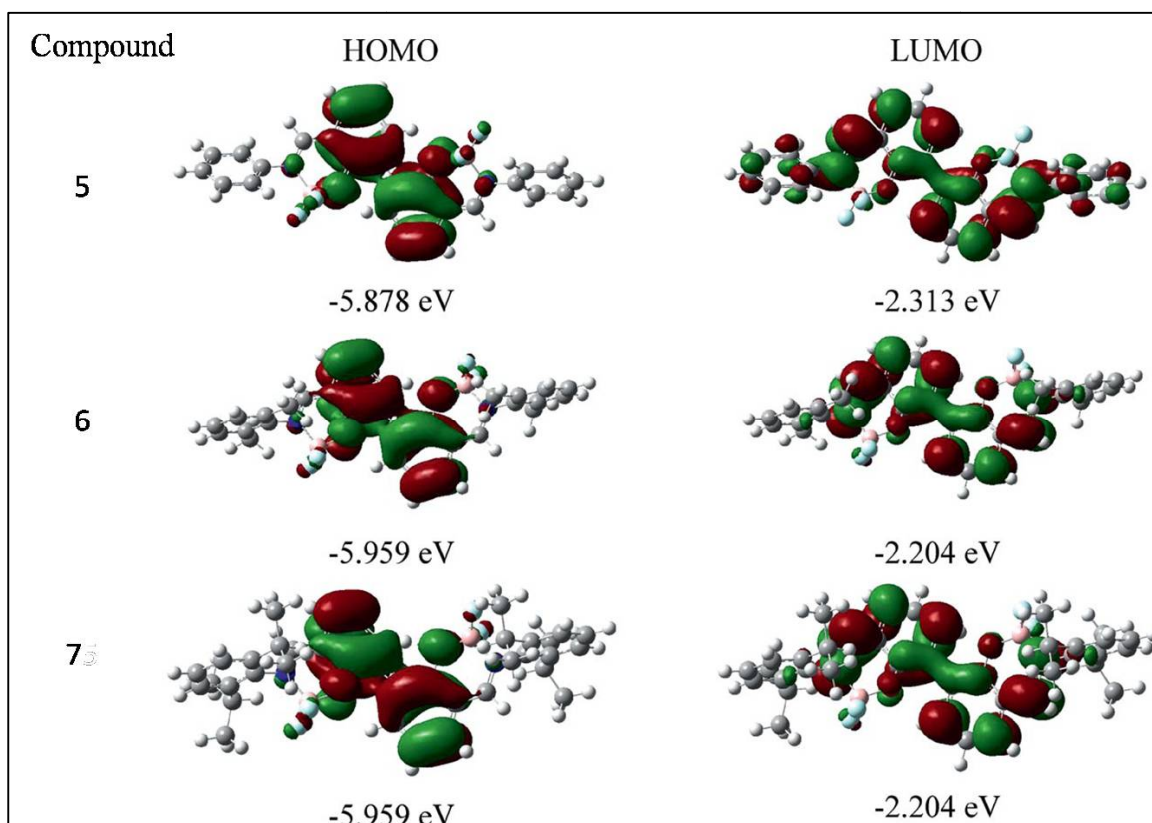


Figure 3B.11: Computed orbitals for 1-3.

more insight into the effect of the biphenyl moiety in our design, we also synthesized the salicylaldehyde monoboron complex **8** (scheme 4B.2) and studied its

photophysical properties. The mononuclear compound **8** showed substantial blueshifts both in absorption (20 nm) and in emission (18 nm) when compared to those of the diboron compound **7** (figures 3B.9); this might be because of the decreased conjugation length, and such a trend is similar to that reported by Gomes and coworkers in their study of iminopyrrolyl boron complexes.²⁸ Density functional theory (DFT)³² computations were performed to model the photophysical properties of the diboron compounds. The geometries of **5–7** were optimized by DFT [B3LYP, 6-31G (d)] calculations, and the excitation energies were computed by using time-dependent DT (TDDFT) calculations. The computed results are consistent with the

Table 3B.4: Calculated electronic transitions for **5–8** from TD-DFT (B3LYP) calculations.

Transition	MO contribution	Energy gap[eV] ([nm])	Oscillator strength (<i>f</i>)	
5 S0→S1	HOMO→LUMO	3.01 (411)	0.2030	
	S0→S2	HOMO→LUMO+1	3.09 (400)	0.0001
	S0→S3	HOMO2→LUMO+1 HOMO-1→LUMO	3.54 (350)	0.0142
6 S0→S1	HOMO→LUMO	3.16 (391)	0.1325	
	S0→S2	HOMO→LUMO+1	3.19 (387)	0.0000
	S0→S3	HOMO-6→LUMO+1	3.71 (333)	0.0080
		HOMO-5→LUMO		
HOMO-4→LUMO+1 HOMO-1→LUMO				
7 S0→S1	HOMO→LUMO	3.16 (391)	0.1324	
	S0→S2	HOMO→LUMO+1	3.19 (387)	0.0000
	S0→S3	HOMO-3→LUMO+1	3.67 (337)	0.0103
		HOMO-2→LUMO		
HOMO-1→LUMO+1				

Table 3B.5: Calculated orbital energies (eV) for compound **5-7** from DFT (B3LYP) calculations

Compound	5	6	7
LUMO+2	-0.734 (bph)	-0.734 (bph)	-0.734 (bph)
LUMO+1	-2.258 (N=CH-bph-CH=N)	-2.204 (N=CH-bph-CH=N)	-2.204 (N=CH-bph-CH=N)
LUMO	-2.313 (N=CH-bph-CH=N)	-2.204 (N=CH-bph-CH=N)	-2.204 (N=CH-bph-CH=N)
HOMO	-5.878 (O-bph-O)	-5.959 (O-bph-O)	-5.959 (O-bph-O)
HOMO-1	-6.285 (Ph-N=CH-bph-CH=N-Ph & O)	-6.449 (N=CH-bph-CH=N & O)	-6.449 (N=CH-bph-CH=N & O)
HOMO-2	-6.585 (Ph-N=CH-bph-CH=N-Ph)	-6.612 (N-Ph(Me ₂))	-6.530 (N-Ph(<i>i</i> Pr ₂))
Bph = Biphenyl			

experimental results, although the absolute excitation data deviate significantly (table 3B.4). Figure 3B.11 shows plots of the highest occupied molecular orbitals (HOMOs) and lowest unoccupied molecular orbitals (LUMOs) of **5-7**; according to the theoretical calculations, the lowest energy excitation corresponds to a π - π^* transition for all three compounds. The HOMOs are mainly contributed to the π orbitals of the biphenyl and oxygen moieties, whereas the LUMOs are composed of π^* orbitals of the biphenyl and imine moieties (tables 3B.5 and 3B.6). There is a clear difference in the electron distribution of **5** and those of **6** and **7**. For **6** and **7**, the electron distribution in the LUMO is confined to the biphenyl and oxygen moieties, whereas the electron distribution in the LUMO of **5** shows a delocalized feature. Owing to this π conjugation, the LUMO level of **5** is lowered and this helps to decrease the band gap and, thus, results in a redshift. Pronounced twists of the *N*-phenyl rings were

observed in **6** and **7** [the rings in **7** are twisted by 77.86 and 85.19°, whereas the rings in **5** are twisted by 48.88 and 44.18° (from X-ray data)] and may be responsible for restricted electronic communication in **6** and **7**.

Table 3B.6: Computed orbitals for compounds **5-7**

Compound	5	6	7
LUMO+2			
LUMO+1			
LUMO			
HOMO			
HOMO-1			
HOMO-2			

3B.2.4 Electrochemical properties of diboron compounds **5-7**

The electron-accepting abilities of the diboron compounds were studied by cyclic voltammetry in dimethylformamide (DMF). All compounds **5-7** underwent two separate reduction waves. The redox potentials for **5** at $E_{1/2}(1) = -1.63$ V and $E_{1/2}(2) = -1.83$ V are slightly less negative than those of **6** and **7** [$E_{1/2}(1) = -1.83$ V, $E_{1/2}(2) = -2.03$ V for **6**; $E_{1/2}(1) = -1.81$ V, $E_{1/2}(2) = -2.0$ V for **7** (Figure 3B.11)], maybe because

of the presence of electron-donating groups in **6** and **7**. The first reduction potentials of diboron compounds **5–7** are comparable with those of the diboron fluorophores reported by Zhang et al. but notably less negative than that of AlQ₃. The HOMO and LUMO energy levels were also calculated from the onset absorption and onset reduction potentials³³ (table 3B.4). The HOMO–LUMO gaps from these measurements are in agreement with the results obtained from the TD-DFT computations.

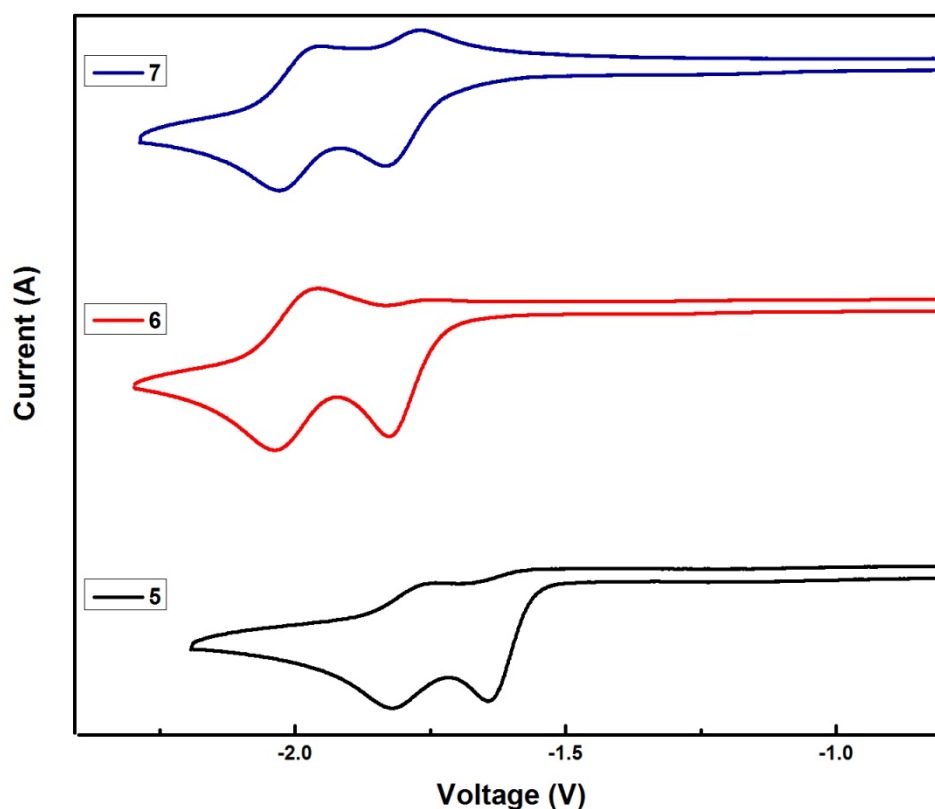


Figure 3B.12: Cyclic voltammograms of **5–7** with 0.1 m Bu₄N(PF₆) in DMF as the supporting electrolyte (scan rate 100 mV/s). Referenced relative to Fc/Fc⁺ couple.

Table 3B.7 Frontier orbital energies [eV] derived from UV/Vis onset absorption and electrochemical data.

Compound	HOMO-LUMO ^a gap (eV)	LUMO ^b (eV)	HOMO ^c (eV)
5	2.91	-3.28	-6.19
6	2.98	-3.11	-6.09
7	2.97	-3.18	-6.15

^[a] Estimated from the absorption onset of the longest-wavelength UV band. ^[b] Calculated from E_{pc} of the first reduction wave referenced to Fc/Fc⁺. ^[c] Calculated from the HOMO–LUMO gap and the LUMO.

3B.3 Conclusions

We have designed and synthesized new salicylaldehyde based diboron fluorophores by a simple synthetic procedure. All three boron compounds showed high thermal stability and interesting photophysical and electrochemical properties. We expect that the new diboron complexes reported here will have potential applications in optoelectronic devices.

3B.4 Experimental Section

3B.4.1 General information

Reagents were used as received unless otherwise noted. THF and toluene were distilled from Na/benzophenone prior to use. Chlorinated solvents were distilled from CaH₂. 2,2-Dihydroxybiphenyl- 3,3'-dicarbaldehyde was prepared according to the literature procedure³⁰. All ¹H (400 MHz), ¹³C (100 MHz), ¹¹B (128 MHz), and ¹⁹F (376 MHz) NMR spectra were recorded with a Bruker ARX 400 spectrometer. All ¹H and ¹³C NMR spectra were referenced internally to solvent signals. ¹¹B NMR spectra were referenced externally to BF₃·Et₂O in CDCl₃ ($\delta = 0$ ppm), and ¹⁹F NMR spectra were referenced to α,α,α -trifluorotoluene (0.05% in CDCl₃; $\delta = -63.73$ ppm). All NMR spectra were recorded at ambient temperature. Elemental analyses of C, H, and N were performed with a Perkin–Elmer 240C elemental analyzer. ESI mass spectra

were recorded with a Bruker microTOF-QII mass spectrometer. The absorbance spectra were recorded with a Perkin–Elmer Lambda 750 UV/Visible spectrometer. The fluorescence spectra were recorded with a Perkin–Elmer LS-55 Fluorescence Spectrometer and corrected for the instrumental response. Quinine sulfate was used as the standard for the determination of the quantum yields. Electrochemical measurements were performed with a conventional three-electrode cell and an electrochemical workstation (CH Instrument 1100A). The three-electrode system consisted of a glassy carbon working electrode, a Pt wire as the secondary electrode, and Ag wire as the reference electrode. The voltammograms were recorded with ca. 1.0×10^{-3} M solutions in DMF containing $\text{Bu}_4\text{N}(\text{PF}_6)$ (0.1 M) as the supporting electrolyte. The scans were referenced after the addition of a small amount of ferrocene as the internal standard. Single-crystal X-ray diffraction data were collected with a Bruker KAPPA APEX-II four angle rotation system with Mo- $K\alpha$ radiation (0.71073 Å). SADABS³³ absorption corrections were applied. Structures were solved by direct methods and completed by subsequent difference Fourier syntheses and refined by full-matrix least-squares procedures on reflection intensities (F^2). All non-hydrogen atoms were refined with anisotropic displacement coefficients. The H atoms were placed at calculated positions and were refined as riding atoms. DFT calculations were performed with the Gaussian03 program. Excitation data were determined by TD-DFT (B3LYP) calculations.

3B.4.2 Synthetic procedure and spectral characterization

[1,1'-Biphenyl]-2,2'-diol-3,3'-bis(phenylimino)methyl (1)

Aniline (0.88 mL, 9.70 mmol) and 2,2'-dihydroxybiphenyl-3,3'-dicarbaldehyde (1.12 g, 4.62 mmol) were dissolved in anhydrous toluene (20 mL). To this solution a catalytic amount of *p*-toluenesulfonic acid was added. The reaction mixture was

heated to reflux for 15 h under Dean–Stark reaction conditions. The reaction mixture was cooled to room temperature, the solvent was removed under vacuum, and the solid was purified by crystallization in chloroform and ethanol, yield 1.50 g, 83 %, m.p. 169 °C. ^1H NMR (400 MHz, C_6D_6): δ = 6.85–6.9 (m, 6 H, ArH), 6.95–6.99 (m, 4 H, ArH), 7.02–7.07 (m, 4 H, ArH), 7.73 (dd, J = 1.6, 8 Hz, 2 H, ArH), 8.07 (s, 2 H, CH=N), 13.97 (s, 2 H, ArOH) ppm. ^{13}C NMR (100 MHz, C_6D_6): δ = 118.54, 119.83, 121.56, 126.74, 126.92, 129.43, 132.26, 135.95, 148.97, 159.96 (ArC), 163.34 (CH=N) ppm. HRMS (ESI): calcd. for $\text{C}_{26}\text{H}_{20}\text{N}_2\text{O}_2$ [$\text{M} + \text{H}$] $^+$ 393.1598; found 393.1595. $\text{C}_{26}\text{H}_{20}\text{N}_2\text{O}_2$ (392.46): calcd. C 79.57, H 5.14, N 7.14; found C 79.31, H 5.22, N 7.01.

[1,1'-Biphenyl]-2,2'-diol-3,3'-bis({[2,6-bis(methyl)phenyl]imino}-methyl) (2)

2,6-Dimethylaniline (0.63 mL, 5.16 mmol), 2,2'-dihydroxybiphenyl-3,3'-dicarbaldehyde (0.50 g, 2.06 mmol), and formic acid (0.1 mL) were dissolved in anhydrous dichloromethane (15 mL). The reaction mixture was heated to reflux for 15 h and then cooled to room temperature. The solvent was removed under vacuum, and the solid was purified by crystallization in chloroform and ethanol, yield 0.65 g, 70 %, m.p. 175 °C. ^1H NMR (400 MHz, C_6D_6): δ = 1.95 (s, 12 H, CH_3), 6.85 (t, J = 8 Hz, 2 H, ArH), 6.90–6.93 (m, 8 H, ArH), 7.71 (s, 2 H, CH=N), 7.73 (d, J = 8 Hz, 2 H, ArH), 13.72 (s, 2 H, ArOH) ppm. ^{13}C NMR (100 MHz, C_6D_6): δ = 18.45 (CH_3), 118.54, 119.42, 125.14, 126.73, 128.58, 128.63, 132.16, 136.19, 148.74, 159.91 (ArC), 167.50 (CH=N) ppm. HRMS (ESI): calcd. for $\text{C}_{30}\text{H}_{28}\text{N}_2\text{O}_2$ [$\text{M} + \text{H}$] $^+$ 449.2224; found 449.2234. $\text{C}_{30}\text{H}_{28}\text{N}_2\text{O}_2$ (448.56): C 80.33, H 6.29, N 6.25; found C 80.12, H 6.01, N 6.08.

[1,1'-Biphenyl]-2,2'-diol-3,3'-bis({[2,6-bis(methylethyl)phenyl]-imino}methyl) (3)

By a similar procedure as that for **2**, the reaction of 2,6-diisopropyl aniline (1.94 mL, 10.32 mmol) and biphenol dialdehyde (1.00 g, 4.13 mmol) gave a yellow solid, which was purified by recrystallization, yield 2.00 g, 86 %, m.p. 192 °C. ¹H NMR (400 MHz, C₆D₆): δ = 1.04 (d, *J* = 8 Hz, 24 H, CH₃), 2.93–3.03 (m, 4 H, CH), 6.82 (t, *J* = 8 Hz, 2 H, ArH), 6.96 (d, *J* = 8 Hz, 2 H, ArH), 7.09–7.10 (m, 6 H, ArH), 7.74 (d, *J* = 8 Hz, 2 H, ArH), 7.99 (s, 2 H, CH=N), 13.75 (s, 2 H, ArOH) ppm. ¹³C NMR (100 MHz, C₆D₆): δ = 23.60 (CH₃), 28.53 (CH), 118.75, 119.36, 123.56, 125.87, 126.60, 132.21, 136.46, 139.08, 147.00, 159.88 (ArC), 167.58 (CH=N) ppm. HRMS (ESI): calcd. for C₃₈H₄₄N₂O₂ [M + H]⁺ 561.3476; found 561.3441. C₃₈H₄₄N₂O₂ (560.78): calcd. C 81.39, H 7.91, N 5.00; found C 81.23, H 7.99, N 4.92.

Synthesis of compound **4**

Compound **4** was prepared following the same procedure used for compound **2**, reaction of 2,6 di-isopropylaniline (1.54 ml, 8.10 mmol,) and salicylaldehyde (0.86 ml, 8.10 mmol) gave a yellow solid; purified by recrystallization. Yield : 2.00 g, 87 %. m.p. 59 °C. ¹H NMR (400 MHz, CDCl₃): δ = 1.24 (d, 12 H, *J* = 4 Hz, CH₃), 3.02–3.09 (m, 2H, CH), 7.02–7.05 (m, 1H, ArH), 7.20 (d, 1H, *J* = 8 Hz, ArH), 7.26–7.30 (m, 3H, ArH), 7.44 (d, 1H, *J* = 8 Hz, ArH), 7.50 (t, 1H, *J* = 8 Hz, ArH), 8.36 (s, 1H, CH = N). ¹³C NMR (100 MHz, CDCl₃): δ = 23.68 (CH₃), 28.32(CH), 117.64, 118.42, 119.35, 123.52, 126.03, 132.63, 134.03, 139.17, 145.36, 161.65 (ArC), 166.98 (CH=N). HR-MS (ESI): calcd. for C₁₉H₂₃N₁O₁ ([M + H]⁺): 282.1852, found: 282.1860.

Synthesis of the boron complex **5**

Under nitrogen, **1** (0.40 g, 1.02 mmol) was added to a suspension of NaH (0.056 g, 2.34 mmol) in anhydrous tetrahydrofuran (15 mL) at 0 °C with stirring. The reaction mixture was warmed to room temperature and stirred at that temperature for 2 h. The resulting solution was added to a solution of BF₃·Et₂O (2.51 mL, 20.40 mmol) in

tetrahydrofuran, and the mixture was stirred for 24 h. The reaction mixture was filtered through Celite, and the resulting filtrate was concentrated to yield a pale yellow solid, which was purified by recrystallization in acetonitrile, yield 260 mg, 52%, m.p. 297–303 °C (dec). ^1H NMR (400 MHz, CDCl_3): δ = 7.17 (t, J = 4 Hz, 2 H, ArH), 7.47–7.58 (m, 12 H, ArH), 8.05 (d, J = 8 Hz, 2 H, ArH), 8.49 (s, 2 H, CH=N) ppm. ^{13}C NMR (100 MHz, CDCl_3): δ = 116.61, 120.40, 123.78, 126.15, 129.49, 129.84, 132.43, 142.01, 142.56, 157.65 (ArC), 163.84 (CH=N) ppm. ^{19}F NMR (376 MHz, CDCl_3): δ = –135.44 (br) ppm. ^{11}B NMR (128 MHz, CDCl_3): δ = 1.01 (s) ppm. Quantum yield (Φ) = 0.12. IR (KBr): $\tilde{\nu}$ = 3030 (w), 2944 (m), 2872 (s), 1622 (s), 1589 (m), 1567 (m), 1454 (s), 1391 (m), 1335 (m), 1255 (s), 1201 (s), 1126 (m), 1048 (s) cm^{-1} . HRMS (ESI): calcd. for $\text{C}_{26}\text{H}_{18}\text{B}_2\text{F}_4\text{N}_2\text{O}_2$ $[\text{M} + \text{Na}]^+$ 511.1392; found 511.1321. $\text{C}_{26}\text{H}_{18}\text{B}_2\text{F}_4\text{N}_2\text{O}_2$ (488.05): calcd. C 63.99, H 3.72, N 5.74; found C 64.27, H 3.79, N 5.63.

Synthesis of the boron complex 6

Compound 6 was prepared by following a similar procedure to that used for 5. The reaction of imine (0.20 g, 0.44 mmol), NaH (0.026 g, 1.11 mmol), and $\text{BF}_3 \cdot \text{Et}_2\text{O}$ (2.7 mL, 22.30 mmol) in anhydrous tetrahydrofuran gave the product as a white solid, which was purified by recrystallization, yield 0.183 g, 75%, m.p. 310 °C (stable to 310 °C). ^1H NMR (400 MHz, CDCl_3): δ = 2.31 (s, 12 H, CH_3), 7.15–7.22 (m, 8 H, ArH), 7.50 (d, J = 8 Hz, 2 H, ArH), 8.14 (d, J = 8 Hz, 2 H, ArH), 8.26 (s, 2 H, CH=N) ppm. ^{13}C NMR (100 MHz, CDCl_3): δ = 18.30 (CH_3), 116.54, 120.35, 126.20, 128.74, 128.92, 132.18, 133.56, 141.15, 142.16, 157.67 (ArC), 167.65 (CH=N) ppm. ^{19}F NMR (376 MHz, CDCl_3): δ = –137.15 (br) ppm. ^{11}B NMR (128 MHz, CDCl_3): δ = 0.89 (s) ppm. Quantum yield (Φ) = 0.28. IR (KBr): $\tilde{\nu}$ = 3032 (w), 2965 (m), 2870 (m), 1626 (s), 1581 (m), 1567 (s), 1436 (s), 1385 (s), 1316 (s), 1245 (s), 1218 (s),

1188 (s), 1048 (m) cm^{-1} . HRMS (ESI): calcd. For $\text{C}_{30}\text{H}_{26}\text{B}_2\text{F}_4\text{N}_2\text{O}_2$ $[\text{M} + \text{Na}]^+$ 567.2019; found 567.2064. $\text{C}_{30}\text{H}_{26}\text{B}_2\text{F}_4\text{N}_2\text{O}_2$ (544.16): calcd. C 66.22, H 4.82, N 5.15; found C 65.94, H 4.42, N 5.38.

Synthesis of the boron complex 7

Compound **7** was prepared by following a similar procedure to that used for **5**. The reaction of imine (1.00 g, 1.78 mmol), NaH (0.107 g, 4.46 mmol), and $\text{BF}_3 \cdot \text{Et}_2\text{O}$ (11 mL, 89.16 mmol) in anhydrous tetrahydrofuran (30 mL) gave the product as a white solid, which was purified by recrystallization, yield 1.05 g, 90%, m.p. 310 °C (stable to 310 °C). ^1H NMR (400 MHz, CDCl_3): δ = 1.15 (d, J = 8 Hz, 12 H, CH_3), 1.29 (d, J = 8 Hz, 12 H, CH_3), 3.03–3.1 (m, 4 H, CH), 7.18 (t, J = 8 Hz, 2 H, ArH), 7.26–7.28 (m, 4 H, ArH), 7.40 (t, J = 8 Hz, 2 H, ArH), 7.48 (d, J = 8 Hz, 2 H, ArH), 8.15 (d, J = 8 Hz, 2 H, ArH), 8.24 (s, 2 H, $\text{CH}=\text{N}$) ppm. ^{13}C NMR (100 MHz, CDCl_3): δ = 23.37 (CH_3), 25.61 (CH_3), 28.60 (CH), 116.35, 120.44, 124.48, 126.17, 129.48, 132.22, 137.87, 142.31, 144.21, 157.63 (ArC), 167.02 ($\text{CH}=\text{N}$) ppm. ^{19}F NMR (376 MHz, CDCl_3): δ = -137.94 (br) ppm. ^{11}B NMR (128 MHz, CDCl_3): δ = 0.80 (s) ppm. Quantum yield (Φ) = 0.16. IR (KBr): $\tilde{\nu}$ = 3065 (w), 2975 (s), 2872 (m), 1626 (s), 1592 (w), 1568 (s), 1465 (m), 1439 (s), 1386 (s), 1311 (s), 1254 (s), 1238 (s), 1183 (s), 1151 (m), 1111 (m), 1057 (m) cm^{-1} . HRMS (ESI): calcd. For $\text{C}_{38}\text{H}_{42}\text{B}_2\text{F}_4\text{N}_2\text{O}_2$ $[\text{M} + \text{Na}]^+$ 679.3273; found 679.3211. $\text{C}_{38}\text{H}_{42}\text{B}_2\text{F}_4\text{N}_2\text{O}_2$ (656.37): calcd. C 69.54, H 6.45, N 4.27; found C 69.83, H 6.31, N 4.11.

Synthesis of the boron complex 8

Compound **8** was prepared following the same procedure used for compound **5**, reaction of imine (1.00 g, 3.5 mmol), NaH (0.25 g, 10.6 mmol), and $\text{BF}_3\text{Et}_2\text{O}$ (4.38 mL, 35.5 mmol) in 30 mL of anhydrous THF gave a white solid. The crude compound was purified by recrystallization in dichloromethane. Yield: 0.93 g, 79 %, m.p. 233 °C.

^1H NMR (400 MHz, CDCl_3): = 1.08 (d, 6H, $J=8\text{Hz}$, CH_3), 1.25 (d, 6H, $J=8\text{Hz}$, CH_3), 2.94-3.05 (m, 2H, CH), 7.02 (t, 1H, $J=8\text{Hz}$, ArH), 7.16 (d, 1H, $J=8\text{Hz}$, ArH), 7.23 (d, 2H, $J=8\text{Hz}$, ArH), 7.36 (t, 1H, $J=8\text{Hz}$, ArH), 7.42-7.45 (m, 1H, ArH), 7.66 (t, 1H, $J=8\text{Hz}$, ArH), 8.16 (s, 1H, $\text{CH}=\text{N}$). ^{13}C NMR (100MHz, CDCl_3): = 23.33 (CH_3), 25.53 (CH_3), 28.55 (CH), 115.56, 120.08, 120.54, 124.44, 129.44, 132.18, 137.81, 139.39, 144.11, 160.35 (ArC), 166.80 ($\text{CH}=\text{N}$). ^1H NMR (376 MHz, CDCl_3): = -138.35 (br). ^{11}B NMR (128 MHz, CDCl_3): = 0.72. HR-MS (ESI): calcd. for $\text{C}_{19}\text{H}_{22}\text{B}_1\text{F}_2\text{N}_1\text{O}_1$ ($[[\text{M} + \text{Na}]^+]$): 352.1658, found: 352.1650

3B.5 References

- (1) Entwistle, C. D.; Marder, T. B. *Chem. Mater.* **2004**, *16*, 4574.
- (2) Wade, C. R.; Broomsgrove, A. E. J.; Aldridge, S.; Gabbaï, F. P. *Chem. Rev.* **2010**, *110*, 3958.
- (3) Yamaguchi, S.; Wakamiya, A. *Pure Appl. Chem.* **2006**, *78*, 1413.
- (4) Rao, Y. L.; Amarne, H.; Wang, S. *Coord. Chem. Rev.* **2012**, *256*, 759.
- (5) Tanaka, K.; Chujo, Y. *Macromol. Rapid Commun.* **2012**, *33*, 1235.
- (6) Zhang, H.; Huo, C.; Ye, K.; Zhang, P.; Tian, W.; Wang, Y. *Inorg. Chem.* **2006**, *45*, 2788.
- (7) Zhang, H.; Huo, C.; Zhang, J.; Zhang, P.; Tian, W.; Wang, Y. *Chem. Commun.* **2006**, 281.
- (8) Hou, Q.; Zhao, L.; Zhang, H.; Wang, Y.; Jiang, S. *J. Lumin.* **2007**, *126*, 447.
- (9) Liddle, B. J.; Silva, R. M.; Morin, T. J.; Macedo, F. P.; Shukla, R.; Lindeman, S. V.; Gardinier, J. R. *J. Org. Chem.* **2007**, *72*, 5637.
- (10) Ren, Y.; Liu, X.; Gao, W.; Xia, H.; Ye, L.; Mu, Y. *Eur. J. Inorg. Chem.* **2007**, 1808.

-
- (11) Macedo, F. P.; Gwengo, C.; Lindeman, S. V.; Smith, M. D.; Gardinier, J. R. *Eur. J. Inorg. Chem.* **2008**, 3200.
- (12) Zhang, Z.; Bi, H.; Zhang, Y.; Yao, D.; Gao, H.; Fan, Y.; Zhang, H.; Wang, Y.; Wang, Y.; Chen, Z.; Ma, D. *Inorg. Chem.* **2009**, *48*, 7230.
- (13) Frath, D.; Azizi, S.; Ulrich, G.; Retailleau, P.; Ziessel, R. *Org. Lett.* **2011**, *13*, 3414.
- (14) Frath, D.; Azizi, S.; Ulrich, G.; Ziessel, R. *Org. Lett.* **2012**, *14*, 4774.
- (15) Massue, J.; Frath, D.; Ulrich, G.; Retailleau, P.; Ziessel, R. *Org. Lett.* **2012**, *14*, 230.
- (16) Loudet, A.; Burgess, K. *Chem. Rev.* **2007**, *107*, 4891.
- (17) Boens, N.; Leen, V.; Dehaen, W. *Chem. Soc. Rev.* **2012**, *41*, 1130.
- (18) Wu, Q.; Esteghamatian, M.; Hu, N. X.; Popovic, Z.; Enright, G.; Tao, Y.; D'Iorio, M.; Wang, S. *Chem. Mater.* **2000**, *12*, 79.
- (19) Cui, Y.; Liu, Q. D.; Bai, D. R.; Jia, W. L.; Tao, Y.; Wang, S. *Inorg. Chem.* **2005**, *44*, 601.
- (20) Qin, Y.; Kiburu, I.; Shah, S.; Jäkle, F. *Macromolecules* **2006**, *39*, 9041.
- (21) Qin, Y.; Kiburu, I.; Shah, S.; Jäkle, F. *Org. Lett.* **2006**, *8*, 5227.
- (22) Li, H.; Jäkle, F. *Macromolecules* **2009**, *42*, 3448.
- (23) Cheng, F.; Jäkle, F. *Chem. Commun.* **2010**, *46*, 3717.
- (24) Cheng, F.; Bonder, E. M.; Jäkle, F. *Macromolecules* **2012**, *45*, 3078.
- (25) Riddle, J. A.; Lathrop, S. P.; Bollinger, J. C.; Lee, D. *J. Am. Chem. Soc.* **2006**, *128*, 10986.
- (26) Zhao, Q.; Zhang, H.; Wakamiya, A.; Yamaguchi, S. *Synthesis* **2009**, 127.
- (27) Li, D.; Zhang, Z.; Zhao, S.; Wang, Y.; Zhang, H. *Dalton Trans.* **2011**, *40*, 1279.
-

-
- (28) Suresh, D.; Gomes, C. S. B.; Gomes, P. T.; Di Paolo, R. E.; Maçanita, A. L.; Calhorda, M. J.; Charas, A.; Morgado, J.; Teresa Duarte, M. *Dalton Trans.* **2012**, *41*, 8502.
- (29) Dhanunjayarao, K.; Mukundam, V.; Ramesh, M.; Venkatasubbaiah, K. *Eur. J. Inorg. Chem.* **2014**, 539.
- (30) Zhang, H. C.; Huang, W. S.; Pu, L. *J. Org. Chem.* **2001**, *66*, 481.
- (31) Steiner, T. *Angew. Chem.* **2002**, *114*, 50.
- (32) Frisch, M. J. *Gaussian 09* **2009**.
- (33) Sheldrick, G. M. *SADABS* **1997**.

CHAPTER 4A**Synthesis and photophysical properties of imidazole based
N,C-chelate boron complexes**

4A.1 Introduction	155
4A.2 Results and discussion	155
4A.2.1 Synthesis and characterization of compounds L1-L4	155
4A.2.2 Synthesis and characterization of compounds B1-B4	157
4A.2.3 Single crystal X-ray analysis	159
4A.2.4 TGA and DSC analysis	162
4A.2.5 Photophysical studies	163
4A.3 Conclusions	167
4A.4 Experimental section	167
4A.4.1 Methods and instruments	167
4A.4.2 Synthetic procedure and spectral characterization	168
4A.5 References	173

4A.1 Introduction

In recent years the design and synthesis of luminescent tetra-coordinate boron compounds has become a subject of extensive research by many groups because of its unique electronic and optical properties such as materials for organic light emitting diodes (OLEDs),^{1,2} fluorescent bio-imaging,^{3,4} photochromic materials.⁵ The ligand design includes mostly *N,O*- and *N,N*- chelate motifs to form five- and six-membered ring boron compounds.⁶ Prominent examples are boron dipyrromethene (BODIPY) dyes,⁷ 8-hydroxyquinolate boron complexes,⁸⁻¹² boranils,¹³⁻¹⁶ formazanate boron compounds.¹⁷⁻²⁰ However *N,C*- chelate boron compounds were studied to a lesser extent. Yamaguchi group first reported thienylthiazole based *N,C*- chelate boron compounds for electron transporting layers in OLEDs.^{21,22} Later Wang group developed several dimesitylboron compounds based on 2-phenylpyridine for photochromic applications.²³⁻²⁵

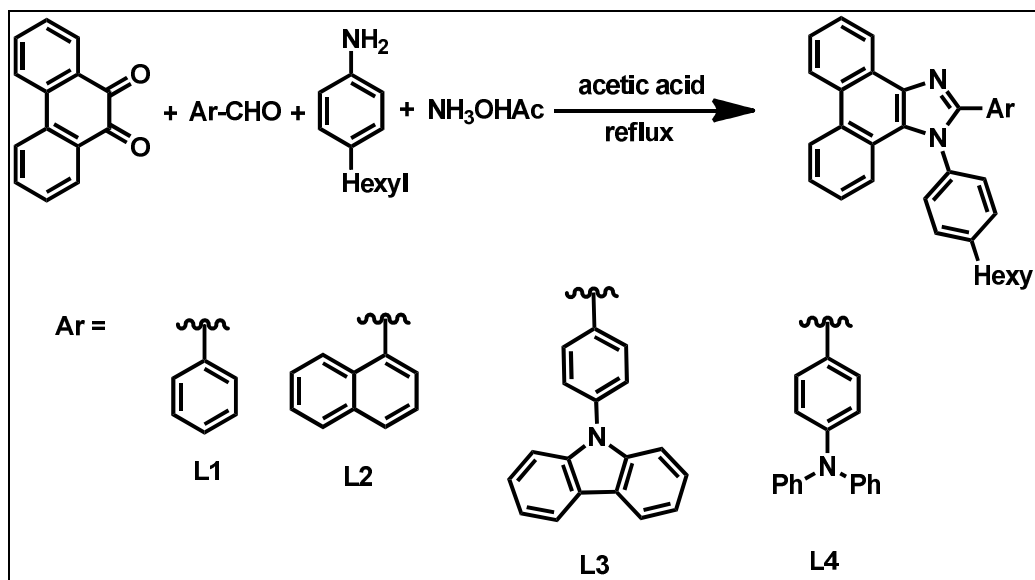
Imidazoles are versatile molecules, greatly studied for their applications in sensors,^{26,27} biological systems²⁸⁻³⁰ and in optoelectronics.^{31,32} Particularly tertaphenyl imidazoles are recently studied for OLEDs,^{33,34} and as a ESIPT based fluorescent materials.³⁵ In this chapter phenanthrene based imidazole boron compounds were prepared by simple synthetic strategy³⁶ with varying substituents on 2-phenyl imidazole moiety.

4A.2 Results and Discussion

4A.2.1 Synthesis and characterization of compounds L1-L4

The synthesis of phenanthrene imidazole ligands (**L1-L4**) are outlined in scheme 4A.1. By taking 9,10-phenanthrenequinone, ammonium acetate, 4-hexylaniline, aldehyde in acetic acid reflux condition gave imidazole ligands (**L1-L4**) in good

yields (scheme 4A.1). All these compounds were well characterized by ^1H , ^{13}C NMR and HRMS analysis. Representative example of ^1H NMR and HRMS spectra of **L1** and **L4** are shown in figure 4A.1 and 4A.2 respectively.



Scheme 4A.1: Synthetic route to compounds **L1**-**L4**.

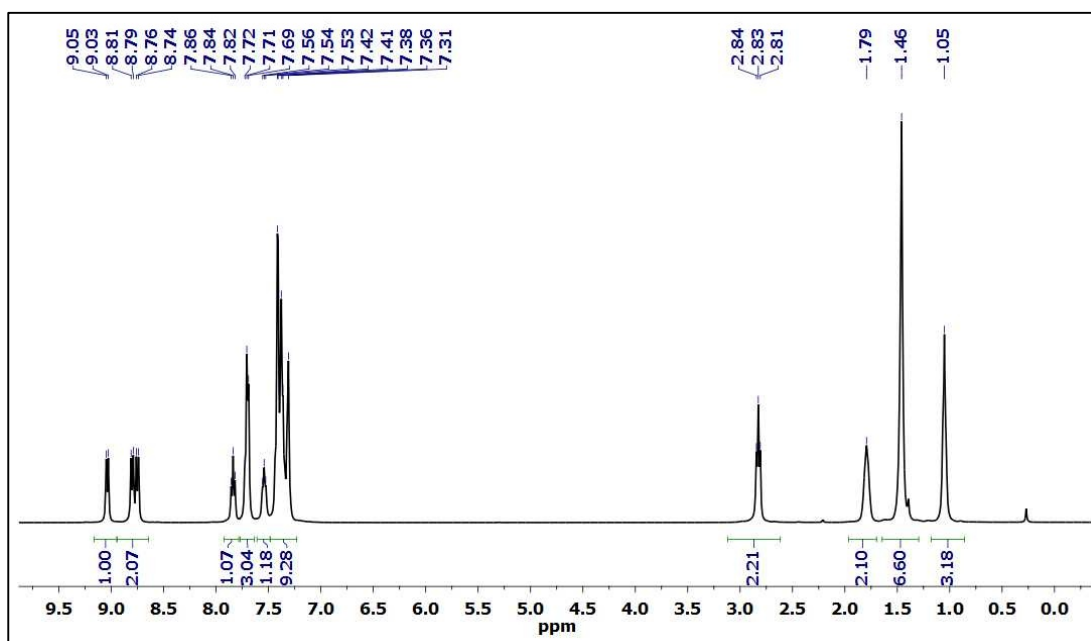


Figure 4A.1: ^1H NMR spectrum of compound **L1**.

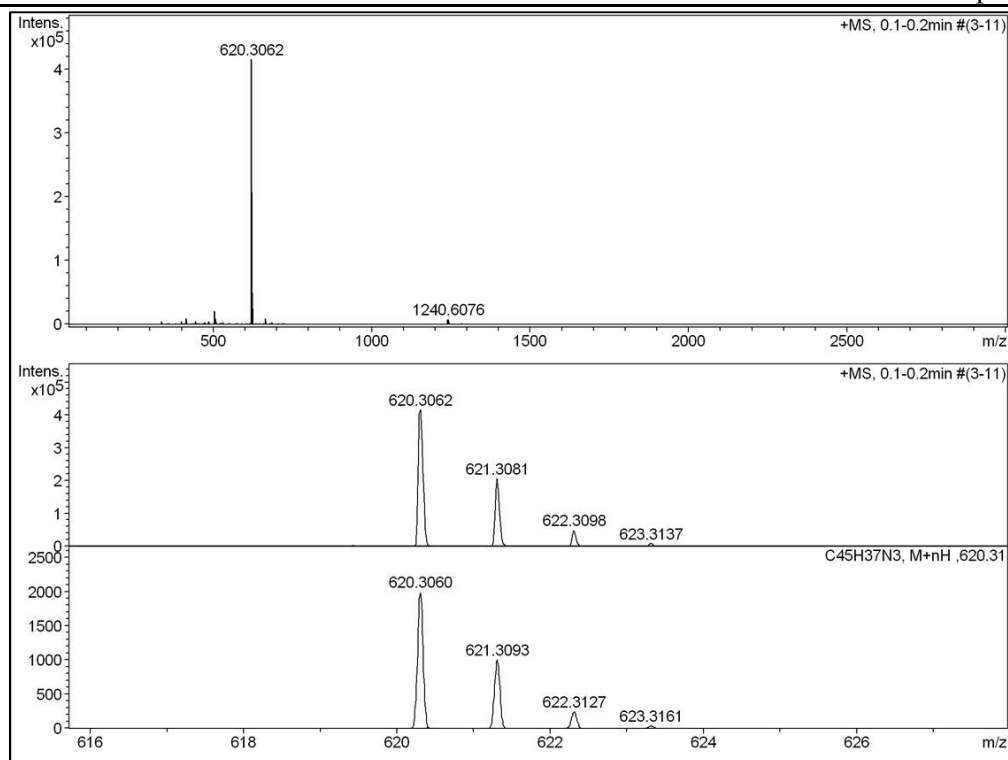


Figure 4A.2: HRMS of compound **L3**.

4A.2.2 Synthesis and characterization of compounds **B1-B4**

Phenanthrene based imidazole *N,C*-chelate dibromoborane compounds were prepared from their corresponding imidazole ligands through an electrophilic aromatic borylation reaction using BBr_3 under basic condition (*i*- Pr_2NEt). Without further purification, the imidazole dibromoborane complexes were treated with trimethylaluminum (AlMe_3) in toluene to afford the desired products **B1-B4** in moderate yields. A representative example for the synthesis of **B1** is shown in scheme 4A.2. All these boron compounds are highly stable towards air and moisture. All these boron compounds were fully characterized by ^1H , ^{13}C , ^{11}B NMR and ESI- mass spectrometry. The characteristic peak at 0.44 (for **B1**), 0.65 (for **B2**), 0.72 (for **B3**), 0.39 (for **B4**) ppm in ^1H NMR, and around 7 ppm (broad) in ^{13}C NMR corresponds to the methyl protons on the boron centre. A representative ^1H , ^{13}C , ESI-MS spectrum of compound **B1** are given in figure 4A.3, 4A.4, and 4A.5 respectively.

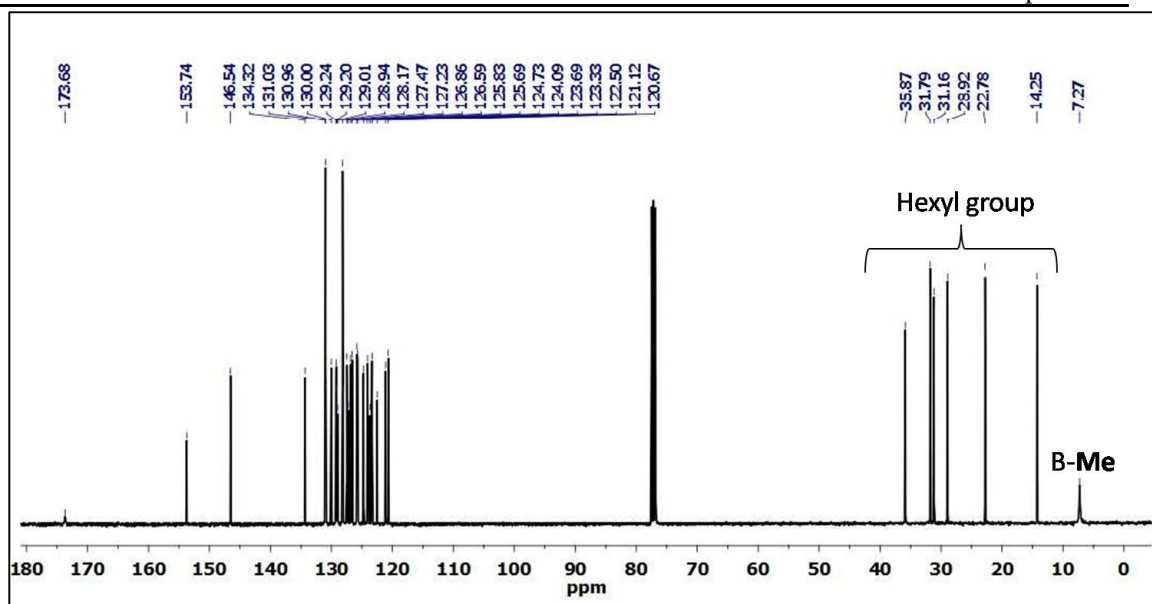


Figure 4A.4: ^{13}C NMR spectrum of compound **B1**.

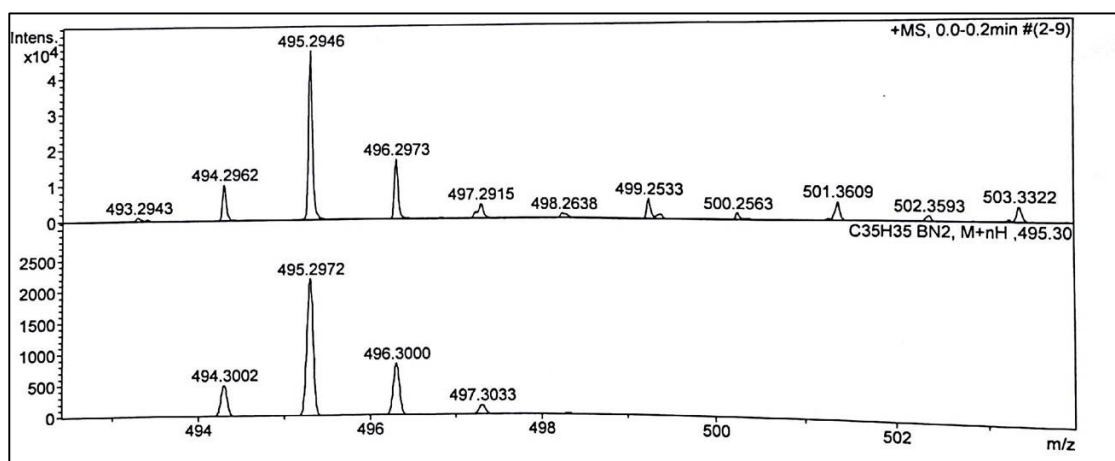


Figure 4A.5: ESI-MS spectrum of compound **B1**.

4A.2.3 Single crystal X-ray analysis

Single crystals of compounds **B1** and **B3** were obtained by slow evaporation of respective solutions in CH_2Cl_2 /ethanol and studied using single crystal X-ray diffraction analysis. Compounds, **B1** and **B3** were crystallized in the monoclinic $\text{P2}_1/\text{c}$, monoclinic $\text{P2}_1/\text{n}$ space groups respectively. The molecular structure of

Table 4A.1: Boron deviation from plane, bond angle and bond lengths of compounds **B1** and **B3**.

Bond length [Å] and bond angles [°]	Compound B1	Compound B3
N2-B1	1.6476(15)	1.6484(28)
C21-B1	1.6182(18)	1.6133(30)
C34-B1	1.6224(17)	1.6138(32)
C35-B1	1.6207(17)	1.6193(29)
C21-B1-N2	95.66(9)	95.30(14)
C21-B1-C34	110.94(10)	110.62(18)
C21-B1-C35	111.09(9)	111.67(18)
C34-B1-N2	110.65(9)	112.45(18)
C34-B1-C35	116.21(10)	116.00(18)
C35-B1-N2	110.41(10)	108.92(17)
Deviation of B1 from C21N2B1 plane (Å)	-0.0154	0.0461

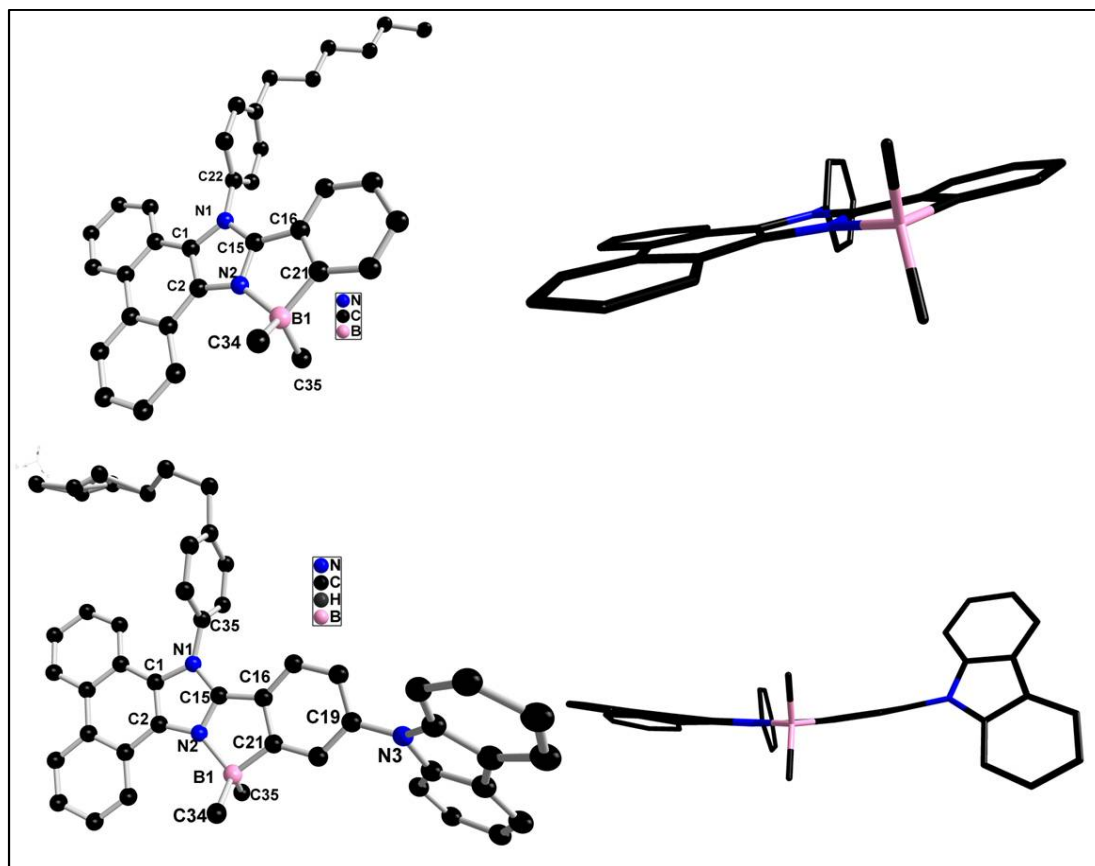


Figure 4A.6: Molecular structure of compounds **B1** (top) and **B3** (bottom).

Table 4A.2: Crystal data and structure refinement parameters for compounds **B1** and **B3**.

	B1	B3
Empirical formula	C ₃₅ H ₃₅ BN ₂	C ₄₇ H ₃₈ BN ₃
Formula weight	494.46	655.61
Temperature/K	100	100
Crystal system	monoclinic	monoclinic
Space group	P2 ₁ /c	P2 ₁ /n
a/Å	19.2965(5)	10.1868(6)
b/Å	11.5420(3)	23.5166(13)
c/Å	12.4695(3)	14.9629(9)
α/°	90	90
β/°	98.5980(10)	92.550(4)
γ/°	90	90
Volume/Å ³	2746.00(12)	3580.9(4)
Z	4	4
ρ _{calc} /cm ³	1.196	1.216
μ/mm ⁻¹	0.068	0.070
F(000)	1056.0	1384.0
Radiation	MoKα (λ = 0.71073)	MoKα (λ = 0.71073)
2 θ range for data collection/°	4.124 to 57.656	5.45 to 58.83
Index ranges	-26 ≤ h ≤ 26, -15 ≤ k ≤ 15, -16 ≤ l ≤ 16	-14 ≤ h ≤ 13, -32 ≤ k ≤ 32, -20 ≤ l ≤ 20
Reflections collected	48011	65428
Independent reflections	7144 [R _{int} = 0.0455, R _{sigma} = 0.0270]	9724 [R _{int} = 0.1229, R _{sigma} = 0.0867]
Data/restraints/parameters	7144/0/346	9724/0/500
Goodness-of-fit on F ²	1.036	1.030
Final R indexes [I ≥ 2σ (I)]	R _I = 0.0438, wR ₂ = 0.1083	R _I = 0.0643, wR ₂ = 0.1515
Final R indexes [all data]	R _I = 0.0568, wR ₂ = 0.1161	R _I = 0.1267, wR ₂ = 0.1824
Largest diff. peak/hole / e Å ⁻³	0.33/-0.23	0.61/-0.27

compounds **B1** and **B3** are shown in figure 4A.6; selected bond lengths and bond angles are summarized in table 4A.1. Crystallographic data for these compounds are presented in table 4A.2. In both the compounds, the boron centre is tetra-coordinate and adopts a typical distorted tetrahedral geometry. The boron atom deviates from the five-membered plane defined by C₃NB (Imidazole N2, C15, C16 and C21); the distance for **B1** is -0.0154 Å and for **B3** is 0.0461 Å. The B–N and B–C distances are in the typical range and are consistent with other literature reported N,C- chelate tetra-coordinate boron complexes (table 4A.1).³⁷

4A.2.4 TGA and DSC analysis

Thermal properties of the imidazole N,C- chelate organoboron compounds (**B1 -B4**) were characterized by thermogravimetric analysis (TGA) and differential scanning calorimetry (DSC) under nitrogen atmosphere at the heating rate of 10 °C min⁻¹ (figure. 4A. 8). The melting points of boron compounds were measured using DSC. As depicted in figure 4A.7 the decomposition temperatures (T_{d5}) (corresponds to 5%

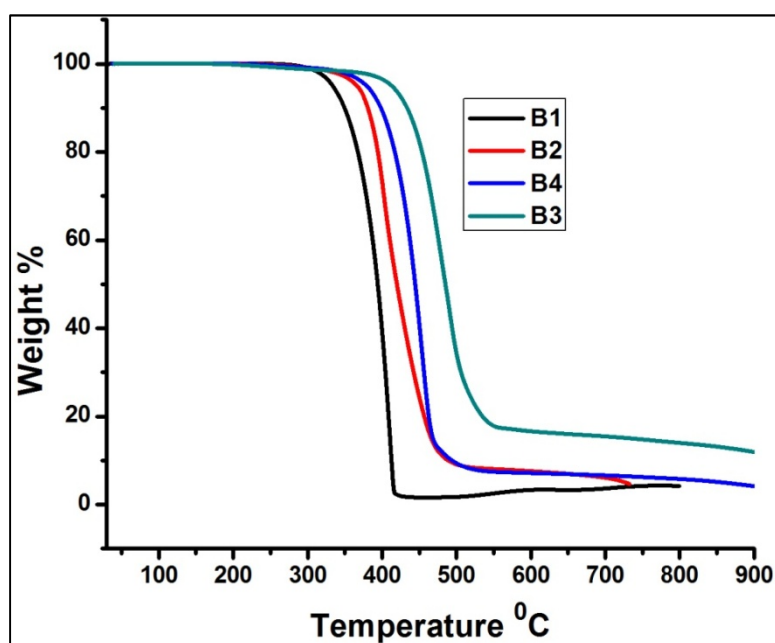


Figure 4A.7: TGA curves of **B1-B4** at a heating rate of 10 °C/min.

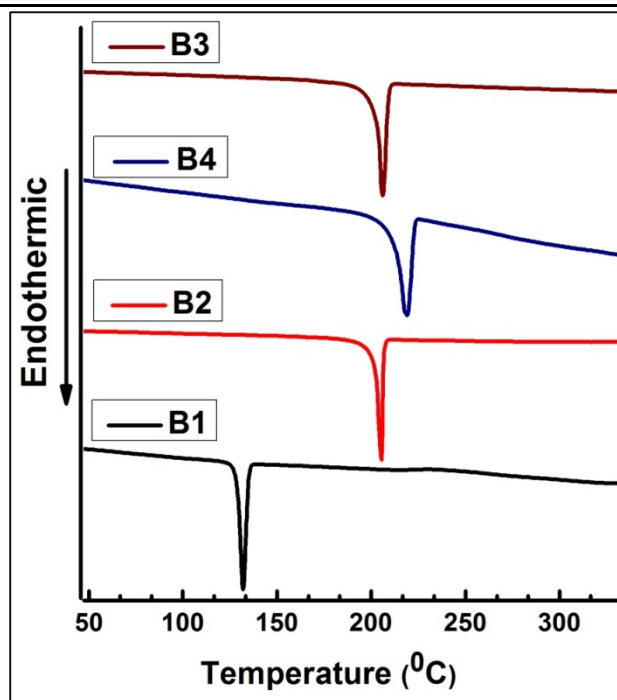


Figure 4A.8: DSC curves of **B1-B4** at a heating rate of 10 °C/min.

weight loss) of compounds **B1-B4** are 329, 366, 412, and 379 °C respectively. These compounds showed low melting temperatures, ranges from 132 °C (**B1**) to 219 °C (**B4**) owing to the presence of hexyl groups. TGA and DSC analysis of these compounds reveal their high thermal stability.

4A.2.5 Photophysical studies

All boron compounds showed limited solubility in protic solvents; hence, the photophysical studies were performed in toluene, CH₂Cl₂, THF and CH₃CN. The normalized absorption spectra of the boron compounds **B1-B4** in CH₂Cl₂ solution (figure 4A.9) showed absorption at *ca.* 384-437 nm with moderate molar extinction coefficient *ca.* 9320-22500 M⁻¹cm⁻¹. The emission spectra of these compounds were recorded by exciting at their longer absorption wavelength, and showed emission maxima at 384 nm (**B1**), 436 nm (**B2**), 407 nm (**B3**), 438 nm, (**B4**) in CH₂Cl₂ solvent (figure 4A.10) with blue colour emission (figure 4A.11). Naphthyl substituted boron compound **B2** showed 52 nm red shift compared to **B1**, because of extended

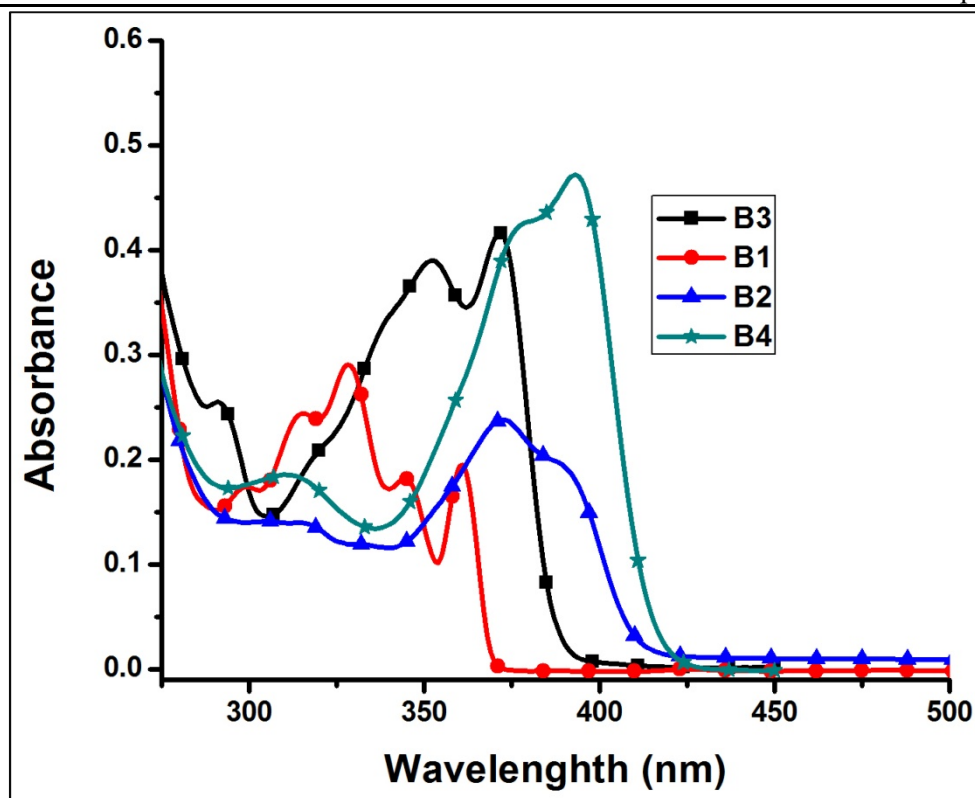


Figure 4A.9: Absorption spectra of boron compounds **B1-B4** (22 μM) in CH_2Cl_2 .

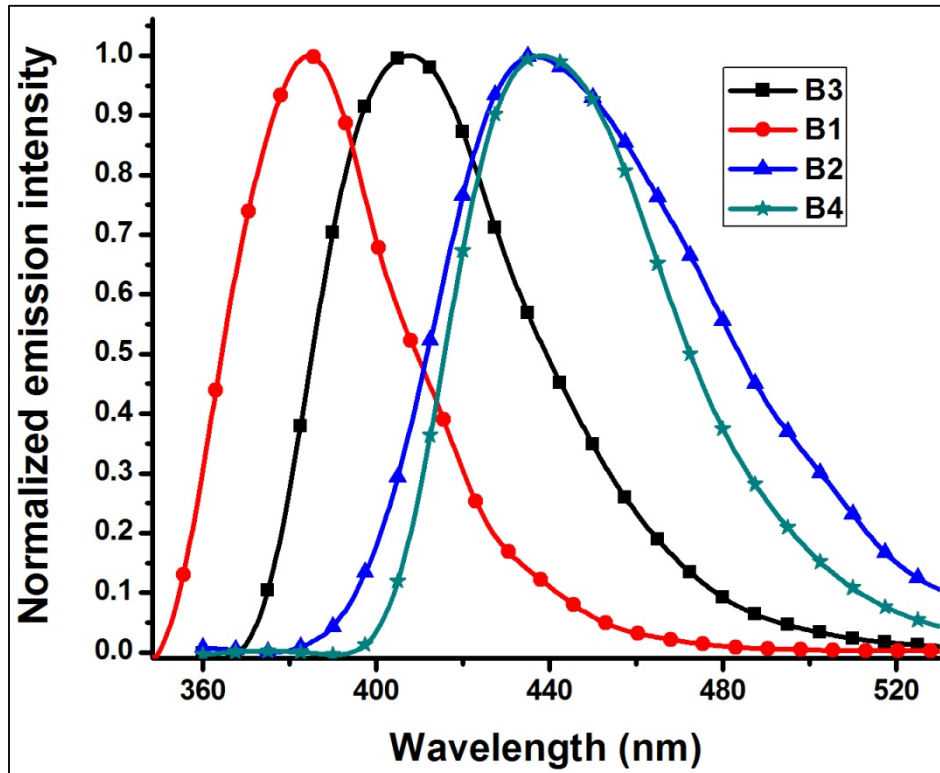


Figure 4A.10: Normalized emission spectra of boron compounds **B1-B4** (22 μM) in CH_2Cl_2 excited at longer wavelength absorption.

conjugation. Compound **B3** and **B4** also red shifted by 23 nm, 54 nm. In order to check the origin of this emission, we recorded emission spectra of **B1-B4** with varying solvent polarity (toluene, THF, CH_2Cl_2 , CH_3CN). Boron compounds **B4** showed significant red shifted emission with increased polarity, where as the emission maxima of compounds **B1**, **B2** and **B3** did not show any change. These results suggest that the intramolecular charge transfer (ICT) process observed in **B4** is because of the

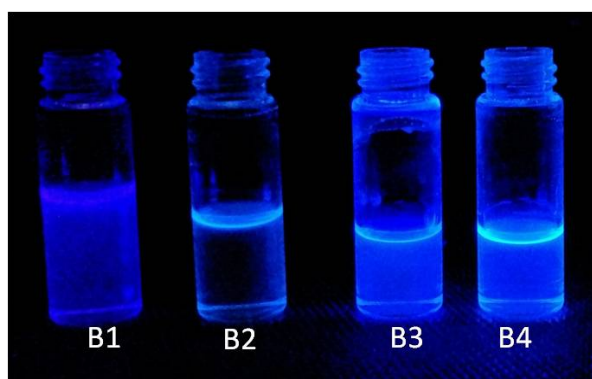


Figure 4A.11: Photograph of compounds **B1-B4** in CH_2Cl_2 under hand held UV lamp of 365 nm.

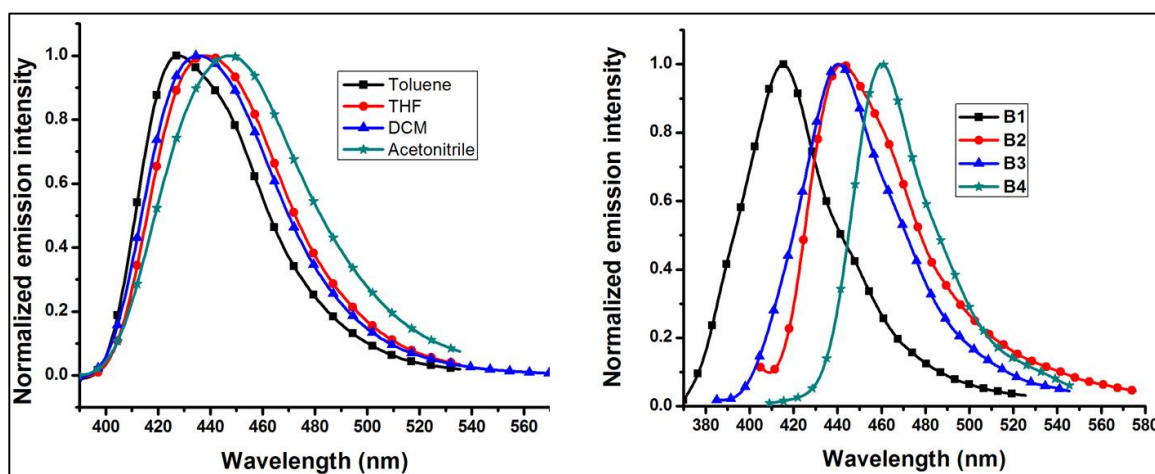


Figure 4A.12: Normalized emission spectra of compound **B4** with increasing solvent polarity (22 μM) (left) and a comparison of emission spectra of boron compounds **B1-B4** in solid state (right).

presence of electron donating NPh₂ group. All these compounds exhibited very good fluorescent quantum yields in solution state ranging from 0.11 to 1.05. These boron compounds **B1-B4** also showed bright solid state emission (figure 4A.12) ranging from 415 nm (**B1**) to 460 nm (**B2**) with red shifted emission maxima in comparison to their emission in solution state. These compounds exhibited solid state quantum yields ranged from 0.04 to 0.51, which are significantly lower than their solution state quantum yields. The observed red shifted emissions and lower quantum yields in solid state might be because of increased intermolecular interactions in the solid state.

Table 4A.3 Photophysical data of compounds **B1-B4**

Compound	Solvent	λ_{\max}^a (nm)	ϵ_{\max} $M^{-1} \text{ cm}^{-1} \times 10^3$	$\lambda_{\text{em}}(\text{nm})^{a,b}$	$\Phi_F^{c,d}$
B1	Toluene	361	8.30	385	0.40
	THF	359	6.08	384	0.46
	CH ₂ Cl ₂	361	8.90	385	0.47
	CH ₃ CN	359	7.25	385	0.37
	Solid			415	0.35
B2	Toluene	393	7.81	444	0.16
	THF	392	7.04	444	0.16
	CH ₂ Cl ₂	390	8.79	435	0.11
	CH ₃ CN	385	8.33	443	0.07
	Solid			442	0.04
B3	Toluene	375	16.59	410	0.95
	THF	370	16.70	409	0.94
	CH ₂ Cl ₂	372	18.92	408	0.96
	CH ₃ CN	369	17.96	409	0.92
	Solid			440	0.32
B4	Toluene	397	21.38	428	1.07
	THF	393	22.66	435	1.01
	CH ₂ Cl ₂	392	21.45	437	1.05
	CH ₃ CN	390	22.50	446	1.06
	Solid			460	0.39

^aAbsorption maximum(22 μ M). ^bExcited at the absorption maximum. ^cQuinine sulphate in 0.1 N H₂SO₄. ^dAbsolute fluorescence quantum yields using an integrating sphere for solids

4A.3 Conclusions

In conclusion, phenanthrene imidazoles (**L1-L4**) were synthesized in a one pot reaction. Later these ligands were borylated *via* simple electrophilic borylation method to get a new *N,C*-chelate boron compounds **B1-B4** with good yields. With substituent variation at 2-position of imidazole, the emission maxima shifted from 385-437 nm. These compounds also exhibited good solid state emission. The photophysical properties suggesting that, the possibility of these boron compounds as emitters and/or electron transporting materials in OLEDs.

4A.4 Experimental section

4A.4.1 Methods and instruments

All reagents were used as received from Spectrochem, Alfa-aesar and Sigma-Aldrich unless otherwise noted. The 4-(9H-Carbazol-9-yl)benzaldehyde and 4-(diphenylamino)benzaldehyde were prepared according to known literature procedures.^{38,39} All solvents were purchased from Spectrochem India. Dichloromethane and toluene were dried using calcium hydride and Na/benzophenone respectively. All experiments were monitored by analytical thin layer chromatography (TLC) under hand held UV lamp at 254 nm.

All ¹H (400 MHz), ¹³C (100 MHz), and ¹¹B (128 MHz) NMR were recorded at room temperature on Bruker ARX 400 spectrometer. Residual protonated solvents were used as internal standards for ¹H and ¹³C NMR. ¹¹B NMR spectra were referenced externally to BF₃·Et₂O in CDCl₃ ($\delta = 0$ ppm). ESI mass spectra were recorded with Bruker micro TOF-QII mass spectrometer. UV-Visible spectra were recorded on Perkin-Elmer Lambda 750 UV/Visible spectrometer. The fluorescence spectra were recorded with a Perkin-Elmer LS-55 Fluorescence spectrometer. 9,10-diphenylanthracene was used as the standard for the determination of the quantum

yields. Single crystals of compound **B1** and **B3** were grown from dichloromethane-ethanol solvent mixture. Single crystal X-ray diffraction data were collected on Bruker APEX-II CCD diffractometer at 100 K using Mo-K α radiation (0.71073 Å). The structure was solved by direct methods using shelXT program and refined with least squares minimization with shelXL using Olex2. The H- atoms were assigned at calculated positions and were refined as riding atoms.

4A.4.2 Synthetic procedures and spectral characterization

General procedure for the synthesis of compounds L1-L4

In a round bottom flask 9,10-phenanthrenequinone, 4-hexylaniline, aldehyde and ammonium acetate were taken. Acetic acid used as a solvent and refluxed for 24 hour under nitrogen atmosphere. The reaction mixture was poured into water and extracted with dichloromethane. The combined organic layers were washed with aqueous NaHCO₃ and brine solution, dried over Na₂SO₄ and concentrated using rotavap. The crude reaction mixture was purified by 100-200 silica gel column chromatography using *n*-hexane/dichloromethane mixture as a mobile phase.

Synthesis of compound L1

The quantities involved are as follows: 9,10-Phenanthrenequinone (3.00 g, 14.41 mmol), 4-hexylaniline (3.61 mL, 18.73 mmol), benzaldehyde (1.53 g, 14.41 mmol), and ammonium acetate (5.55 g, 72.05 mmol). Yield: 4.72 g, (72 %). Mp: 125 °C. ¹H NMR (400 MHz, CDCl₃): δ 9.04 (d, J = 7.8 Hz, 1H), 8.78 (dd, J = 20.0, 8.3 Hz, 2H), 7.84 (t, J = 7.3 Hz, 1H), 7.71 (t, J = 6.8 Hz, 3H), 7.56 - 7.53 (m, 1H), 7.42 - 7.31 (m, 9H), 2.83 (t, J = 7.4 Hz, 2H), 1.79 (dd, J = 16, 8 Hz, 2H), 1.52 - 1.41 (m, 6H), 1.05 (t, J = 8 Hz, 3H) ppm. ¹³C NMR (100 MHz, CDCl₃): δ 150.95, 144.71, 137.34, 136.14, 130.66, 130.01, 129.41, 129.22, 128.75, 128.72, 128.26, 128.21, 128.14, 127.32,

127.22, 126.18, 125.53, 124.81, 124.04, 123.14, 123.12, 122.77, 120.89, 35.60, 31.70, 31.05, 28.71, 22.68, 14.17 ppm. HR-MS (ESI). Calcd. for $C_{33}H_{31}N_2$ ($[M + H]^+$): 455.2482, found: 455.2498.

Synthesis of compound L2

The quantities involved are as follows: 9, 10-Phenanthrenequinone (3.00 g, 14.41 mmol), 4-hexylaniline (3.61 mL, 18.73 mmol), 1-napthaldehyde (2.25 g, 14.41 mmol), and ammonium acetate (5.55 g, 72.05 mmol). Yield: 3.70 g, (51 %). Mp: 174 °C. 1H NMR (400 MHz, $CDCl_3$): δ 8.91 (d, $J = 7.4$ Hz, 1H), 8.79 (dd, $J = 24.5, 8.3$ Hz, 2H), 8.00 (d, $J = 8.2$ Hz, 1H), 7.85 - 7.83 (m, 2H), 7.75 (t, $J = 7.1$ Hz, 1H), 7.68 (t, $J = 8$ Hz, 1H), 7.57 - 7.53 (m, 1H), 7.51 - 7.44 (m, 3H), 7.36 (t, $J = 8$ Hz, 1H), 7.31 - 7.23 (m, 5H), 7.14 (d, $J = 8.1$ Hz, 2H), 2.61 (t, 2H), 1.60 (dd, $J = 14.3, 7.5$ Hz, 2H), 1.32 - 1.2 (m, 6H), 0.89 (t, $J = 6.8$ Hz, 3H) ppm. ^{13}C NMR (100 MHz, $CDCl_3$): δ 150.58, 144.18, 137.29, 135.48, 133.51, 133.24, 129.67, 129.54, 129.48, 129.29, 128.36, 128.19, 128.15, 127.56, 127.42, 127.37, 126.84, 126.32, 126.14, 125.62, 125.00, 124.49, 124.14, 123.22, 123.14, 122.93, 121.14, 35.48, 31.65, 30.87, 28.69, 22.65, 14.16 ppm. HR-MS (ESI): Calcd. for $C_{37}H_{34}N_2$ ($[M + H]^+$): 505.2638, found: 505.2697.

Synthesis of compound L3

The quantities involved are as follows: 9, 10-Phenanthrenequinone (3.00 g, 14.41 mmol), 4-hexylaniline (3.61 mL, 18.73 mmol), 4-(9H-carbazol-9-yl)benzaldehyde (3.90 g, 14.41 mmol), and ammonium acetate (5.55 g, 72.05 mmol). Yield: 5.53 g, (62 %). Mp: 211 °C. 1H NMR (400 MHz, $CDCl_3$): δ 8.96 (bs, 1H), 8.77 (dd, $J = 25.4, 8.3$ Hz, 2H), 8.14 (d, $J = 7.7$ Hz, 2H), 7.87 (d, $J = 8.4$ Hz, 2H), 7.78 (t, $J = 7.3$ Hz, 1H), 7.69 (t, $J = 7.3$ Hz, 1H), 7.57 - 7.46 (m, 7H), 7.43 - 7.39 (m, 3H), 7.32 - 7.24 (m, 5H), 2.83 (t, $J = 7.3$ Hz, 2H), 1.80 - 1.73 (m, 2H), 1.42 - 1.31 (m, 6H), 0.88 (t, $J = 8$

Hz, 3H) ppm. ^{13}C NMR (176 MHz, CDCl_3): δ 150.13, 145.27, 140.65, 138.18, 137.58, 136.24, 130.84, 130.40, 129.70, 129.48, 128.93, 128.55, 128.45, 127.46, 127.36, 126.64, 126.41, 126.12, 125.81, 125.10, 124.24, 123.66, 123.29, 122.85, 121.07, 120.46, 120.29, 109.89, 35.81, 31.77, 31.28, 28.88, 22.75, 14.21 ppm. HR-MS (ESI): Calcd. for $\text{C}_{45}\text{H}_{38}\text{N}_3$ ($[\text{M} + \text{H}]^+$): 620.3060, found: 620.3062

Synthesis of compound L4

The quantities involved are as follows: 9, 10-Phenanthrenequinone (3.00 g, 14.41 mmol), 4-hexylaniline (3.61 mL, 18.73 mmol), 4-(diphenylamino)benzaldehyde (3.93 g, 14.41 mmol), and ammonium acetate (5.55 g, 72.05 mmol). Yield: 4.75 g, (53 %). Mp: 213 °C. ^1H NMR (400 MHz, CDCl_3): δ 8.92 (bs, 1H), 8.73 (dd, $J = 25.2, 8.3$ Hz, 2H), 7.74 (t, $J = 7.4$ Hz, 1H), 7.65 (t, $J = 7.4$ Hz, 1H), 7.52 - 7.39 (m, 7H), 7.28 - 7.23 (m, 6H), 7.17 (d, $J = 8.2$ Hz, 1H), 7.10 - 7.03 (m, 5H), 6.94 (d, $J = 8.8$ Hz, 2H), 2.80 (t, $J = 7.6$ Hz, 2H), 1.73 (m, 2H), 1.40 - 1.30 (m, 6H), 0.90 (t, $J = 7.0$ Hz, 3H) ppm. ^{13}C NMR (100 MHz, CDCl_3): δ 150.90, 148.39, 147.35, 144.92, 137.33, 136.49, 130.19, 130.17, 129.42, 129.20, 128.93, 128.30, 128.20, 127.28, 126.25, 125.55, 125.07, 124.73, 124.14, 123.53, 123.25, 123.18, 122.88, 122.14, 120.91, 35.76, 31.77, 31.18, 28.83, 22.74, 14.23 ppm. HR-MS (ESI): Calcd. for $\text{C}_{45}\text{H}_{40}\text{N}_3$ ($[\text{M} + \text{H}]^+$): 622.3217, found: 622.3209

General procedure for the synthesis of compounds B1-B4

Oven dried two neck round bottom flask charged with dichloromethane solution of compounds (**L1-L4**) under argon atmosphere. To this solution diisopropylethylamine (*i*-Pr₂NEt) was added at 0 °C and stirred. After 10 min BBr₃ (1.0 M in dichloromethane) was added slowly at the same temperature and allowed to warm to room temperature. After being stirred at room temperature for 24 h, saturated K₂CO₃ aqueous solution was added to the reaction mixture and extracted with CH₂Cl₂. The

combined organic layers were washed with water, dried over MgSO_4 and concentrated using rotary evaporator to afford the crude dibromo boron compound. Without further purification the crude product was taken in a round bottom flask and dried using high vacuum then filled with argon. To the dried compounds toluene was added. To this stirred solution, AlMe_3 (2.0 M in toluene) was added at room temperature. After being stirred for half an hour, the reaction was quenched by adding water and extracted with CH_2Cl_2 . The combined organic layers were washed with water, and brine. The organic layer was dried was over Na_2SO_4 and concentrated using rotavap. The crude product was purified by silica gel column chromatography using *n*-hexane/dichloromethane mixture as a mobile phase.

Synthesis of boron compound B1

The quantities involved are as follows: Compound **L1** (2.47 g, 5.43 mmol), N,N-diisopropylethylamine (0.94 mL, 5.43 mmol), BBr_3 (1.0 M in CH_2Cl_2 , 16.30 mL, 16.29 mmol) and AlMe_3 (2.0 M in toluene, 5.43 mL, 10.87 mmol). Yield: 1.61 g, (60 %). Mp: 132 °C. ^1H NMR (400 MHz, CDCl_3): δ 9.26 (d, $J = 8.1$ Hz, 1H), 8.76 (t, $J = 7.7$ Hz, 2H), 7.84 (t, $J = 7.5$ Hz, 1H), 7.72 (t, $J = 7.5$ Hz, 1H), 7.66 - 7.53 (m, 6H), 7.37 - 7.25 (m, 3H), 6.94 (t, $J = 7.5$ Hz, 1H), 6.46 (d, $J = 7.8$ Hz, 2H), 2.91 (t, $J = 8$ Hz, 2H), 1.88 - 1.80 (m, 2H), 1.49 - 1.37 (m, 6H), 0.96 (t, $J = 7.0$ Hz, 3H), 0.44 (s, 6H) ppm. ^{13}C NMR (100 MHz, CDCl_3): δ 173.68, 153.74, 146.54, 134.32, 131.03, 130.96, 130.00, 129.24, 129.20, 129.01, 128.94, 128.17, 127.47, 127.23, 126.86, 126.59, 125.83, 125.69, 124.73, 124.09, 123.69, 123.33, 122.50, 121.12, 120.67, 35.87, 31.79, 31.16, 28.92, 22.78, 14.25, 7.27 ppm. ^{11}B NMR (128 MHz, CDCl_3): δ 0.26 ppm. HR-MS (ESI): Calcd. for $\text{C}_{35}\text{H}_{36}\text{B}_1\text{N}_2$ ($[\text{M} + \text{H}]^+$): 495.2972, found: 495.2946.

Synthesis of boron compound B2

The quantities involved are as follows: Compound **L2** (2.74 g, 5.43 mmol), N,N-diisopropylethylamine (0.94 mL, 5.43 mmol), BBr₃ (1.0 M in CH₂Cl₂, 16.30 mL, 16.29 mmol) and AlMe₃ (2.0 M in toluene, 5.43 mL, 10.87 mmol). Yield: 0.91 g, (31 %). Mp: 205 °C. ¹H NMR (400 MHz, CDCl₃): δ 9.66 (d, *J* = 8.3 Hz, 1H), 8.76 (dd, *J* = 8.2, 3.3 Hz, 2H), 7.90 - 7.83 (m, 3H), 7.75 (t, *J* = 8 Hz, 1H), 7.68 - 7.63 (m, 2H), 7.55 - 7.40 (m, 5H), 7.22 (t, *J* = 8 Hz, 1H), 7.08 (dd, *J* = 7.5, 0.9 Hz, 1H), 7.01 (t, *J* = 7.8 Hz, 1H), 6.95 (d, *J* = 8.3 Hz, 1H), 2.89 (t, *J* = 7.5 Hz, 2H), 1.86 - 1.79 (m, 2H), 1.49 - 1.40 (m, 6H), 1.01 (t, *J* = 8 Hz, 3H), 0.66 (s, 6H) ppm. ¹³C NMR (100 MHz, CDCl₃): δ 159.50, 146.51, 145.83, 136.51, 132.67, 132.34, 131.86, 131.25, 131.06, 130.50, 129.69, 129.58, 129.27, 128.79, 128.76, 127.43, 126.70, 126.50, 126.45, 125.01, 124.12, 123.83, 123.25, 123.19, 122.98, 121.73, 121.67, 121.29, 35.83, 31.82, 31.29, 29.84, 28.81, 22.83, 14.29. ¹¹B NMR (128 MHz, CDCl₃): δ -3.44 ESI-MS: Calcd. for C₃₉H₃₈B₁N₂ ([M + H]⁺): 545.3129, found: m/z 545.3052.

Synthesis of boron compound B3

The quantities involved are as follows: Compound **L3** (3.36 g, 5.43 mmol), N,N-diisopropylethylamine (0.94 mL, 5.43 mmol), BBr₃ (1.0 M in CH₂Cl₂, 16.30 mL, 16.29 mmol) and AlMe₃ (2.0 M in toluene, 5.43 mL, 10.87 mmol). Yield: 1.64 g, (46 %). Mp: 206 °C. ¹H NMR (400 MHz, CDCl₃): δ 9.44 (d, *J* = 8.1 Hz, 1H), 8.79 (t, *J* = 7.6 Hz, 2H), 8.23 (d, *J* = 7.7 Hz, 2H), 8.04 (bs, 1H), 7.97 (t, *J* = 7.6 Hz, 1H), 7.80 (t, *J* = 7.4 Hz, 1H), 7.70 - 7.56 (m, 74H), 7.51 (t, *J* = 7.6 Hz, 2H), 7.40 - 7.33 (m, 4H), 7.29 (dd, *J* = 8.1, 1.8 Hz, 1H), 6.78 (d, *J* = 8.2 Hz, 1H), 2.97 (t, *J* = 7.6 Hz, 2H), 1.94 - 1.86 (m, 2H), 1.56 - 1.44 (m, *J* = Hz, 6H), 1.06 (t, *J* = 6.8 Hz, 3H), 0.72 (s, 6H) ppm. ¹³C NMR (100 MHz, CDCl₃): δ 176.07, 152.97, 146.72, 140.75, 139.06, 134.16, 131.17,

131.06, 129.32, 129.14, 129.02, 128.32, 128.11, 127.55, 127.11, 126.93, 126.72, 125.99, 125.92, 125.61, 124.12, 123.62, 123.59, 123.40, 123.06, 122.41, 122.25, 120.67, 120.32, 120.03, 110.30, 35.84, 31.72, 31.09, 28.91, 22.75, 14.23, 7.32 ppm. ^{11}B NMR (128 MHz, CDCl_3): δ -0.26 ppm. HR-MS (ESI): Calcd. for $\text{C}_{47}\text{H}_{43}\text{B}_1\text{N}_3$ ($[\text{M} + \text{H}]^+$): 660.3552, found: 660.3536.

Synthesis of boron compound B4

The quantities involved are as follows: Compound **L4** (3.37 g, 5.43 mmol), N,N-diisopropylethylamine (0.94 mL, 5.43 mmol), BBr_3 (1.0 M in CH_2Cl_2 , 16.30 mL, 16.29 mmol) and AlMe_3 (2.0 M in toluene, 5.43 mL, 10.87 mmol). Yield: 1.90 g, (53 %). Mp: 219 °C. ^1H NMR (400 MHz, CDCl_3): δ 9.22 (bs, 1H), 8.75 (t, $J = 8\text{Hz}$, 2H), 7.83 - 7.53 (m, 7H), 7.06 - 6.38 (m, 13H), 6.57 (bs, 1H), 6.32 (bs, 1H), 2.86 (t, $J = 8\text{Hz}$, 2H), 1.90 - 1.70 (m, 2H), 1.52 - 1.25 (s, 6H), 0.93 (t, $J = 8\text{Hz}$, 3H), 0.39 (s, 6H) ppm. ^{13}C NMR (100 MHz, CDCl_3): δ 175.31, 153.77, 149.63, 147.77, 146.41, 134.49, 131.10, 130.87, 129.34, 129.04, 128.84, 128.63, 128.30, 127.40, 126.80, 126.43, 125.65, 125.57, 125.28, 124.11, 123.68, 123.32, 123.29, 123.02, 122.55, 121.95, 120.96, 120.58, 119.45, 35.88, 31.76, 31.19, 28.98, 22.74, 14.20, 7.33 ppm. ^{11}B NMR (128 MHz, CDCl_3): δ -0.51. ESI-MS: Calcd. for $\text{C}_{47}\text{H}_{45}\text{B}_1\text{N}_3$ ($[\text{M} + \text{H}]^+$): 662.3709, found: m/z 662.3685.

4A.5 References

- (1) Li, D.; Zhang, H.; Wang, Y. *Chem. Soc. Rev.* **2013**, *42*, 8416.
- (2) Suresh, D.; Gomes, C. S. B.; Lopes, P. S.; Figueira, C. A.; Ferreira, B.; Gomes, P. T.; Di Paolo, R. E.; Macanita, A. L.; Duarte, M. T.; Charas, A.; Morgado, J.; Vila-Vicosa, D.; Calhorda, M. J. *Chem. Eur. J.* **2015**, *21*, 9133.

-
- (3) Pais, V. F.; Alcaide, M. M.; Lopez-Rodriguez, R.; Collado, D.; Najera, F.; Perez-Inestrosa, E.; Alvarez, E.; Lassaletta, J. M.; Fernandez, R.; Ros, A.; Pischel, U. *Chem. Eur. J.* **2015**, *21*, 15369.
- (4) Jäkle, F. *Chem. Rev.* **2010**, *110*, 3985.
- (5) Rao, Y.-L.; Amarne, H.; Wang, S. *Coord. Chem. Rev.* **2012**, *256*, 759.
- (6) Frath, D.; Massue, J.; Ulrich, G.; Ziessel, R. *Angew. Chem. Int. Ed.* **2014**, *53*, 2290.
- (7) Ge, Y.; O'Shea, D. F. *Chem. Soc. Rev.* **2016**, *45*, 3846.
- (8) Wu, Q.; Esteghamatian, M.; Hu, N.-X.; Popovic, Z.; Enright, G.; Tao, Y.; D'Iorio, M.; Wang, S. *Chem. Mater.* **1999**, *12*, 79.
- (9) Anderson, S.; Weaver, M. S.; Hudson, A. J. *Synth. Met.* **2000**, *111–112*, 459.
- (10) Qin, Y.; Pagba, C.; Piotrowiak, P.; Jäkle, F. *J. Am. Chem. Soc.* **2004**, *126*, 7015.
- (11) Cui, Y.; Wang, S. *J. Org. Chem.* **2006**, *71*, 6485.
- (12) Qin, Y.; Kiburu, I.; Shah, S.; Jäkle, F. *Org. Lett.* **2006**, *8*, 5227.
- (13) Frath, D.; Azizi, S.; Ulrich, G.; Retailleau, P.; Ziessel, R. *Org. Lett.* **2011**, *13*, 3414.
- (14) Frath, D.; Azizi, S.; Ulrich, G.; Ziessel, R. *Org. Lett.* **2012**, *14*, 4774.
- (15) Hou, Q.; Zhao, L.; Zhang, H.; Wang, Y.; Jiang, S. *J. Lumin.* **2007**, *126*, 447.
- (16) Dhanunjayarao, K.; Mukundam, V.; Ramesh, M.; Venkatasubbaiah, K. *Eur. J. Inorg. Chem.* **2014**, 539.
- (17) Barbon, S. M.; Reinkeluers, P. A.; Price, J. T.; Staroverov, V. N.; Gilroy, J. B. *Chem. Eur. J.* **2014**, *20*, 11340.
- (18) Barbon, S. M.; Staroverov, V. N.; Gilroy, J. B. *J. Org. Chem.* **2015**, *80*, 5226.
-

-
- (19) Hesari, M.; Barbon, S. M.; Staroverov, V. N.; Ding, Z.; Gilroy, J. B. *Chem. Commun.* **2015**, *51*, 3766.
- (20) Maar, R. R.; Barbon, S. M.; Sharma, N.; Groom, H.; Luyt, L. G.; Gilroy, J. B. *Chem. Eur. J.* **2015**, *21*, 15589.
- (21) Wakamiya, A.; Taniguchi, T.; Yamaguchi, S. *Angew. Chem. Int. Ed.* **2006**, *45*, 3170.
- (22) Job, A.; Wakamiya, A.; Kehr, G.; Erker, G.; Yamaguchi, S. *Org. Lett.* **2010**, *12*, 5470.
- (23) Rao, Y.-L.; Amarne, H.; Zhao, S.-B.; McCormick, T. M.; Martić, S.; Sun, Y.; Wang, R.-Y.; Wang, S. *J. Am. Chem. Soc.* **2008**, *130*, 12898.
- (24) Amarne, H.; Baik, C.; Murphy, S. K.; Wang, S. *Chem. Eur. J.* **2010**, *16*, 4750.
- (25) Hudson, Z. M.; Ko, S.-B.; Yamaguchi, S.; Wang, S. *Org. Lett.* **2012**, *14*, 5610.
- (26) Coll, C.; Ros-Lis, J. V.; Martinez-Manez, R.; Marcos, M. D.; Sancenon, F.; Soto, J. *J. Mater. Chem.* **2010**, *20*, 1442.
- (27) Chen, X.; Kang, S.; Kim, M. J.; Kim, J.; Kim, Y. S.; Kim, H.; Chi, B.; Kim, S.-J.; Lee, J. Y.; Yoon, J. *Angew. Chem., Int. Ed.* **2010**, *49*, 1422.
- (28) Bhandari, K.; Srinivas, N.; Marrapu, V. K.; Verma, A.; Srivastava, S.; Gupta, S. *Bioorg. Med. Chem. Lett.* **2010**, *20*, 291.
- (29) Vlahakis, J. Z.; Hum, M.; Rahman, M. N.; Jia, Z.; Nakatsu, K.; Szarek, W. A. *Bioorg. Med. Chem.* **2009**, *17*, 2461.
- (30) Bellina, F.; Cauteruccio, S.; Monti, S.; Rossi, R. *Bioorg. Med. Chem. Lett.* **2006**, *16*, 5757.
- (31) Fang, Z.; Wang, S.; Zhao, L.; Xu, Z.; Ren, J.; Wang, X.; Yang, Q. *Mater. Chem. Phys.* **2008**, *107*, 305.
-

-
- (32) Ge, Z.; Hayakawa, T.; Ando, S.; Ueda, M.; Akiike, T.; Miyamoto, H.; Kajita, T.; Kakimoto, M.-a. *Chem. Mater.* **2008**, *20*, 2532.
- (33) Mukundam, V.; Dhanunjayarao, K.; Chuang, C. N.; Kang, D. Y.; Leung, M. K.; Hsieh, K. H.; Venkatasubbaiah, K. *Dalton Trans.* **2015**, *44*, 10228.
- (34) Mukundam, V.; Dhanunjayarao, K.; Samal, S.; Venkatasubbaiah, K. *Asian J. Org. Chem.* **2017**, *6*, 1054.
- (35) Kwon, J. E.; Park, S. Y. *Adv. Mater.* **2011**, *23*, 3615.
- (36) Ishida, N.; Moriya, T.; Goya, T.; Murakami, M. *J. Org. Chem.* **2010**, *75*, 8709.
- (37) Shaikh, A. C.; Ranade, D. S.; Thorat, S.; Maity, A.; Kulkarni, P. P.; Gonnade, R. G.; Munshi, P.; Patil, N. T. *Chem. Commun.* **2015**, *51*, 16115.
- (38) Shao, H.; Chen, X.; Wang, Z.; Lu, P. *J. Lumin.* **2007**, *127*, 349.
- (39) Meng, G.; Chen, Z.; Tang, H.; Liu, Y.; Wei, L.; Wang, Z. *New J. Chem.* **2015**, *39*, 9535.

CHAPTER 4B**Synthesis and photophysical properties of *N,C*-chelate tetrahydro phenanthridine boron complexes**

4B.1 Introduction	179
4B.2 Results and discussion	180
4B.2.1 Synthesis and characterization of compounds 1a-1g	180
4B.2.2 Synthesis and characterization of compounds 2-8	182
4B.2.3 Thermal properties	188
4B.2.4 Photophysical properties	189
4B.3 Conclusions	194
4B.4 Experimental section	195
4B.4.1 Methods and instruments	195
4B.4.2 Synthetic procedure and spectral characterization	196
4B.5 References	204

4B.1 Introduction

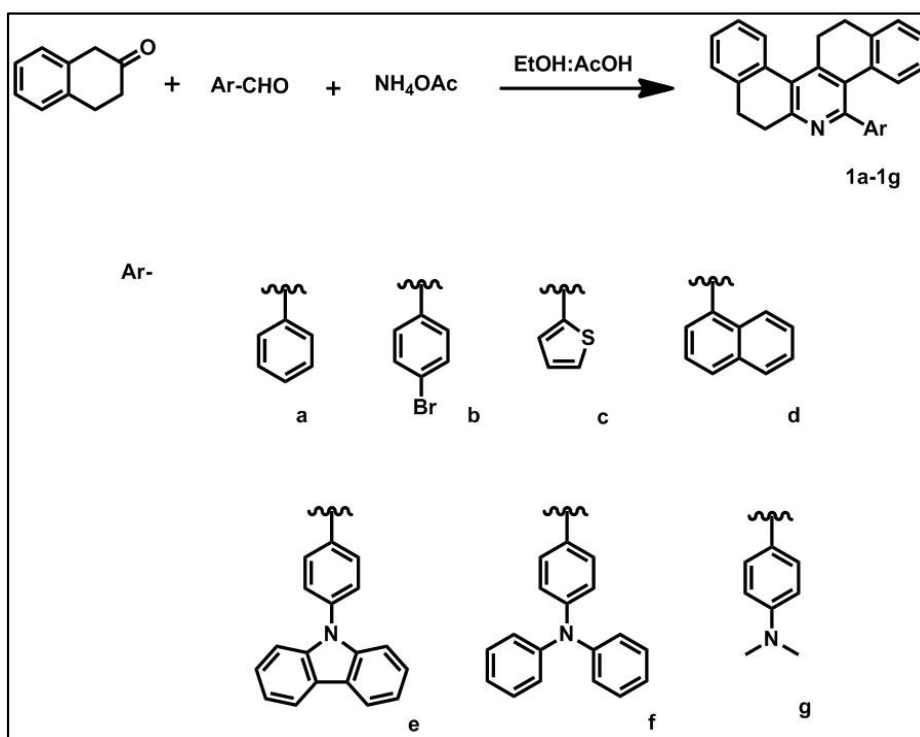
Organic luminophores based on small molecules have attracted great attention on account of their broad range applications ranging from bio-imaging,¹⁻³ photodynamic therapy (PDT)^{4,5} to organic electronics such as in OLEDs,⁶ organic light emitting field effect transistors⁷ and solar energy conversion.^{7,8} In order to tune the electronic properties of organic luminophores different methods are used; among them incorporation of main group elements has become a powerful strategy to produce unusual electronic properties. Boron containing molecules especially tetra-coordinate boron compounds are emerged as efficient materials for potential applications in OLEDs⁹, organic field effect transistors, photoresponsive materials¹⁰, sensory¹¹ and biological imaging materials.¹² Structural as well as photophysical properties of different class of different boron compounds have been reported. Among them *N,N*-chelate BODIPY dyes¹³ are widely studied. However these dyes often exhibit small Stokes shifts as well as less emissive in the solid state. The *N,O*-chelate ligands mainly hydroxyquinolate,^{14,15} Schiff bases,¹⁶⁻¹⁸ iminoketones¹⁹ and 2-(2'-hydroxyphenyl)imidazoles/oxazoles,^{20,21} including wide range structural modifications with single and multiple boron²²⁻²⁴ cores have been reported for various applications.²⁵ *N,C*-Chelate boron compounds based on thienylthiazole ligand were reported by Yamaguchi group,²⁶ meanwhile, Kawashima and co-workers reported highly luminescent azobenzene or imine based *N,C*-chelate boron compounds.²⁷ Later, Wang group developed photochromic *N,C*-chelate boron compounds based on 2-phenylpyridine moiety.²⁸ However, all these *N,C*-chelate boron compounds involves tedious synthesis such as lithiation reactions and need of bromo functionalized heteroarenes. In 2010 Murakami and coworkers reported the aromatic electrophilic borylation strategy²⁹ to synthesize phenylpyridine boron complexes.

Later using the same electrophilic borylation method, few reports came for the synthesis of highly luminescent *N,C*-chelate boron compounds.³⁰⁻³³ In this chapter, we disclose the synthesis of tetrahydrodibenzo[*a,i*]phenanthridine boron compounds and their photophysical properties.

4B.2 Results and discussion

4B.2.1 Synthesis and characterization of compounds 1a-1g

The synthetic route to a series of substituted tetrahydrodibenzo[*a,i*]phenanthridine compounds is outlined in scheme 4B.1. Compounds **1a-1g** were obtained in one pot reaction using 2-tetralone, aldehyde, and ammonium acetate in ethanol-acetic acid solvent mixture. All compounds (**1a-1g**) were characterized by ¹H, ¹³C NMR, and also by



Scheme 4B.1: Synthetic route to compounds **1a-1g**.

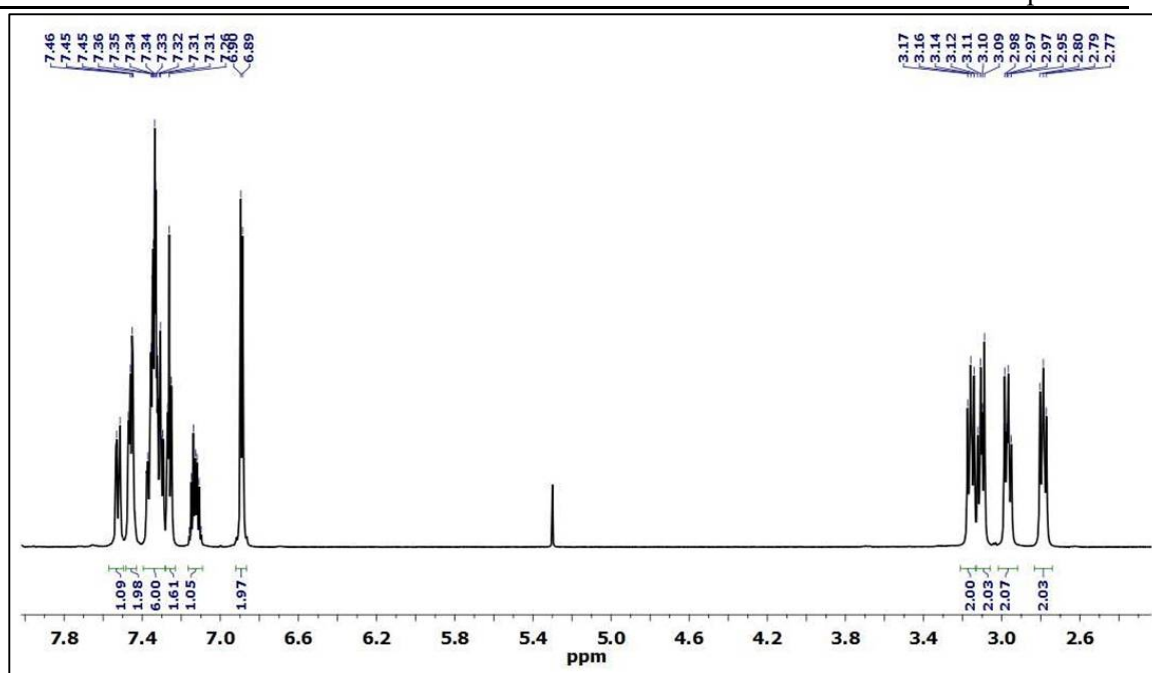


Figure 4B.1: ^1H NMR spectrum of compound 1a.

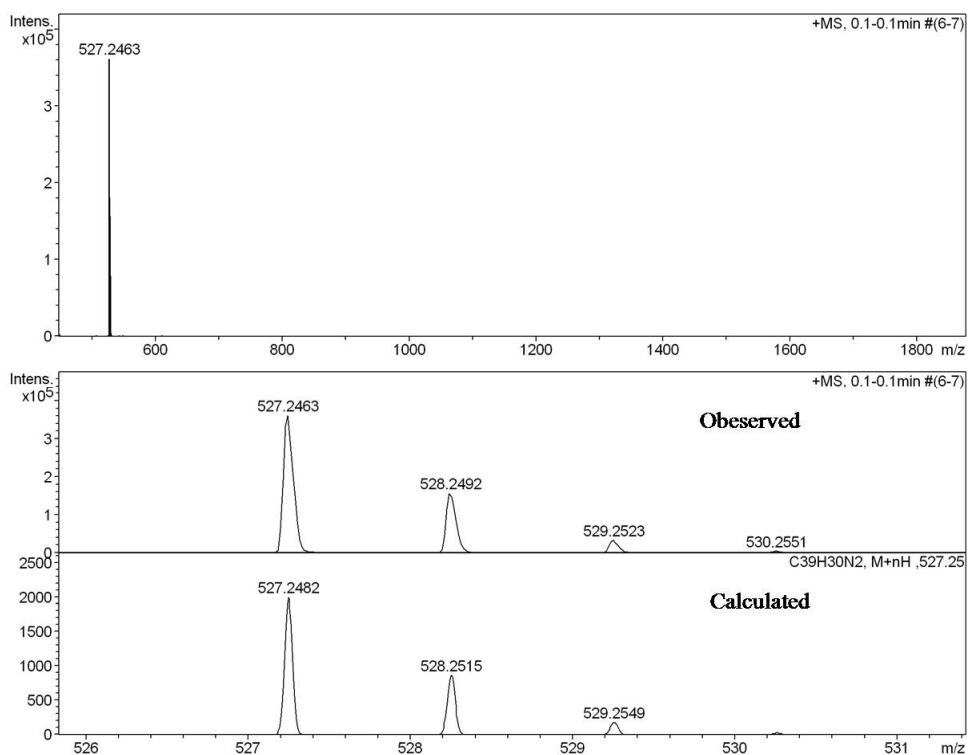
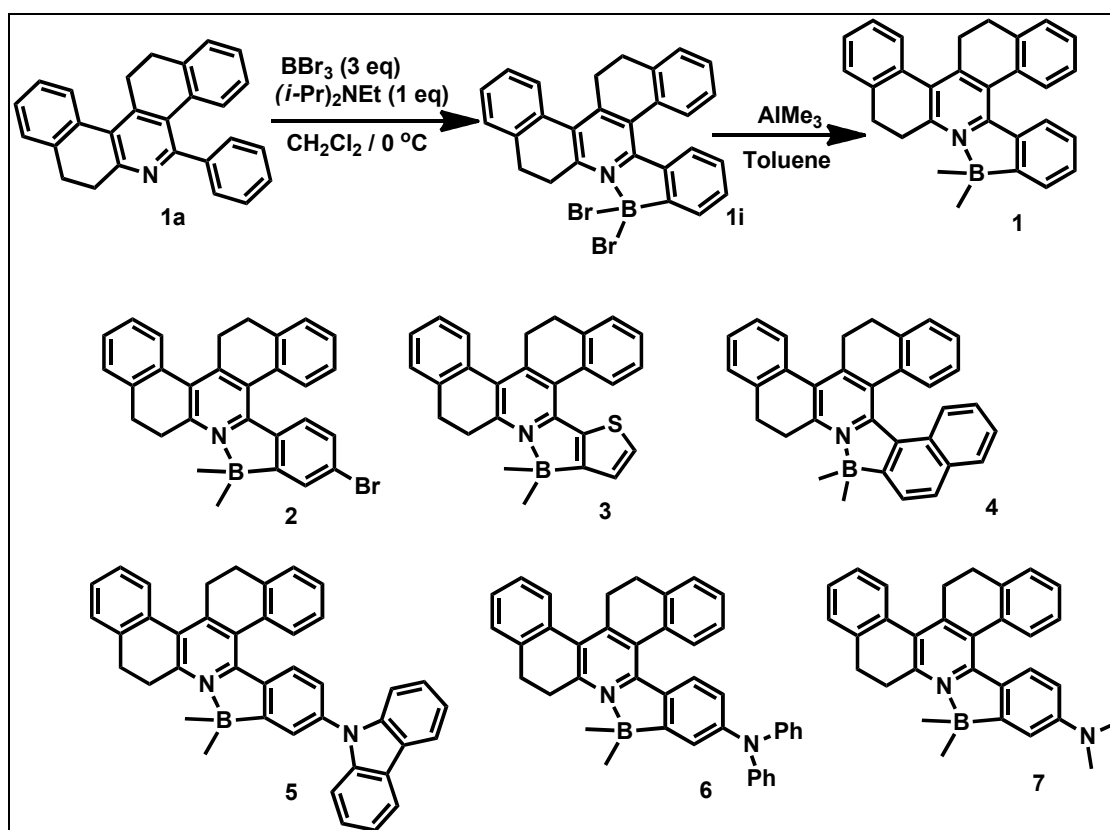


Figure 4B.2: HRMS of compound 1f.

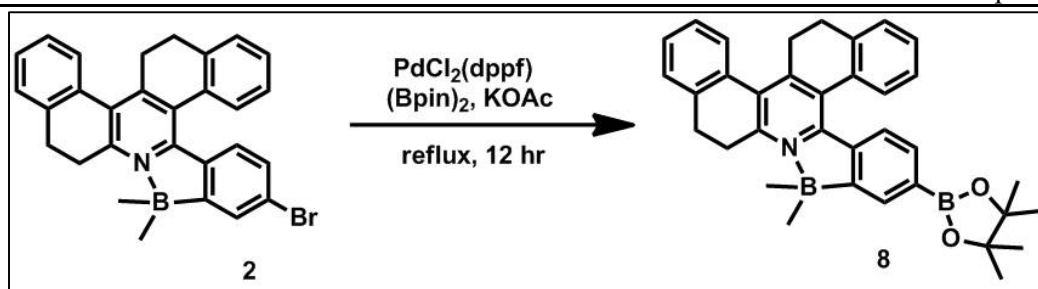
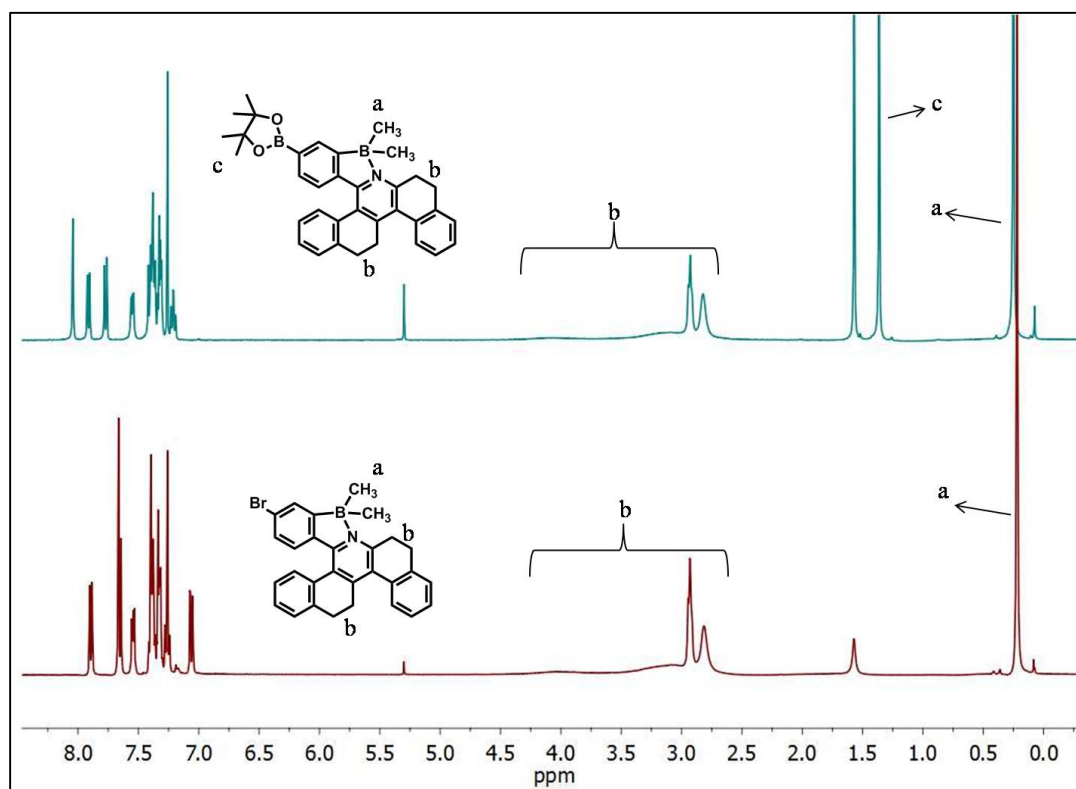
HRMS analysis. Representative ^1H NMR spectrum of compound **1a** and HRMS of compound **1f** are shown in figure 4B.1 and figure 4B.2 respectively.

4B.2.2 Synthesis and characterization of compounds 2-8

The tetrahydrodibenzo[*a,i*]phenanthridine *N,C*- chelate boron compound **1** was prepared as shown in scheme 4B.2. The aromatic electrophilic borylation of compound **1a** using BBr_3 under basic condition given dibromoborane compound. Without further purification, the dibromoborane intermediate **1i** was treated with trimethylaluminum (AlMe_3) to afford the desired product **1** in good yield. The crude product was purified by column chromatography over silica gel. By similar way, the other *N,C*- chelate boron compounds **2-7** were synthesized from their corresponding



Scheme 4B.2: Synthetic route to *N,C*- chelate boron compound **1** and chemdraw representations of compounds **2-7**.

Scheme 4B.3: Synthetic route to compound **8**.Figure 4B.3: ^1H NMR spectrum of compound **2** (bottom) and **8** (top).

starting materials (**1a-1g**) (Scheme 4B.2). All the boron compounds are highly stable towards air and moisture. We also successfully post functionalized the boron compound **2** by using palladium catalyst to get boronate functional group on *N,C*-chelate phenanthridine boron (**8**) (Scheme 4B.3). All the *N,C*-chelate boron compounds **1-8** were successfully characterized by ^1H and ^{13}C NMR spectroscopy. The appearance of new signal around 0.2 ppm in ^1H , and 4 ppm (broad) in ^{13}C NMR corresponds to the methyl groups on boron. For sample, ^1H NMR spectrum of

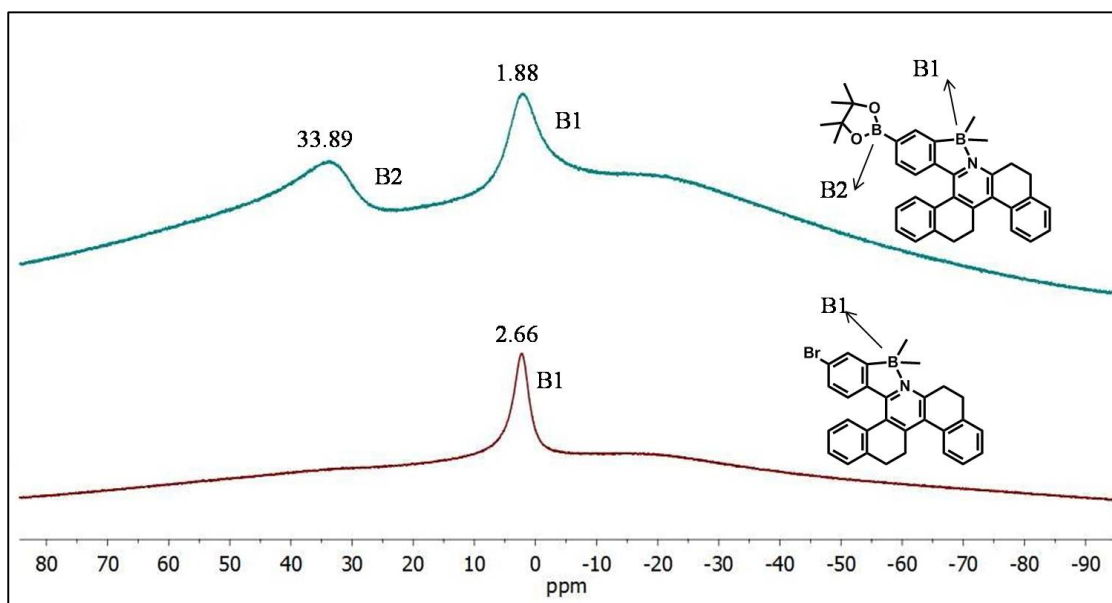


Figure 4B.4: ^{11}B NMR spectrum of compound **2** (bottom) and **8** (top).

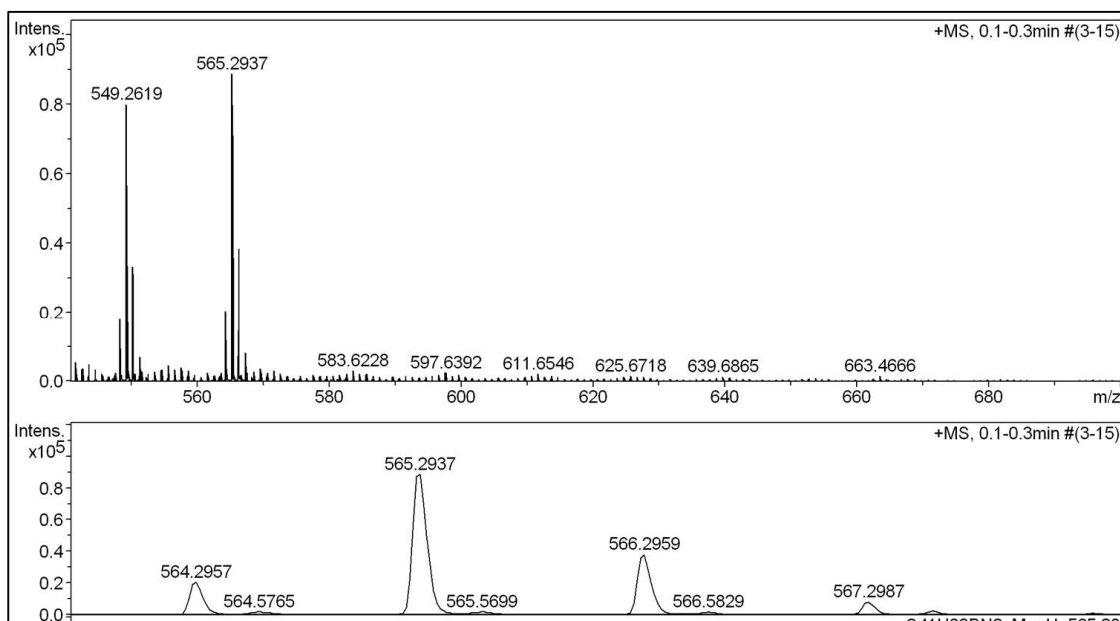


Figure 4B.5: ESI-MS of compound **5**.

compound **2** and **8** are shown in figure 4B.3. Furthermore ^{11}B NMR spectra of the compounds **1-8** shows a signal at $\delta \approx 1-3$ ppm, which clearly indicates the presence of a four-coordinate boron atom. As shown in figure 4B.4, the existence of a new down-

fielded signal at δ 33.89 ppm which corresponds to tri-coordinate boron along with its tetra-coordinate boron atom (δ 1.88 ppm) indicates the formation of compound **8**. Moreover, the proposed structures of *N,C*-chelate boron compounds were confirmed by parent ion peak $[M + H]^+$ in LC-MS analysis (Figure 4B.5) and single-crystal X-ray analysis of **1**, **2**, **4**, **6** and **8**.

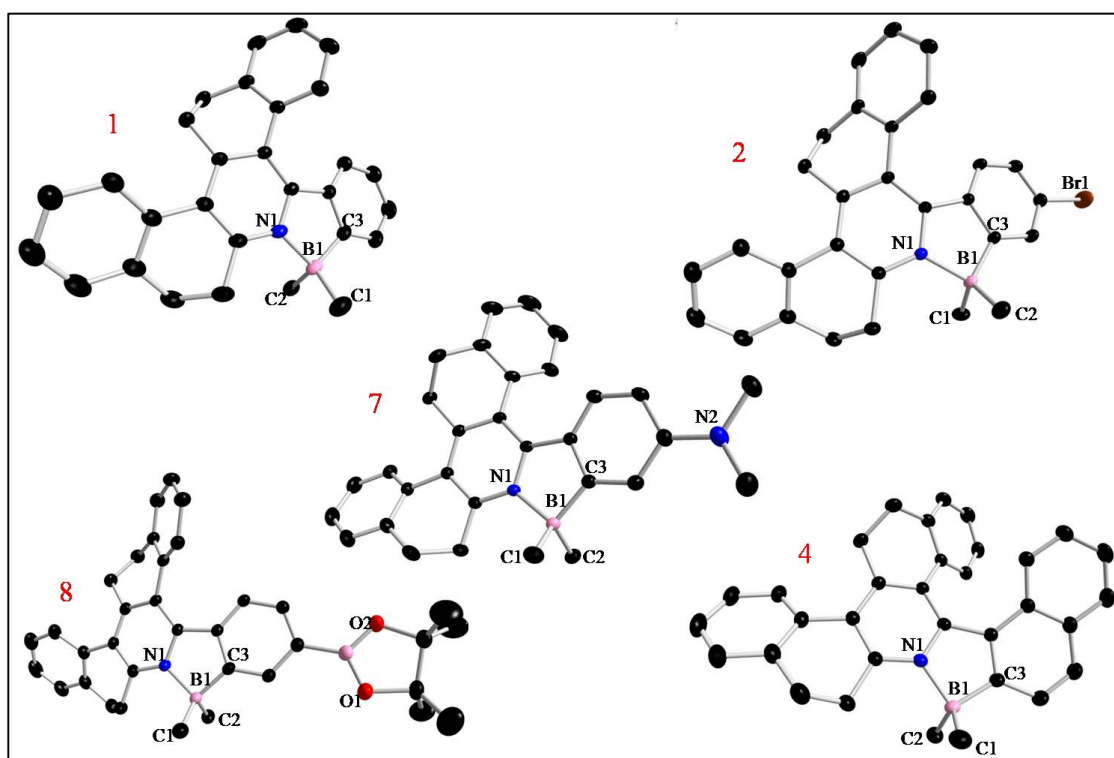


Figure 4B.6: Molecular structure of compounds **1**, **2**, **4**, **7** and **8**. Hydrogen atoms are omitted for clarity. Thermal ellipsoids are drawn at 30% probability level.

Single crystals of compounds **1-8** were grown from CH_2Cl_2 -hexane/ethanol and has been analyzed using single crystal X-ray diffraction studies (Table 4B.2 and 4B.3). The molecular structures of compounds **1-8** are shown in figure 4B.6; selected bond lengths and bond angles around the boron centre are summarized in table 4B.2. In all these compounds, the boron atom adopts a slightly distorted tetrahedral geometry and deviate from the plane passing through a five-membered ring which is formed by the

N,C-chelation with boron; the distance ranging from 0.0079 to 0.0297 Å. The B–N and B–C distances are in the typical range (Table 4B.1) and are consistent with values reported in literature for tetra-coordinated *N,C*-chelate boron complexes.³³

Table 4B.1: Selected bond angle and bond lengths of compounds **1**, **2**, **4**, **7** and **8**.

Bond length [Å] and bond angles [°]	Compound 1	Compound 2	Compound 4	Compound 7	Compound 8
N1-B1	1.646(3)	1.669(2)	1.6559(18)	1.6603(16)	1.663(2)
C1-B1	1.627(3)	1.625(3)	1.622(2)	1.6234(18)	1.616(3)
C2-B1	1.625(3)	1.616(3)	1.617(2)	1.6210(18)	1.631(3)
C3-B1	1.583(3)	1.599(3)	1.599(2)	1.5976(17)	1.591(3)
C1-B1-N1	111.58(18)	111.19(16)	111.97(12)	111.52(10)	111.99(14)
C1-B1-C3	114.5(2)	111.14(17)	107.30(13)	111.2(1)	114.29(15)
C1-B1-C2	115.01(19)	113.67(16)	115.33(12)	113.02(10)	113.95(15)
C2-B1-N1	108.97(17)	110.64(15)	109.00(12)	110.55(10)	109.68(14)
C2-B1-C3	108.71(19)	113.26(17)	116.02(13)	113.56(10)	109.67(15)
C3-B1-N1	96.50(16)	95.59(13)	95.56(10)	95.80(8)	95.82(12)
Deviation of B1 from C ₂ N ₂ B plane (Å)	-0.0187	0.0297	-0.0097	-0.0293	-0.0079

Table 4B.2: Crystal data and structure refinement parameters for compounds **1**, **2** and **4**.

	1	2	4
Empirical formula	C ₂₉ H ₂₆ NB	C ₂₉ H ₂₅ NBBR	C ₃₃ H ₂₈ NB
Formula weight	399.32	478.22	449.37
Temperature/K	296.15	296.15	296.15
Crystal system	orthorhombic	triclinic	triclinic
Space group	Pbca	P-1	P-1
<i>a</i> /Å	18.0934(14)	9.3225(3)	10.6815(5)
<i>b</i> /Å	10.3514(7)	10.3040(3)	11.1873(5)
<i>c</i> /Å	22.9774(18)	12.4417(3)	11.5693(7)
α /°	90	93.391(2)	61.340(3)
β /°	90	94.105(2)	89.736(4)
γ /°	90	108.647(2)	88.253(3)
Volume/Å ³	4303.5(6)	1125.23(6)	1212.47(11)

Z	8	2	2
$\rho_{\text{calc}}/\text{cm}^3$	1.233	1.411	1.231
μ/mm^{-1}	0.070	1.844	0.070
F(000)	1696.0	492.0	476.0
Radiation	MoK α ($\lambda =$ 0.71073)	MoK α ($\lambda =$ 0.71073)	MoK α ($\lambda =$ 0.71073)
2 θ range for data collection/ $^\circ$	4.2 to 52.868	4.188 to 58.33	3.816 to 54.348
Index ranges	$-22 \leq h \leq 22$, $-12 \leq$ $k \leq 10$, $-28 \leq l \leq$ 28	$-12 \leq h \leq 12$, $-$ $14 \leq k \leq 13$, -17 $\leq l \leq 16$	$-13 \leq h \leq 13$, -14 $\leq k \leq 14$, $-14 \leq l \leq$ 14
Reflections collected	37451	19333	18226
Independent reflections	4399 [$R_{\text{int}} =$ 0.0829, $R_{\text{sigma}} =$ 0.0460]	6053 [$R_{\text{int}} =$ 0.0345, $R_{\text{sigma}} =$ 0.0405]	5346 [$R_{\text{int}} =$ 0.0466, $R_{\text{sigma}} =$ 0.0439]
Data/restraints/parame ters	4399/0/282	6053/0/291	5346/0/318
Goodness-of-fit on F2	1.030	1.024	1.039
Final R indexes [$I \geq 2\sigma(I)$]	$R_I = 0.0556$, wR_2 $= 0.1235$	$R_I = 0.0410$, $wR_2 = 0.0936$	$R_I = 0.0469$, wR_2 $= 0.1146$
Final R indexes [all data]	$R_I = 0.0878$, $wR_2 =$ 0.1471	$R_I = 0.0710$, $wR_2 = 0.1057$	$R_I = 0.0698$, wR_2 $= 0.1280$
Largest diff. peak/hole / $e \text{ \AA}^{-3}$	0.19 and -0.24	0.27 and -0.87	0.18 and -0.21

Table 4B.3: Crystal data and structure refinement parameters for compounds **7** and **8**.

	7	8
Empirical formula	C ₃₁ H ₃₁ N ₂ B	C ₃₅ H ₃₆ NO ₃ B ₂
Formula weight	442.39	540.27
Temperature/K	296.15	296.15
Crystal system	triclinic	triclinic
Space group	P-1	P-1
a/ \AA	9.1788(5)	10.2364(6)
b/ \AA	10.4056(5)	12.5523(7)
c/ \AA	13.3256(7)	12.9221(8)
$\alpha/^\circ$	95.086(3)	105.759(4)
$\beta/^\circ$	95.827(3)	97.135(4)
$\gamma/^\circ$	105.348(3)	96.594(4)
Volume/ \AA^3	1212.12(11)	1566.28(16)
Z	2	2

$\rho_{\text{calc}}/\text{cm}^3$	1.212	1.146
μ/mm^{-1}	0.070	0.071
F(000)	472.0	574.0
Radiation	MoK α ($\lambda =$ 0.71073)	MoK α ($\lambda =$ 0.71073)
2 θ range for data collection/ $^\circ$	3.094 to 59.27	5.408 to 57.606
Index ranges	$-12 \leq h \leq 12$, $-14 \leq$ $k \leq 14$, $-18 \leq l \leq$ 18	$-13 \leq h \leq 12$, $-$ $16 \leq k \leq 16$, -17 $\leq l \leq 17$
Reflections collected	22249	28165
Independent reflections	6829 [$R_{\text{int}} =$ 0.0285, $R_{\text{sigma}} =$ 0.0311]	8101 [$R_{\text{int}} =$ 0.0663, $R_{\text{sigma}} =$ 0.0658]
Data/restraints/parame ters	6829/0/311	8101/0/367
Goodness-of-fit on F^2	1.028	0.986
Final R indexes [$I \geq 2\sigma(I)$]	$R_1 = 0.0506$, wR_2 $= 0.1336$	$R_1 = 0.0601$, $wR_2 = 0.1469$
Final R indexes [all data]	$R_1 = 0.0700$, wR_2 $= 0.1491$	$R_1 = 0.1108$, $wR_2 = 0.1657$
Largest diff. peak/hole / $e \text{ \AA}^{-3}$	0.27 and - 0.22	0.30 and -0.25

4B.2.3 Thermal properties

Thermal properties of the *N,C*-chelate organoboron compounds (**1-6** and **8**) were characterized by thermogravimetric analysis (TGA) (Figure 4B.7) and differential scanning calorimetry (DSC) under nitrogen atmosphere at the heating rate of 10 $^\circ\text{C}$ per minute. The melting points of **1-6** and **8** were measured using DSC (Figure 4B.8). As depicted in figure 4B.7 the decomposition temperatures (T_{d5}) (corresponds to 5% weight loss) of compounds **1-6** and **8** are 274, 305, 277, 284, 372, 356 and 325 respectively. Compounds **6** (295 $^\circ\text{C}$) and **8** (293 $^\circ\text{C}$) showed high melting point over other compounds. TGA and DSC analysis reveal that these compounds exhibit high thermal stability.

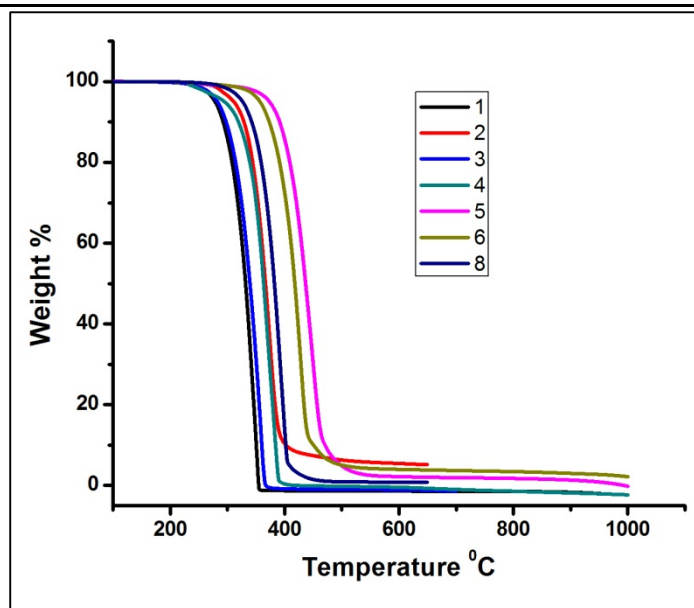


Figure 4B.7: TGA curves of 1-6 and 8 at a heating rate of 10 °C/min.

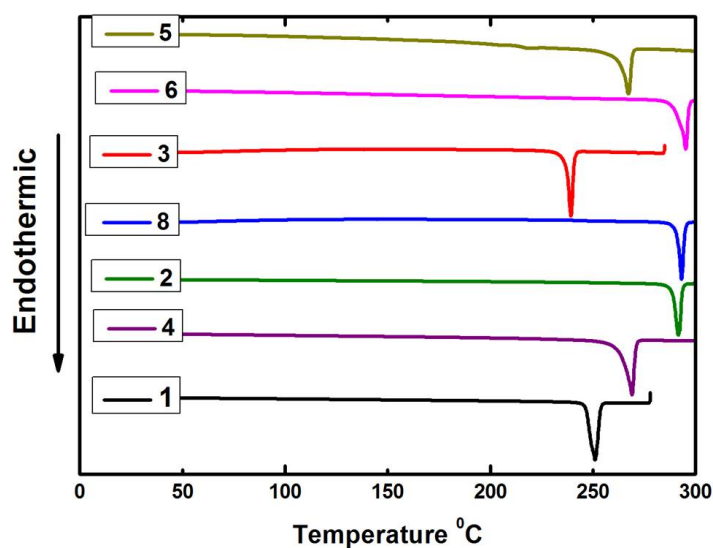


Figure 4B.8: DSC curves of 1-6 and 8 at a heating rate of 10 °C/min.

4B.2.4 Photophysical properties

All compounds showed good solubility in polar aprotic solvents and also in non polar solvent like toluene. The photophysical properties of all these compounds were studied in four different solvents with varying polarity *viz* toluene, dichloromethane, THF and acetonitrile and are presented in table 4B.4. As shown in figure 4B.9 the

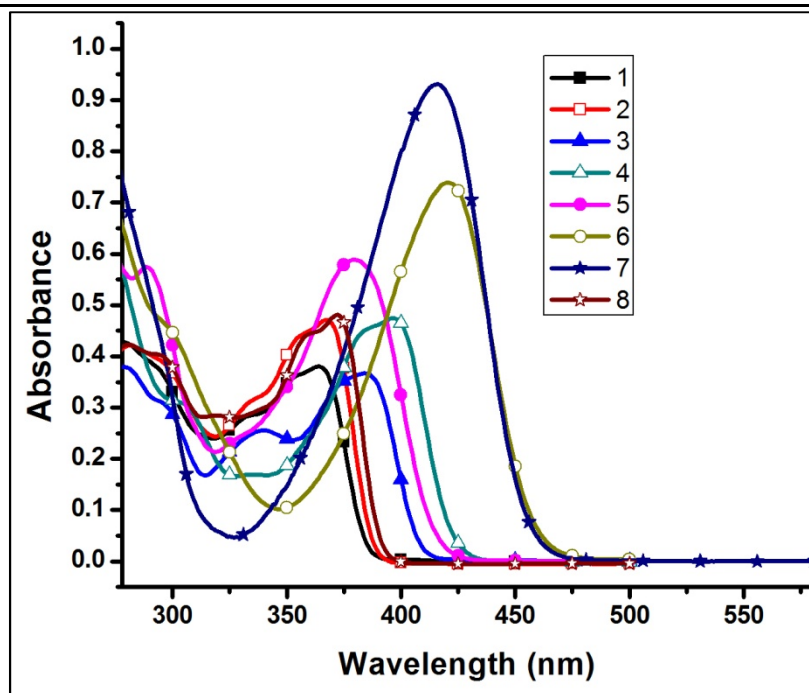


Figure 4B.9: Absorption spectra of boron compounds **1-8** (24 μ M) in CH₂Cl₂.

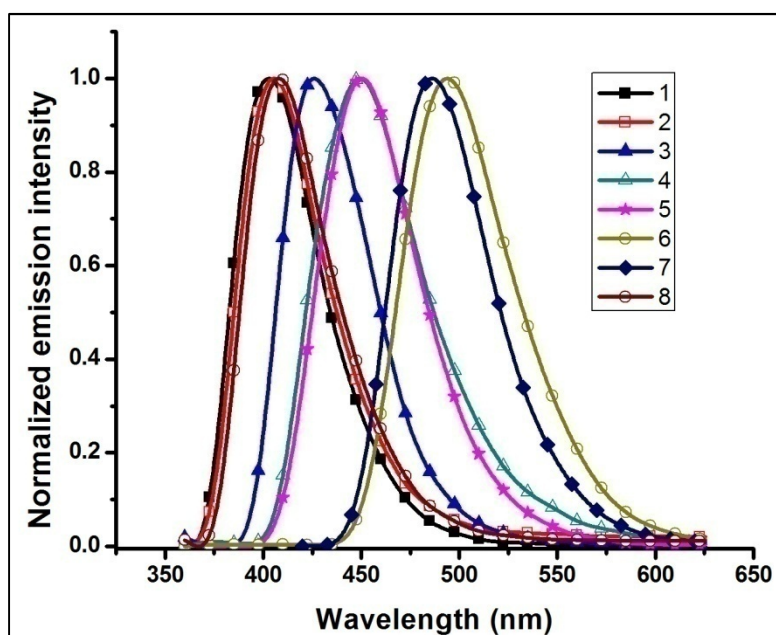


Figure 4B.10: Normalized emission spectra of boron compounds **1-8** (24 μ M) in CH₂Cl₂ excited at longer wavelength absorption maxima.

absorption spectra of CH₂Cl₂ solutions of compounds **1-8** showed absorption maxima from 364-420 nm with molar extinction coefficient ranges from

$15800\text{-}38700\text{ M}^{-1}\text{cm}^{-1}$. Because of extended conjugation compounds **3** and **4**, exhibits red shifted absorption compared to compound **1**. Most of these compounds did not show any solvatochromism except compounds **5**, **6** and **7**. However the absorption maxima got blue shifted with increased solvent polarity of compounds **5**, **6** and **7** (Table 4B.3).

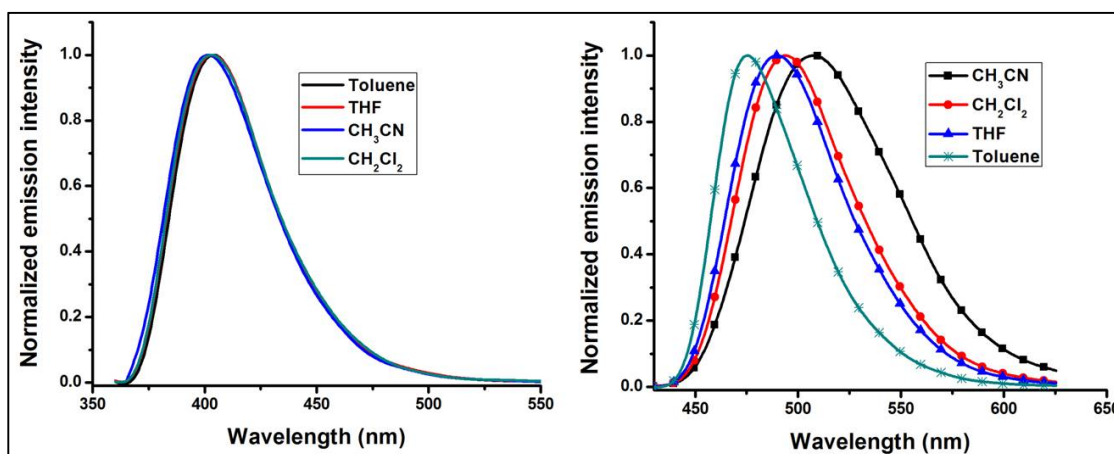


Figure 4B.11: Normalized emission spectra of compounds **1**(left) and **6**(right) with increasing solvent polarity (24 μM).

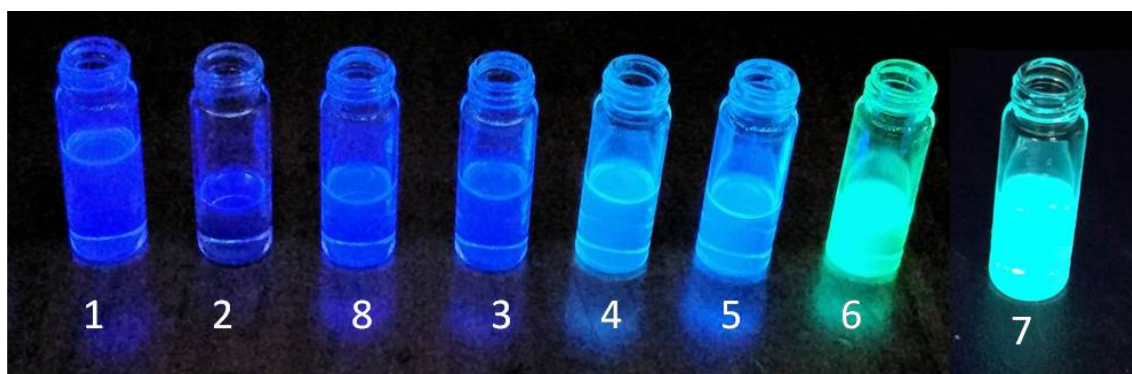


Figure 4B.12: Photograph of compounds **1-8** in THF under hand held UV lamp of 365 nm.

Table 4B.4 Photophysical data of compounds 1-8

Compound	Solvent	λ_{\max}^a (nm)	ϵ_{\max}^a $M^{-1}cm^{-1} \times 10^4$	$\lambda_{em}(nm)^{a,b}$	Φ_F^d
1	Toluene	368	1.67	403	0.45
	THF	366	1.64	402	0.52
	CH ₂ Cl ₂	364	1.58	403	0.66
	CH ₃ CN	361	1.51	402	0.47
	Solid			466	0.21
2	Toluene	371	2.00	404	0.14
	THF	370	2.03	404	0.15
	CH ₂ Cl ₂	368	1.96	406	0.13
	CH ₃ CN	364	1.87	403	0.12
	Solid			463	0.05
3	Toluene	389	1.51	426	0.36
	THF	384	1.53	427	0.40
	CH ₂ Cl ₂	384	1.52	426	0.41
	CH ₃ CN	380	1.41	425	0.34
	Solid			471	0.16
4	Toluene	401	1.89	446	0.51
	THF	398	1.84	448	0.46
	CH ₂ Cl ₂	397	1.97	448	0.53
	CH ₃ CN	392	1.87	449	0.38
	Solid			492	0.06
5	Toluene	388	2.25	438	0.95
	THF	380	2.38	448	0.86
	CH ₂ Cl ₂	379	2.45	450	0.67
	CH ₃ CN	376	2.35	460	0.73
	Solid			470	0.38
6	Toluene	430	3.00	475	0.68
	THF	421	2.99	490	0.62
	CH ₂ Cl ₂	420	3.07	494	0.99
	CH ₃ CN	413	2.74	507	0.51
	Solid			531	0.46
7	Toluene	424	3.7	476	0.60
	THF	418	3.42	489	0.63
	CH ₂ Cl ₂	415	3.87	485	0.55
	CH ₃ CN	410	3.49	504	0.24
	Solid			550	0.94
8	Toluene	376	1.87	409	0.48
	THF	375	2.18	408	0.49
	CH ₂ Cl ₂	373	1.99	408	0.54
	CH ₃ CN	369	1.96	406	0.45
	Solid			455	0.34

^aAbsorption maximum(24 μ M). ^bExcited at the absorption maximum. ^cQuinine sulphate standard in 0.1 N H₂SO₄. ^dAbsolute quantum yields measured using an integrating sphere for solids

Normalized emission spectra of compounds **1-8** are shown in figure 4B.10 where all the compounds excited at their longer absorption wavelength maxima. The emission wavelength of *N,C*- chelate boron compounds are finely tuned from 402 nm (compound **1**) to 495 nm (compound **6**) in dichloromethane. Naphthalene (**4**) and thiophene (**3**) substituted *N,C*- chelate boron chromophores showed red-shifted emission due to increased conjugation. Compounds **1-4** and **8** did not show any emission changes with solvent polarity which indicates that the interaction of fluorophores with solvent molecules in excited state is less significant. However, in case of compounds **5**, **6** and **7**, the emission maxima got red shifted due to intramolecular charge transfer from carbazole, -NPh₂, and -NMe₂ groups respectively. The charge transfer emission of these compounds further supported by the positive solvatochromism with increased solvent polarity from toluene to acetonitrile (Figure 4B.11). The emission efficiencies of boron compounds **1-8** in CH₂Cl₂ were measured using quinine sulphate as reference in 0.1N H₂SO₄ which are presented in table 4B.4. Compound **2** showed less fluorescence quantum yield (0.13) over compound **1** (0.4) because of the presence of heavy bromine atom which induces non radiative pathways. The *N,N*- diphenyl amine substituted *N,C*- chelate boron compound **6** achieved highest quantum yield (0.99) with large stock shifted (74 nm) emission. The solid state emission spectra of compounds **1-8** are represented in figure 4B.13. The solid state emission of compounds **1-8** ranges from 455 nm (deep blue **8**) to 550 nm (yellow **7**) and all are red shifted compared to their solution state (CH₂Cl₂) emission by ≈ 40 nm, suggesting that the substituents at 2-position of tetrahydrodibenzo[a,i]phenanthridine indeed effective in fine tuning the emission wavelength of *N,C*- chelate tetra-coordinate organoboron. Moreover, the absolute solid state fluorescence quantum yields of compounds **1-8** suggest that they are highly

emissive even in their solid state as well. The highest solid state quantum yield (0.94) was observed for compound **7** with red shifted emission at 550 nm.

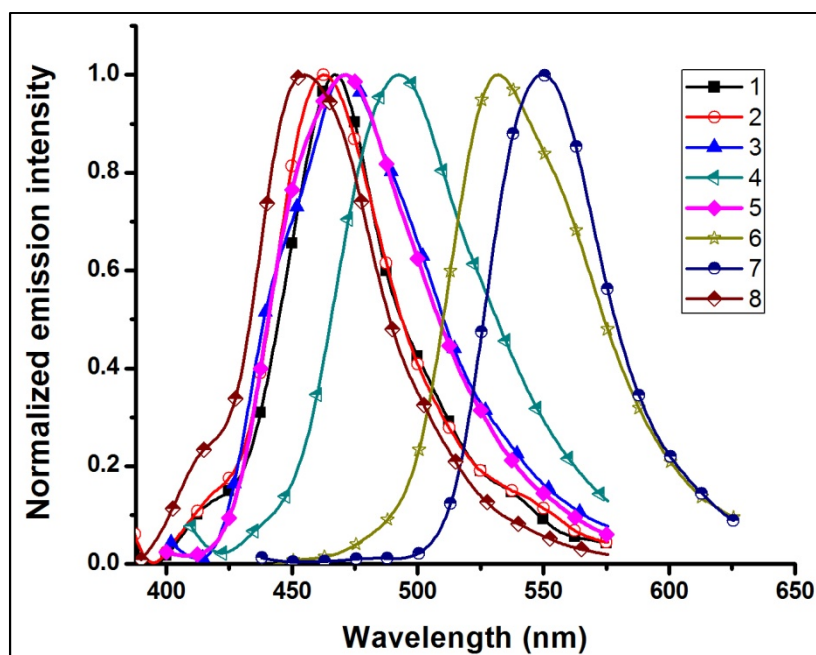


Figure 4B.13: A comparison of normalized emission spectra of boron compounds **1-8** in solid state.

4B.3 Conclusion

A series of tetrahydrodibenzo[*a,i*]phenanthridine compounds (**1a-1g**) were synthesized in one pot. By simple electrophilic borylation of these compounds, *N,C*-chelated boron compounds **1-8** were obtained with good yields. All these compounds were successfully characterized by NMR and X-ray analysis. Large Stokes shifts as well as better quantum yields in both solution and solid state of the compounds suggest that this class of compounds could have potential applications in imaging and optoelectronic devices.

4B.4 Experimental section

4B.4.1 Methods and instruments

All reagents were used as received from Spectrochem, Alfa-aesar and Sigma-Aldrich unless otherwise noted. The 4-(9H-carbazol-9-yl)benzaldehyde and 4-(diphenylamino)benzaldehyde were prepared according to known literature procedures.^{34,35} All solvents were purchased from Spectrochem India. Dichloromethane and toluene were dried using calcium hydride and Na/benzophenone respectively. All experiments were monitored by analytical thin layer chromatography (TLC) under hand held UV lamp at 254 nm. All ¹H (400 and 700 MHz), ¹³C (100 and 176 MHz), and ¹¹B (128 MHz) NMR were recorded at room temperature on Bruker ARX 400 and 700 spectrometer. Residual protonated solvents were used as internal standards for ¹H and ¹³C NMR. ¹¹B NMR spectra were referenced externally to BF₃·Et₂O in CDCl₃ ($\delta = 0$ ppm). ESI mass spectra were recorded with Bruker micro TOF-QII mass spectrometer. UV-Visible spectra were recorded on JASCO V-730 UV/Visible spectrometer. The fluorescence spectra were recorded with a Perkin-Elmer LS-55 Fluorescence spectrometer. Quinine sulphate was used as the standard for the determination of fluorescence quantum yields. For solid state quantum yields integrating sphere method has been used. Single crystals of all compounds were grown from dichloromethane-hexane/ethanol solvent mixture. Single crystal X-ray diffraction data were collected on Bruker APEX-II CCD diffractometer at 296 K using Mo-K α radiation (0.71073 Å). The structure was solved by direct methods using shelXT program and refined with least squares minimization with shelXL using Olex2. The H- atoms were assigned at calculated positions and were refined as riding atoms.

4B.4.2 Synthetic procedures and spectral characterization

General procedure for the synthesis of compounds 1a-1g

In a 100 mL conical flask ethanol and acetic acid (4:1) were taken. To this solvent mixture, benzaldehyde (1 eq) and ammonium acetate (4 eq) were added and warmed under water bath until the solids form a homogeneous solution. To this reaction mixture 2-tetralone (2 eq) was added, and the mixture heated for 5 min at 75 °C. Later the reaction mixture was kept for 24 hour at room temperature in open air. The progress of the reaction was monitored by TLC. The reaction mixture was poured into water and extracted with dichloromethane. The combined organic layers were washed with brine solution, dried over Na₂SO₄ and concentrated using rotavap. The crude reaction mixture was purified by 100-200 silica gel chromatography using *n*-hexane/dichloromethane mixture as the mobile phase.

Synthesis of compound 1a

The quantities involved are as follows. Benzaldehyde (0.57 mL, 5.67 mmol), 2-tetralone (1.5 mL, 11.34 mmol), and ammonium acetate (1.75 g, 22.68 mmol). Yield: 1.66 g, (82 %). Mp: 215 °C. ¹H NMR (400 MHz, CDCl₃): δ 7.54 - 7.51 (m, 1H), 7.46 (dd, *J* = 6.5, 3.0 Hz, 2H), 7.39 - 7.29 (m, 6H), 7.27 - 7.24 (m, 2H), 7.16 - 7.10 (m, 1H), 6.89 (d, *J* = 3.9 Hz, 2H), 3.17 - 3.14 (m, 2H), 3.12 - 3.09 (m, 2H), 2.98 - 2.95 (m, 2H), 2.79 (t, *J* = 8 Hz, 2H) ppm. ¹³C NMR (100 MHz, CDCl₃): δ 158.11, 153.97, 145.71, 142.08, 139.68, 138.71, 133.07, 133.05, 129.87, 129.68, 128.87, 128.74, 128.40, 127.91, 127.83, 127.69, 127.51, 127.00, 126.91, 126.08, 125.67, 33.20, 29.59, 29.51, 29.25 ppm. HRMS (ESI): Calcd. for C₂₇H₂₂N₁ ([M + H]⁺): 360.1747, found: 360.1719.

Synthesis of compound 1b

The quantities involved are as follows: 4-Bromobenzaldehyde (1.04 g, 5.67 mmol), 2-tetralone (1.50 mL, 11.34 mmol), and ammonium acetate (1.75 g, 22.68 mmol). Yield: 1.96 g, (79 %). Mp: 219 °C. ^1H NMR (400 MHz, CDCl_3): δ 7.53 - 7.48 (m, 3H), 7.38 - 7.27 (m, 6H), 7.17 (td, $J = 7.3, 1.4$ Hz, 1H), 6.98 - 6.91 (m, 2H), 3.18 - 3.11 (m, 4H), 2.99 - 2.96 (m, 2H), 2.79 (t, $J = 8$ Hz, 2H) ppm. ^{13}C NMR (100 MHz, CDCl_3): δ 158.24, 152.35, 146.27, 140.66, 139.72, 138.82, 132.85, 132.63, 131.73, 131.63, 129.65, 129.10, 128.80, 128.04, 127.98, 127.39, 127.16, 126.22, 125.97, 122.35, 33.01, 29.57, 29.46, 29.32 ppm. HR-MS (ESI): Calcd. for $\text{C}_{27}\text{H}_{21}\text{Br}_1\text{N}_1$ ($[\text{M} + \text{H}]^+$): 438.0852, found: 438.0841.

Synthesis of compound 1c

The quantities involved are as follows: Thiophene-2-carbaldehyde (0.53 mL, 5.67 mmol), 2-tetralone (1.5 mL, 11.34 mmol), and ammonium acetate (1.75 g, 22.68 mmol). Yield: 1.38 g, (67 %). Mp: 220 °C. ^1H NMR (400 MHz, CDCl_3): δ 7.52 - 7.50 (m, 1H), 7.36 - 7.26 (m, 6H), 7.19 (t, $J = 7.4$ Hz, 1H), 7.07 (d, $J = 4$ Hz, 1H), 7.03 (t, $J = 7.6$ Hz, 1H), 6.94 (dd, $J = 5.0, 3.7$ Hz, 1H), 3.13 - 3.06 (m, 4H), 2.98 - 2.94 (m, 2H), 2.76 (t, $J = 7.4$ Hz, 1H) ppm. ^{13}C NMR (100 MHz, CDCl_3): δ 158.35, 147.07, 146.07, 144.65, 139.77, 138.99, 133.06, 132.95, 129.35, 129.09, 128.74, 128.10, 128.01, 127.85, 127.72, 127.51, 127.26, 127.09, 126.82, 126.18, 125.83, 33.23, 29.62, 29.60, 29.49 ppm. HR-MS (ESI): Calcd. for $\text{C}_{25}\text{H}_{20}\text{N}_1\text{S}_1$ ($[\text{M} + \text{H}]^+$): 366.1311, found: 366.1289.

Synthesis of compound 1d

The quantities involved are as follows: 1-Naphthaldehyde (0.77 mL, 5.67 mmol), 2-tetralone (1.5 mL, 11.34 mmol), and ammonium acetate (1.75 g, 22.68 mmol). Yield:

1.44 g, (62 %). ^1H NMR (400 MHz, CDCl_3): δ 7.88 (dd, $J = 8.0, 4.4$ Hz, 2H), 7.70 (d, $J = 8.4$ Hz, 1H), 7.58 - 7.56 (m, 1H), 7.47-7.42 (m, 2H), 7.40 - 7.31 (m, 5H), 7.19 (d, $J = 7.4$ Hz, 1H), 6.99 (td, $J = 7.2, 1.8$ Hz, 1H), 6.63 - 6.57 (m, 2H), 3.34 - 3.27 (m, 1H), 3.20 - 3.11 (m, 3H), 3.02 - 2.96 (m, 2H), 2.83 - 2.74 (m, 2H) ppm. ^{13}C NMR (176 MHz, CDCl_3): δ 158.00, 153.25, 145.49, 139.92, 139.84, 138.58, 134.20, 133.16, 132.91, 132.01, 130.49, 129.00, 128.40, 128.36, 128.06, 127.98, 127.92, 127.05, 126.90, 126.31, 126.23, 126.10, 125.88, 125.72, 33.22, 29.78, 29.55, 29.38 ppm. HR-MS (ESI): Calcd. for $\text{C}_{31}\text{H}_{24}\text{N}_1$ ($[\text{M} + \text{H}]^+$): 410.1903, found: 410.1904.

Synthesis of compound 1e

The quantities involved are as follows: 4-(9H-Carbazol-9-yl)benzaldehyde (1.53 g, 5.67 mmol), 2-tetralone (1.5 mL, 11.34 mmol), and ammonium acetate (1.75 g, 22.68 mmol). Yield: 1.54 g, (52%). Mp: 267 °C. ^1H NMR (400 MHz, CDCl_3): δ 8.16 (d, $J = 7.7$ Hz, 2H), 7.74 (d, $J = 8.0$ Hz, 2H), 7.60 - 7.55 (m, 3H), 7.50 - 7.29 (m, 11H), 7.25 - 7.22 (m, 1H), 7.05 (d, $J = 4.0$ Hz, 2H), 3.31 - 3.22 (m, 4H), 3.04 - 3.01 (m, 2H), 2.83 - 2.76 (m, 2H) ppm. ^{13}C NMR (100 MHz, CDCl_3): δ 158.45, 153.02, 146.07, 141.23, 140.91, 139.81, 139.01, 137.34, 133.05, 132.98, 131.58, 129.80, 129.26, 128.87, 128.06, 127.99, 127.95, 127.44, 127.24, 127.01, 126.24, 126.09, 125.82, 123.56, 120.43, 120.08, 109.97, 33.36, 29.68, 29.59, 29.35 ppm. HR-MS (ESI): Calcd. for $\text{C}_{39}\text{H}_{29}\text{N}_2$ ($[\text{M} + \text{H}]^+$): 525.2325, found: 525.2320.

Synthesis of compound 1f

The quantities involved are as follows: 4-(Diphenylamino)benzaldehyde (1.55 g, 5.67 mmol), 2-tetralone (1.5 mL, 11.34 mmol), and ammonium acetate (1.75 g, 22.68 mmol). Yield: 1.49 g, (50%). Mp: 238 °C. ^1H NMR (400 MHz, CDCl_3): δ 7.53 - 7.51 (m, 1H), 7.37 - 7.24 (m, 10H), 7.17 - 7.12 (m, 5H), 7.07 - 6.97 (m, 6H), 3.16 - 3.09

(m, 4H), 2.98 -2.95 (m, 2H), 2.77 (t, $J = 8.0$ Hz, 2H) ppm. ^{13}C NMR (100 MHz, CDCl_3): δ 158.20, 153.71, 147.73, 147.55, 145.78, 139.72, 138.80, 136.15, 133.36, 133.21, 130.93, 129.68, 129.29, 128.85, 128.75, 127.95, 127.68, 127.33, 127.07, 126.97, 126.12, 125.56, 124.48, 123.67, 122.93, 33.36, 29.64, 29.60, 29.32 ppm. HR-MS (ESI): Calcd. for $\text{C}_{39}\text{H}_{31}\text{N}_2$ ($[\text{M} + \text{H}]^+$): 527.2482, found: 527.2463.

Synthesis of compound 1g

The quantities involved are as follows: 4-(dimethylamino)benzaldehyde (0.85 g, 5.67 mmol), 2-tetralone (1.5 mL, 11.34 mmol), and ammonium acetate (1.75 g, 22.68 mmol). Yield: 1.27 g, (56%). ^1H NMR (700 MHz, CDCl_3): δ 7.51 (d, $J = 8$ Hz, 1H), 7.36 (t, $J = 8$ Hz, 3H), 7.31 (t, $J = 8$ Hz, 1H), 7.27 (dd, $J = 12, 8$ Hz, 2H), 7.17 - 7.07 (m, 2H), 6.96 (t, $J = 8$ Hz, 1H), 6.69 (d, $J = 8.0$ Hz, 2H), 3.14 - 3.09 (m, 4H), 2.98 (s, 6H), 2.97 - 2.93 (m, 2H), 2.79 - 2.72 (m, 2H) ppm. ^{13}C NMR (176 MHz, CDCl_3): δ 158.13, 154.29, 150.41, 145.73, 139.71, 138.66, 133.86, 133.46, 130.86, 130.13, 129.59, 128.71, 128.37, 127.89, 127.45, 126.85, 126.73, 126.66, 126.06, 125.77, 112.37, 40.67, 33.35, 29.74, 29.69, 29.47 ppm. ESI-MS: Calcd. for $\text{C}_{29}\text{H}_{27}\text{N}_2$ ($[\text{M} + \text{H}]^+$): 403.2169, found: 403.2155.

General procedure for the synthesis of compounds 1-8

Oven dried three neck round bottom flask with addition funnel was degassed and purged using vacuum - nitrogen cycle and charged with dichloromethane solution of compounds (**1a-1g**). To this solution diisopropylethylamine (*i*-Pr₂NEt) was added at 0 °C and stirred. After 10 min BBr_3 (1.0 M in dichloromethane) was added slowly at the same temperature and allowed to warm to room temperature. After being stirred at room temperature for 24 h, saturated K_2CO_3 aqueous solution was added to the reaction mixture and extracted with CH_2Cl_2 . The combined organic layers were

washed with water, dried over MgSO_4 and concentrated using rotary evaporator to afford the crude dibromo boron compound. Without further purification the crude product was taken in a round bottom flask and dried using high vacuum and then filled with argon and added toluene. To this stirred solution AlMe_3 (2.0 M in toluene) was added at room temperature. After stirring for half an hour, the reaction was quenched by adding water and extracted with CH_2Cl_2 . The combined organic layers were washed with water, and brine. The organic layer was dried over Na_2SO_4 and concentrated using rotavap. The crude product was purified by silica gel column chromatography using *n*-hexane/dichloromethane mixture as the mobile phase.

Boron compound 1

The quantities involved are as follows: Compound **1a** (0.60 g, 1.67 mmol), *N,N*-diisopropylethylamine (0.29 mL, 1.67 mmol), BBr_3 (1.0 M in CH_2Cl_2 , 5.01 mL, 5.01 mmol) and AlMe_3 (2.0 M in toluene, 1.67 mL, 3.34 mmol). Yield: 0.43 g, (65 %). Mp: 251 °C. ^1H NMR (400 MHz, CDCl_3): δ 7.97 (d, $J = 7.7$ Hz, 1H), 7.81 (d, $J = 8.1$ Hz, 1H), 7.58 - 7.54 (m, 2H), 7.41 - 7.24 (m, 7H), 6.95 (t, $J = 8$ Hz, 1H), 2.81 - 4.04 (m, 8H), 0.25 (s, 1H) ppm. ^{13}C NMR (100 MHz, CDCl_3): δ 170.22, 155.71, 151.05, 149.83, 139.46, 139.03, 135.70, 131.67, 131.61, 129.70, 129.61, 129.27, 128.94, 128.63, 128.57, 128.40, 127.89, 127.84, 127.26, 126.37, 126.03, 124.82, 123.98, 30.29, 29.35, 28.78, 28.32, 9.16 ppm. ^{11}B NMR (128 MHz, CDCl_3): δ 2.12 ppm. ESI-MS: Calcd. for $\text{C}_{29}\text{H}_{27}\text{B}_1\text{N}_1$ ($[\text{M} + \text{H}]^+$): 400.2236, found: m/z 400.2340.

Boron compound 2

The quantities involved are as follows: Compound **1b** (0.73 g, 1.67 mmol), *N,N*-diisopropylethylamine (0.29 mL, 1.67 mmol), BBr_3 (1.0 M in CH_2Cl_2 , 5.01 mL, 5.01 mmol) and AlMe_3 (2.0 M in toluene, 1.67 mL, 3.34 mmol). Yield: 0.49 g, (62 %).

Mp: 291 °C. ^1H NMR (400 MHz, CDCl_3): δ 7.89 (d, $J = 7.7$ Hz, 1H), 7.65 (d, $J = 8.3$ Hz, 2H), 7.56 – 7.53 (m, 1H), 7.41 – 7.30 (m, 5H), 7.28 – 7.24 (m, 1H), 7.06 (dd, $J = 8.5, 2.0$ Hz, 1H), 4.04 – 2.81 (m, 8H), 0.22 (s, 6H) ppm. ^{13}C NMR (100 MHz, CDCl_3): δ 172.87, 155.84, 150.11, 150.08, 139.47, 139.17, 134.42, 131.50, 131.40, 129.76, 129.19, 129.08, 128.67, 128.61, 128.31, 127.97, 127.45, 127.13, 126.47, 126.32, 126.19, 125.42, 30.30, 29.34, 28.75, 28.33, 8.79 ppm. ^{11}B NMR (128 MHz, CDCl_3): δ 2.66 ppm.

Boron compound 3

The quantities involved are as follows: Compound **1c** (0.61 g, 1.67 mmol), N,N-diisopropylethylamine (0.29 mL, 1.67 mmol), BBr_3 (1.0 M in CH_2Cl_2 , 5.01 mL, 5.01 mmol) and AlMe_3 (2.0 M in toluene, 1.67 mL, 3.34 mmol). Yield: 0.20 g, (30 %). Mp: 239 °C. ^1H NMR (400 MHz, CDCl_3): δ 8.28 - 8.24 (m, 1H), 7.48 - 7.45 (m, 1H), 7.42 - 7.37 (m, 4H), 7.32 - 7.29 (m, 3H), 7.12 (d, $J = 4.7$ Hz, 1H), 3.44 (brs, 2H), 3.12 (t, $J = 8$ Hz, 2H), 2.94 (t, $J = 6.7$ Hz, 2H), 2.73 (t, $J = 8$ Hz, 2H), 0.23 (s, 6H) ppm. ^{13}C NMR (100 MHz, CDCl_3): δ 156.09, 149.48, 148.49, 139.02, 138.82, 133.66, 131.78, 131.24, 130.25, 129.00, 128.68, 128.16, 127.86, 127.71, 127.24, 127.07, 126.60, 126.49, 126.42, 126.14, 30.31, 29.31, 28.68, 28.17, 7.92 ppm. ^{11}B NMR (128 MHz, CDCl_3): δ 1.67. ESI-MS: Calcd. for $\text{C}_{27}\text{H}_{25}\text{B}_1\text{N}_1\text{S}_1$ ($[\text{M} + \text{H}]^+$): 406.1800, found: m/z 406.1905.

Boron compound 4

The quantities involved are as follows: Compound **1d** (0.68 g, 1.67 mmol), N,N-diisopropylethylamine (0.29 mL, 1.67 mmol), BBr_3 (1.0 M in CH_2Cl_2 , 5.01 mL, 5.01 mmol) and AlMe_3 (2.0 M in toluene, 1.67 mL, 3.34 mmol). Yield: 0.32 g, (42 %). Mp: 269 °C. ^1H NMR (400 MHz, CDCl_3): δ 7.87 (d, $J = 7.9$ Hz, 1H), 7.76 (t, $J = 8.1$

Hz, 2H), 7.68 (d, $J = 7.2$ Hz, 1H), 7.40 - 7.31 (m, 4H), 7.19 - 7.11 (m, 2H), 7.06 (d, $J = 8.5$ Hz, 1H), 6.93 (d, $J = 7.7$ Hz, 1H), 6.83 (t, $J = 7.6$ Hz, 1H), 6.69 (t, $J = 7.4$ Hz, 1H), 3.76 - 3.69 (m, 2H), 3.30 - 3.22 (m, 1H), 3.08 - 3.05 (m, 2H), 2.95 (t, $J = 8$ Hz, 2H), 2.86 - 2.77 (m, 1H), 0.32 (s, 3H), 0.21 (s, 3H) ppm. ^{13}C NMR (100 MHz, CDCl_3): δ 173.20, 155.68, 152.10, 148.91, 139.46, 137.22, 133.78, 133.13, 131.95, 131.27, 130.69, 128.65, 128.56, 128.52, 128.16, 128.08, 128.01, 127.94, 127.77, 127.07, 126.85, 126.74, 126.51, 125.75, 124.38, 123.55, 29.17, 29.09, 28.83, 28.38, 8.46 ppm. ^{11}B NMR (128 MHz, CDCl_3): δ 2.63 ppm. ESI-MS: Calcd. for $\text{C}_{33}\text{H}_{29}\text{B}_1\text{N}_1$ ($[\text{M} + \text{H}]^+$): 450.2393, found: m/z 450.2515.

Boron compound 5

The quantities involved are as follows: Compound **1e** (0.88 g, 1.67 mmol), *N,N*-diisopropylethylamine (0.29 mL, 1.67 mmol), BBr_3 (1.0 M in CH_2Cl_2 , 5.01 mL, 5.01 mmol) and AlMe_3 (2.0 M in toluene, 1.67 mL, 3.34 mmol). Yield: 0.44 g, (47 %). Mp: 267 °C. ^1H NMR (400 MHz, CDCl_3): δ 8.15 (d, $J = 7.7$ Hz, 2H), 8.09 (d, $J = 7.6$ Hz, 1H), 8.04 (d, $J = 8.5$ Hz, 1H), 7.77 (d, $J = 1.8$ Hz, 1H), 7.59 (t, $J = 7.2$ Hz, 3H), 7.44 - 7.40 (m, 5H), 7.36 - 7.33 (m, 3H), 7.30 - 7.27 (m, 2H), 7.17 (dd, $J = 8.4, 2.0$ Hz, 1H), 4.10 - 2.85 (m, 8H), 0.31 (s, 6H) ppm. ^{13}C NMR (100 MHz, CDCl_3): δ 172.54, 155.96, 150.26, 150.10, 140.82, 139.49, 139.19, 138.70, 134.47, 131.57, 131.56, 129.82, 129.24, 129.17, 128.70, 128.56, 128.06, 127.96, 127.45, 126.47, 126.24, 126.21, 126.00, 125.95, 123.62, 122.18, 120.31, 119.92, 110.50, 30.38, 29.41, 28.81, 28.41, 9.02 ppm. ^{11}B NMR (128 MHz, CDCl_3): δ 2.28 ppm. ESI-MS: Calcd. for $\text{C}_{41}\text{H}_{34}\text{B}_1\text{N}_2$ ($[\text{M} + \text{H}]^+$): 565.2816, found: m/z 565.2937.

Boron compound 6

The quantities involved are as follows: Compound **1f** (0.88 g, 1.67 mmol), N,N-diisopropylethylamine (0.29 mL, 1.67 mmol), BBr₃ (1.0 M in CH₂Cl₂, 5.01 mL, 5.01 mmol) and AlMe₃ (2.0 M in toluene, 1.67 mL, 3.34 mmol). Yield: 0.42 g, (45 %). Mp: 295 °C. ¹H NMR (400 MHz, CDCl₃): δ 8.08 (d, *J* = 7.5 Hz, 1H), 7.77 (d, *J* = 8.7 Hz, 1H), 7.57 - 7.55 (m, 1H), 7.40 - 7.24 (m, 15H), 7.09 (t, *J* = 7.1 Hz, 2H), 6.66 (dd, *J* = 8.6, 1.8 Hz, 1H), 4.01 - 2.80 (m, 8H), 0.27 (s, 6H) ppm. ¹³C NMR (100 MHz, CDCl₃): δ 171.95, 155.51, 150.84, 149.61, 149.11, 147.73, 139.27, 138.95, 131.80, 131.77, 129.65, 129.26, 129.00, 128.66, 128.59, 128.50, 128.13, 127.81, 127.18, 126.72, 126.32, 125.94, 125.61, 125.27, 123.19, 121.34, 118.80, 30.27, 29.35, 28.79, 28.29, 9.16 ppm. ¹¹B NMR (128 MHz, CDCl₃): δ 2.09 ppm. ESI-MS: Calcd. for C₄₁H₃₆B₁N₂ ([M + H]⁺): 567.2972, found: m/z 567.2960.

Boron compound 7

The quantities involved are as follows: Compound **1g** (0.67 g, 1.67 mmol), N,N-diisopropylethylamine (0.29 mL, 1.67 mmol), BBr₃ (1.0 M in CH₂Cl₂, 5.01 mL, 5.01 mmol) and AlMe₃ (2.0 M in toluene, 1.67 mL, 3.34 mmol). Yield: 0.43 g, (58 %). Mp: 260 °C. ¹H NMR (700 MHz, CDCl₃) δ 8.03 (d, *J* = 7 Hz, 1H), 7.71 (d, *J* = 7 Hz, 1H), 7.50 (d, *J* = 7 Hz, 1H), 7.36 - 7.24 (m, 6H), 6.83 (s, 1H), 6.36 (d, *J* = 7 Hz, 1H), 0.24 (s, 6H), 2.78 - 2.92 (m, 6H), 3.06 (s, 6H), 3.4 - 4.4 (m, 2H). ¹³C NMR (176 MHz, CDCl₃) δ 172.59, 155.35, 151.84, 151.39, 149.31, 139.27, 138.96, 132.35, 132.13, 128.81, 128.45, 128.36, 127.80, 127.76, 127.56, 127.12, 126.27, 125.88, 125.69, 124.51, 110.12, 108.99, 40.46, 30.25, 29.43, 28.90, 28.33, 9.57. ESI-MS: Calcd. for C₃₁H₃₂B₁N₂ ([M + H]⁺): 443.2658, found: m/z 443.2795.

Boron compound 8

Degassed 1,4-dioxane was added to compound **2** (1.92 g, 4.01 mmol), potassium acetate (1.18 g, 12.04 mmol), bis(pinacolato)diboron (1.12 g, 4.41 mmol),

Pd(dppf)Cl₂ (88 mg, 0.12 mmol) under nitrogen atmosphere in a 250 mL round bottom flask fitted with reflux condenser. After being stirred at 100 °C temperature for 12 h, the reaction mixture was poured into water, extracted with CH₂Cl₂. The combined organic layers were washed with brine solution, dried over Na₂SO₄ and concentrated. The residue was purified by silica gel column chromatography using *n*-hexane/ ethyl acetate mixture as eluent. Yield: 1.87 g, (89 %). Mp: 293 °C. ¹H NMR (400 MHz, CDCl₃): δ 8.04 (s, 1H), 7.91 (d, *J* = 7.7 Hz, 1H), 7.77 (d, *J* = 8.0 Hz, 1H), 7.55 (dd, *J* = 5.4, 3.6 Hz, 1H), 7.42 - 7.31 (m, 6H), 7.21 (d, *J* = 8 Hz, 1H), 2.82 - 4.05 (m, 8H), 1.36 (s, 12H), 0.25 (s, 6H) ppm. ¹³C NMR (100 MHz, CDCl₃): δ 168.52, 155.84, 150.82, 149.76, 139.53, 139.01, 138.42, 135.14, 131.60, 131.58, 130.42, 130.01, 129.38, 129.03, 128.66, 128.47, 128.21, 127.90, 127.25, 126.39, 126.00, 123.94, 83.72, 30.25, 29.33, 28.76, 28.32, 25.05, 8.73 ppm. ¹¹B NMR (128 MHz, CDCl₃): δ 33.88, 1.88 ppm. ESI-MS: Calcd. for C₃₅H₃₇B₂N₁O₂Na₁ ([M + Na]⁺): 548.2914, found: m/z 548.2887.

4B.5 References

- (1) Kobayashi, H.; Choyke, P. L. *Acc. Chem. Res.* **2011**, *44*, 83.
- (2) Schäferling, M. *Angew. Chem. Int. Ed.* **2012**, *51*, 3532.
- (3) Jelinek, R.; Kolusheva, S. *Chem. Rev.* **2004**, *104*, 5987.
- (4) Boens, N.; Leen, V.; Dehaen, W. *Chem. Soc. Rev.* **2012**, *41*, 1130.
- (5) Chatterjee, T.; Srinivasan, A.; Ravikanth, M.; Chandrashekar, T. K. *Chem. Rev.* **2017**, *117*, 3329.
- (6) Entwistle, C. D.; Marder, T. B. *Chem. Mater.* **2004**, *16*, 4574.
- (7) Qu, S.; Tian, H. *Chem. Commun.* **2012**, *48*, 3039.
- (8) Kalyanasundaram, K.; Graetzel, M. *Curr. Opin. Biotechnol.* **2010**, *21*, 298.
- (9) Li, D.; Zhang, H.; Wang, Y. *Chem. Soc. Rev.* **2013**, *42*, 8416.

-
- (10) Rao, Y.-L.; Amarne, H.; Wang, S. *Coord. Chem. Rev.* **2012**, *256*, 759.
- (11) Jäkle, F. *Chem. Rev.* **2010**, *110*, 3985.
- (12) Ge, Y.; O'Shea, D. F. *Chem. Soc. Rev.* **2016**, *45*, 3846.
- (13) Loudet, A.; Burgess, K. *Chem. Rev.* **2007**, *107*, 4891.
- (14) Kappaun, S.; Rentenberger, S.; Pogantsch, A.; Zojer, E.; Mereiter, K.; Trimmel, G.; Saf, R.; Möller, K. C.; Stelzer, F.; Slugovc, C. *Chem. Mater.* **2006**, *18*, 3539.
- (15) Wu, Q.; Esteghamatian, M.; Hu, N.-X.; Popovic, Z.; Enright, G.; Tao, Y.; D'Iorio, M.; Wang, S. *Chem. Mater.* **1999**, *12*, 79.
- (16) Hou, Q.; Zhao, L.; Zhang, H.; Wang, Y.; Jiang, S. *J. Lumin.* **2007**, *126*, 447.
- (17) Frath, D.; Azizi, S.; Ulrich, G.; Retailleau, P.; Ziessel, R. *Org. Lett.* **2011**, *13*, 3414.
- (18) Zhou, Y.; Kim, J. W.; Kim, M. J.; Son, W.-J.; Han, S. J.; Kim, H. N.; Han, S.; Kim, Y.; Lee, C.; Kim, S.-J.; Kim, D. H.; Kim, J.-J.; Yoon, J. *Org. Lett.* **2010**, *12*, 1272.
- (19) Kubota, Y.; Hara, H.; Tanaka, S.; Funabiki, K.; Matsui, M. *Org. Lett.* **2011**, *13*, 6544.
- (20) Kwak, M.-J.; Kim, Y.-M. *Bull. Korean Chem. Soc.* **2009**, *30*, 2865.
- (21) Massue, J.; Frath, D.; Ulrich, G.; Retailleau, P.; Ziessel, R. *Org. Lett.* **2012**, *14*, 230.
- (22) Qiu, F.; Zhang, F.; Tang, R.; Fu, Y.; Wang, X.; Han, S.; Zhuang, X.; Feng, X. *Org. Lett.* **2016**, *18*, 1398.
- (23) Cui, Y.; Wang, S. *J. Org. Chem.* **2006**, *71*, 6485.
- (24) Zhang, Z.; Bi, H.; Zhang, Y.; Yao, D.; Gao, H.; Fan, Y.; Zhang, H.; Wang, Y.; Wang, Y.; Chen, Z.; Ma, D. *Inorg. Chem.* **2009**, *48*, 7230.
-

-
- (25) Frath, D.; Massue, J.; Ulrich, G.; Ziessel, R. *Angew. Chem. Int. Ed.* **2014**, *53*, 2290.
- (26) Wakamiya, A.; Taniguchi, T.; Yamaguchi, S. *Angew. Chem. Int. Ed.* **2006**, *45*, 3170.
- (27) Yoshino, J.; Kano, N.; Kawashima, T. *Chem. Commun.* **2007**, 559.
- (28) Rao, Y.-L.; Amarne, H.; Zhao, S.-B.; McCormick, T. M.; Martić, S.; Sun, Y.; Wang, R.-Y.; Wang, S. *J. Am. Chem. Soc.* **2008**, *130*, 12898.
- (29) Ishida, N.; Moriya, T.; Goya, T.; Murakami, M. *J. Org. Chem.* **2010**, *75*, 8709.
- (30) Zhu, C.; Guo, Z.-H.; Mu, A. U.; Liu, Y.; Wheeler, S. E.; Fang, L. *J. Org. Chem.* **2016**.
- (31) Yusuf, M.; Liu, K.; Guo, F.; Lalancette, R. A.; Jakle, F. *Dalton Trans.* **2016**, *45*, 4580.
- (32) Wong, B. Y.-W.; Wong, H.-L.; Wong, Y.-C.; Chan, M.-Y.; Yam, V. W.-W. *Chem. Eur. J.* **2016**, *22*, 15095.
- (33) Shaikh, A. C.; Ranade, D. S.; Thorat, S.; Maity, A.; Kulkarni, P. P.; Gonnade, R. G.; Munshi, P.; Patil, N. T. *Chem. Commun.* **2015**, *51*, 16115.
- (34) Shao, H.; Chen, X.; Wang, Z.; Lu, P. *J. Lumin.* **2007**, *127*, 349.
- (35) Meng, G.; Chen, Z.; Tang, H.; Liu, Y.; Wei, L.; Wang, Z. *New J. Chem.* **2015**, *39*, 9535.

Summary

